

BUILDINGS IN A HOT CLIMATE WITH VARIABLE VENTILATION AT NIGHT

by

Mohammad-Reza Hafezi

*Submitted in accordance with the requirements  
for the degree of  
doctor of philosophy*

Department of Civil Engineering  
University of Leeds  
March 1989

## ABSTRACT

During the summer, buildings in hot dry climates have the inevitable problem of cooling. These climates are characterized by hot summer days with cold nights, a high degree of solar radiation, low humidity and with a nearly fixed seasonal and daily pattern of wind. These natural phenomena could be exploited by nocturnal ventilation to cool the building fabric, thus saving energy during the day and providing comfort at night.

The procedures to evaluate thermal performance of buildings with special reference to nocturnal ventilation are studied. Various approaches to building thermal response are first reviewed. Dynamic thermal simulation computer models are developed to predict hourly 'internal temperatures'. These are used to study the various constituents of models. They are based on:

- the Admittance Method (as suggested by the CIBSE Guide);
- a similar procedure but with higher harmonics;
- the Response Factor Method (suggested by ASHRAE);
- and the Finite Difference Method.

A room surrounded by similar rooms in a multi-storey building, having only one external wall, was simulated in the laboratory. It was subjected to typical variations of a hot climate. Predictions of the computer simulations are compared with laboratory results and it is shown that:

- the closest agreement was obtained with the Response Factor and Finite Difference methods which are equally good;
- for higher rates of ventilation, representation of a room by a simple three nodes model thermal network will give sufficiently accurate results; while for lower rates of ventilation a more detailed model gives more accurate results;
- the standard Admittance Method gives adequate results, especially with higher rates of ventilation. It could also be used for hourly temperature calculations and variable ventilation without losing significant accuracy;
- a fuller treatment in the Admittance Method of time-lag and time-lead associated with the dynamic thermal factors, will not greatly improve the results. An increase in the number of harmonics in the procedure did not also result in significant improvements, especially with a high rate of ventilation.

Natural ventilation into rooms through open windows in these climates is theoretically investigated. It is shown that the rate of natural air flow obtained may be sufficient to meet the requirements of passive cooling by nocturnal ventilation.

A computer program is developed to calculate the rate of air flow in multi-zone buildings, and a new relationship is suggested, which will reduce the complexity of natural air flow calculations in multi-zone buildings subjected to cross ventilation.

---

 TABLE OF CONTENTS
 

---

Abstract	II
Table of contents	III
Acknowledgements	VII
Nomenclature	VIII
CHAPTER ONE	
<i>INTRODUCTION</i>	
1.1 General	1
1.2 Hot and dry climates of Iran	2
1.3 Night ventilation requirements	3
1.4 The architecture of hot and dry climates of Iran	3
1.5 Thermal comfort in hot arid regions	5
1.6 Thermal simulation of buildings	8
1.6.1 Existing thermal models	8
1.7 The objects and scope of the present work	9
CHAPTER TWO	
<i>HEAT TRANSFER MECHANISM IN BUILDINGS</i>	
2.1 General	11
2.2 Convective heat transfer	12
2.3 Radiative heat transfer	14
2.4 Conductive heat transfer	15
2.4.1 Harmonic method	16
2.4.2 Response factor method	20
2.4.4 Finite difference method	24
CHAPTER THREE	
<i>THERMAL MODELLING TECHNIQUES THROUGH LITERATURE</i>	
3.1 Introduction	27
3.2 Thermal models in buildings	27
3.3 Traditional models	28

3.4 Environmental temperature model	29
3.4.1 Basis of the model	29
3.4.2 Conductance between elements	31
3.4.3 Development in application of the model	35
3.4.4 Admittance procedure	36
3.4.5 Basis of the procedure	37
3.4.6 Development of the Admittance procedure	37
3.4.7 Multizone buildings	38
3.4.8 Validations of the model	39
3.5 Other models	40
3.5.1 Multi-exchange model	44
3.6 Summary and discussion	46

## CHAPTER FOUR

### *NATURAL VENTILATION IN BUILDINGS*

3.1 Introduction	49
3.1.1 Health	49
3.1.2 Ventilation for thermal comfort	49
3.1.3 Cooling the structure which surrounds the body	50
3.2 Modelling room ventilation	51
3.2.1 Single sided ventilation	52
3.2.2 Cross ventilation	54
3.3 Results	58
3.3.1 Single sided ventilation	58
3.3.2 Cross ventilation	58
3.3.3 Cross ventilation in multi-zone buildings	63
3.4 Summary and conclusion	70

## CHAPTER FIVE

### *MATHEMATICAL MODELS AND COMPUTER PROGRAMS*

5.1 Introduction	74
5.2 The models	74
5.2.1 Number of nodes	75
5.2.2 Unsteady heat conduction	79
5.2.3 Air ventilation	79
5.2.4 Convection coefficient	80
5.2.5 Long-wave radiation through open windows	82
5.3 Finite difference model	83
5.3.1 Heat balance equations for different nodes	84

5.3.2 Finite difference computer program	90
5.4 Response factor program	92
5.4.1 Room thermal response factor	93
5.4.2 Heat balance equation	93
5.4.3 Response factor computer program	95
5.5 Harmonic method model	97
5.5.1 Admittance method	97
5.5.2 Harmonic method computer program	103

## CHAPTER SIX

### *THE OBSERVATIONS*

6.1 Introduction	105
6.2 Background	105
6.3 Physical description and measurements technique	106
6.3.1 Test room	107
6.3.2 Environmental chamber	110
6.3.3 Temperature measurement	111
6.3.4 Air flow measurement	112
6.4 Measurements procedure	112
6.5 Measurements accuracy and uncertainties	116
6.6 Results and discussion	118

## CHAPTER SEVEN

### *COMPARISON BETWEEN THE MEASUREMENTS AND CALCULATED DATA*

7.1 Introduction	133
7.2 Errors and uncertainties	133
7.2.1 Methods of uncertainty analysis	134
7.2.2 Results of error analysis	137
7.3 Results and comparison of thermal models	137
7.3.1 Results of different models	150
7.3.2 Discussion and conclusion	159
7.4 Harmonic method	160

## CHAPTER EIGHT

### *CONCLUSION AND DISCUSSION*

#### *Suggestions for further work*

166

169

REFERENCES	171
APPENDIX A <i>CALCULATIONS OF VIEW FACTOR IN A ROOM</i>	178
APPENDIX B <i>DERIVATION OF THERMAL RESPOSE FACTOR</i>	181
APPENDIX C <i>COMPARISON OF MEASUREMENTS AND PREDICTIONS OF DIFFERENT MODELS</i>	184

## ACKNOWLEDGEMENTS

Many people have come to my aid throughout this project. Space limitation prevents me mentioning all. In particular I would like to give my special thanks to

Dr. W. Houghton Evans and Dr. D. Fitzgerald, my supervisors, for their constant encouragement and useful discussions and advice.

Mr. J. Higgins and the technical staff of the department for their great help and understanding during difficulties of the experimental work.

Mr. G. Broadhead from Department of Electrical Engineering for his skill and help in the period of experiment.

The Ministry of Higher Education of Iran for their financial support.

My special thanks is also extended to my wife and my son for their great patience and sacrifice during this study.

And last and by no means least I would like to give my greatest appreciation to my parents without whose constant encouragement this work would have never been completed.

## NOMENCLATURE

This nomenclature is used throughout this thesis, unless indicated locally.

Symbol		Unit
A	area	$m^2$
$C_v$	ventilation conductance	W/K
$C_d$	discharge coefficient	—
$c_p$	specific heat capacity	J/kg K
d	distance	m
F	surface factor	—
f	decrement factor	—
g	Accelaration due to gravity	$m/s^2$
Gr	Grashof number	—
$h_r$	radiation conductance	$W/m^2K$
$h_c$	heat transfer coefficient for convection	$W/m^2K$
I	total solar intensity	$W/m^2$
l	thickness	m
N	number of air changes per hour	$h^{-1}$
Nu	Nusselt number	—
P	pressure	Pa
Pr	Prandtl number	—
Q	rate of heat flow	W
R	thermal resistance	$m^2K/W$
$R_{si}$	inside surface resistance	$m^2K/W$
$R_{so}$	outside surface resistance	$m^2K/W$
T	temperature	$^{\circ}C$
$T_c$	dry resultant temperature	$^{\circ}C$
$T_{el}$	environmental temperature	$^{\circ}C$
$\bar{T}_r$	mean surface temperature	$^{\circ}C$
t	time	s
U	thermal transmittance	$W/m^2K$
Vol	volume	$m^3$



V	air velocity	m/s
v	ventilation rate	m <sup>3</sup> /s
x	distance	m
Y	admittance	W/m <sup>2</sup> K

### *Greek*

---

$\alpha$	thermal diffusivity	m/s
$\beta$	glass reflectance	—
$\epsilon$	Surface emissivity	—
$\lambda$	thermal conductivity	W/mK
$\omega$	time lead for admittance	h
$\phi$	time lag for decrement factor	h
$\psi$	time lag for surface factor	h
$\rho$	density	kg/m <sup>3</sup>
$\tau$	glass absorptance	—
$\sigma$	Stefan Boltzman constant $5.67 \times 10^{-8}$	W/m <sup>2</sup> K <sup>4</sup>

### *Subscripts*

---

ai	inside air
ao	outside air
s	surface
si	internal surface
ri	mean surface temperature of a room
si	internal surface
so	external surface

### *Superscripts*

---

-	daily mean of a value
~	swing about the mean of a value

## CHAPTER ONE

### *INTRODUCTION*

#### **1.1 General**

The most basic function of a building is to control the internal environment, in order to make it suitable for healthy and comfortable living. Buildings in hot climates like those in parts of Iran have the inevitable problem of cooling during the hot summer days.

In the past people who lived in these areas have learned to cope, and make use of the outside environment, to create and control comfort in their buildings. This was mainly achieved by experience through generations and many years of trial and error. With the modern change in life style, construction techniques and architecture generally, the old solutions tend to be neglected.

If energy is freely spent, with present knowledge and equipment the internal environment of a building can be comfortable regardless of how uncomfortable the outside environment is. But the customary energy source will not last indefinitely and also the techniques and equipment are not universally available, especially in developing countries, and they are also expensive to build and use.

In a mild climate, like that of the U.K., cooling a dwelling on a warm summer day could be achieved by natural ventilation through open windows, but in the hot climate of Iran, the outside air is so hot during the day that it cannot be allowed in for cooling purposes. From late afternoon until early morning the outside air drops to a lower temperature, suitable for cooling the body as well as the structure. Night ventilation is consequently the dominant method of cooling buildings for many months of the hot season. A well designed building could be kept comfortable by natural ventilation, without air conditioning. Even with air conditioning, night ventilation reduces the internal temperatures, (air and surfaces) and consequently energy will be saved.

In recent years attention has been given to passive cooling, but

most studies are qualitative descriptions of past experience.

It is desirable early in the design stages to predict the thermal response of buildings and evaluate comfort attainable by night ventilation. A suitable procedure would be a compromise between accuracy, reliability, simplicity and ease of use. The purpose of this study is to examine existing techniques and to develop such a procedure with reference especially to night ventilation in hot arid climates. In this study special attention is paid to hot arid climates of Iran and similar climatological data is used where required.

### 1.2 Hot and dry climate of Iran:

Iran is a large country, between latitudes  $25^{\circ}$  and  $39^{\circ}$  North and longitude of  $25^{\circ}$  to  $45^{\circ}$  East. In world climatology Iran is classified as a tropical and subtropical region. (Tavassoli 1976) Nevertheless because of its special geographical location it contains other climates, such as those around the Caspian sea in the north (mild and wet); the Persian Gulf and Oman Sea in the south (hot and humid); and mountainous areas of the west and north (cold and dry).

The hot and dry climatic regions of Iran have special characteristics, which include high solar intensity, hot days and cold nights, very high energy loss to the sky during the night, low relative humidity, very low rainfall, and a dominant pattern of prevailing wind.

The low relative humidity, the clear sky and low cloud cover cause a quick rise in air temperature during the day. At night because of the low thermal capacity of the dry air, its energy will be lost quickly and its temperature will fall. This variation of temperature between day and night becomes as much as 20 K in some summer months. The high angle of incidence will also cause a high energy gain by building surfaces during the day, while absence of cloud permits easy release of stored heat, by long wave radiation to the sky. These climates have a fixed pattern of wind, and usually a desirable wind blows at a fixed direction at a lower temperature than that of the ambient air. In some directions the wind might be warm and carry sand. Temperature diversion is also a significant phenomenon.

Table 1-1 summarizes some climatological data for cities during the summer.

Table 1-1 Weather data for some cities in Iran

	Latitude N	Air temperature °C					Relative humidity(%)	
		daily mean	mean		absolute		min.	max.
			max.	min.	max.	min.		
Tehran	34° 41'	32.3	39.3	25.7	43.0	21.0	11	24
Kerman	30° 15'	25.7	35.7	15.8	38.0	11.0	12	27
Kashan	33° 59'	35.6	44.0	27.3	47.0	24.0	16	30
Yazd	31° 54'	32.2	40.0	23.8	43.0	21.0	9	15
Isfahan	32° 37'	29.7	37.3	22.0	39.0	19.0	17	32

### 1.3 Night ventilation requirements

In a theoretical examination of cooling buildings in Yazd in the hot arid parts of Iran, Golneshan and Yaghoubi(1984) has shown that comfort could be achieved during hot summer days by ventilation at night and suitable design. A ventilation rate of 12 to 30 air changes per hour during the cold period of the night is suggested and infiltration during the day is discouraged. In another investigation for Aswan in Egypt, Al-Awa (1981) has suggested the same range of ventilation rate during the night. He has shown that 40 air changes per hour will result in reasonable room air temperature, if the house is suitably designed.

Such rates of ventilation could be achieved by cross ventilation, using the dominant wind direction and an appropriate configuration of openings. In rooms with all windows only on one wall; (single sided ventilation) the rate of air flow may not be sufficient for cooling purposes. The air flow rate could be enhanced by certain devices. One such device is the wind tower traditionally used in passive cooling in Iranian architecture, described below. The air flow rate could be increased by adding baffle walls besides windows. With an oblique wind the average air speed in a room with single sided ventilation, may be increased in this way from 8% to 35% of that of the wind outside. (Givoni 1981)

### 1.4 The architecture of the hot and dry climate of Iran

The people in the hot arid regions of Iran have adapted their way of living and their dwellings to the conditions imposed by the

outside environment with methods such as:

- reduction of the exposed surfaces of buildings by attaching them to each other;

- use of thick heavy brick and adobe walls to exploit the high daily fluctuation in outside air temperature;

- reduction of the area of glass to decrease the rate of solar gain;

- by living and sleeping outside during the night and opening doors and windows to exploit long wave radiation loss to the sky.

They also avoided the high solar radiation by constructing court-yards and earth-sheltered dwellings. This also allowed them to move around the house according to the season; using south facing parts during the winter and north facing parts in the summer. They built ponds and planted trees and shrubs in the court-yard to increase the relative humidity of the air.

Such methods and innovations have resulted in an especial architecture of the hot and dry regions of Iran. Tavassoli(1975) has outlined their main architectural elements as: court-yard houses; large terraces in front of buildings (eivans); domed roofs and wind towers ( Baud Geers); of which the last two are used for cooling; by heat transfer by convection and increasing the rate of air movement.

Domes and vaults are the essential elements of Iranian architecture, used for both public buildings and dwellings. Apart from their structural advantages (being lighter and cheaper than flat roofs where timber is scarce), they are also of great use in passive cooling for example a domed roof provides more air flow in the room below. A hole at its apex will increase the rate of natural air flow in the room. Haghghat and Bahadori (1983) have studied the rate of natural ventilation in buildings employing domed roofs, with openings at the crown. When compared with flat roofs the domed roofs always increase the air flow rate through the buildings. This increase becomes significant in buildings with all windows and doors on one side (single sided ventilation), or when the building envelope cannot provide enough pressure difference across openings. This increase in air flow rate could be as high as 250%. Cavity domes (or double layered domes) are also widely used in larger buildings. By providing openings on the outer dome and on the apex of both layers, the air would circulate between the layers and through the building below. It will decrease the temperature of the surfaces. This large air flow rate in buildings may be utilized to store night air coolness in the

structure more effectively and keep the temperature of the interior surfaces low, thus decreasing the mean radiant temperature for better summer comfort.

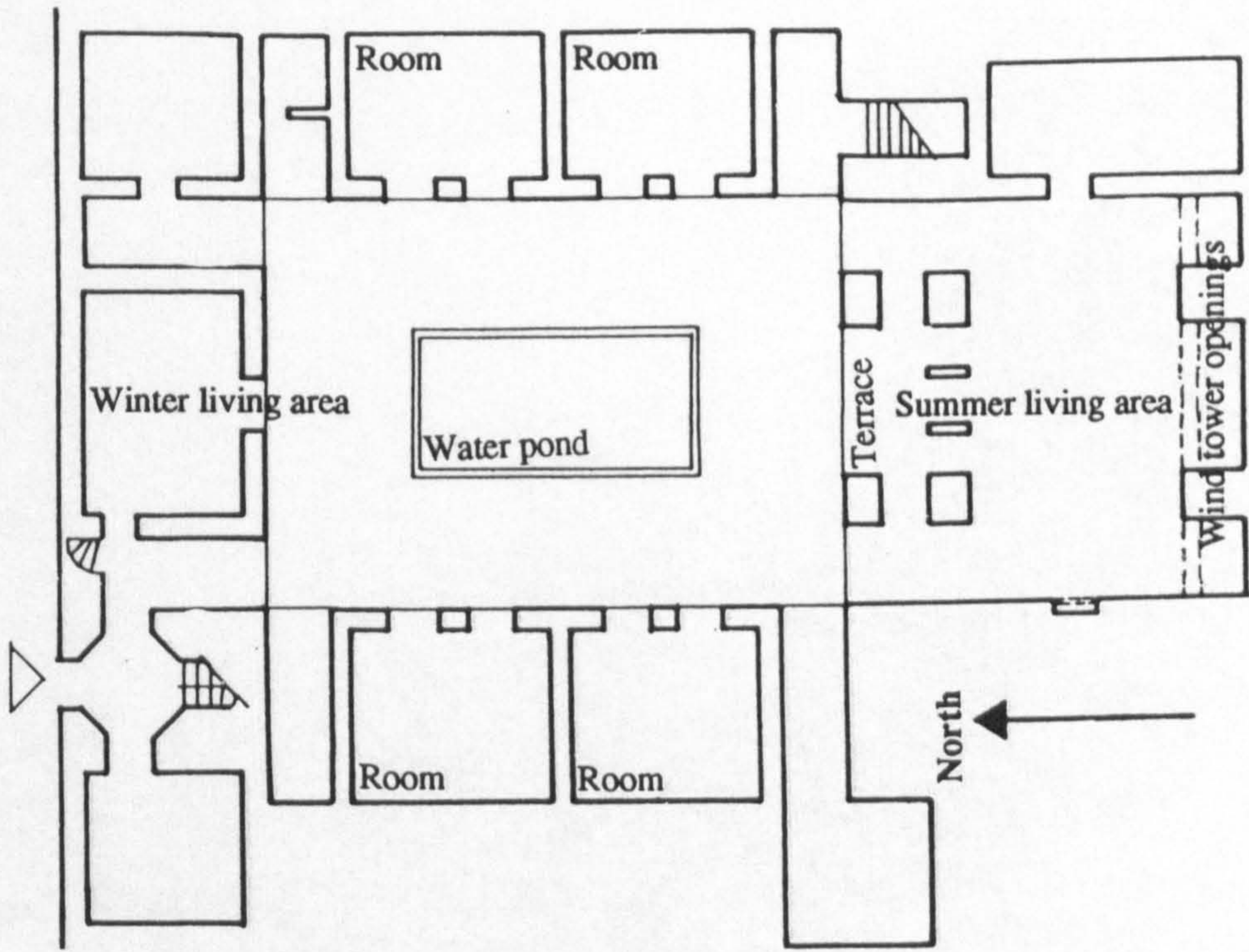
One of the finest examples of the use of natural ventilation in buildings are wind towers which are widely used in the hot arid regions of Iran. (Bahadori 1978)

Wind towers are masonry structures designed to provide natural circulation of air through the building. They collect cooler air at higher level and lead it into the building. There is always a circulation of air through wind towers. (Bahadori 1979) Their function differs between day and night. At night, when there is no wind they act as a chimney to maintain a circulation of air through the attached building, and, when there is wind, the air moves in the opposite direction. The cooling of its structure is accomplished both by long wave radiation loss to the sky and by convection with cool night air. During the day when there is no wind, the tower works as a reverse chimney. The hot outside air will enter and pass through the tower, and during its journey loses energy to the structure of the tower, cooled during the previous night, and enters the room. When there is wind, the air enters the room at a higher rate. There are different types of wind tower shapes, various tower heights and openings, cross section and structure. Some of them are connected to an underground room (sardab), to circulate air through it, in order to increase humidity and use the coldness of the underground air. They were also connected to cisterns to cool the space for storing ice during hot summer days. (Bahadori ) Figure 1.1 shows an example of a dwelling with a wind tower in Iranian architecture.

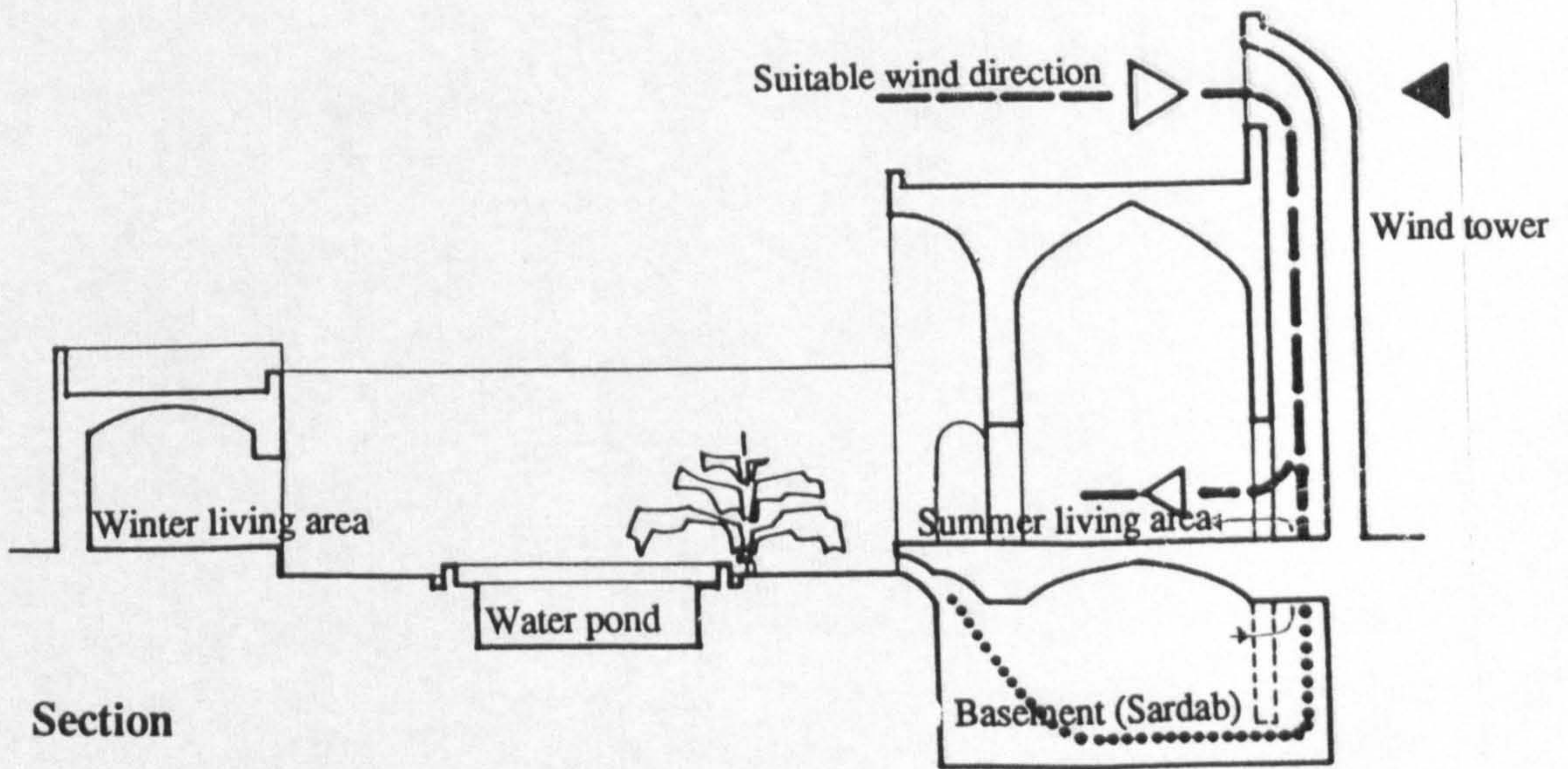
### 1.5 Thermal comfort in hot arid climates

The human body's thermal comfort depends on the combined effect of the mean radiant temperature, the ambient air temperature, the relative humidity and the air velocity, besides the type of clothing and the level of activity. Various thermal indices have been developed to give a basis for comfort evaluation, which differ in their approach to the problem, assigning different importance to the factors, their range of applicability, the precision and data required etc. (Eleven such indices are reviewed by Sodha et al. 1986)

In the U.K., "resultant temperature" (or dry resultant temperature) is accepted as an index for thermal comfort evaluation. This temperature may be measured by a globe thermometer at the centre



Plan



Section

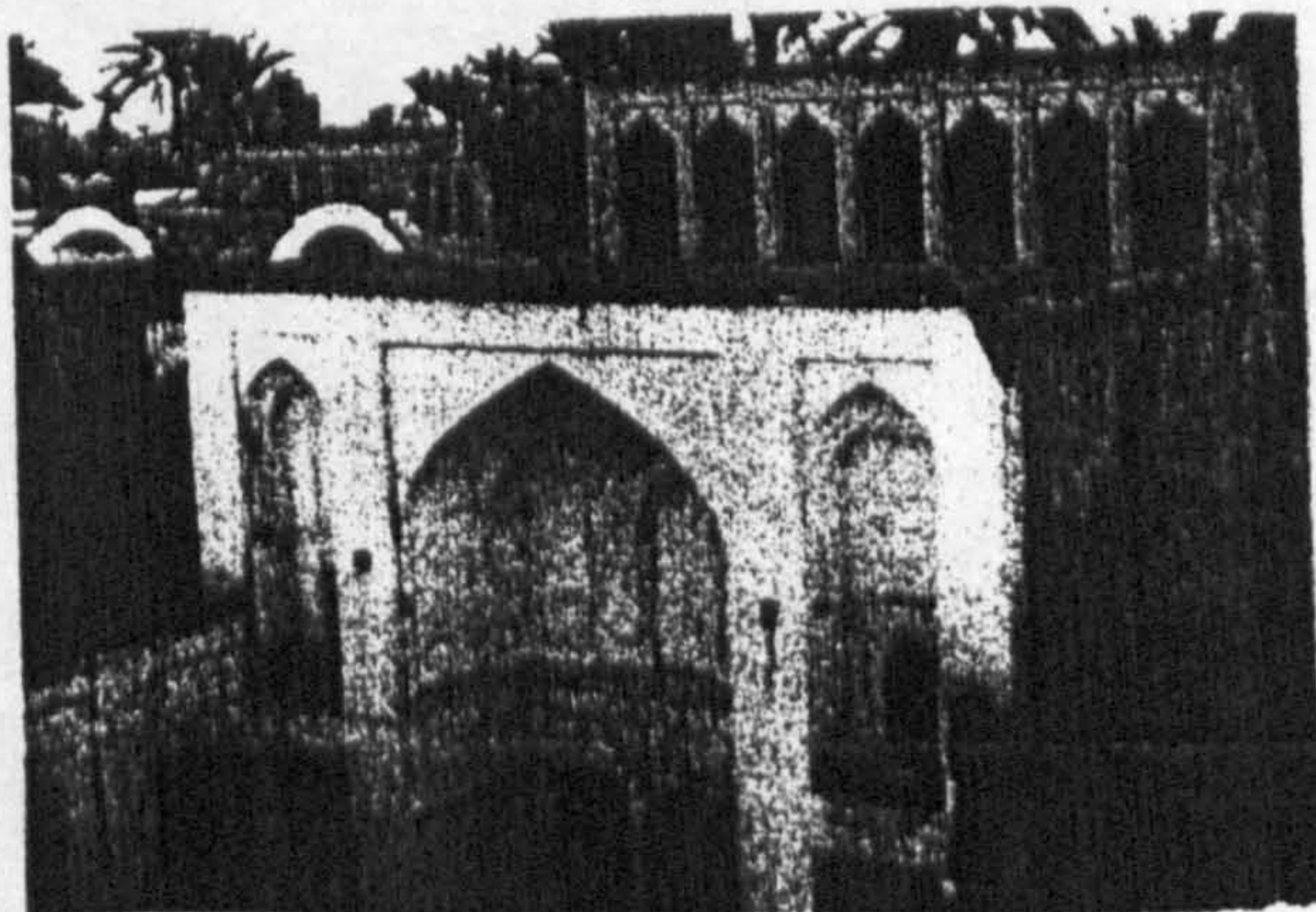


Figure 1.1: One example of a court-yard, earth sheltered dwelling employing wind tower and underground room (sardab). (Tavassoli 1975)

of a room. (CIBSE Guide part A1 1986) It is also shown to be a suitable index for comfort in hot arid climates. (Nicol 1975) This temperature correlates the effect of mean radiant temperature, ambient air temperature and air velocity and is given by:

$$T_c = \frac{\bar{T}_r + T_{ai} (10v)^{0.5}}{1 + (10v)^{0.5}} \quad ^\circ\text{C} \quad (1.1)$$

where

$T_c$  = dry resultant temperature  $^\circ\text{C}$

$T_{ai}$  = air temperature  $^\circ\text{C}$

$\bar{T}_r$  = mean radiant temperature  $^\circ\text{C}$

$v$  = air velocity m/s

The effect of humidity on comfort can be ignored if the resultant temperature is not much greater than the preferred values and if the relative humidity lies between 40% to 70%. As a change of  $\pm 1.5$  K on the preferred comfort temperature will not significantly affect comfort under normal conditions. With the air velocity about 0.1 m/s, the above equation could be simplified to

$$T_c = (T_{ai} + \bar{T}_r) / 2 \quad ^\circ\text{C} \quad (1.2)$$

The preferred indoor temperature is also related to the outdoor air temperature. When the building is not air conditioned - a "free running building" - this relation is linear, such that one degree increase in outdoor air temperature would be compensated by half a degree increase in comfort temperature.

Nicol (1975) has studied observations related to comfort in two hot arid cities during June and July: in Roorkee in India and Baghdad in Iraq. His investigation has shown that none of the several thermal comfort indices which were tested, correlated significantly better than the globe temperature. He also found that the people in these climates were comfortable in much warmer conditions than people in temperate climates.

By comparing the results with observations of comfort among English workers at similar conditions, he has shown that while English subjects are comfortable at a globe temperature of 20 to 25  $^\circ\text{C}$ , in a hot arid climate little thermal discomfort was shown at temperature up to 32  $^\circ\text{C}$  provided the air velocity exceeded 0.25 m/s.



It was also found that the discomfort vote did not exceed 20% until the globe temperature rose above 36 °C.

Nicol has also shown that while the effect of relative humidity was insignificant, the air velocity had a constant and statistically significant effect on thermal comfort. Air movement reduced discomfort from heat at temperatures above 31 °C, and below this temperature there was little discomforts. At temperatures above 40 °C discomfort was experienced at any air velocity. More detailed discussion about the effect of air movement on thermal comfort is given in chapter four.

## 1.6 Thermal simulation techniques

The importance of a building as a modifier of outdoor conditions has necessitated the development of dynamic thermal simulation techniques. These models are required as a tool to predict the thermal response of buildings and to evaluate the relative significance of variables at the design stage. Such models should be a compromise of accuracy, reliability, flexibility and ease of use.

A dynamic thermal model depends on how the physical laws of heat transfer are used and how a room is presented as a thermal network. The accuracy, flexibility and simplicity of a thermal model is affected by its treatment of

- unsteady heat transfer by conduction
- energy input to the room
- radiation between surfaces
- convection between surfaces and air
- ventilation
- presentation of the elements of the thermal system

### 1.6.1 Existing thermal techniques

Mathematical techniques currently used to estimate the indoor "temperature" and the cooling or heating load of a building can be divided into three groups: (Gupta et al. 1976)

- a: the harmonic method
- b: the response factor method
- c: numerical methods

The fundamental assumption made by the harmonic method is that the climatological information can be approximated by a series of periodic cycles, which is usually the case for design studies. This

is also the basic assumption of the Admittance Method used in the U.K. and given by the CIBSE Guide and practiced since 1970.

The response factor method is devised to handle both periodic, non-periodic and intermittent inputs, where the harmonic method is no longer applicable. This could also be used when energy demands are required to be calculated over a fairly long time. The method is recommended by the American Society of Heating, Refrigerating and Air Conditioning Engineers (ASHRAE) for heat transfer calculations in buildings.

Numerical methods are used when the solution to the unsteady heat conduction equation under varied boundary conditions of interest is not possible by the analytical approach.

### 1.7 The objects and scope of this work

The object of this study is the evaluation and improvement of design procedures for hot arid climates with special reference to natural nocturnal ventilation.

Emphasis is given to different established techniques currently in practice in order to predict the thermal response of buildings. Several unsteady mathematical models are developed varying:

- the number of nodes in the thermal circuit
- the treatment of unsteady heat transfer
- the treatment of convective and radiative heat transfer in a room
- the treatment of ventilation

To evaluate the models and the relative significance of each parameter, the results of mathematical analysis had to be compared with measurements. A special test room was built and was subjected to variations of "outside air temperature" similar to those of hot climates. It was ventilated during the night. The precision of the results obtained from models is evaluated in comparison with the data obtained from observations.

In chapter two different mechanisms of heat transfer between building elements are described. Chapter three is concerned with a review of different techniques of thermal modelling in buildings in the literature. In chapter four natural ventilation flow calculations in a room with different opening configuration were performed using a mathematical model developed to simulate typical rooms. The experimental procedure and the results are described in chapter five

and the effects of timing and the rate of ventilation are discussed. In chapter six the detailed procedures of the mathematical models developed in this study are given. Chapter seven deals in detail with the comparison between calculations and observations, describing the effect of each parameter and indicating the precision of each technique. In chapter eight concluding remarks are made and suggestions for further work are given.

## CHAPTER TWO

### *HEAT TRANSFER MECHANISMS IN BUILDINGS*

#### 2.1 General

One of the main purposes of buildings is to provide a healthy environment for living. The degree and level of its control becomes more important when artificial air conditioning is not possible.

The desired environment is usually different from that outside. This difference in the two environments consists of a substantial "temperature" difference between indoors and outdoors. The thermal response of a building is a function of a number of parameters which in physical terms may be grouped into three broad classes : climatic, occupancy ,and enclosure factors.(GUPTA 1970)

-Climatic factors include the air temperature, relative humidity of the air, direct and diffuse solar radiation, wind speed and direction.

-Occupancy factors include the number of occupants, and how they live and the conditions they want including ventilation and humidity, and the heat emitted by their activities.

-Enclosure factors include the geographical location and type of neighbourhood (urban or rural) ,geometrical factors such as: dimensions, orientation, lay out, insulation and its distribution, the size and position of windows, solar control and shading devices and the physical properties of the building materials.

On account of the variations of climatic factors the thermal response of a building is unsteady, so that a building behaves as a complicated thermal system which is subjected to unsteady thermal excitation. The internal environment will be provided by the interaction of these parameters through different heat transfer processes. The mechanism of heating or cooling imply basically the transfer of heat by virtue of existing temperature difference among two or more objects and can take place in three different ways: by conduction, convection and radiation. These heat transfer modes are interdependent and the calculation of any one of them requires the

simultaneous consideration of the other heat transfer modes. A brief review of these mechanisms and the way they are usually applied in building application and also as used in the present study follows.

## 2.2 Convective heat transfer :

The rate of heat transfer in  $W/m^2$  between a surface and a fluid, air, may be calculated from:

$$Q/A = h_c (T_a - T_s) \quad W/m^2 \quad (2.1)$$

where

$T_a$  = air temperature °C

$T_s$  = surface temperature °C

$h_c$  = convective heat transfer coefficient  $W/m^2K$

Here the convective heat transfer coefficient  $h_c$  is some surface-averaged value. The value of  $h_c$  depends upon the geometry of the system, the velocity and mode of the fluid flow (laminar or turbulent), and upon the temperature difference between the air and the surface ( $T_a - T_s$ ).

Heat transfer by convection, is either "natural" or "forced". Natural convection is caused by the buoyancy forces arising from density variations of the air as the result of changes in temperature, and forced convection will occur if the fluid motion is caused by "external" forces independent of the temperature difference in the fluid .

Many empirical formulations may be found in the literature which give the convective coefficient and could be used in buildings. e.g. ASHRAE 1985 , WONG 1977, O'CALLAGHAN 1980. These are usually a function of surface and air temperature difference, characteristics and dimensions of the surface and direction of flow under given conditions, and whether the flow is laminar or turbulent .

The convective heat transfer coefficient for surfaces of naturally ventilated buildings in case of buoyancy-driven convection (natural convection) which could be applied to the full range of laminar, transitional, and turbulent air flow is given by ALAMDARI & HAMMOND (1983). For vertical surfaces

$$h_c = \left\{ \left[ 1.5 \left( \frac{dT}{l} \right)^{0.25} \right]^6 + \left[ 1.23 (dT)^{0.33} \right]^6 \right\}^{1/6} \quad (2.2)$$

for horizontal surfaces with heat flow upwards:

$$h_c = \left\{ \left[ 1.4 \left( \frac{dT}{l} \right)^{0.25} \right]^6 + \left[ 1.63 (dT)^{0.33} \right]^6 \right\}^{1/6} \quad (2.3)$$

and for horizontal surfaces with heat flow downwards:

$$h_c = 0.6 \left( \frac{dT}{l^2} \right)^{0.2} \quad (2.4)$$

where:

$dt$  is the temperature difference between air and surface

$l$  is the hydraulic diameter  $4A/P$

$A$  is the area  $m^2$

$P$  is the perimeter  $m$

This formula is valid over the range of  $10 < Gr.Pr < 10^{12}$  which covers the conditions in buildings. For forced convection the coefficient can be found from : (McADAMS 1954).

$$h_c = 5.7 \left[ a + b \left( V/0.31 \right)^n \right] \quad (2.5)$$

where

$V$  is the speed of air  $m/s$

$a, b, n$  are empirical constants.

When the air velocity is less than  $4.8 m/s$ , for smooth surfaces  $a, b,$  and  $n$  are  $0.99, 0.22$  and  $1$ , and  $1.09, 0.23$  and  $1$  for rough surfaces respectively.

Natural convection is believed to be the main mechanism of heat transfer by convection in a naturally ventilated room, but in cases when natural and forced convection taking place at the same time,

McADAMS (1954) recommends that both values be calculated and the larger used.

According to the above formulation  $h_c$  might change over a wide range, For example  $h_c$  is equal to  $0.8 \text{ W/m}^2\text{K}$  for natural convection and a temperature difference of  $0.1 \text{ K}$  between air and the surface or it could be as high as  $10.5 \text{ W/m}^2\text{K}$  for forced convection and an air speed of  $1 \text{ m/s}$ .

It is not always possible to use a time dependent coefficient, and a mean value might be required. The CIBSE Guide suggests values of  $4.5, 3.0, 1.5 \text{ W/m}^2\text{K}$  for floors, ceiling and walls respectively. (CIBSE 1986)

### 2.3 Radiative heat transfer :

The heat exchange by radiation between two surfaces in "visual" communication can be calculated from:

$$Q_R = E_{12} \sigma A_1 \left( T_2^4 - T_1^4 \right) \quad \text{W} \quad (2.6)$$

where

$T$  is the surface temperature  $^{\circ}\text{K}$

$A$  is the area of the surface  $\text{m}^2$

$\sigma$  is the Stefan Boltzman constant ( $= 5.67 \times 10^{-8} \text{ W/m}^2\text{K}^4$ )

$E_{12}$  is the configuration factor with a value up to 1.0 depending upon the emissivity of the surfaces and relative view factor,  $F_{12}$ , between them. If one side has an emissivity  $\epsilon_1$  and other  $\epsilon_2$ , it can be shown that for radiant heat exchange between two "non black" surfaces at different temperature

$$E_{12} = \left[ \frac{1 - \epsilon_1}{\epsilon_1} + \frac{1}{F_{12}} + \frac{A_1 (1 - \epsilon_2)}{A_2 (\epsilon_2)} \right]^{-1} \quad (2.7)$$

The relative view factor can be obtained from many texts on heat transfer. Clarke (1985) shows how to calculate the view factors for rectangular building components. Appendix A. gives the view factor for the special case between the room surfaces and room windows for both cases of adjacent and parallel positions.

The use of a constant value for radiation conductance is studied by Buchberg (1971). He has developed a finite difference model to

compare the response of different types of buildings and different regimes of energy input, with a fixed and variable radiation conductance. To linearize the radiation in a thermal network of a room, the radiation resistance is given by:

$$R_{12} = \frac{1}{AE_{12} \sigma (T_2^2 + T_1^2) (T_2 + T_1)} \quad (2.8)$$

The value of  $R_{12}$  is computed at each time step using the new values of surface temperatures,  $T_1$ ,  $T_2$ . The comparison is made between the time dependent and fixed radiation conductance. The maximum deviation in mean air and surface temperature is less than 10%.

In building application  $T_1$  and  $T_2$  in equation 2.7 usually differ by about 10 K and each is order of 300 °K. The heat flux is nearly proportional to the difference of temperature and equation 2.6 could be approximated by:

$$Q_R = E_{12} A_{12} 4\sigma \bar{T}^3 (T_2 - T_1) \quad (2.9)$$

where

$\bar{T}$  is the mean surface temperature  $(T_1 + T_2)/2$ . °C

By defining the radiant heat transfer coefficient as :

$$h_{r12} = 4\sigma \bar{T}^3 E_{12} \quad \text{W/m}^2 \text{ K} \quad (2.10)$$

From equation 2.10 a mean value of  $h_r = 5.7 \times E_{12}$  W/m °C is usually used for building application. The final equation for heat transfer by radiation is given by:

$$Q_R = A h_r (T_2 - T_1) \quad (2.11)$$

#### 2.4.1 Conductive heat transfer

The general equation representing the unsteady-state, one dimensional heat flow within a solid by conduction is found from



$$\frac{\partial^2 T}{\partial x^2} = \frac{1}{\alpha} \frac{\partial T}{\partial t} \quad (2.12)$$

where

$\alpha$  is the thermal diffusivity m/s

$t$  is the time s

$x$  is the distance m

Different methods exist to deal the underlying heat transfer problem, some reviewed by Muncey (1979). These different techniques give their names to the approaches to the thermal simulations of buildings. They are based upon the assumptions and the conditions imposed on the environmental system and the characteristics of the building materials. These are the Harmonic Method, the Response Factor method and the Finite Differences Method.

#### 2.4.1 Harmonic Method

In the case of building design it is a reasonable assumption to consider that the climatic conditions are cyclic over a given time. If this condition be imposed on equation 2.12, the variation of temperature is sinusoidal and the solution of this equation is given by MUNCEY (1979) and PIPES (1957) as:

$$\begin{vmatrix} T_o \\ Q_o \end{vmatrix} = \begin{vmatrix} A & B \\ D & A \end{vmatrix} \times \begin{vmatrix} T_1 \\ Q_1 \end{vmatrix} \quad (2.13)$$

where for a sinusoidal input

$T_n$  is the temperature of surface n °C

$Q_n$  is the heat flux at surface n W/m<sup>2</sup>

$A = \cosh (1+i) \phi$

$B = R \sinh(1+i) \phi / (1+i) \phi$

$D = (1+i) \phi \sinh(1+i) \phi / R$

$\phi = (\omega l^2 / 2 \alpha)^{0.5}$

$\alpha$  is the thermal diffusivity m/s

$R$  is the thermal resistance of the slab m<sup>2</sup>K/W

$l$  is the slab thickness m

$\omega$  is the angular frequency s<sup>-1</sup>

$$= 2\pi \text{ frequency of heat input} \quad \text{s}^{-1}$$

and in case of a high diffusivity, and with a total thermal resistance the matrix becomes:

$$\begin{vmatrix} A & B \\ D & A \end{vmatrix} = \begin{vmatrix} 1 & R \\ 0 & 1 \end{vmatrix} \quad (2.14)$$

The exchange between two environmental points, inside and outside through a multi layer slab may be written as

$$\begin{vmatrix} T_o \\ Q_o \end{vmatrix} = \begin{vmatrix} 1 & R_{so} \\ 0 & 1 \end{vmatrix} \times \begin{vmatrix} E & F \\ G & H \end{vmatrix} \times \begin{vmatrix} 1 & R_{sl} \\ 0 & 1 \end{vmatrix} \times \begin{vmatrix} T_i \\ Q_i \end{vmatrix} \quad (2.15)$$

where

$$\begin{vmatrix} E & F \\ G & H \end{vmatrix} = \begin{vmatrix} A_1 & B_1 \\ D_1 & A_1 \end{vmatrix} \times \begin{vmatrix} A_2 & B_2 \\ D_2 & A_2 \end{vmatrix} \times \dots \times \begin{vmatrix} A_n & B_n \\ D_n & A_n \end{vmatrix} \quad (2.16)$$

where  $A_1$ ,  $B_1$  and  $D_1$  are the coefficients calculated from equation 2.12 for each layer.

Some simplifications are made in building application which are the basis of the Admittance Method which is the standard procedure of heat and energy analysis in buildings in the U.K. suggested by CIBSE. From the above solution three factors may be obtained each dependant on the thermal properties of the material as well as the frequency of the sinusoidal excitation. These factors are: (MILBANK 1974)

The Admittance which is the amount of energy ( $Q_1$ ) entering the surface for each degree of temperature difference at the environmental point

$$Y = \frac{\tilde{Q}_1}{\tilde{T}_1} \quad (2.17)$$

which might be used to calculate the equivalent swing in temperature above some mean value due to cyclic load on an enclosure.

The Decrement factor  $f$  is the ratio of the cyclic transmittance

to the steady state U value.

$$f = \frac{\tilde{Q}_o}{\tilde{t}U} \quad (2.18)$$

The Surface factor F is the equivalent cyclic energy at the environmental point due to a cyclic energy input at the surface. It is the proportion of the heat gain at the surface which is readmitted to the environmental point when the temperatures are held constant.

$$F = \frac{\tilde{Q}_1}{\tilde{Q}} \quad (2.19)$$

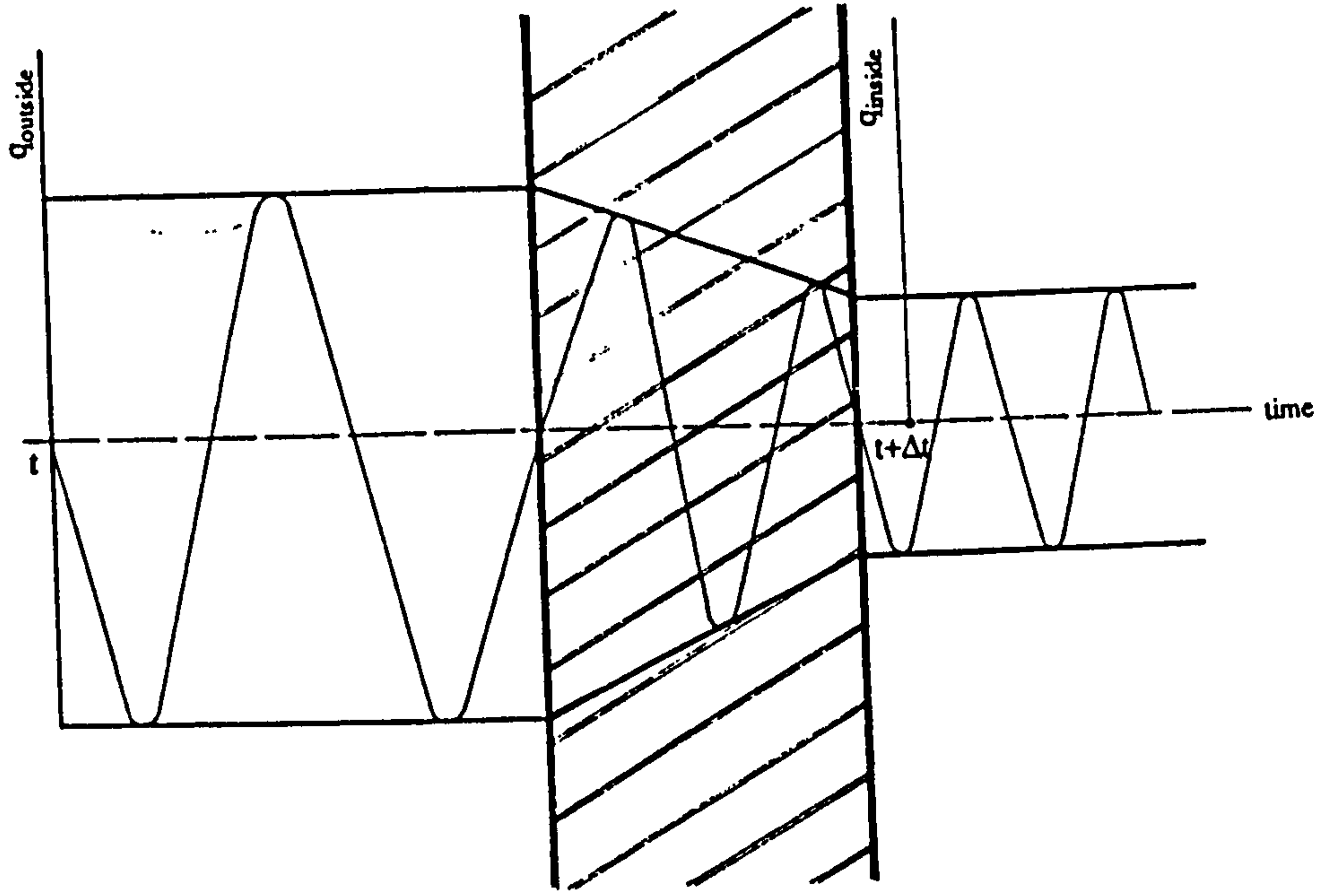
These factors are expressed as complex numbers so that each has a time lag associated with it. The detailed procedure for computation of each factor is given by Milbank (1974).

As mentioned above, this method of solution of the underlying heat transfer problem is applied when the energy input is considered to be periodic cycles over a period of time, so that the external climatic data should be analyzed into a steady term accompanied by a series of sine terms with decreasing amplitude and increasing frequency. Each harmonic will be treated with the thermal factors appropriate to its frequency. The final result will be obtained by summing the results from each harmonic. Figure 2.2 shows an analysis of actual solair temperature for different harmonics.

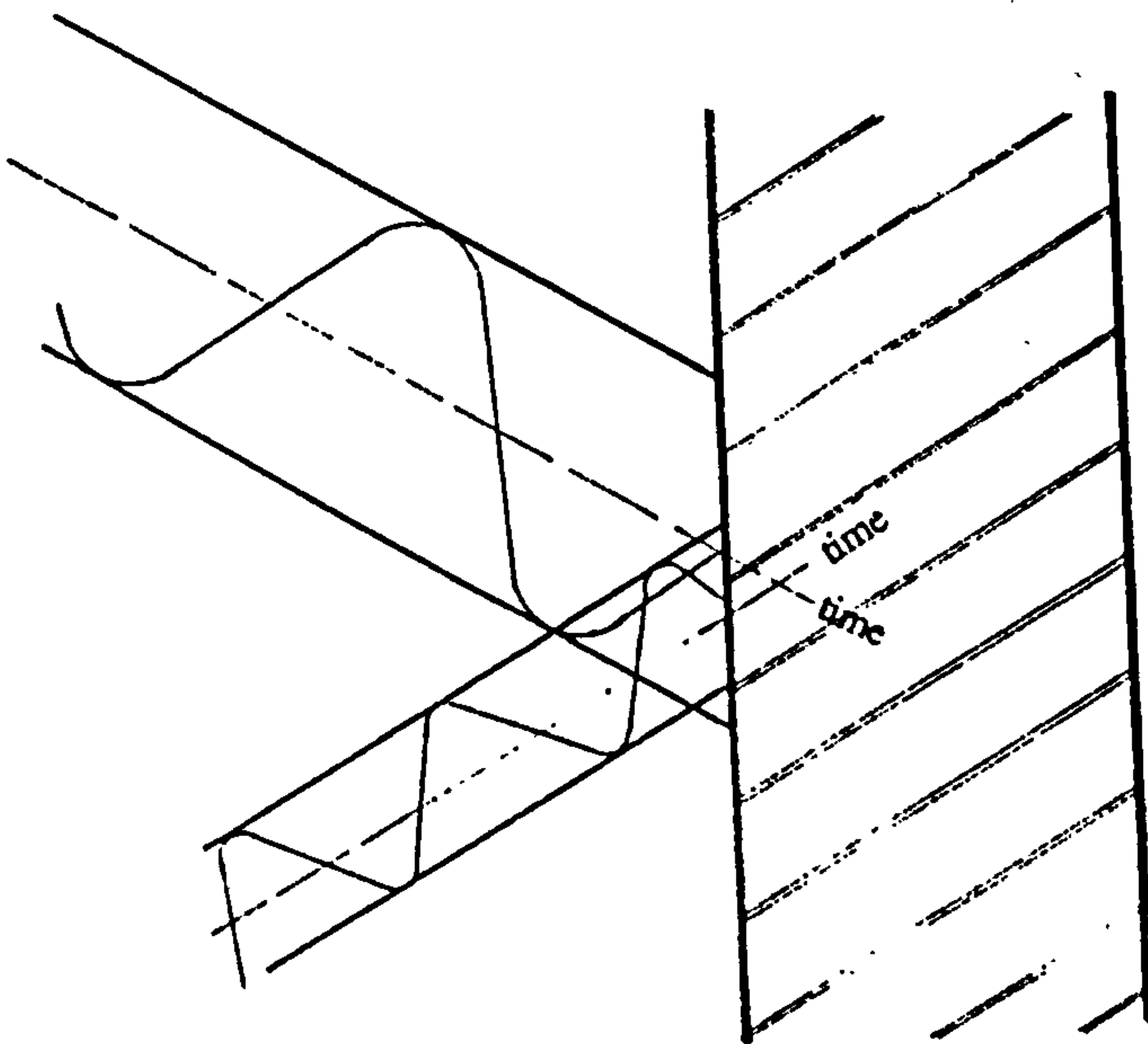
The division of a real climatic time series into components of sinusoidal variations about some mean value can be readily achieved by Fourier series representation, through which a given function can be approximated to a series of sine and cosine functions, or sine or cosine only, such that for some continuous function  $f(x)$ , for example a 24 hour values of temperature may be represented as: (CHATFIELD 1975)

$$T_t = a_0 + \sum_{j=1}^{\infty} a_j \cos\left(\frac{2\pi t}{24}\right) + \sum_{j=1}^{\infty} b_j \sin\left(\frac{2\pi t}{24}\right) \quad (2.20)$$

where



a: Effect of Decrement Factor and time lag



b: Effect of Surface Factor and time lag

**Figure 2.1: Definition of Surface Factor and Decrement Factor.**

$$a_0 = \frac{1}{24} \sum_{n=1}^{24} T_n$$

$$a_j = \frac{2}{24} \sum_{n=1}^{24} T_n \cos\left(\frac{2 \pi j n}{24}\right)$$

$$b_j = \frac{2}{24} \sum_{n=1}^{24} T_n \sin\left(\frac{2 \pi j n}{24}\right)$$

$j$  = number of frequency

$T_n$  = temperature at time  $n$

In recent years Milbank and Harrington-Lynn at the Building Research Station have developed the mean and swing technique introduced by Danter (1960) which is commonly referred to as the Admittance Method and is given in CIBSE Guide (1985) This method employs the factors for the first harmonic (24 hours frequency) which is applied to the actual climatic data, and is believed to be sufficiently accurate for application to buildings, with the advantage of *not requiring* the use of computers. Sodha et al.(1986) have compared the idea of the Admittance Method with the Fourier method for hourly calculation of heat flow through a wall. They concluded that the Admittance Method could be employed for hourly calculation without losing much accuracy with a maximum deviation of 10% in air temperature(in °C). In this research programme a computer model based on the Admittance Method is developed and the results are compared with those of the other calculation methods. This will be discussed in more detail below.(Chapter three)

#### 2.4.2 The Response Factor Method

When the energy requirement over a fairly long time is to be assessed, or the climatic conditions are believed to be non-periodic, the harmonic method is no longer applicable. The response factor method was developed to handle both periodic and non periodic situations, and perhaps this is the main reason why it is more applied in the field of energy calculation of buildings and is suggested by ASHRAE. The method is developed based on some previous work by Stephenson and Mitalas (1967 a,b)

The main feature of the method is based upon the use of of the "time series" and "response function".

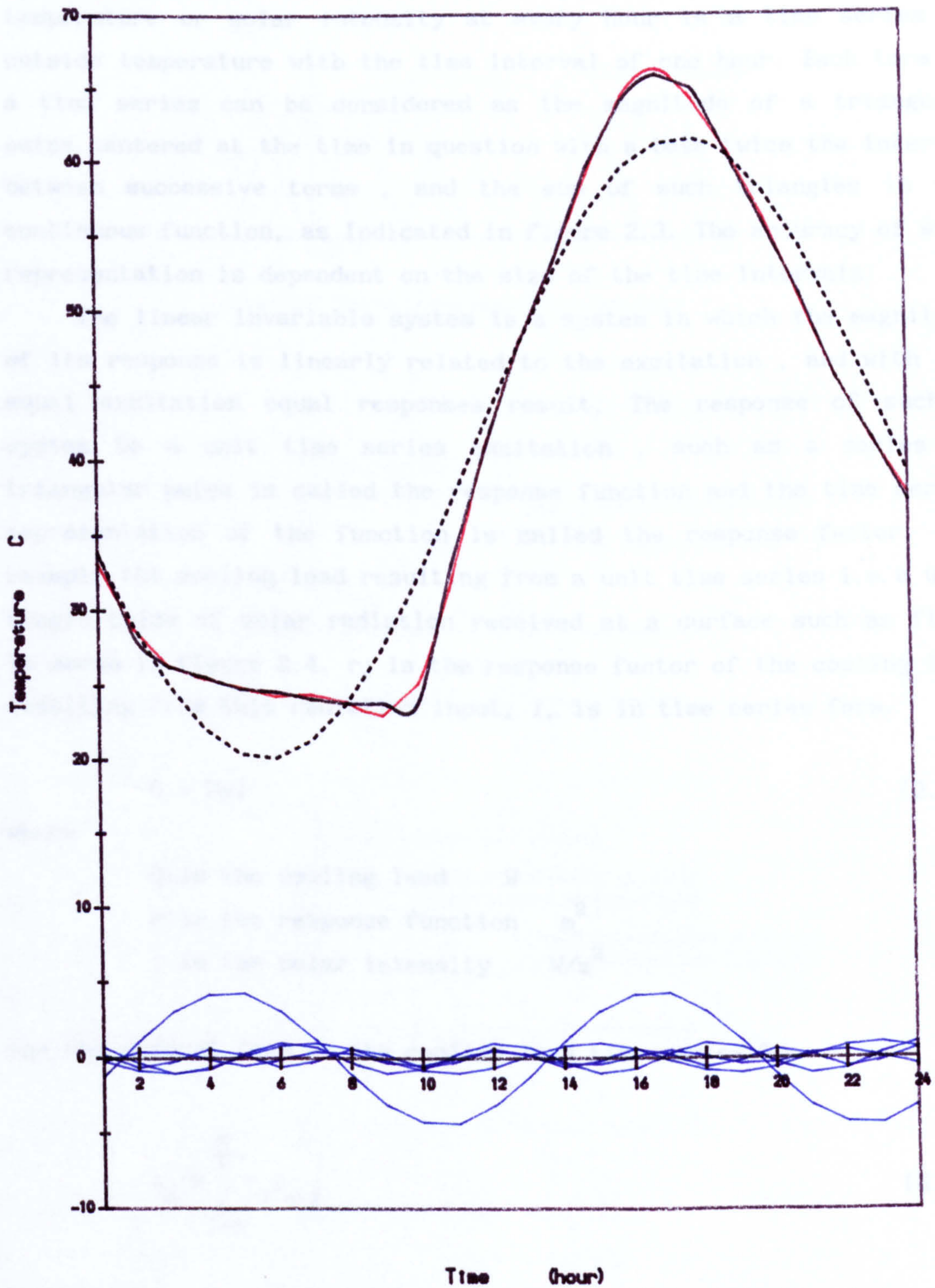


Figure 2.2 : Example of a solar temperature cycle similar to hot climate analyzed into first six harmonics

Time series are defined as an array of number of quantities representing the value of a function at successive equal interval of time. For example a series of numbers representing the air temperature or solar intensity at every hour is a time series of outside temperature with the time interval of one hour. Each term in a time series can be considered as the magnitude of a triangular pulse centered at the time in question with a base twice the interval between successive terms , and the sum of such triangles is the continuous function, as indicated in figure 2.3. The accuracy of such representation is dependent on the size of the time intervals.

The linear invariable system is a system in which the magnitude of its response is linearly related to the excitation , and with the equal excitation equal responses result. The response of such a system to a unit time series excitation , such as a series of triangular pules is called the response function and the time series representation of the function is called the response factor. For example the cooling load resulting from a unit time series i.e. a unit single pulse of solar radiation received at a surface such as floor is shown in figure 2.4.  $r_j$  is the response factor of the cooling load resulting from this radiation input,  $I$ , is in time series form.

$$Q = R \times I \quad (2.21)$$

where

$$\begin{aligned} Q & \text{ is the cooling load} & W \\ R & \text{ is the response function} & m^2 \\ I & \text{ is the solar intensity} & W/m^2 \end{aligned}$$

and the general form of the cooling load time series is:

$$q_n = \sum_{j=0}^{\infty} r_j i_{n-j} \quad (2.22)$$

This idea is used in the development of response factor method for calculating transient heat flow.

If two surfaces of a wall are assigned A and B the heat flux  $Q$  can be expressed in terms of surface temperature and response factors by: (see figure 2.5)

$$Q_A = T_A \cdot X - T_B \cdot Y \quad (2.23)$$

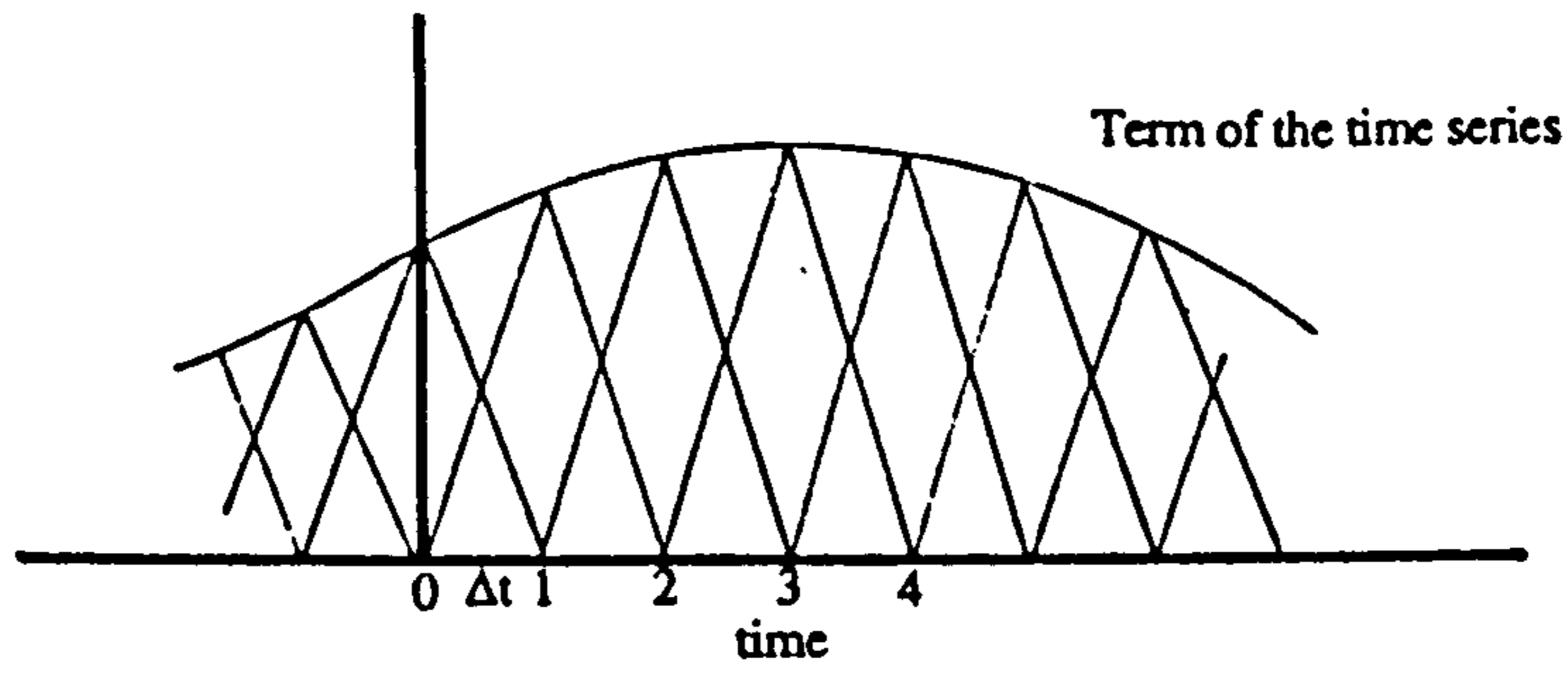


Figure 2.3: Time series representation of a function.

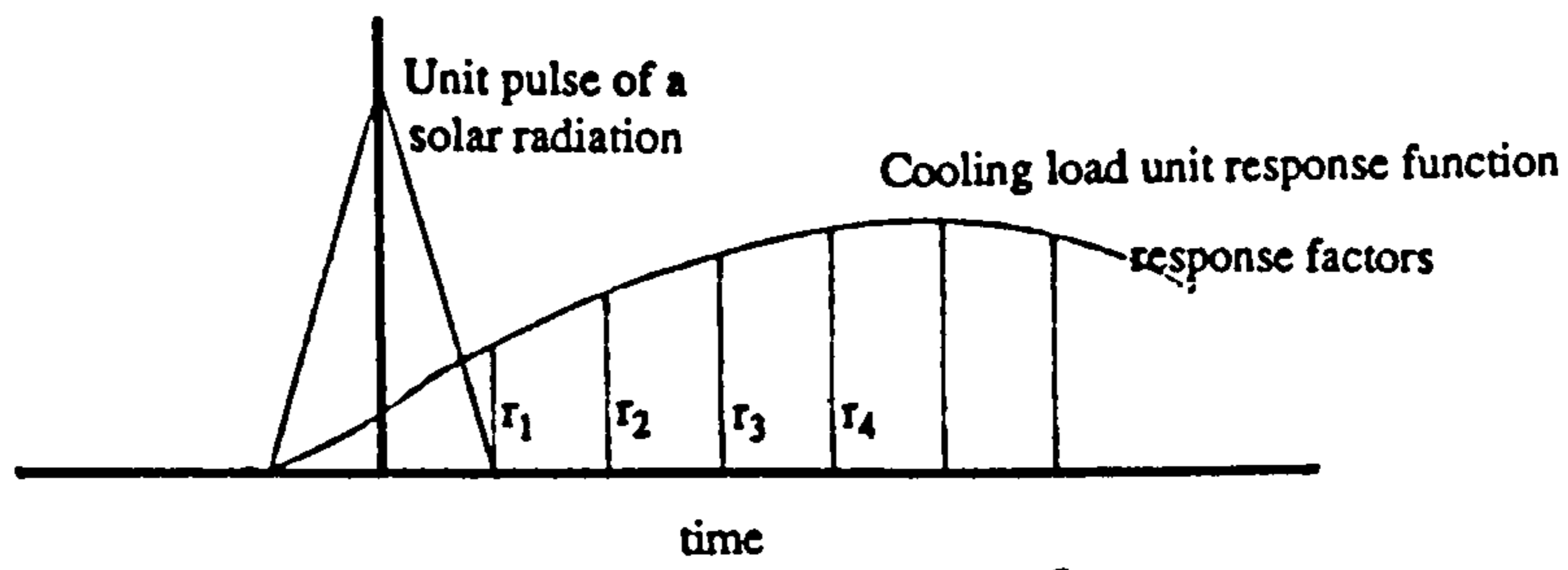


Figure 2.4: A unit excitation and unit response function.

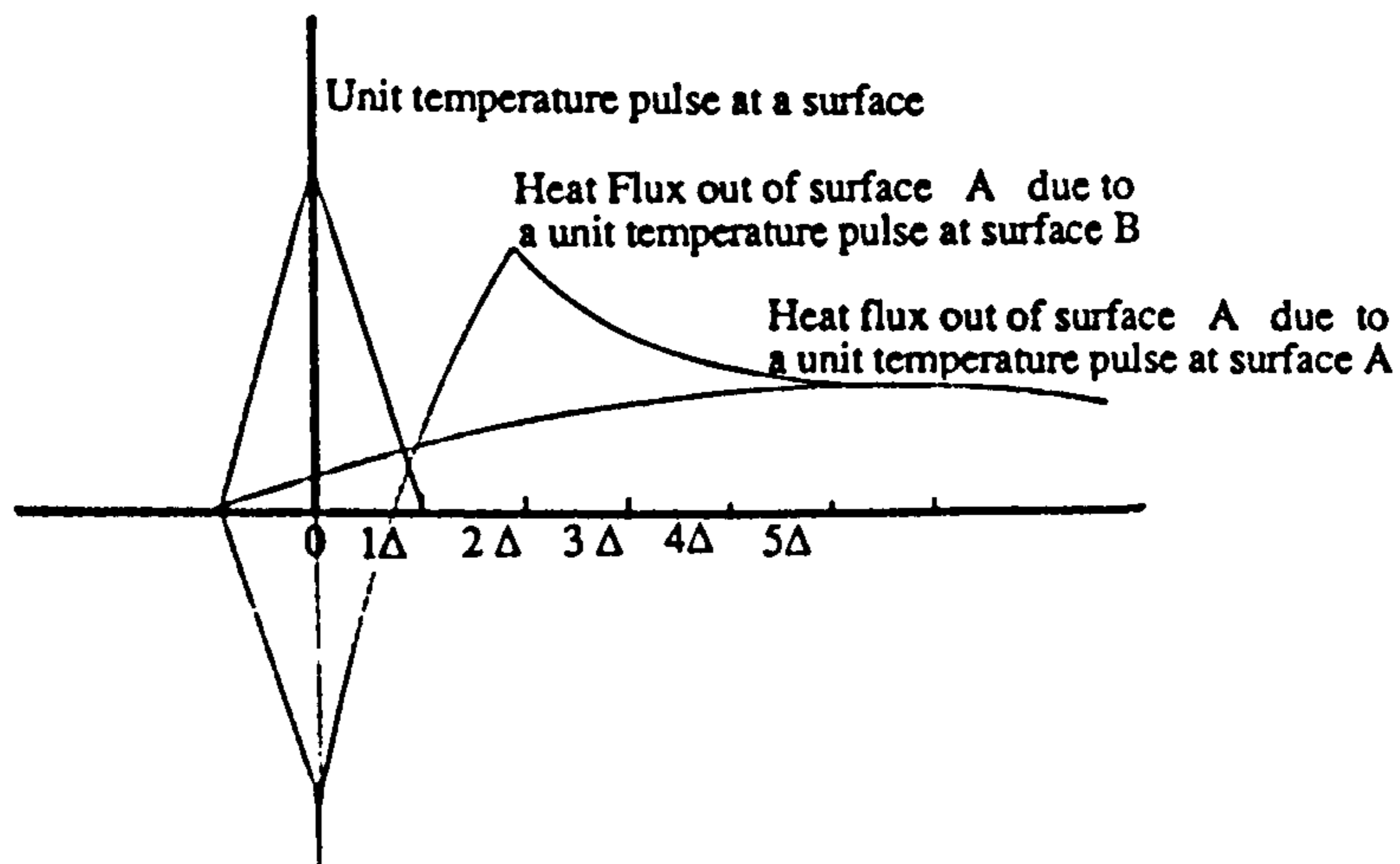


Figure 2.5: Heat flux at surface A due to Unit temperature pulse at surface A and B. (Stephenson and Mitalas 1967)



where

$Q_A$  and  $Q_B$  are the time series of heat flow into surface A and out of surface B

$T_A$  and  $T_B$  are the time series for temperature at surface A and B

X and Y are the time series for the heat flux at surface A and B respectively, due to a unit time-series of temperature at surface A ( $T_A=1,0,0,\dots$ ,  $T_B=0,0,\dots$ )

Y and Z are the time series for the flux at surface A and B respectively, due to a unit time-series of temperature at surface B ( $T_B=1,0,0,\dots$ ,  $T_A=0,0,\dots$ )

The conduction heat flux at wall surfaces in the form of a time series, at some time, t is the product of the surface temperature time series and the appropriate response factors:

$$Q_t = - \sum_{p=0}^{\infty} T_{i,(t-p)} \cdot X_p + \sum_{p=0}^{\infty} T_{j,(t-p)} \cdot Y_p \quad (2.24)$$

where the subscript j indicates the other surface of the wall. The number of terms involved for the calculation of heat flux through the slabs is a function of the slab's structure. Heavy structures require larger values for response factors and past history surface temperature. The number of terms seldom exceeds 20 for most conventional building structures as the response factors tend to zero. (KUSUDA 1976).

The procedure for calculating the response factors for homogeneous slabs and multilayer structures are given in Appendix B

### 2.4.3 The Finite Difference Method

Boundary conditions of thermal systems are not always simple. There are cases when transient heat conduction within multilayer slabs are non linear, or thermal properties are considered to be temperature dependant and consequently time dependant.

The finite difference method employs the numerical approximation of the first and second order derivative of the heat conductance equation. If  $(T_{x,t+dt} - T_{x,t})$  is the temperature gradient at one interface x, at the time interval t, between time t and t+dt, as a

consequence of the temperature variation at the interfaces  $x+dx$ ,  $x$ ,  $x-dx$ , the second derivative of the partial differential equation of heat conductance, equation 2.11 could be replaced by:

$$\frac{\partial^2 T}{\partial x^2} = \frac{T_{x+dx,t} - 2T_{x,t} + T_{x-dx,t}}{dx^2} \quad (2.25)$$

and similarly the time derivative approximated by:

$$\frac{\partial T}{\partial t} = \frac{T_{x,t+dt} - T_{x,t}}{dt} \quad (2.26)$$

Thus the overall equation could be written as:

$$\frac{T_{x+dx,t} - 2T_{x,t} + T_{x-dx,t}}{dx^2} = \frac{1}{\alpha} \frac{T_{x,t+dt} - T_{x,t}}{dt} \quad (2.27)$$

and may be solved to give the temperature at time  $t+dt$  and interface  $x$  provided all temperature at the time  $t$  are known.

$$T_{x,t+dt} = \frac{\lambda}{\rho c_p} \frac{dt}{dx^2} T_{x-dx,t} + \left[ 1 - \frac{2\lambda}{\rho c_p} \frac{dt}{dx^2} \right] T_{x,t} + \frac{\lambda}{\rho c_p} \frac{dt}{dx^2} T_{x+dx,t} + Q_t \frac{\lambda dt}{\rho c_p} \quad (2.28)$$

The above solution is the explicit method of solution. The coefficient

$$\frac{\lambda}{\rho c_p} \frac{dt}{dx^2} \quad (2.29)$$

is the Fourier number. To avoid negative coefficients in the above equation, in order to get a stable numerical solution, the values for  $dt$  and  $dx$  should be chosen to result in the coefficients to be greater than zero, so that

$$1 - \frac{2\lambda}{\rho c_p} \frac{dt}{dx^2} \geq 0 \quad (2.30)$$

and

$$\frac{2\lambda}{\rho c_p} \frac{dt}{dx^2} \geq 1/2 \quad (2.31)$$

Using the explicit numerical technique to solve one dimensional heat conduction problems through any slab, and writing the heat balance equation for any node (i.e. at different surfaces and interface points and air point) at time  $t+dt$ , a set of independent equation will be obtained equal to the number of unknown temperatures which, by introducing initial values for  $dx$ , and  $dt$ , permits the equations to be solved for consecutive time intervals.

If equation 2.25 be rewritten for time interval  $t+dt$  (instead of  $t$ ), we obtain

$$T_{x+dx,t+dt} - 2T_{x,t+dt} + T_{x-dx,t+dt} = \frac{1}{\alpha} \frac{T_{x,t+dt} - T_{x,t}}{dt} \quad (2.32)$$

Rearrangement of the above equation for  $T_{x,t+dt}$  gives

$$\left[1 + \frac{2\lambda dt}{\rho c_p dx^2}\right] T_{x,t+dt} = T_{x,t} + \frac{\lambda dt}{\rho c_p dx^2} T_{x+dx,t+dt} + \frac{\lambda dt}{\rho c_p dx^2} T_{x-dx,t+dt} \quad (2.33)$$

This method is the implicit solution and it is unconditionally stable for all distances and time increments, although the accuracy depends on their values.

Writing a heat balance equation for each node in a thermal system, will result in a set of equations each simultaneously dependent on the temperature of other nodes at the same time. These could be solved simultaneously to give the temperatures at each interface and time interval which is essentially a computer task. A weighted average of equations 2.33 and 2.26 may be used to establish a generalized formula, which is discussed in detail for example by MUNCEY (1979), and CLARKE (1985)

## CHAPTER THREE

### *LITERATURE REVIEW OF THERMAL MODELING TECHNIQUES*

#### 3.1 Introduction

Buildings are subjected to different forms of energy transfer. Heat is conducted to the inside of external walls either by the temperature difference between the internal and the external environment or by the absorbed insolation. Heat will be exchanged between room surfaces by long wave radiation and between the room air and surfaces by convection. Solar radiation may also enter the room by striking the glass, where some is reflected and absorbed and most entering the room as short wave radiation, which may raise the internal surface temperatures. Ventilation replaces inside air with outside air which eventually exchanges energy with internal surfaces by convection.

Full evaluation of this complicated system of heat exchange among building elements requires a set of complicated heat transfer equations. If each surface of a room be assigned a mean temperature, 27 flow paths of heat exchange by different mechanisms result. Consideration of the unsteady behaviour will add to this complication.

#### 3.2 Thermal models in buildings

Various methods exist for the evaluation of building response to energy input. They vary from simple to complicated. The proper model is the multi-exchange model, in which any element in a space, is shown as a single node, and heat exchanges among nodes are expressed by separate equations. This level of complication is not always appropriate. With some approximations a model could be greatly simplified. This could be achieved by introducing an index point in a room at which radiation exchange could take place, (DAVIES 1983); or the index point could be used for both radiation and convection exchange, like in the environmental temperature model. Some models divide different element of a thermal network and lump

them into smaller nodes. (MATHEWS 1986, CRABB et al. 1987)

A short review of some of the existing models relevant to this study follows. Presenting a thorough review of all of them is beyond the scope of this study. Some are reviewed by Hanna(1974). Special attention is paid to the development of the environmental temperature model used in the Admittance Procedure of the CIBSE Guide.

### 3.3 The traditional method

Air temperature is the basis of the traditional heat loss calculations. Three quantities are taken into account, Heat loss between air and surfaces:

$$Q_{cv} = Ah_c (T_{ai} - T_w) \quad (3.1)$$

the radiative heat exchange

$$Q_{rd} = AEh_r (T_{ai} - T_{ao}) \quad (3.2)$$

which means the remainder of room surfaces are at the same temperature as the air. The ventilation loss :

$$Q_{cv} = c_p \rho Vol (T_{ai} - T_{ao}) \quad (3.3)$$

and the fabric loss:

$$Q_f = AU(T_{ai} - T_{ao}) \quad (3.4)$$

where

$$U = (R_{si} + R_1 + R_2 + \dots + R_{so})$$

$R_{si}$  = Inside surface resistance

$R_{so}$  = Outside surface resistance

$R_j$  = Thermal resistance of the slabs

According to the above procedure, the energy input to the room with all be at the air point. This could only be true if the energy source is convective and not radiative, as solar radiation. Furthermore it is an oversimplification to consider the surface temperatures the same as air temperature. Evaluation of comfort also requires consideration of both radiant and air temperatures. The traditional method does not consider the radiant temperature. Inside air temperature is a poor index for the heat loss calculation. Loudon

(1970) has shown errors of up to 40% percent, if heat losses are calculated in terms of air temperature only.

### 3.4 Environmental temperature model

The deficiency of the traditional method might be avoided by using a model with a central index temperature. This central index temperature is a weighted value between air and mean radiant temperature, known as the environmental temperature, leading to a model developed by Danter and other workers at the U.K. Building Research Station. Danter (1974) has shown that with such an assumption the errors will decrease to about 5%. The model is the basis of the Admittance Method, which is the accepted standard procedure for temperature prediction, heating, cooling requirement and energy calculation in the U.K. It was first published in the IHVE (now CIBSE) Guide (1970). The method is based on two assumptions: the representation of heat exchange in a room via a central index temperature, the environmental temperature; and the solution to the problem of unsteady heat conductance/capacitance of the building structure, by using the harmonic method with the dynamic thermal factors from the first harmonic only. (see chapter two) As suggested by the Guide(CIBSE Chapter 5) it is most suitable for calculations where the temperature swings and/or the energy during the day are changing steadily. It is less suitable for step inputs, especially if transient temperature calculations are needed at the time of change. (CIBSE A5 1986)

#### 3.4.1 The basis of the model

The general application of the method was first published by Loudon (1968) and was used to investigate overheating problems in buildings during the summer. (LOUDON 1970)

The fundamental theory of the model was given by Danter.(1974) If a room is considered with all internal walls at the same temperature,  $T_{ri}$ , the rate of heat flow between the inside surface of the external wall and its enclosing space is

$$Q_s = A E h_r (T_{ri}' - T_{si}) + A h_{sc} (T_{ai} - T_{si}) \quad (3.5)$$

Using relation 3.5 the surface heat transfer  $Q_s$  is:

$$Q_s = A_s \left[ E h_r \left( \frac{(T_{ri} - T_{si}) \sum(A)}{\sum(A) - A_s} \right) + (T_{ai} - T_{si}) h_c \right] \quad (3.6)$$

or

$$Q_s / A_s = h'_r (T_{ri} - T_{si}) + h_c (T_{ai} - T_{si}) \quad (3.7)$$

where

$$T'_{ri} - T_{si} = (T_{ri} - T_{si}) \frac{\sum(A)}{\sum(A) - A_s} \quad K \quad (3.8)$$

$$h'_r = E h_r \frac{\sum(A)}{\sum(A) - A_s} \quad W/m^2K \quad (3.9)$$

$E h_r$  = Coefficient for heat transfer by radiation  $W/m^2K$

$T_{ri}$  = Mean surface temperature of room  $^{\circ}C$

$A_s$  = Area of the external wall  $m^2$

$\sum(A)$  = Total area of the room  $m^2$

The factor  $h'_r$  depends on the ratio  $\frac{\sum(A)}{\sum(A) - A_s}$ , which depends on the shape of the room. For a room of approximate ratio 1 : 4 : 4 the values of the ratio are 1.09 and 1.50. For a cubical room (1 : 1 : 1) the ratio is 1.2. This is a reasonable approximation for many room configurations, and will be discussed below.

To obtain a conventional form of equation 3.5 with regard to an index temperature

$$Q/A_s = (h'_r + h_c) (T_x - T_s) \quad (3.10)$$

where

$$T_x = \frac{h'_r T_{ri} + h_c T_{ai}}{h_c + h'_r} \quad (3.11)$$

The value of  $h'_r$  differs in a range depending on the type of surface and heat flux. With typical values for  $E=0.9$  and  $h_r=5.7$  a mean value  $h'_r=3.0$  and the shape configuration ratio as  $h_r=6/5$ , will result

$$T_x = \frac{6/5(0.9 \times 5.7) T_{ri} + 3 T_{ai}}{3 + 6/5(0.9 \times 5.7)} \quad (3.12)$$

$$\text{or nearly} = 2/3 T_{ri} + 1/3 T_{ai}$$

This is a weighted mean temperature between air and mean radiant temperature in a room, biased towards the latter, as the heat

transfer coefficient for radiation is almost twice that for convection under conditions normal in a room. It is also a central point for energy input. The ventilation conductance, which is actually an input to the air or the solar radiation which is a radiant input to the surfaces, now could be input to the environmental point after appropriate scaling. The heat interchange in a room via the central point as discussed by Loudon is given in figure 3.1. (LOUDON 1970)

### 3.4.2 Conductances between the elements of the model

The detailed basis and background of the model is discussed by Davies (1978) in a later paper. Different conductances based on the  $T_{ei}$  are derived and discussed. (figure 3.2) The fabric heat loss is given by

$$Q_f = \left[ \left\{ A(h_c + 6/5Eh_r)^{-1} + (A.U_1)^{-1} \right\}^{-1} (T_{ei} - T_{ao}) \right] \quad (3.13)$$

where

$$U_1 = \left( \frac{d_1}{\lambda_1} + \frac{d_2}{\lambda_2} + \dots + \frac{1}{h_o} \right)$$

$h_o$  is the outer surface transmittance  $W/m^2K$

and the heat loss by ventilation through the environmental point is given by:

$$Q_v = C_v (T_{ei} - T_{ao}) \quad (3.14)$$

where

$C_v$  is the ventilation conductance

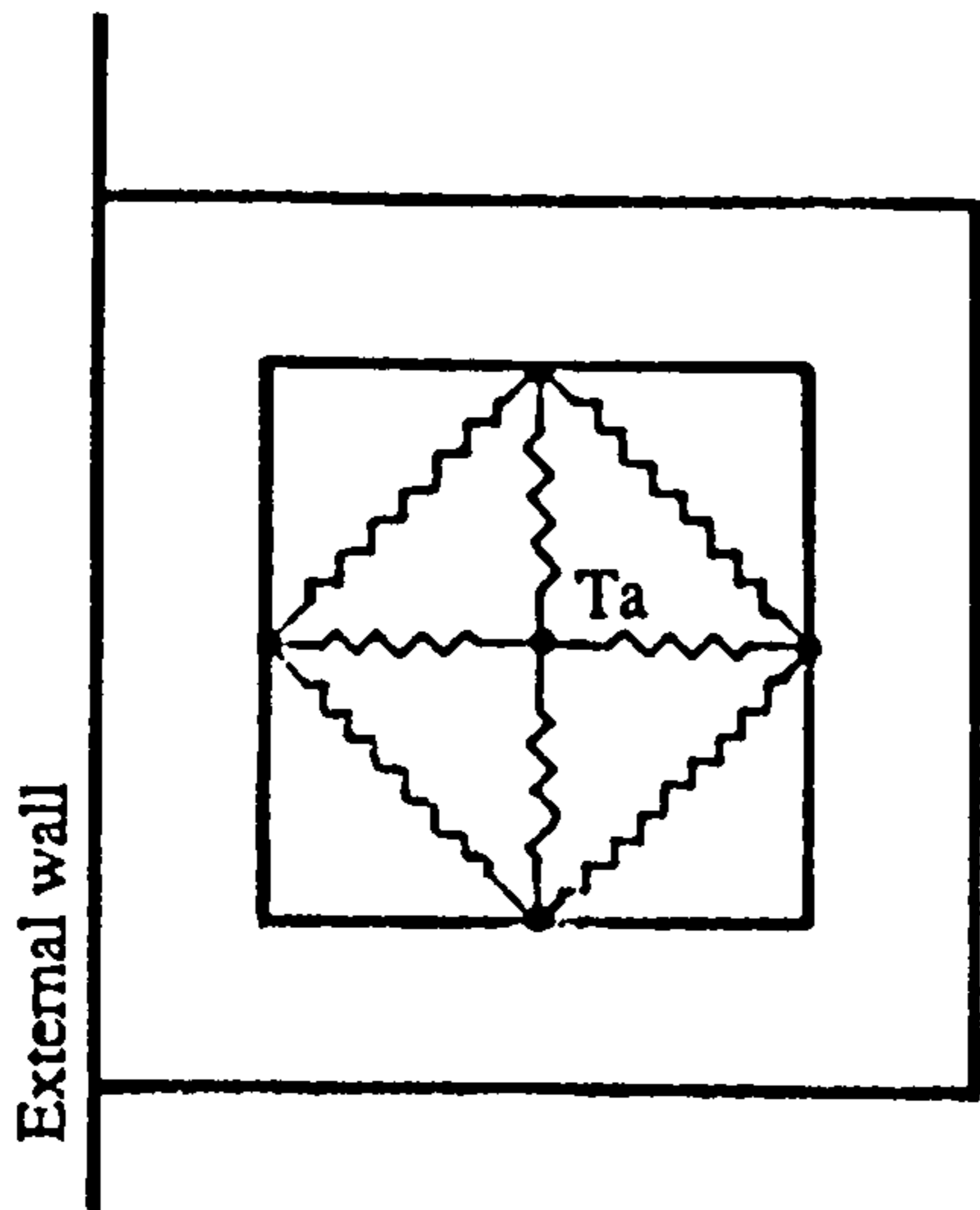
$$= \left[ \left\{ 6A(h_c + 6/5Eh_r) \frac{h_c}{6/5Eh_r} \right\}^{-1} + (c_p \cdot \rho \cdot V)^{-1} \right]^{-1}$$

and the conductance between the environmental point and the air is given by:

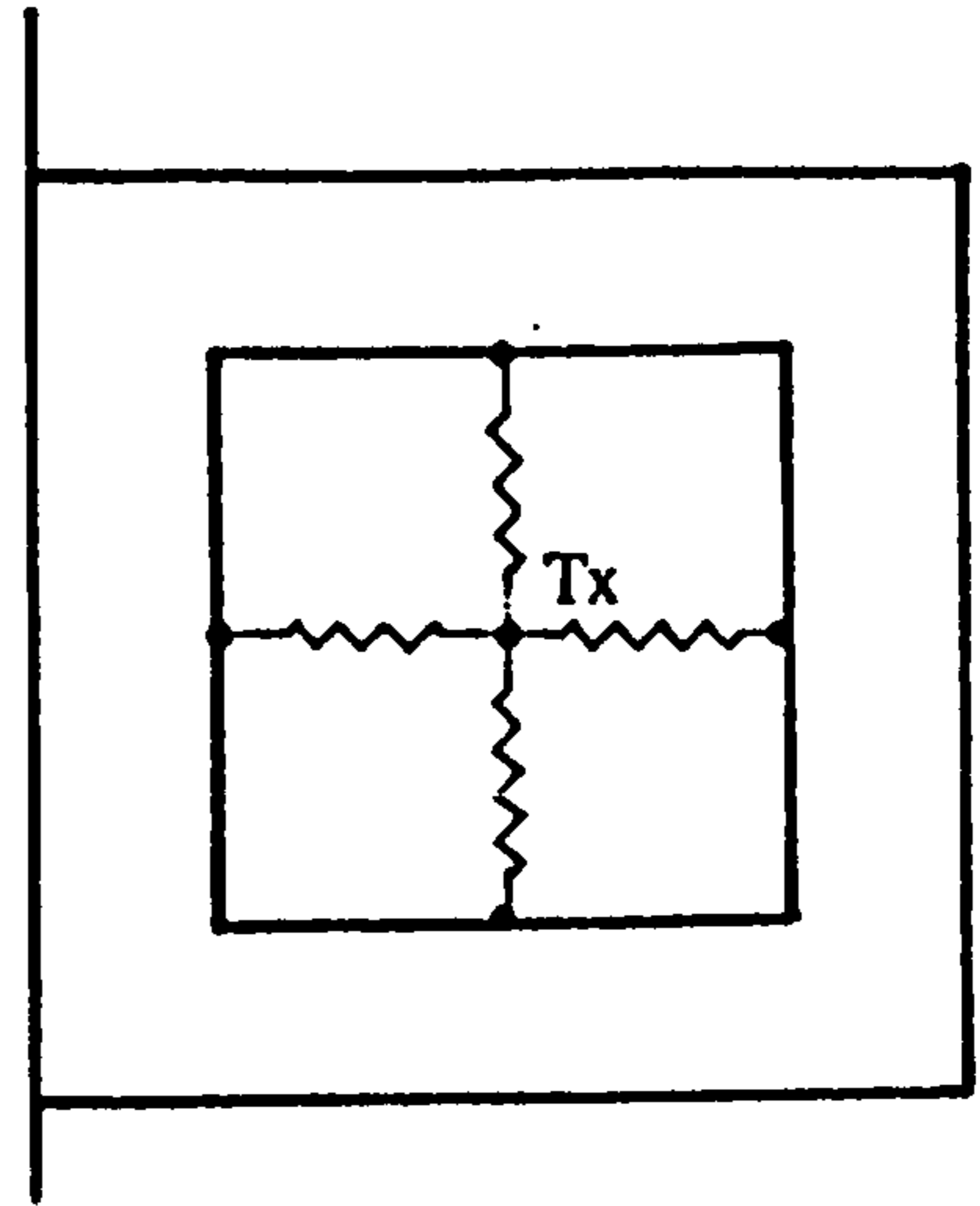
$$C_a = 6A(h_c + 6/5Eh_r) \frac{h_c}{6/5Eh_r} \quad (3.15)$$

The above conductances are considered to be in a cubic room. As there may be considerable variations in the values of  $h_c$  and  $Eh_r$ , accuracy is not sacrificed by ignoring the 6/5 coefficient in the eq.

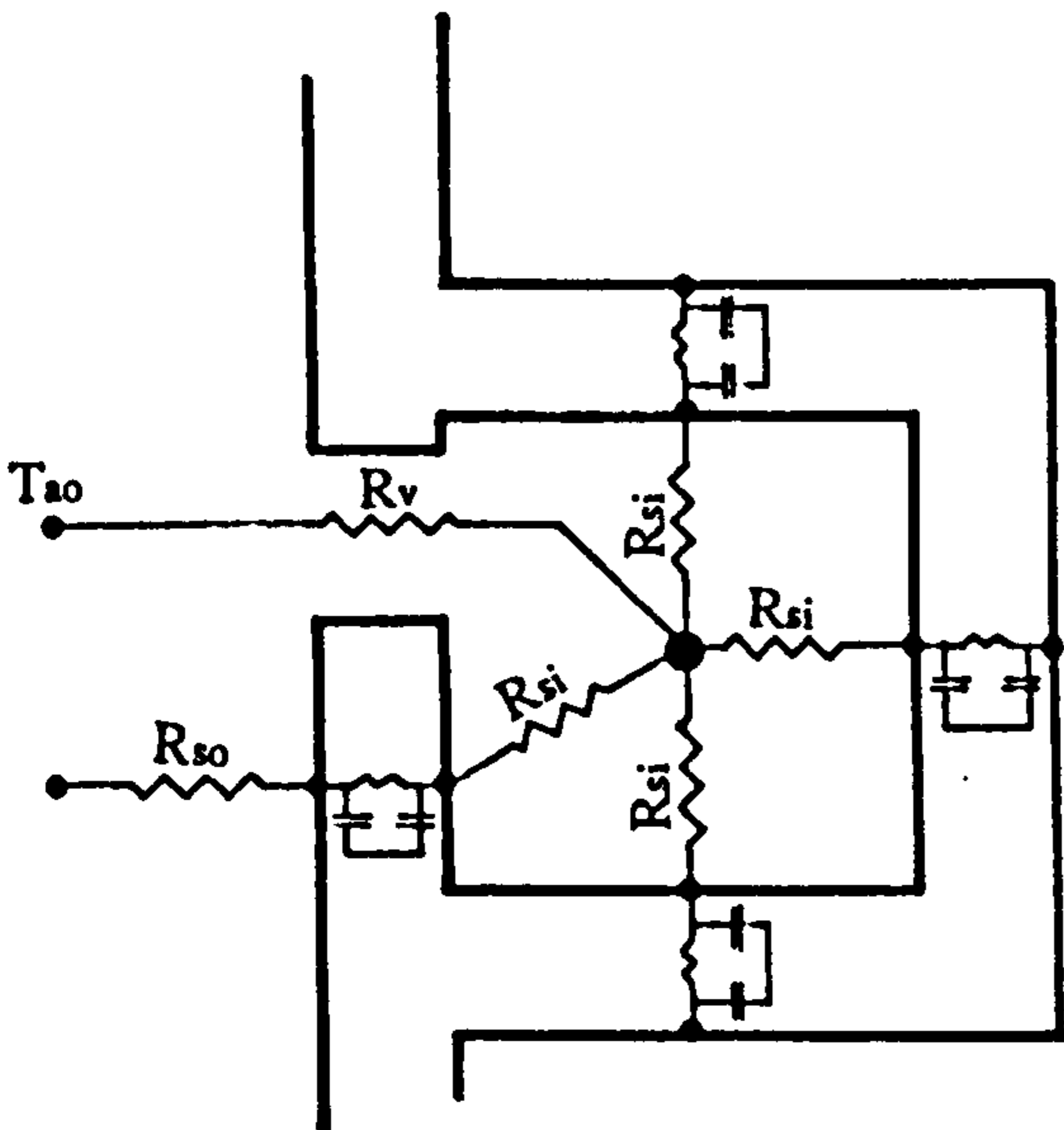




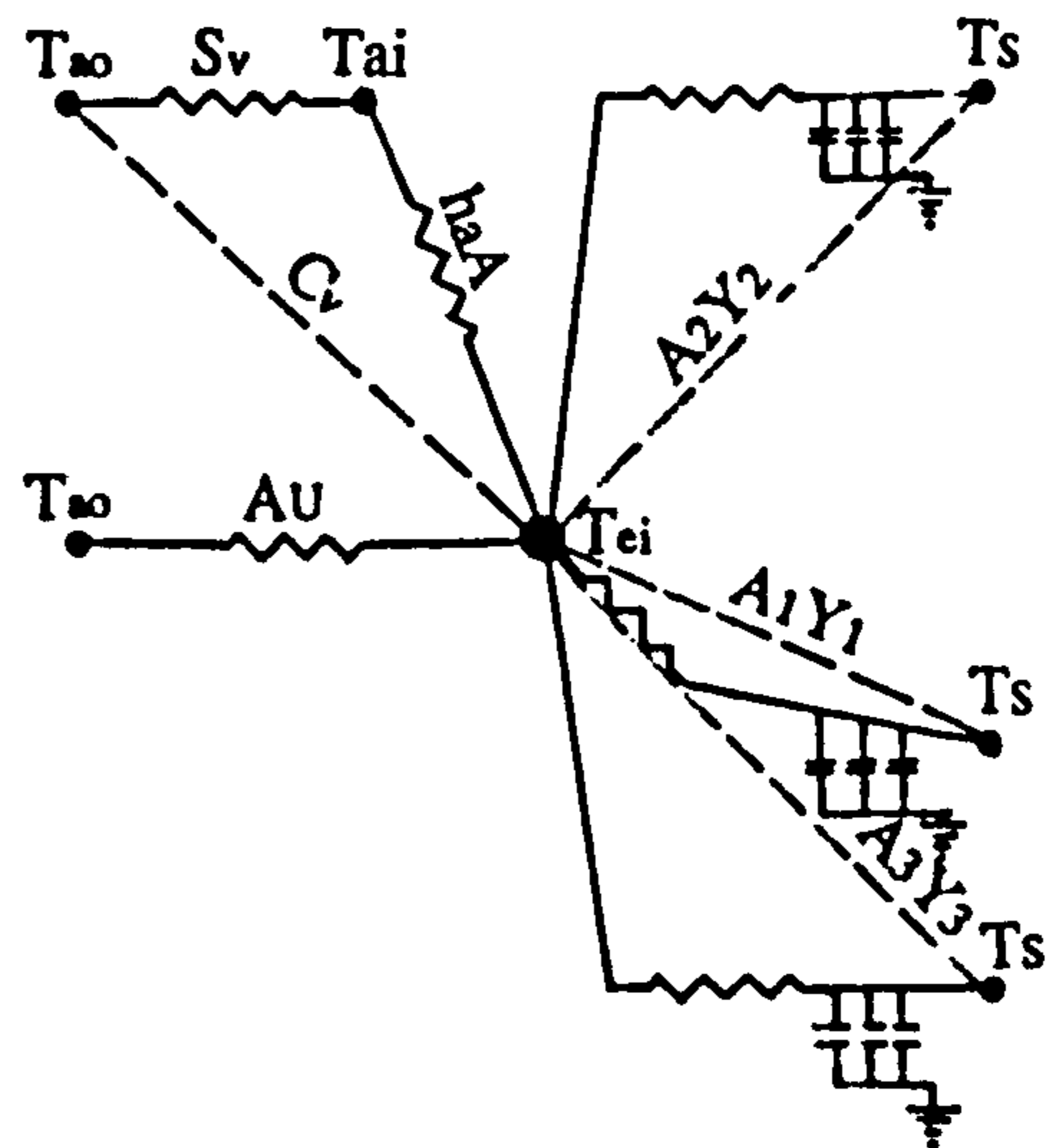
a: Actual interchanges in a room



b: Equivalent interchanges with a central index temperature



c: Thermal network of a room with central point .



d: equivalent thermal network index mode with resistances and capacitances in a central index model.

Figure 3.1: Heat interchanges within a room. (Loudon 1970)

3.12 to 3.15 . The numerical values of the above conductances are given by:

$$R_{si} = (h_c + Eh_r)^{-1} \quad (3.16)$$

$$C_v = \left( \frac{1}{4.8 \sum(A)} + \frac{1}{c_p \rho V} \right)^{-1} \quad (3.17)$$

$$C_a = \sum(A) (h_c + Eh_r) \frac{h_c}{Eh_r} \quad (3.18)$$

$$= \sum(A) \cdot 4.8$$

It is also shown that the energy input to the room, either to the air or at surfaces, should be scaled before being input at the environmental point. One of the applications of the scaling procedure is for solar gain in the room. From the solar radiation which falls on the glazing, some is transmitted through the glass and absorbed by the internal surfaces ( $\alpha$ ) and a little is absorbed by the glass ( $\tau$ ) and some is reflected by the glass ( $\beta$ ). If the scaling procedure is applied to put this energy gain to the environmental point, the total solar gain at  $T_{ei}$  is given by:

$$\sum \bar{Q}_e = \frac{h_c + 6/5Eh_r}{U_1 + h_c (6/5Eh_r)} \alpha \bar{Q}_{inc} + \tau \bar{Q}_{inc} \quad (3.19)$$

$$\bar{Q}_e = \frac{h_c + 6/5Eh_r}{U_1 + h_c (6/5Eh_r)} \alpha \bar{Q}_{inc} + \frac{h_c + 6/5Eh_r}{Y_s + h_c (6/5Eh_r)} \tau \bar{Q}_{inc} \quad (3.20)$$

or

$$\sum \bar{Q}_e = S \bar{Q}_{inc} \quad (3.21)$$

$$\sum Q_e = S_a \bar{Q}_{inc} \quad (3.22)$$

where

$Q_{inc}$  is the incident solar energy  $W/m^2$

$Y_s$  is the total admittance of the structures  $\left( \frac{\sum AY}{\sum A} \right) m^2/W$

$U_1$  is the transmittance of the glass  $m^2 K/W$

Equations 3.21 and 3.22 give the definitions of mean and alternating solar gain factors  $S$  and  $S_a$ . The solar gain factors depend upon the absorbance and transmittance of the glass, which depend on the position of the sun. The mean solar gain factor is not affected by the type of the room construction, but the alternating solar gain factor depends on the room's construction. (e.g. heavy or

lightweight ). The mean numerical values given in the CIBSE Guide are correct for the U.K. and should be corrected according to the altitude and climate for use otherwise.

Cornell (1976) has demonstrated the use of environmental temperature to analyze the variations of comfort in a space. The temperature of the internal surface of the external wall is given by: (figure 3.2)

$$T_{si} = T_{ei} - \frac{Q}{A(6/5Eh_r + h_c)} \quad (3.23)$$

The above equation could be used for both opaque and window surfaces separately. Local comfort could be evaluated by using the mean radiant temperature of internal walls, external walls and the air temperature. To evaluate comfort at any point the effect of the radiant temperature of each surface is considered according to the view factor between the point and the surface.

### 3.4.3 Development and the application of the model

The environmental temperature described above, was considered to be an index temperature in a cubic room, and the numerical values given by the CRIBS Guide are also based on this assumption. The factors of 6/5 and 6 in equation 3.12 to 3.23 have a general form of  $h_r'$  and  $\sum A$  where

$$h_r' = \frac{\sum(A)}{\sum(A) - A_s} \quad (3.24)$$

Baxter (1975) has compared the environmental temperature model with  $h_r'$  for a cubic room as 6/5, and a weighted correction factor for any type of building shape using a detailed mathematical model, which considers convection and radiative heat transfer separately for each surface of the room, in the steady state. He concluded that the index temperature must be an area weighted temperature. Errors of up to 20% are reported for some kind of energy input and room shapes. This is also reported by Davies (1986) as one of the defects in the standard environmental temperature model.

The environmental temperature also depends on the convective heat transfer coefficient,  $h_c$ , but the error from the variations of  $h_c$ , is shown normally to be very small. It is also difficult to deal with this problem in the model, because of the lack of knowledge of

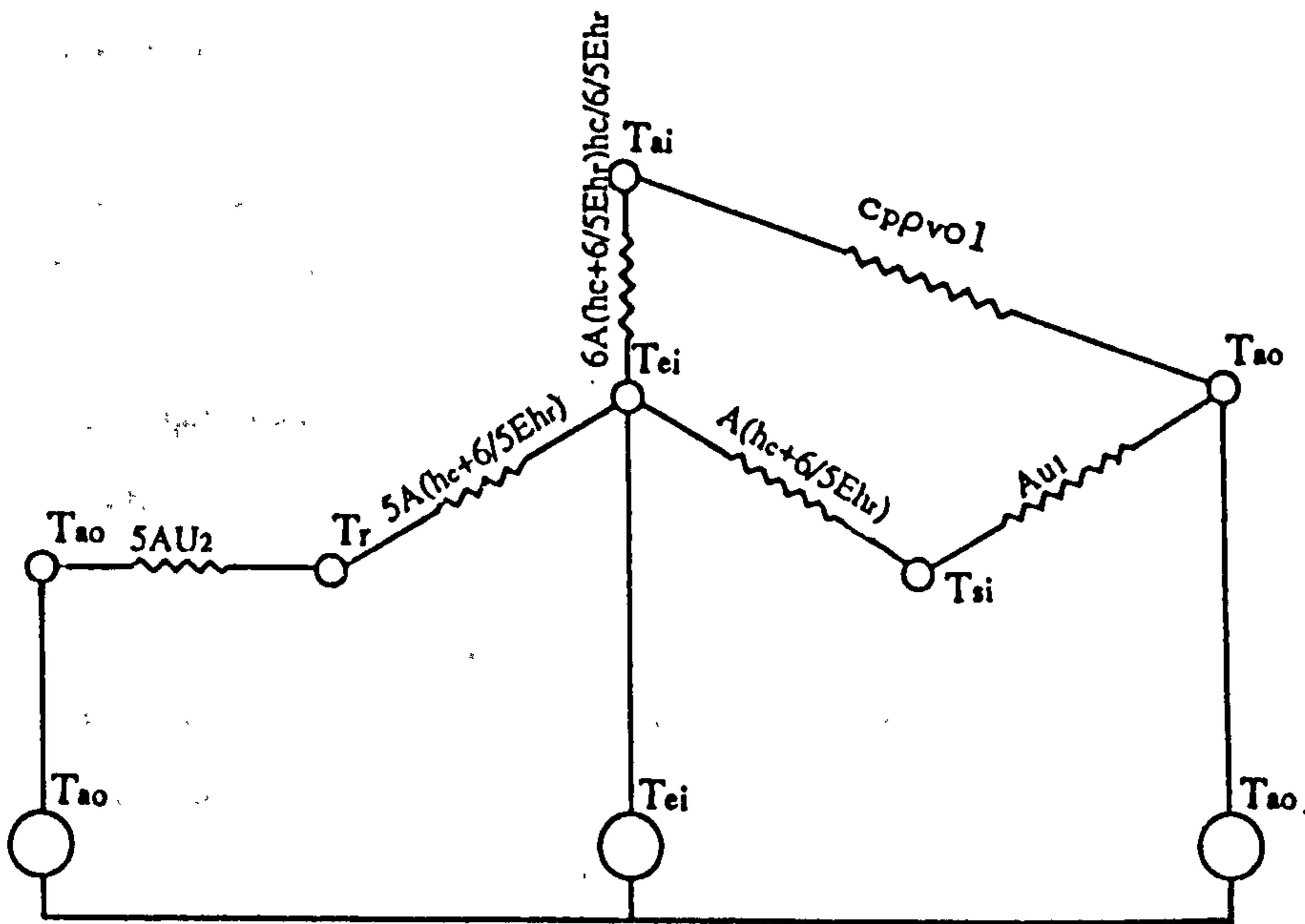
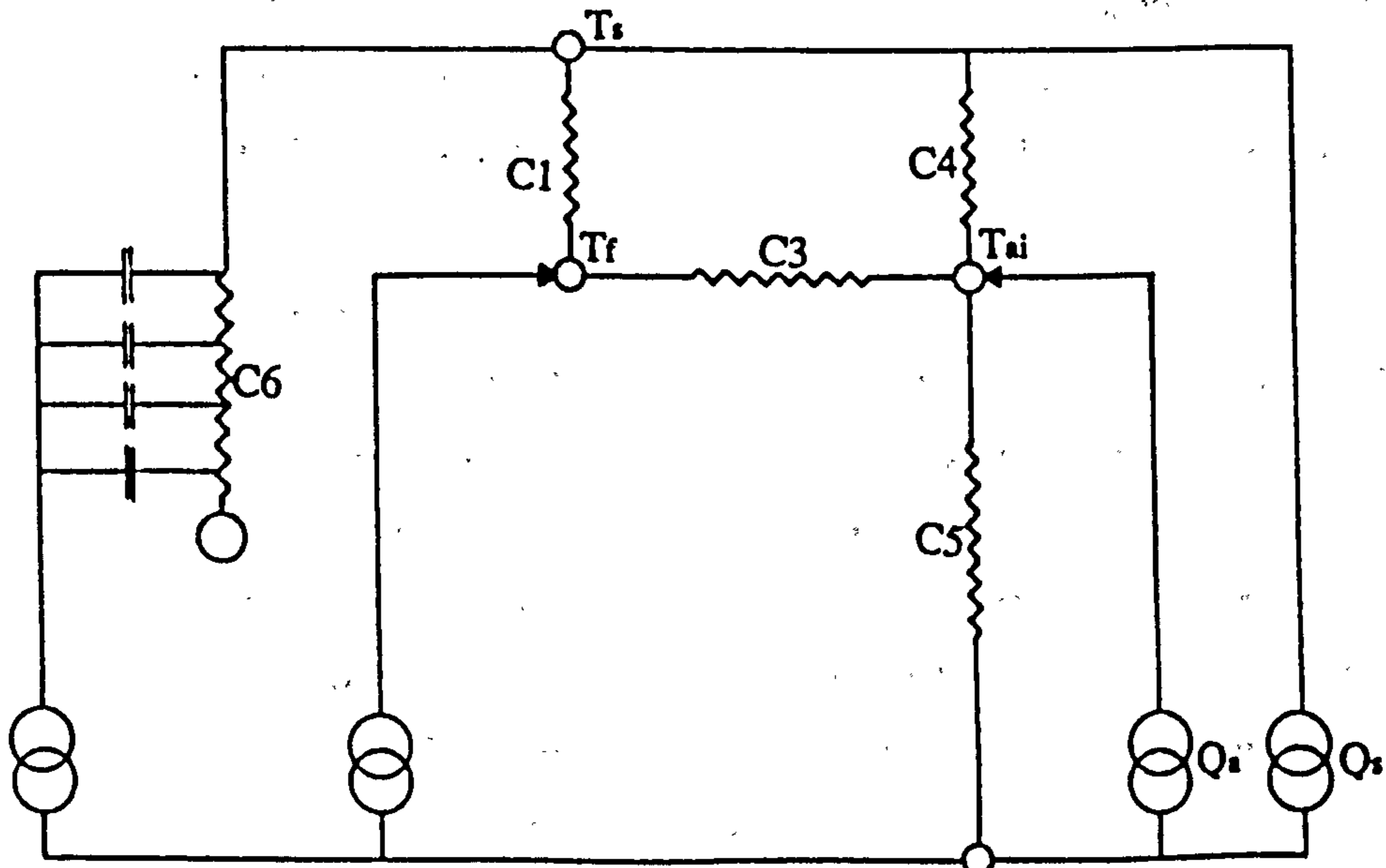


Figure 3.2: Presentation of heat exchange in the environmental temperature model with heat loss through five internal walls and the conductance between elements.  
(Davies 1978)



C1= Radiative conductance  
C2= Conductive conductance  
C3= Convective conductance  
C4= Convective conductance  
C5= Ventilation conductance

T<sub>s</sub>= Surface of internal walls  
T<sub>r</sub>= Internal surface of external walls  
T<sub>ai</sub>= Inside air  
T<sub>ao</sub>= Outside air  
C6= Storage

Figure 3.3: The 6 element model of a thermal enclosure including storage  
(Davies 1974)

individual surface temperatures.

As the index temperature for assessment of human comfort is approximately the average of the air and of the mean radiant temperatures, the environmental temperature has a slight bias. Humphrey (1974) has shown the bias is proportional to the difference between the air temperature and the mean radiant temperature and could be removed by appropriate adjustments suggested in table form.

#### 3.4.4 Admittance procedure

When the environmental temperature is used to calculate the radiation and convection interchange in a space, the unsteady response of the internal environmental temperature, to a steady cyclic energy input, can be determined by the factors obtained from the harmonic solution to conductive/storage of the structure. (Chapter two 2.4.1) This will make the energy input into a constant term with a number of pure sine wave harmonics, with, in general, decreasing amplitude at increasing frequency. The overall result will be obtained by the sum of the response to each harmonic. The Admittance Method only uses the steady state term and the first harmonic for the swing about the mean, but applied to the actual energy input. The technique of mean and swing was developed by Danter (1960), to calculate the heat flux across slabs. He has shown that the approximation of mean and swing will in commonly used materials result in negligible errors in heat flux calculation, compared with the exact analysis with separate consideration of the harmonics.

#### 3.4.5 Basic form of the Procedure

The use of 24 hours frequency values of the 3 factors for a practical manual solution in the calculation of the internal environmental temperature in buildings was demonstrated by Milbank (1974). By comparison with the first six harmonics, he showed that the use of higher frequencies will not result in a greater accuracy, and a difference of 10% is reported in room air temperature swing resulting from solar radiation falling onto the floor of a room. In a similar comparison Sodha et al. (1986) have compared the results from the ordinary Admittance Method and the Fourier method. Good agreement is found even for the hourly total heat flux entering a room caused by solar radiation and outside air temperature changes.

The basic equations used in Admittance Method are (chapter 8 of CIBSE Guide 1987)

$$\bar{Q}_t = \sum(A.U)(\bar{T}_{ei} - \bar{T}_{eo}) + (\sum A U_g + C_v)(\bar{T}_{ei} - \bar{T}_{ao}) \quad (3.25)$$

$$\tilde{Q}_t = (\sum(A.Y) + C_v)\tilde{T}_{ei} \quad (3.26)$$

$$\frac{1}{\bar{C}_v} = \frac{1}{0.33NV_{o1}} + \frac{1}{4.8\sum(A)} \quad (3.27)$$

where

$$\begin{aligned} \bar{Q}_t &\text{ is the mean total heat gain} && W \\ &= \bar{Q}_c + \bar{Q}_s \end{aligned}$$

$$\begin{aligned} \tilde{Q}_t &\text{ is the swing in total heat gain} && W \\ &= \tilde{Q}_c + \tilde{Q}_s + \tilde{Q}_f + \tilde{Q}_a \end{aligned}$$

$$Q_c = \text{Casual heat gain} \quad W$$

$$Q_s = \text{Solar heat gain} \quad W$$

$$Q_f = \text{Swing in effective heat input due to structural gain}$$

$$Q_a = \text{Swing in effective heat input due to outside air}$$

### 3.4.6 Development of the Admittance Procedure

In this way the above solution is only applied with constant ventilation during the day and without plant operation. (or constant plant operation). In real situations, this is seldom practiced. Ventilation varies by opening windows or by intermittent use of ventilation plant, like what is practiced in hot climates. The extension of the model to intermittent plant operation and variable ventilation was first described by Harrington-Lynn (1974 a&b). The procedure uses the environmental point as the index temperature of the space and assumes that heat input occurs at this point. Waters (1981) removed this restriction to allow the "dry resultant temperature" which is the average of air and mean surface temperature, to be considered as the index temperature by appropriate adaptation. His method also enables the radiative and convective component of heat input to the air and environmental point to be treated separately. It further suggests a general relation to calculate the dry resultant temperature directly.

Danter (1983) in further work, suggests a general solution for intermittent plant operation and variable ventilation. The instantaneous heat balance equation is used to calculate the hourly air and environmental temperature, for hourly values of ventilation rate and plant operation. In the case of variable ventilation and in a free running building the environmental temperature is given by

$$T_{c,t} = T_{ao} + \frac{Q_{g,t}}{Y_t} + \frac{Y_s \sum^{24} (Q_{g,t}/Y_t)}{Y_t \sum^{24} (U_t/Y_t)} \quad (3.28)$$

where

$$Q_{g,t} = F_Y Q_{eg,t} - (F_Y - F_U) Q_{eg} + F_v Q_{am,t} + F_{v,t} c_{pp} V_t \quad W$$

$Q_{am,t}$  is the energy gain at air point from other sources W

$Q_{eg}$  is the energy gain at environmental point W

$V_t$  is the ventilation rate at time t  $m^3/s$

$$Y_t = F_Y \sum (AY) + F_{v,t} c_{pp} V_t \quad W/m^2K$$

$$U_t = F_U \sum (AU) + F_{v,t} c_{pp} V_t \quad W/m^2K$$

$$F_Y = \frac{h_{ac} \sum(A)}{h_{ac} \sum(A) + \sum(AU)}$$

$$F_U = \frac{h_{ec} \sum(A)}{h_{ec} \sum(A) + \sum(AU)}$$

$$F_v = \frac{h_{ac} \sum(A)}{h_{ac} \sum(A) + c_{pp} V_t}$$

As shown above the energy input to the system could be divided into convective and radiative parts as input to the air and surfaces but here combined to the environmental point.

### 3.4.7 Multi-zone buildings

The method in its standard form considers a single room with no heat transfer to or from other rooms, through internal walls. This is only suitable and correct when the room in question is surrounded by similar rooms or the effect of heat transfer through internal walls be neglected. Dow (1985) has extended the model for the multi-zone buildings. The temperature in each room is first calculated with no internal heat. A new temperature is calculated for one of the rooms, with inter-zone heat transfer, using the old temperature. The new temperature is used to calculate the new temperature in other rooms. The process is repeated for all the rooms in turn for a number of iterations. The iteration process continues until the overall change in temperature between successive iterations falls below a chosen value and the "steady state" is reached.

The fundamental theory of the Admittance Procedure is such that it is fairly successful at estimating mean and peak temperatures. If the hourly values are required the harmonics of periods 12,6 hours

etc. are needed but this is not featured in the model. (DAVIES 1985) Nevertheless the approximation is believed to be acceptable in building application. Any further application of the model needs to be justified. A method is suggested by Ulaah et al. (1977) to take into account effectively the influence of multiple harmonics in equivalent decrement factors and time lags. Comparison is made between the surface temperatures obtained from the proposed technique, and both analytical method (12 harmonics) and the first harmonic. In the case of light structures no difference is found, but for heavy structures results from different models do not agree with each other.

#### 3.4.8 Validation of the model

The empirical validation and evaluation of the method is restricted to its early stages of development. Milbank et al. have published results comparing measured temperatures with the predictions of an electrical analogue. They also showed that predictions by the Admittance Method agreed with the results of the electric analogue. On this basis they claim this proved the method's validity. (MILBANK et al. 1970 reported by WATERS 1977). Loudon (1970) published the results of a comparison between measurement and calculations performed by the Admittance Method in a free running building during summer. The agreement was thought to be satisfactory.

Attempts have been made to modify the BRE admittance procedure, so that it may be used in hot climates. A suggested modification by Harris Bass (1981 a&b). includes the external temperature profile, solar data, sky clarity, ground reflectance, external surface resistance, long wave radiation and heat loss due to ventilation. By comparison with observations, using specially designed test cells, the prediction is claimed to be good and the method useful. No detail is given.

Some comparisons between the analytical methods and Admittance Method are also reported for a few isolated examples. (SODHA 1986, MILBANK 1974). Although the environmental temperature model was first introduced to investigate the thermal response of buildings for simple cases, such as overheating problem in buildings during the summer, the literature shows that it is capable of tackling different



aspects of thermal investigation of buildings.

Davies in recent work has criticized the model and argued against its "logical shortcomings". (DAVIES 1987) and that "the procedure .. has not proved easy to understand. The model is based on three erroneous ideas: it reduces the 21 conductances network .. just to a single conductance, and so failed to distinguish between emissivity and geometrical aspects of radiant exchange, the argument appeared to suggest- wrongly -that the temperature  $T_{e1}$ , so arrived at was a meaningful enclosure parameter, it assumed wrongly that the heat could be input at  $T_{e1}$ ".

The main point raised is the way the radiation is treated, and as an example Davies argues that the mean surface temperature  $T_m$  as used in

$$h_r = 4\sigma\bar{T}_m^3 \quad (3.29)$$

is irrelevant. The radiation between surfaces depends on the temperature difference and not their mean. Or if  $E=0$  (say for polished aluminum)  $T_{e1}$  is independent of all surface temperature. (equation 3.11) This means that comfort does not depend on surface temperatures. Nevertheless it is admitted "the model is crude, but simple to use and probably adequate for many applications..... and in convective heat exchanges presents no problem".

The conceptual difficulties in the environmental temperature model has lead to the introduction of another model. This model also uses a new point as the index point of heat transfer, but it is used as a central point only for radiative exchange. Whether in practice its use leads to significantly better results, with regard to the inherent inaccuracies of much of the data (eg. casual gains infiltration, convective heat transfer treatment) is doubtful. (BILLINGTON 1987)

### 3.5 Other models

Davies (1974) has suggested a model of an enclosure having one external wall and five internal walls at the same temperature, surrounded by similar rooms, through which on average no heat flows. All internal walls are assumed to be at a uniform temperature ( $T_s$ ). The model when storage is included, has six elements and is called a "six element model". Figure 3.3 shows such a thermal network and the conductances between its elements. To solve the unsteady

behaviour, the admittance of the walls is used. In fact the environmental temperature model may be considered as a simplified form of the six element model. Hanna (1977) has extended the six elements model to eleven elements, by assuming different nodes for the glazed and opaque parts of the external wall, (figure 3.4) The unsteady behaviour of the model is solved by a finite differences technique. By this comparison it is concluded that no significant improvement is achieved by increasing the number of the nodes from six to eleven.

To overcome the shortcomings of the environmental temperature model as discussed by Davies, the radiative and convective exchange in a room may be separated in a further corrections to the model. (DAVIES 1987 a & b) First the network of the surface to surface system of radiant exchange may be reduced to a surface-to-star point  $T_r$  exchange by a least square fit. (DAVIES 1984) Then the radiant output from any source is taken acting at  $T_r$ . In this way the surface nodes are not linked to one another directly. It is normally assumed that convective gains can be treated at the space average air point. In certain well defined conditions these two points,  $T_r$  and  $T_{ai}$ , may be replaced by a single star point, to a composite "air index node". This model is similar to the environmental temperature model. The complete network of the model and conductances between the nodes are given in Figure 3.5. The heat balance equations at each node in the model are

at  $T_{ai}$

$$Q_a = (T_{ai} - T_{ao})V + \sum (T_{ai} - T_{sj}) A_j h_{cj} \quad (3.30)$$

at  $T_r$

$$Q_r = (T_r - T_{ao})W + \sum (T_r - T_j) A_j E_j^* h_{jr} \quad (3.31)$$

and at each surface node

$$Q_j = (T_{sj} - T_{ai}) A_j h_{cj} + (T_{sj} - T_r) A_j E_j^* h_{jr} + (T_{sj} - T_{ao}) A_j U_j^* \quad (3.32)$$

leading the matrix:

$$\begin{bmatrix} \sum A_j h_{cj} + V & & & & \\ & \sum A_j E_j^* h_{jr} + W & -A_1 E_1 h_{1r} & & -A_2 E_2^* h_{2r} \\ -A_1 h_{c1} & -A_1 E_1^* h_{1r} & A_1 h_{c2} + A_1 U_1 + A_1 E_1^* h_{1r} & & \\ & & & & \\ -A_2 & -A_2 E_2^* h_{2r} & & & A_2 h_{c2} + A_2 U_2 + A_2 E_2^* h_{2r} \end{bmatrix} \times \begin{bmatrix} T_a \\ T_r \\ T_1 \\ T_2 \end{bmatrix}$$

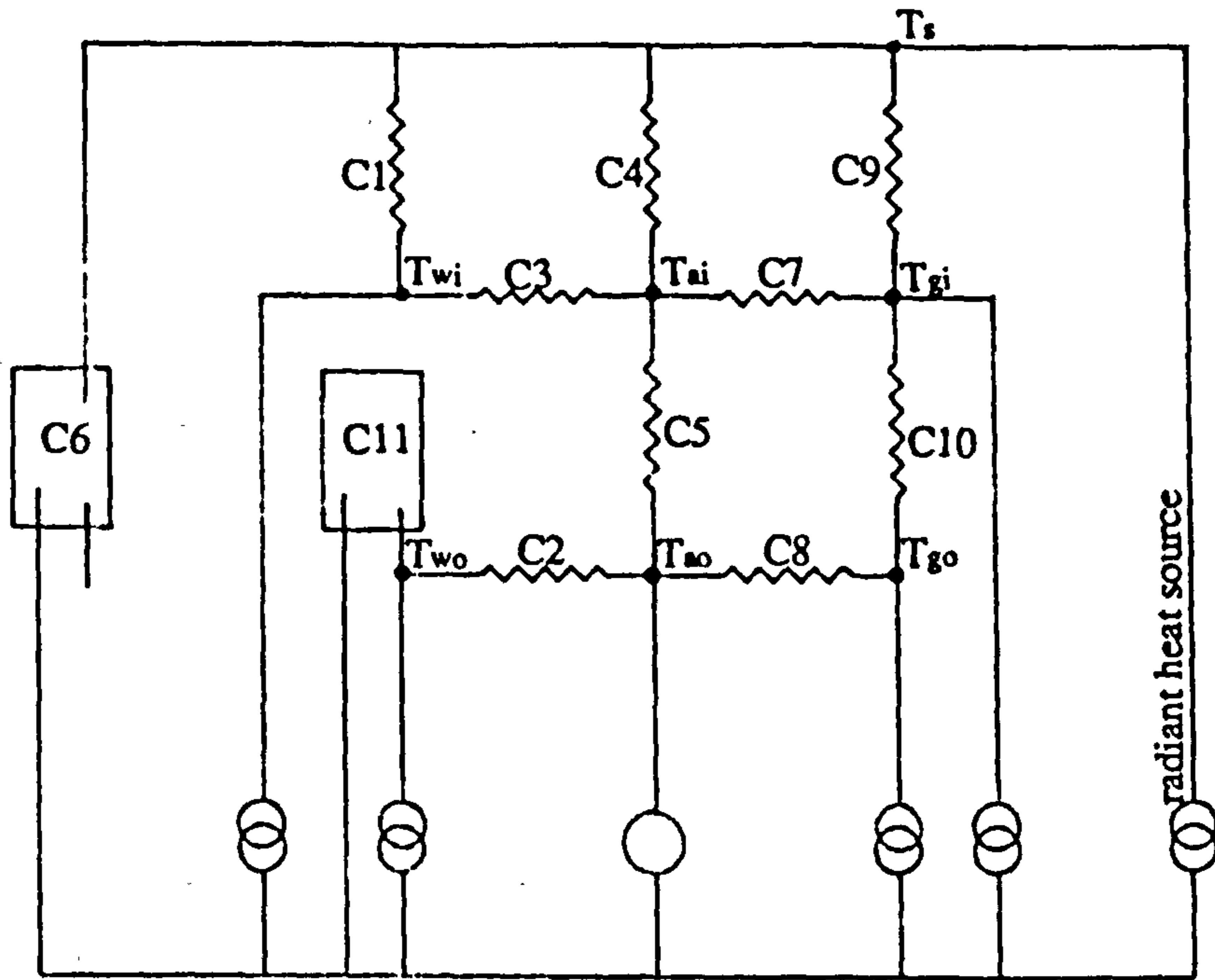


Figure 3.4: The 11 element model of a thermal enclosure (with an outer wall partly glazed and partly opaque) (Hanna 1979)

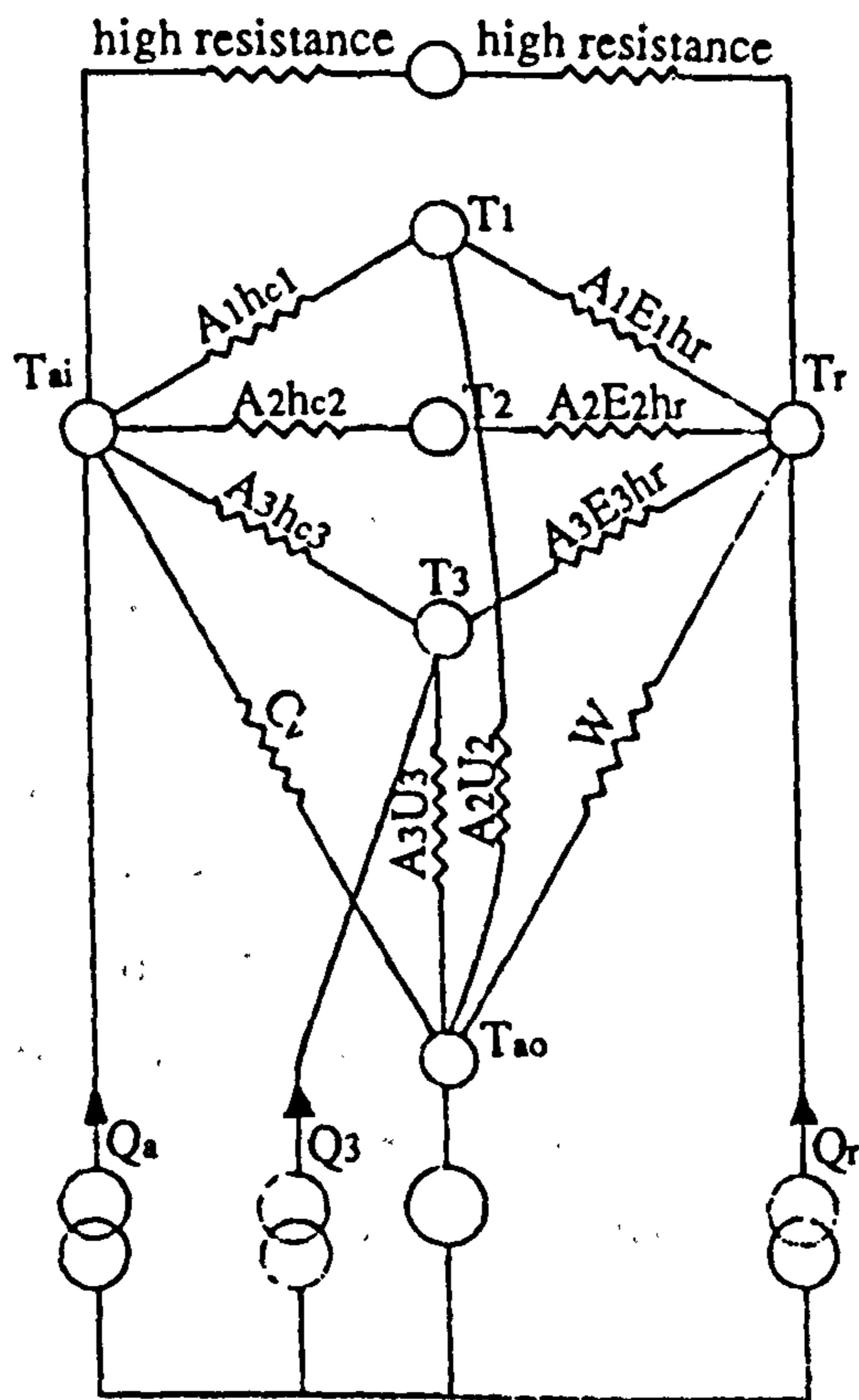


Figure 3.5 Thermal network of a room with a central point for radiation exchange (Davies 1987)

$$A_j E_j hr = A_j \epsilon_j hr / (1 - \epsilon_j + \beta \epsilon_j)$$

$$\beta_j = 1 - f_j - 3.53(f_j^2 - 1/2f_j) + 5.04(f_j - 0.25f_j)$$

$$f_j = A_j / \Sigma(A)$$

$W$  = Direct path by long wave radiation through open windows

$$T_c = (T_{ai} + T_r) / 2$$

$$= \begin{bmatrix} Q_a + T_{ao} V \\ Q_r + T_{ao} V \\ Q_1 + T_{ao} A U_1^* \\ Q_2 + T_{ao} A U_2^* \end{bmatrix} \quad (3.33)$$

where

$$A_j E_j^* h_r = A_j \epsilon_j h_r (1 - \epsilon_j + \beta_j \epsilon_j)$$

$$1/U_j^* = 1/U_i - 1/(E_j^* h_r + h_c)$$

$\epsilon_j$  is the emissivity of surface  $j$

The elements of the square matrix consist of conductances, which are assumed to be known. The model although physically unattractive, provides separate treatment for convection and radiation and is believed to be a better design procedure. The model has lost the great advantage of the Admittance Method, which was originally designed for use without a computer.

One of the early studies of unsteady heat conduction in buildings was performed by Muncey (1953), known as the matrix method, based on a harmonic solution to the unsteady heat transfer through the slabs. The results from calculations are compared with measurements in an unconditioned small scale test cell, subjected only to varying outside air temperature. Radiation exchange between surfaces is ignored. Gupta (1964) overcame this shortcoming by including the internal heat exchange between room surfaces into the thermal circuit. Gupta's calculation is performed for a single unconditioned and unventilated room with all surfaces exposed. The results are compared with observations obtained from a especially made test room, and significant improvement is reported.

A simplified method is developed by Mathews (1986) in which an electrical analogy is used to represent a room's thermal network. The main feature of the method is that empirical constants in some equations account for the typical rate of natural ventilation in conventional buildings. A single temperature is used instead of the sol-air and the outside air temperature. The final unsteady temperature is found for the first harmonic approximation of the indoor air temperature. The method is not suitable for a wide range of applications. On the one hand, empirical constants are used in

its development, and, on the other, the air temperature is the only temperature to be calculated.

### 3.5.1 Multi-exchange models

The most appropriate way to present a space in a mathematical model is to consider separate, independent nodes for each component of the enclosure ( air node and surfaces). The final mathematical model would be made by the establishment of relations between these nodes. The solution to the system of equations obtained from the heat balance at each node enables the prediction of each node temperature. Stephenson et al. (1968 a & b) have developed a thermal network for a room. Each surface of the room is given a node. In their model even the furniture in the room is presented by separate nodes. The air temperature is kept constant and known. The radiation exchange between surfaces is treated correctly but the convection coefficient is kept constant for the whole day. The response factor method is used to solve the unsteady heat conduction through the walls. The heat balance equations are written for every hour of the day in matrix form. The final result is obtained by matrix algebra. The main advantage of the response factor method over finite difference technique is claimed to be that it uses less computer time. The only lengthy calculation is to find the response factors for a room.

Buchberg and Naruishi (1967) and Buchberg (1969, and 1971) developed a perfect multi- exchange model to represent a single test enclosure exposed on all surfaces, with windows on two parallel walls. To study the effect of various external walls, different mathematical models are used to represent the wall. Figure 3.6 shows one of the models. The unsteady state heat conduction was achieved by application of the explicit forward finite difference method in space and time. The model is also used to study the sensitivities to outdoor wind speed and solar and longwave radiation inputs to the room, and opaque or transparent walls, for different types of building construction (1969). It is also developed to study the influence of radiation coupling between inside surfaces, and to investigate the use of constant inside surface coefficients for combined convection and radiation. (1971)

To study the effect of walls on indoor temperature, Hassan and Hanna (1972) developed a multi exchange model. The model is assumed to be isolated from all effects, except those of the variable outside air temperature and solar radiation on one of the external

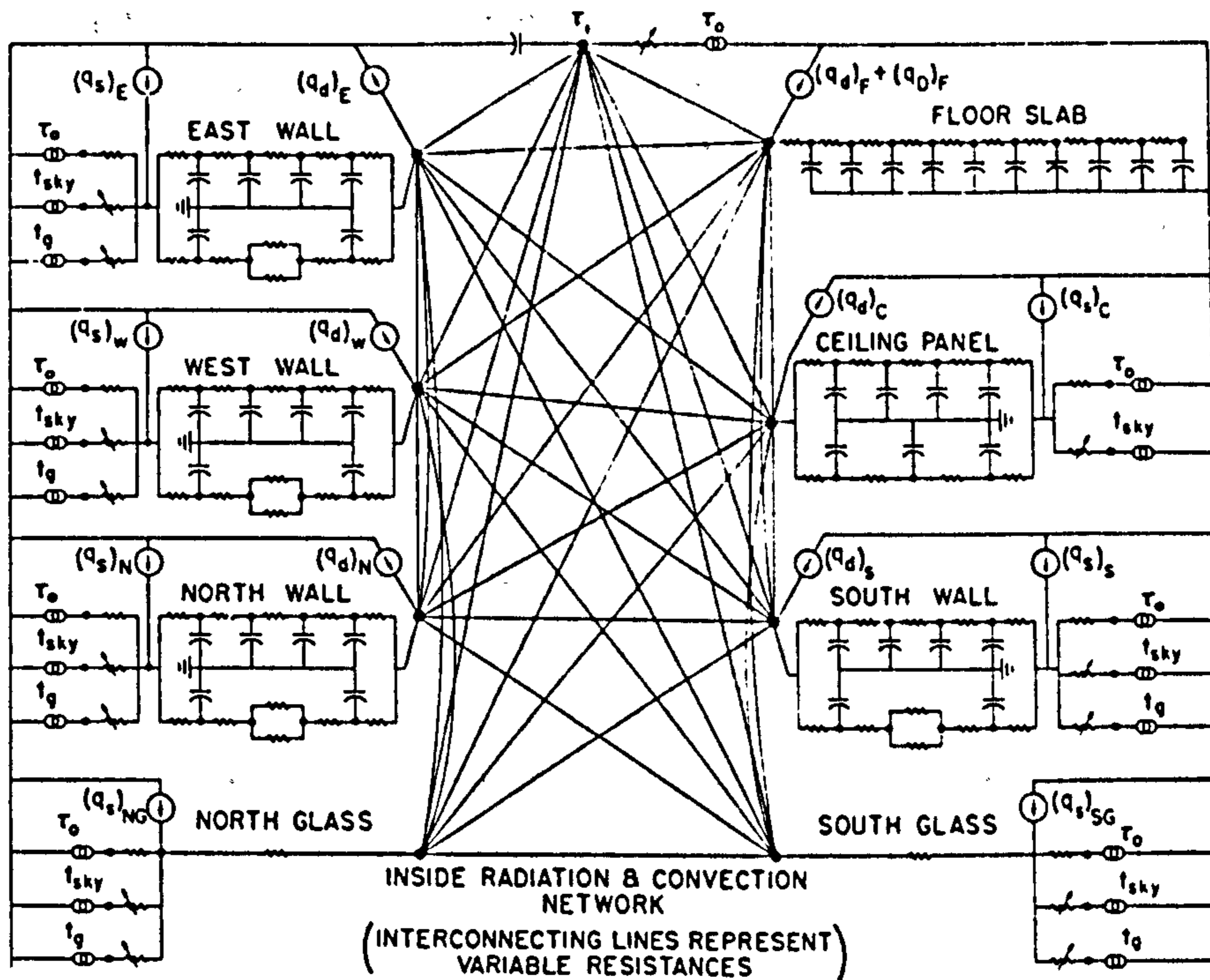


**Figure 3.6: Multi-exchange of a room exposed on all surfaces  
(hollow concrete walls, Finite Difference Technique)  
(Buchberg and Naruishi 1967)**

walls. A finite difference technique is used to solve the unsteady heat conduction equation. The main feature of their study is that they include forms of dimensionless groups which represent different variables in the model

### 3.6 Summary and discussion:

A number of methods representing heat exchange in a room are discussed. These vary from simple operating techniques, originally designed for hand calculations, (Admittance Method), to complicated multi-exchange models with finite difference technique using the computer.

It is the designer, at the early stages of design, who will decide what temperature is to be established in an enclosure. If comfort is to be evaluated, either the dry resultant temperature directly, or separate mean radiant and the air temperature, are required. This could be found by the Admittance Procedure. The multi-exchange models could provide the individual surface temperature. The finite difference technique enables the prediction of temperature profile across a slab. It is the required degree of precision which determines the suitability of a model.

Simple models and techniques, in order to simplify heat exchange among the elements, usually reduce the thermal network to simple index points. Among these the Admittance Procedure is the most important.

Each technique has certain assumptions and limitations, outlined below.

#### 3.6.1 Admittance procedure

The procedure has assumptions and limitations. The main interest in the present study is the validity of the method in the special case of variable ventilation and its use in conditions and climates different from those for which the technique was developed.

The concept of a combined coefficient for both radiation and convection is used which leads to the 'environmental temperature'. This is a fictitious temperature at which all heat transfer and energy input is assumed to take place. As was said above, this has been investigated (Danter 1974) and for most circumstances errors less than 5% of temperature, are reported, but Danter's investigation does not cover variable ventilation and is confined to the steady state.

The idea of the 'environmental temperature point', in its standard form, is developed for a cubic room. This might lead to errors in some cases. (BAXTER 1975) This affects the internal surface resistance, the conductance between the environmental and other points in the model and also on the scaling procedure of energy input to the index point. The dynamic factors in the Admittance Method i.e. admittance, decrement and surface factor, and also their associated time lags, are also affected by the internal surface resistance. The overall effect of the variation caused by changes in  $R_{si}$  might result in serious error.

The internal surface resistance is also a function of the radiative and convective heat transfer coefficients. The variation in the radiative part is negligible, but the convective part will change over a wide range, 3.0 to 7.0  $W/m^2K$ . (CHANDRA 1984) The standard value recommended by the CIBSE Guide is 3.0 ( $W/m^2K$ ) In case of sudden change to the rate of ventilation this will change. In these cases a fixed value for  $hc$  and  $R_{si}$  is not appropriate.

The environmental temperature model is based on the assumption of a unique temperature for the external wall, which is usually partly glazed and partly opaque. As shown above, this will not lead to great error in building application. (HANNA 1977)

The heat flux through the structure is considered to be one dimensional, so that the effect of corners is also neglected. It is also assumed that the physical properties of the building materials are constant during the day. These two are the common assumptions in most of the models and are not expected to cause problems.

In the standard form of the method, as suggested by the CIBSE Guide, all the dynamic characteristics of the structure are calculated for pure sinusoidal energy input for a 24-hours period. The external temperature are also assumed to vary sinusoidally. It is believed that this assumption will be accurate enough in normal cases, but it needs further examination.

In the method and its adaptation for wider use, (DANTER 1985, WATERS 1981, HARRINGTON LYNN 1974, CIBSE Guide A-5 1986) the time lag associated with the dynamic factors is not considered. The method is simplified either to ignore the time lag or to use a fixed value. A more correct solution could be obtained by the simultaneous heat balance equation at the air and environmental point, for each time step. Although this will diminish the great advantage of the procedure as a "manual method", in this research it is inevitable.



The thermal model as used in the procedure, considers the room as a single zone, and assumes the surrounding building at the same temperature. A method is suggested by Dow (1985) to extend the model for multi-zone cases. But there are some doubts about whether his procedure results in accurate answers. The original background of the model assumes no radiation exchange among surfaces of internal walls. The method does not take this into account. It is possible to use it only if the temperature difference between surfaces are small.

### 3.6.2 Other models

Multi-exchange models and finite difference technique are the most flexible methods for calculating the heat loss and thermal response in a building. Two approaches are normally used.

Implicit methods have the great advantage of being stable for all time intervals and distances between nodes in a slab, but the computations are more complicated.

In the explicit methods the stability criterion causes many restrictions in choosing steps in time and distance, but the computation is much easier.

Like the finite difference technique, the response factor method becomes practical only when a computer is used to carry out the many calculations required. In the response factor method, the procedure is simple, provided the conductance matrix is kept constant. This is only so if parameters such as convection coefficient or the ventilation rate are kept constant. In this case it is only the excitation matrix which needs to be calculated at each time interval. But if some parameters are also subjected to change the elements of the conductance matrix, the square matrix, are also subject to change. This will make the whole process more complicated and for such cases the finite difference technique is preferable.

The model developed by Davies(1987,1988), to overcome the shortcomings of the environmental temperature model, allow the temperature of individual surfaces of interest to be calculated, without going to the process of considering long wave radiation heat exchange between different nodes separately. This will for example, allow the surface temperature of an external window to be treated separately and enable the calculation of heat loss by long wave radiation through open windows.

## CHAPTER FOUR

### *NATURAL VENTILATION IN BUILDINGS*

#### 4.1 Introduction

Natural ventilation in buildings in hot and dry climates may serve several functions, which can be summarized into three main groups:

- health
- thermal comfort
- cooling the structure

##### 4.1.1 Health

This is determined by a minimum rate of fresh air for diluting odours and contaminants and removal of excessive moisture generated in building. The rate of fresh air required to satisfy health conditions is low, compared with the rate of ventilation necessary to cool the body and structure, and is achieved easily by infiltration and by ventilation through small openings.

##### 4.1.2 Ventilation for thermal comfort

The removal of excess heat, and air motion past the body must be sufficient to provide adequate cooling and rapid sweat evaporation. In hot dry climates, because of high outside air temperatures during the day, air cannot then be used for cooling, except in the evening and at night. At high air temperature, convective heat loss from the body is low, even when the air speed is high. On the other hand, the low humidity in dry climates allows adequate sweat evaporation rate from the body, even in still air, and thus air motion need not be great to prevent discomfort (GIVONI 1981), but in the evening and at night, air motion helps to increase comfort. The air speed required for comfort depends on the air temperature and relative humidity.

The relation between air speed and thermal comfort is studied by Fanger(1970). He has shown that an increase from a very low air velocity of less than 0.1 m/s to 1.5 m/s can be compensated by a

temperature decrease of 2.5 to 6 K, depending on the type of clothing, relative humidity and level of activity. He has shown that the effect of air velocity is more important at lower speeds. An increase in air velocity from 0.1 m/s to 0.3 m/s is compensated by 1.5 K.

Nicole(1974) in an investigation of comfort in hot dry climates, has shown that the control of air movement has a significant role in achieving thermal comfort. He has also shown that the major effect on comfort was when air speed exceeded 0.25 m/s , and when it exceeded 1 m/s there was little difference in discomfort.

Through the studies of Nicole and Fanger, one may conclude that an air speed in the range 0.25 to 1 m/s is desirable and provide comfort in these climates. Air speeds of up to 2 m/s is generally considered to be desirable and above this level may be disturbing. Air speed more than 4 m/s is generally considered to be uncomfortable at any temperature.(BOWEN and LOMAS 1981)

#### 4.1.3 Cooling the structure which surrounds the body.

In an unventilated room, in hot and dry climates, the maximum internal temperatures;(air and average of surfaces), occurs with some time lag after the maximum temperature of the air outside. This difference in time depends on whether the structure is heavy or light. When the internal air approaches its maximum temperature, the outside air will drop to a lower temperature, cooler than that of the air inside. Ventilation of a room with the cool outside evening air will help to provide comfort and also store 'coolth' for the following day, when the building is left unventilated. Both night ventilation and thermal capacity are required.

The effect of night ventilation on the "coolth" stored in the structure depends on the ventilation rate, the heat transfer between the building surfaces and the air, the surface area and the thermal capacity of the building material. Givoni(1981) has made series of observations on the performance of buildings cooled by night ventilation. Based on the results he has suggested that the effectiveness of the thermal capacity for storage of "coolness" in the summer increases with:

- the surface area of the mass at the interface with the indoor spaces.
- the thermal conductivity and thermal capacity of the structure.

-the heat transfer among the surfaces including the mass and the air.

It is possible to direct the air flow within buildings in such way that flow is greatest to the surface of the building, where thermal capacity is concentrated. Increase of the heat transfer coefficient for convection ( $h_c$ ) will also increase the rate of heat exchange at surfaces. This could be achieved by a higher rate of ventilation, and by means of higher air velocity near the surfaces. In a windless condition this could be achieved by use of a ceiling fan. From full scale measurements in a naturally ventilated room, Chandra et al. (1984) have shown  $h_c$  will increase from 4 to 8  $W/m^2K$  when the local air speed changes from 0.2 to 1 m/s. Through field measurements they have also reported an increase in  $h_c$  from 3.0  $W/m^2K$ , when the building is only naturally ventilated, (up to 30 air changes per hour), to 6.7  $W/m^2K$  with a ceiling fan for the same building. A ceiling fan will also increase the rate of ventilation. In one experiment in a passive cooling laboratory with no external wind, the rate of ventilation through open windows reached 4 air changes per hour. With the ceiling fan, the ventilation rate increased to 20 air changes per hour. (CHANDRA 1986).

It is generally believed that the rate of natural ventilation through windows will in general be adequate for cooling the structure. In hot climates, however, the openings must be designed to do two tasks: they must decrease the infiltration rate and heat gain during the day, and provide as much ventilation as possible at night.

The appropriate use of architectural elements and the right choice of the size and configuration of openings, orientation and location of buildings with regard to climate, facilitates the control of the rate and level of ventilation to a great extent.

Quantification of natural ventilation flow rate for typical rooms, with various types of openings etc. is needed for realistic evaluation of the functioning of design facilities and understanding of passive cooling with natural ventilation.

#### 4.2 Modelling room ventilation

The natural ventilation of a room depends on two sets of factors:

-environmental factors :

- local wind speed and its direction
- shelter from surrounding buildings
- temperature difference between inside and outside air
- built form :
  - the shape of the building (length to width ratio etc.)
  - dimensions, configuration and location of openings
  - design of the windows( air tightness, type etc.).

Methods used to predict the ventilation rate into buildings divide them into two classes: those with single sided ventilation and those with cross ventilation.

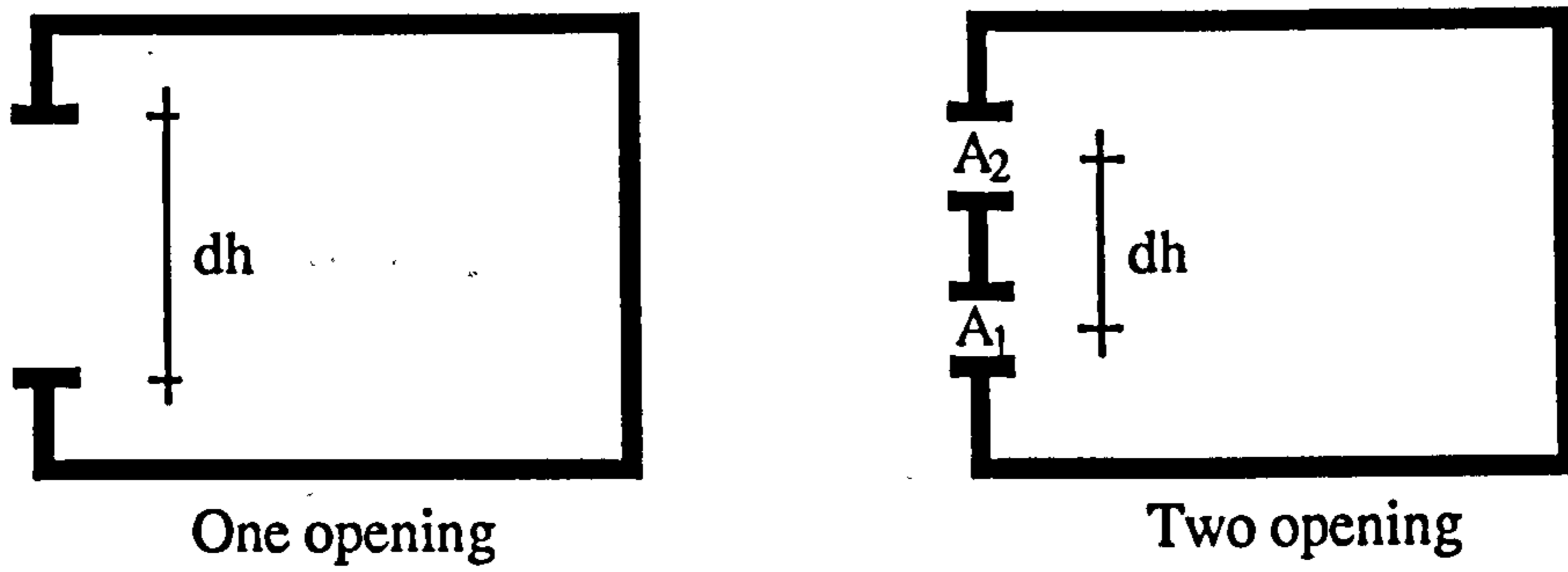
#### 4.2.1 Single sided ventilation

By single-sided ventilation is meant natural ventilation of buildings with all openings on one wall only, or that the internal partitions provide a barrier to ventilation air so that the effect of cross air flow becomes unimportant. Single sided ventilation is provided either by stack effect (due to temperature difference between inside and outside air) or by pressure difference due to wind.

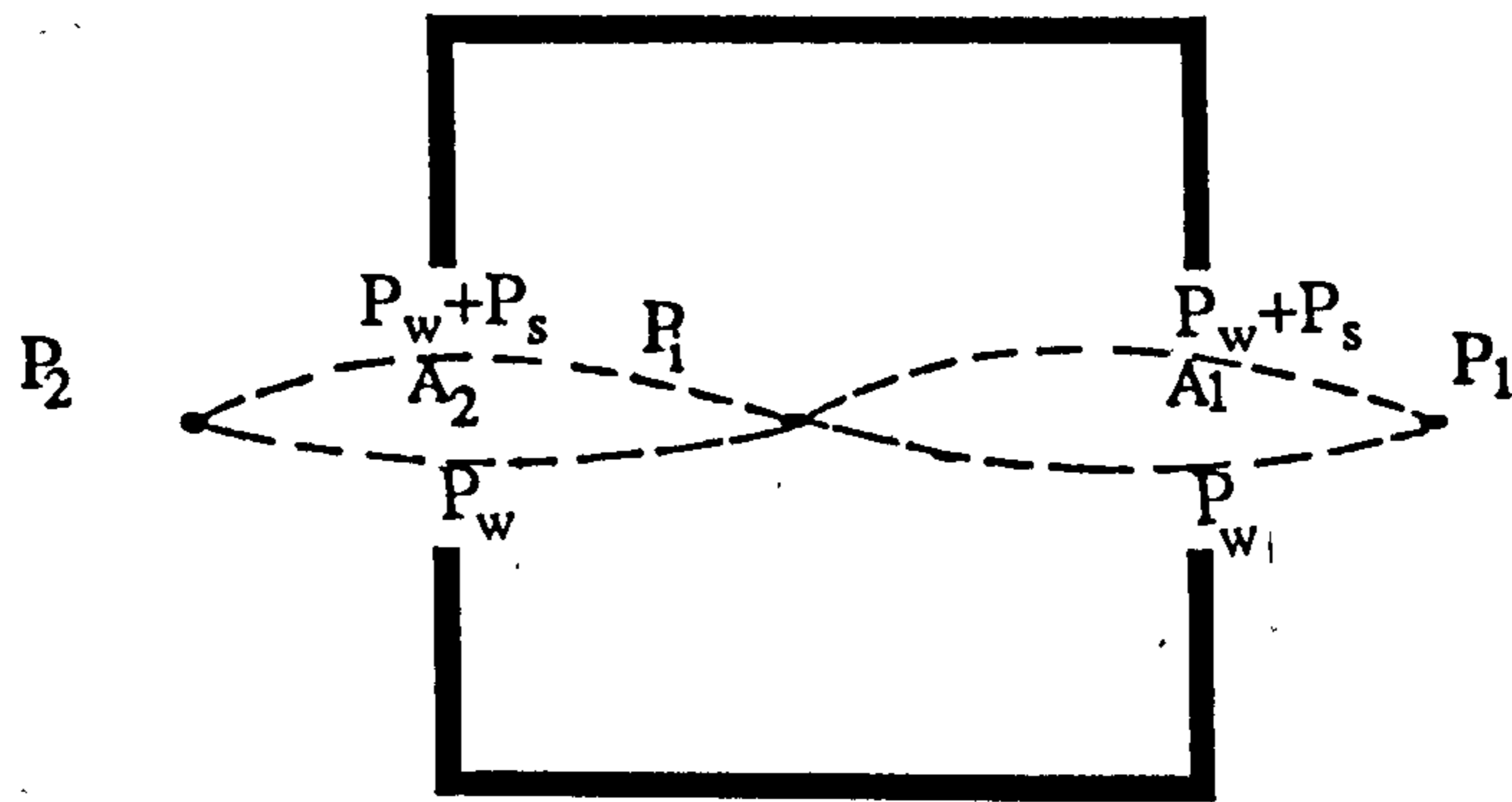
To predict wind-induced ventilation, most of the existing models take two factors into account: area of openings and wind velocity. (WARREN 1986 ,SWAMI and CHANDRA 1987, CIBSE 1986, BRE 1978, PHAFF et al.1980)

Changes in the angle of incident wind will change the ventilation rate. To incorporate the effect of wind angle is too complicated and has not yet been considered in the existing models. In the model proposed by ASHRAE the incident wind is divided into "perpendicular" and "oblique". Perpendicular wind will produce twice as much air flow as oblique wind. (ASHRAE 1985). Cockroft (1976) has suggested that wind velocity be resolved into perpendicular wind using the angle of incidence, for the wind angles up to 60 degrees from normal to the surface. Cormellin et al. (1988) have shown that the air flow rate will be halved if the incident wind changes from being perpendicular to the opening facade to being perpendicular to the leeward side of the building. Narasaki (1987) has shown the air flow rate is proportional to mean air velocity , the opening area and the "turbulence intensity", and becomes greater at an incident angle of 75 degrees. This agrees with results obtained by Warren.(1986)

In this study, the model suggested by CIBSE Guide and British



a: Single sided ventilation (section)



Single zone Cross ventilation flow network (section)

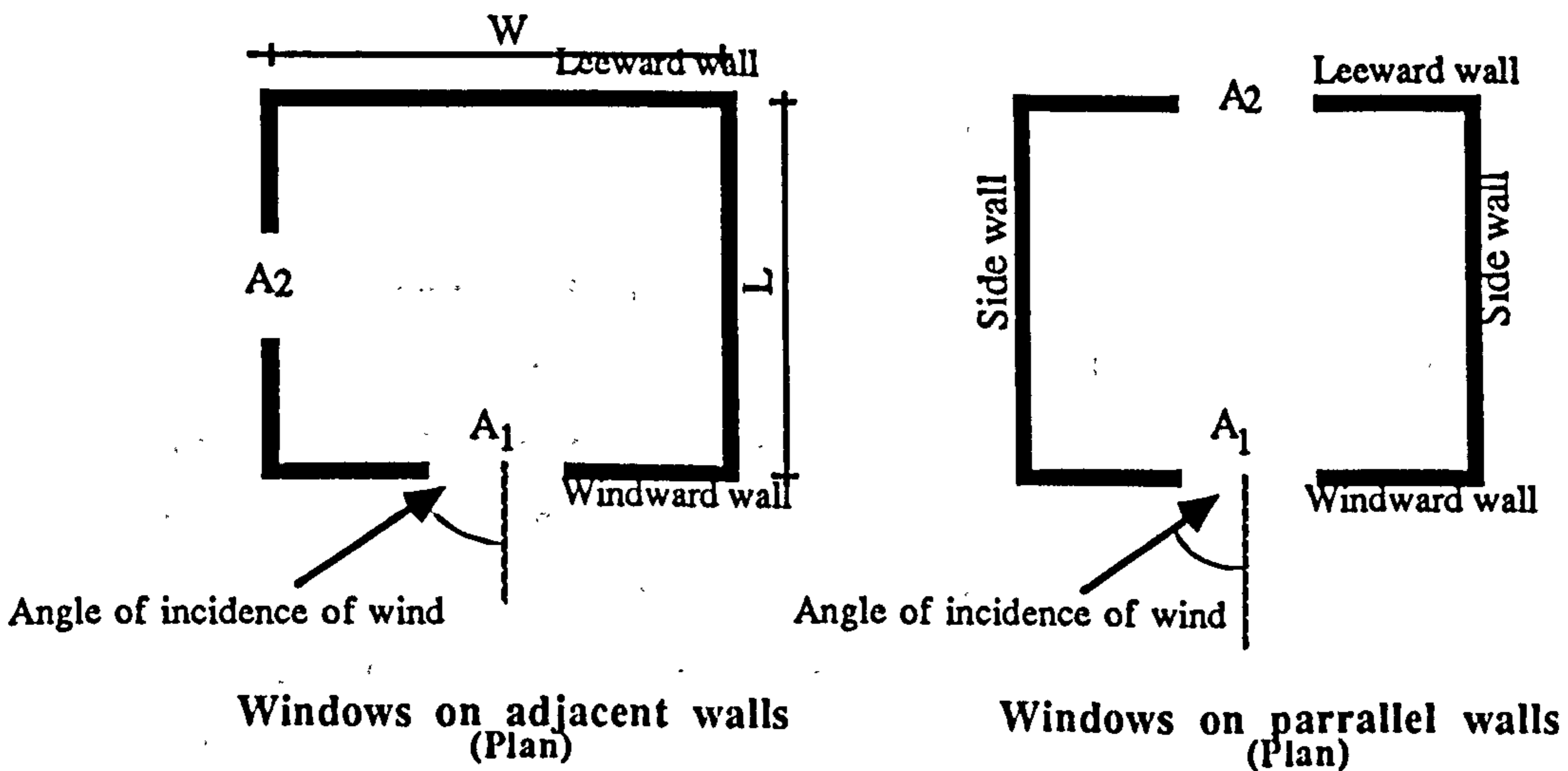


Figure 4.1 : Single zone ventilation

Standard 5925 (1980) is used. This is found to be sufficient to evaluate the effect of some alternatives in design such as orientation, area of the openings, inlet/outlet ratio etc. The air flow generated by the wind could be estimated by

$$Q_w = 0.025A\bar{V}_r \quad \text{m}^3/\text{s} \quad (4.1)$$

and by stack effect with openings all at the same height from

$$Q_s = C_d \frac{A}{3} \left( \frac{\Delta T \, dh \, g}{\bar{T} + 273} \right)^{0.5} \quad \text{m}^3/\text{s} \quad (4-2)$$

and in cases with two openings at a height difference  $h_a$  (figure 4.1) from

$$Q_s = C_d (A_1 + A_2) \frac{2^{0.5} \epsilon}{(1 + \epsilon)(1 + \epsilon^2)^{0.5}} \quad \text{m}^3/\text{s} \quad (4-3)$$

where

$$\begin{aligned} Q_s &= \text{stack induced air flow} \quad \text{m}^3/\text{s} \\ Q_w &= \text{wind induced air flow} \quad \text{m}^3/\text{s} \\ A_1, A_2 &= \text{area of the openings at different height} \quad \text{m}^2 \\ \epsilon &= A_1/A_2 \\ C_d &= \text{discharge coefficient} \\ \bar{V}_r &= \text{air velocity at the reference height} \quad \text{ms}^{-1} \\ dh &= \text{height of the window or the distance between} \\ &\quad \text{windows (figure 4.1a, 4.1b)} \quad \text{m} \end{aligned}$$

#### 4.2.2 Cross ventilation model

Cross ventilation is defined as the ventilation provided by circulation of air from one side of a room to the other. The air flow through an opening is a function of pressure difference across the opening. The most common representation for the air flow are a power law or a quadratic. The power law was found to be the most suitable technique according to Liddament(1987). This approach as suggested by AIVC (Air Infiltration and Ventilation Centre) Guide is used in the present study. (Liddament 1986).

The flow through an opening is given by :

$$Q = K(\Delta P)^n \quad \text{m}^3/\text{s} \quad (4.4)$$

where

$$\begin{aligned}
 Q &= \text{flow rate} \quad \text{m}^3/\text{s} \\
 \Delta p &= \text{pressure difference across opening} \quad \text{Pa} \\
 K &= \text{flow coefficient} \quad \text{m}^3/\text{s} \\
 n &= \text{flow index}
 \end{aligned}$$

In the case of natural ventilation the pressure difference across an opening is caused by wind and the temperature difference between inside and outside air (stack effect). The total pressure caused by stack and wind is given by

$$P = P_s + P_w \quad (4.5)$$

where

$$\begin{aligned}
 P_w &= \text{wind induced pressure difference} \quad \text{Pa} \\
 P_s &= \text{stack induced pressure difference} \quad \text{Pa}
 \end{aligned}$$

The pressure caused by wind is proportional to the velocity pressure

$$P_w = c_p(\rho V^2/2) \quad (4.6)$$

where

$$\begin{aligned}
 \rho &= \text{air density} \quad \text{kg/m}^3 \\
 c_p &= \text{pressure coefficient} \\
 V &= \text{mean air velocity at the reference height} \quad \text{m/s}
 \end{aligned}$$

and pressure caused by temperature difference is given by

$$P_s = -\rho_o g 273 \left( \frac{1}{T_{ao}} - \frac{1}{T_{ai}} \right) (h_2 - h_1) \quad (4-7)$$

where

$$\begin{aligned}
 \rho_o &= \text{air density at } 273^\circ\text{K} \text{ (1.294 kg/m}^3 \text{ for dry air)} \\
 g &= \text{acceleration due to gravity} \quad \text{m/s}^2 \\
 h_2 \text{ \& } h_1 &= \text{height of the opening of the facade} \quad \text{m} \\
 T_{ao} \text{ \& } T_{ai} &= \text{outside and inside absolute temperature} \\
 &\quad \text{respectively} \quad ^\circ\text{K}
 \end{aligned}$$

The effect of water vapour content of the air is here ignored, an uncertainty of little significance when the air is dry.

In a room with a number of flow paths, a mass flow balance equation is applied



$$\sum \rho_i Q_i = 0 \quad (4.8)$$

Using the power law of equation 4.4 the mass balance equation becomes

$$\sum K_i (P_i - P_{int})^{nl} \left( \frac{|P_i - P_{int}|}{P_i - P_{int}} \right) = 0 \quad (4.9)$$

Note that in equation 4.8 the variations of  $\rho_i$  between inside and outside is negligible in comparison with the magnitude of the overall density of air and could be ignored. It should also be mentioned that the third term in equation 4.9 is to keep the sign of flow and its direction.

In the case of a multizone model, each zone having different flow paths, the mass balance equation may be presented as

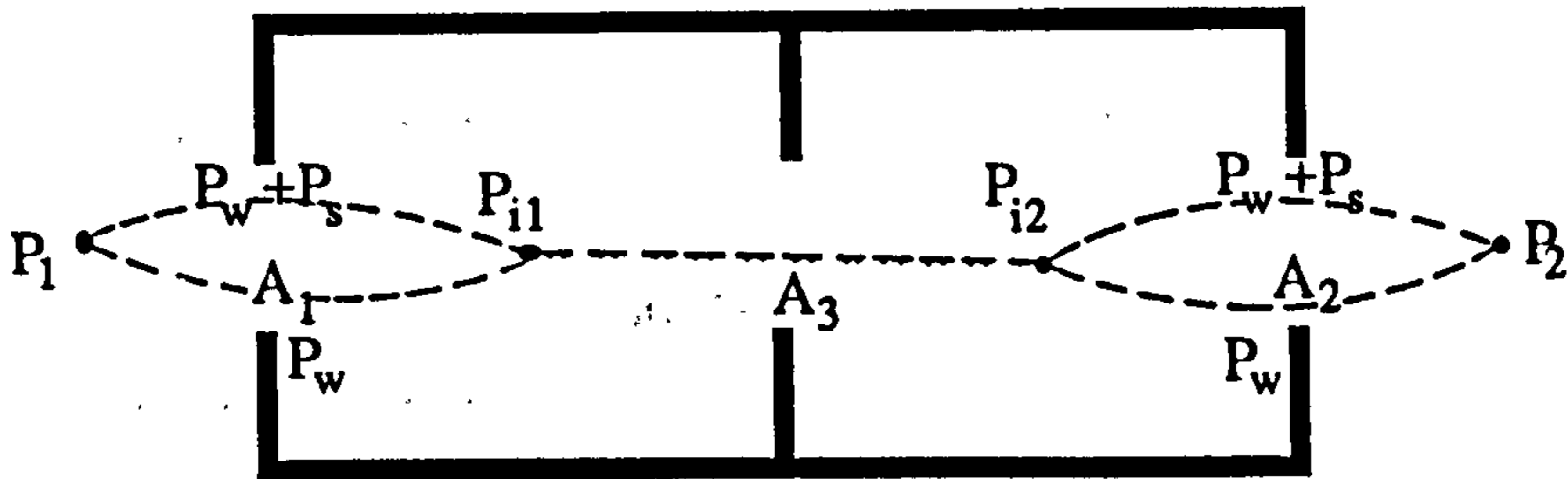
$$\sum_{i=1}^I \sum_{j=1}^J K_{ij} (P_i - P_j)^{nl} \left( \frac{|P_i - P_j|}{P_i - P_j} \right) = 0 \quad (4-10)$$

The procedure for correcting the wind velocity due to the surroundings i.e urban, city centres etc., the values of flow coefficient and flow exponents are used according to the AIVC Guide. The values of  $c_p$  used are as given by the same guide.

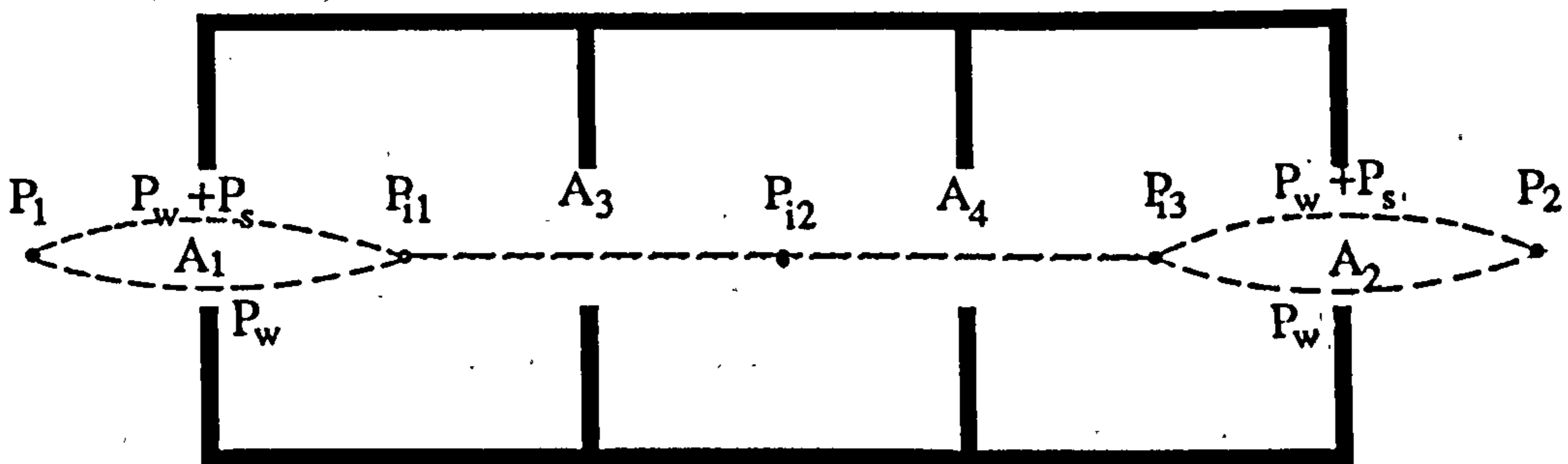
The above models are used below to predict the ventilation rate in the following cases

- Single sided-ventilation with all openings at the same height. Figure 4.1
- single sided-ventilation with two openings at different height. Figure 4.1
- cross-ventilation in a single-zone building. Figure 4.1
- cross ventilation in a two-zone building. Figure 4.2
- cross ventilation in three-zone buildings. Figure 4.1

As the rate of air flow is linearly proportional to the area of the opening, and in order to give a general form of representation and better understanding of the design parameters affecting the ventilation rate, a standard height of 3 meters for rooms, (which is common in the architecture of hot dry climates) is assumed. The area of openings are represented per metre length of the facade.



a: two-zone-building



b: Three-zone building

Figure 4.2: Cross ventilation flow network in multi-zone buildings

In the case of cross ventilation three types of building shapes are considered:

- square
- oblong with a width/length ratio of 1/2 having the longer wall exposed
- oblong plan with a width/length ratio of 1/2 having the shorter wall exposed

The temperature difference between inside and outside is assumed to be constant during the night, when ventilation occurs. This is a fair assumption, usually practiced as with open windows. The difference between inside and outside temperature is small and fairly constant, and in the presence of a moderate wind the main factor causing air flow would be pressure difference caused by the wind, and the stack effect would be negligible.

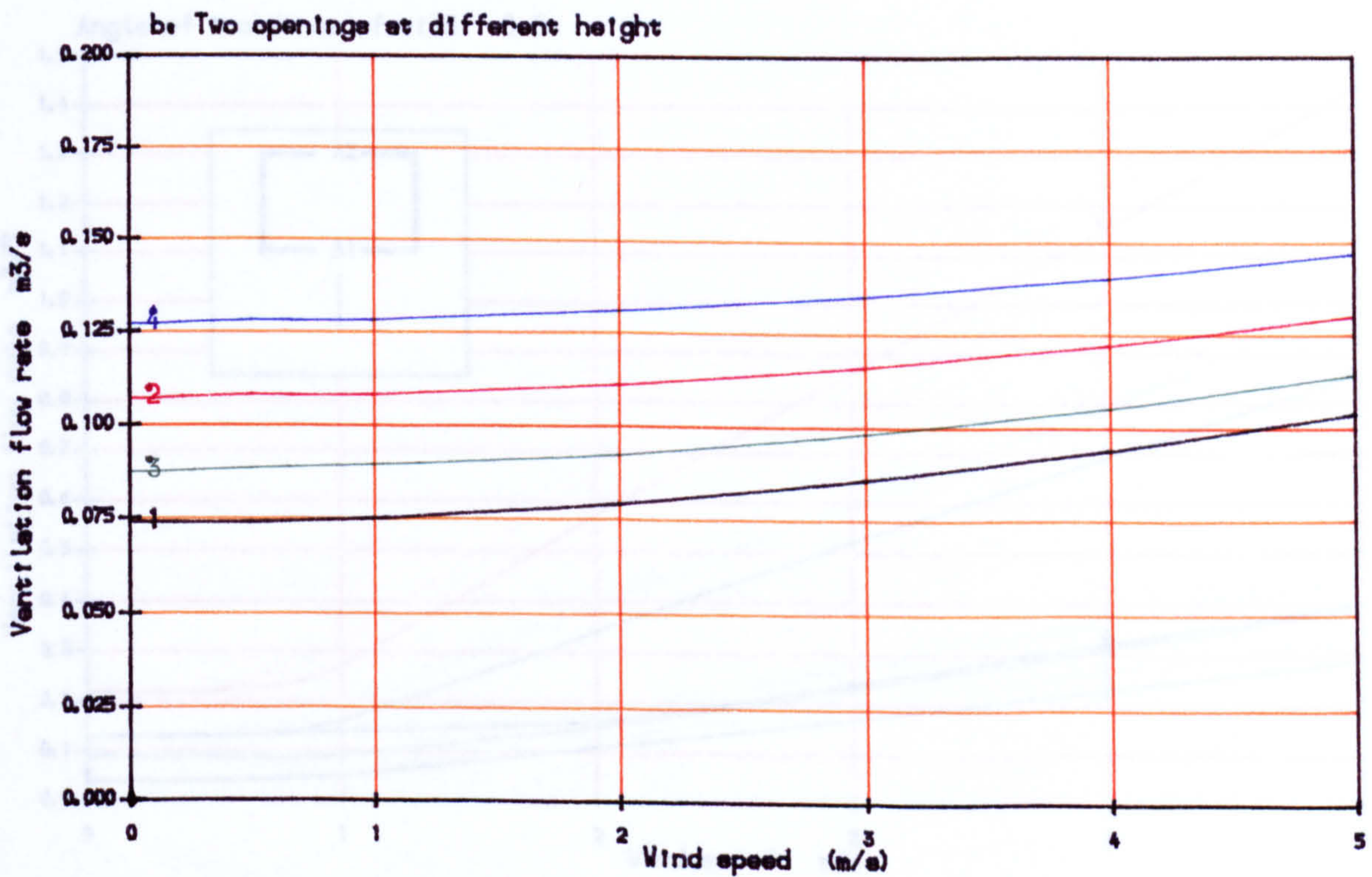
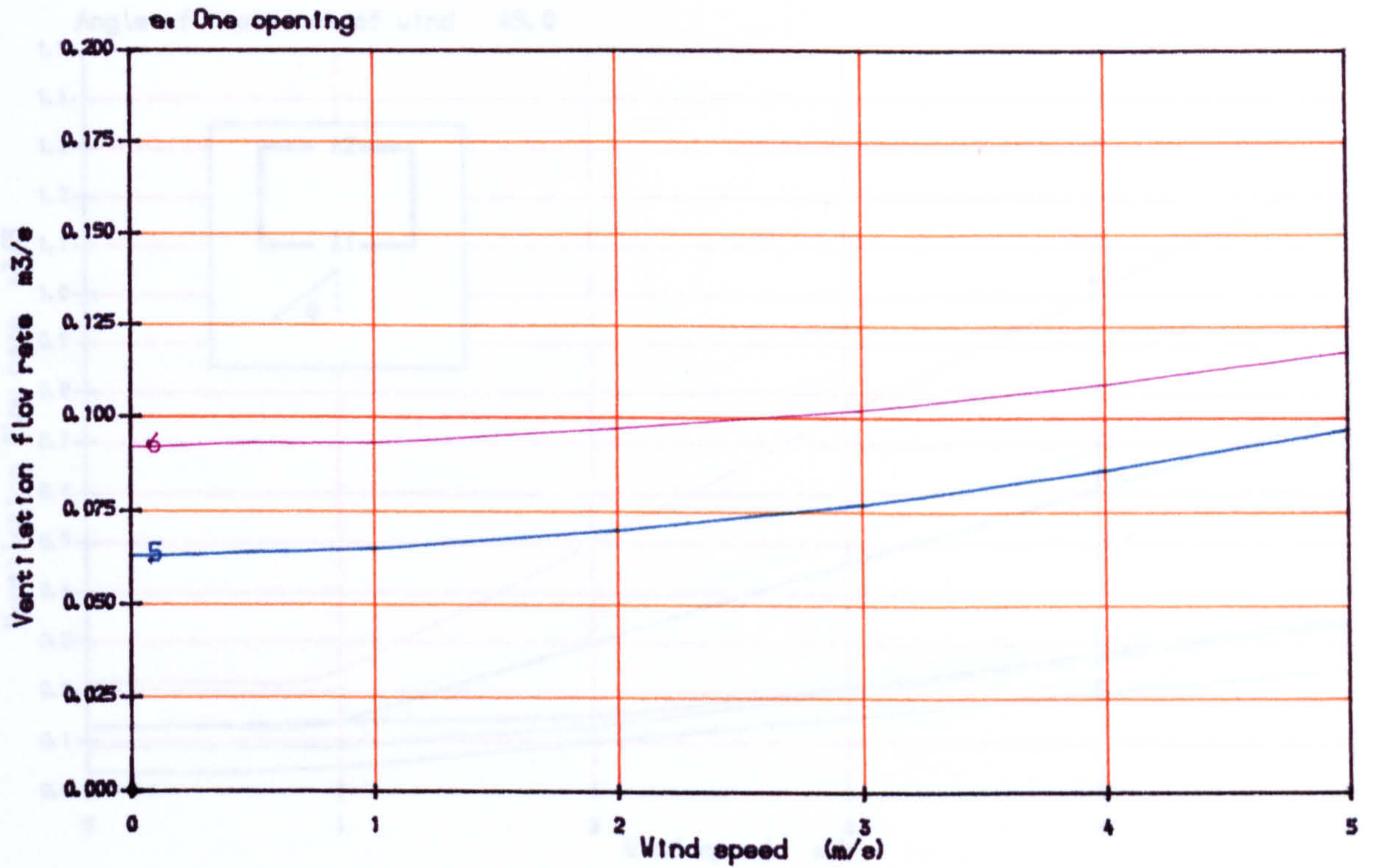
### 4.3 Results

#### 4.3.1 Single sided ventilation

Figure 4.3a and figure 4.3b show for different types of openings the air flow rates of single sided ventilation with different wind speeds and with 3 K temperature difference between inside and outside air. The sum of open areas is the same for both. It is shown that for a wind speed of 1 m/s the dominant mechanism of air flow is stack effect. For a single opening a ventilation rate about 30% higher is obtained with a 2.55 m high window than with a 1.2 m high window. In case of two openings, when the distance between the openings is kept constant, and the area of openings are equal, the air flow is about 20% more than with unequal windows. With the same type of openings a higher ventilation rate is achieved when there is a greater difference in their height. Figure. 4.3a and 4.3b show that with the same area of opening an improvement of up to 50% in ventilation flow rate could be achieved by appropriate adjustment of openings.

#### 4.3.2 Cross ventilation

Figure 4.4 shows the air flow rate for different areas of openings and wind speed, in a room with a square plan, and with windows located on either parallel walls or on adjacent walls. The building is assumed to be in a sheltered area i.e. surrounded by buildings of the same height. Figures 4.5 and 4.6 show results for a semi-sheltered area, (i.e. surrounded by buildings or obstructions of



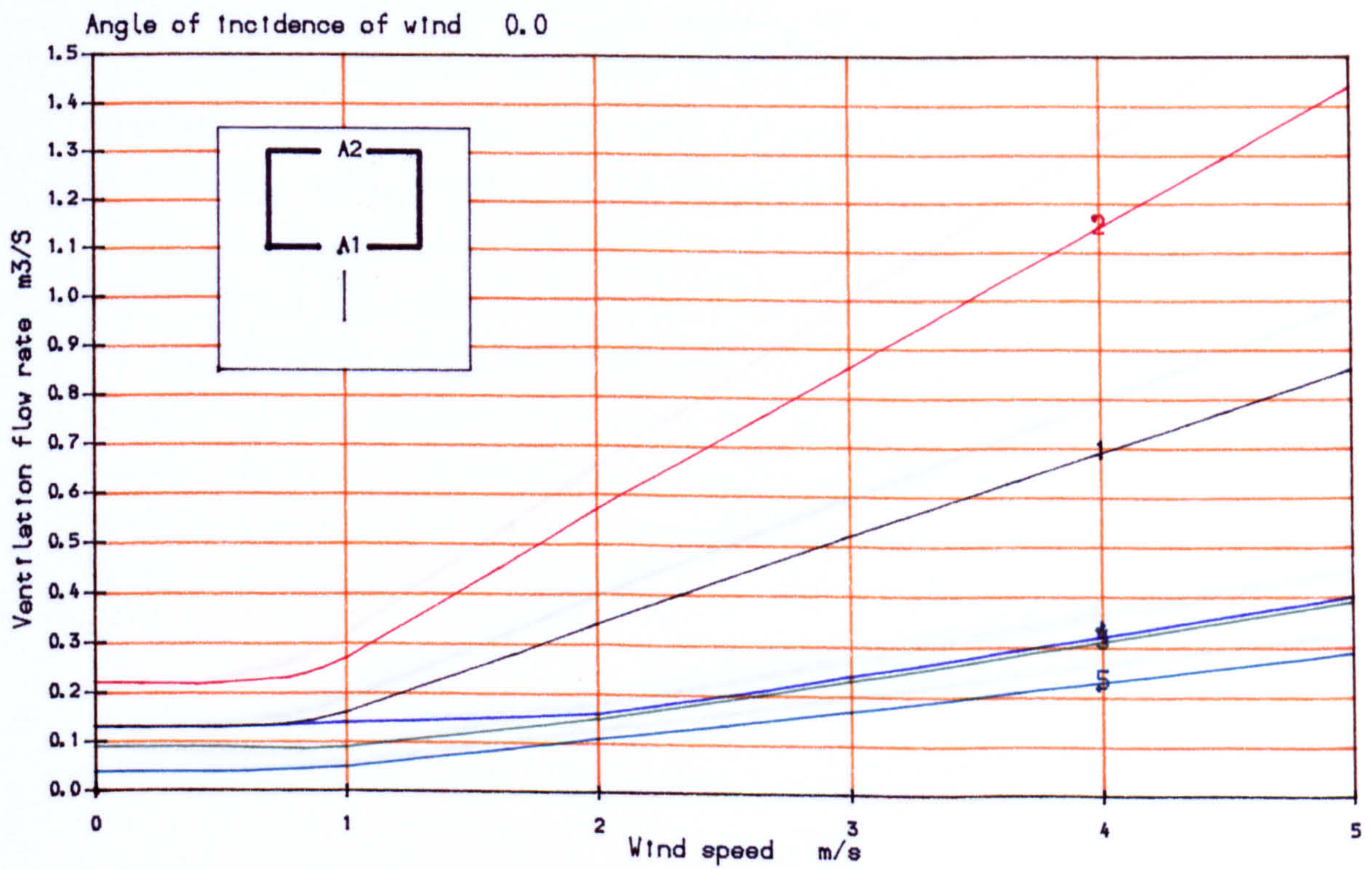
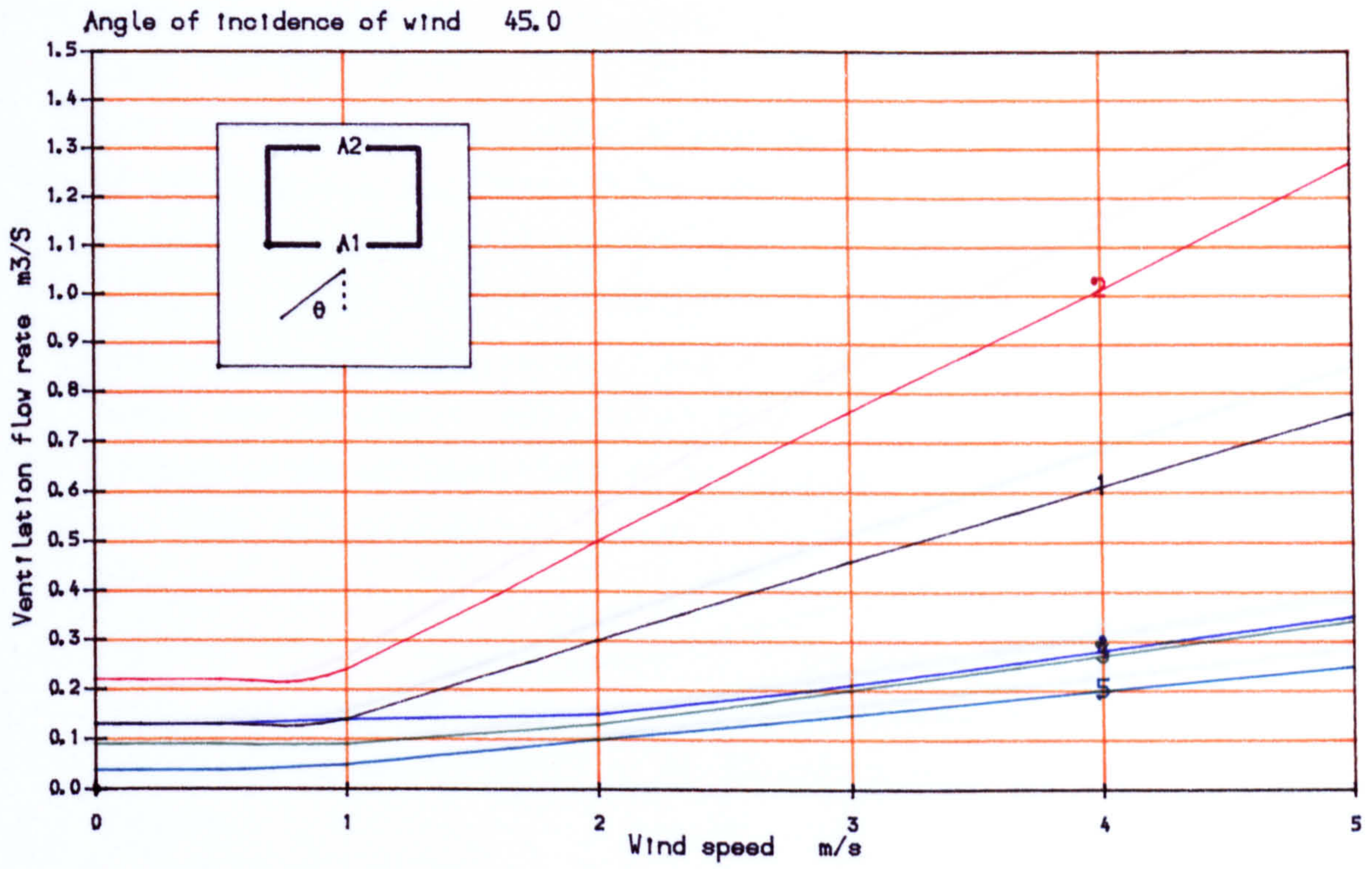
1  $A1/A2 = 1/2$   $dH = 1.20$   
 3  $A1/A2 = 1$   $dH = 1.20$   
 5 One opening  $H=1.20$

2  $A1/A2 = 1/2$   $dH = 2.55$   
 4  $A1/A2 = 1$   $dH = 2.55$   
 6 One opening  $H=2.55$

Figure 4.3 : Flow rate through openings on one wall

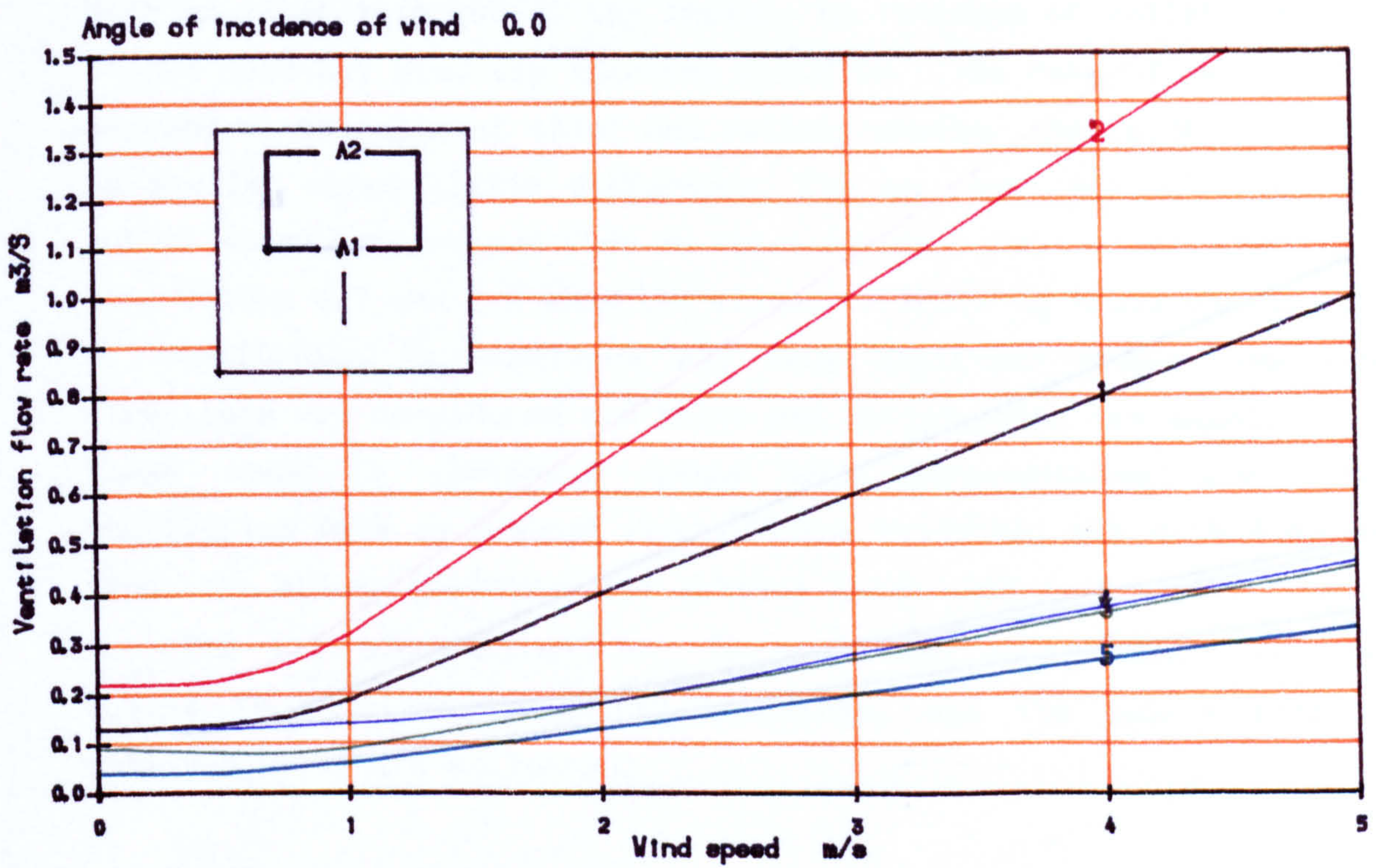
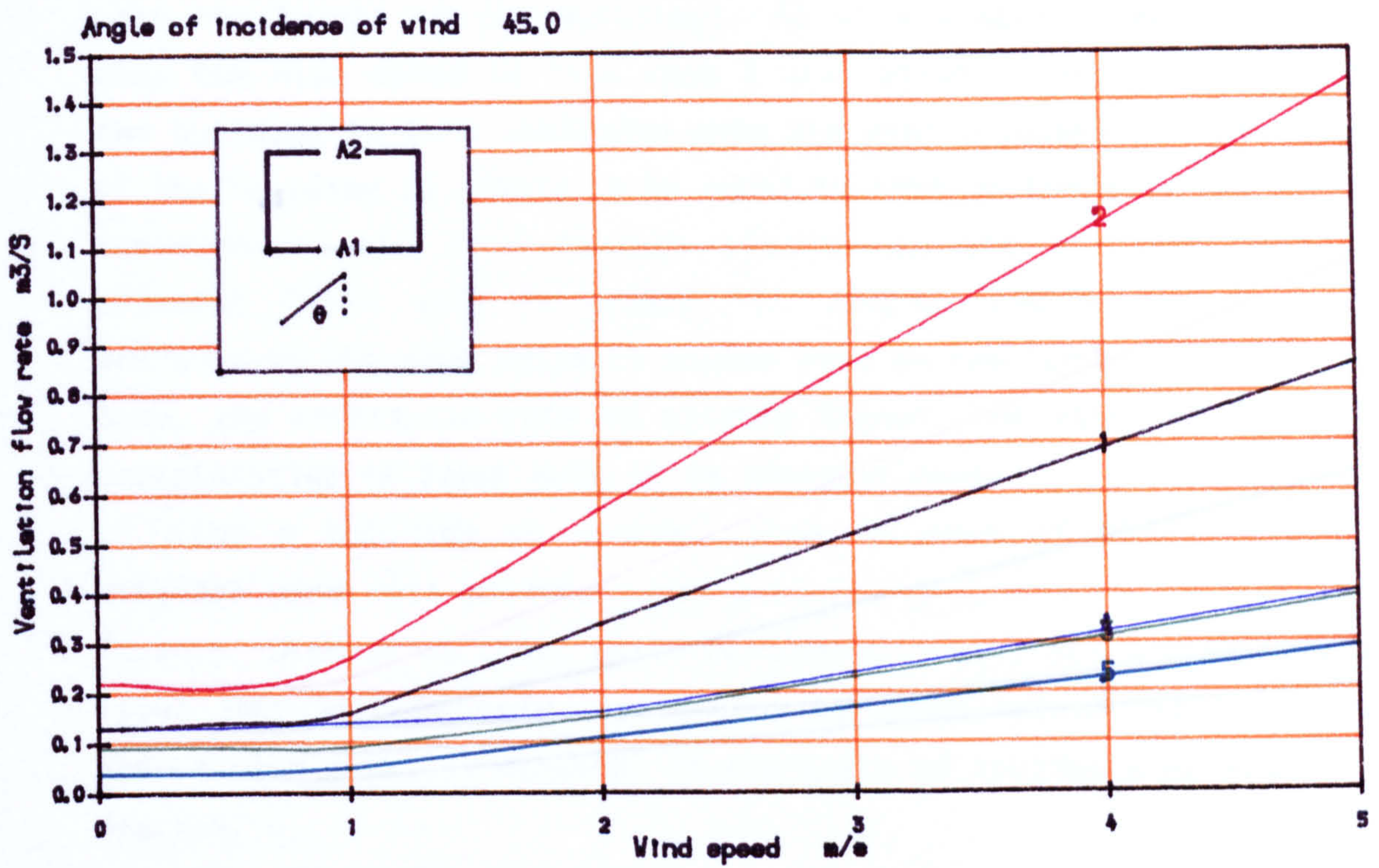
Sheltered area

Sum of open areas in all plots 0.9 m<sup>2</sup>



1	$A1 = 0.9 m^2$	$A2 = 0.9 m^2$	4	$A1 = 0.3 m^2$	$A2 = 1.5 m^2$
2	$A1 = 0.5 m^2$	$A2 = 1.5 m^2$	5	$A1 = 0.3 m^2$	$A2 = 0.3 m^2$
3	$A1 = 0.3 m^2$	$A2 = 0.9 m^2$			

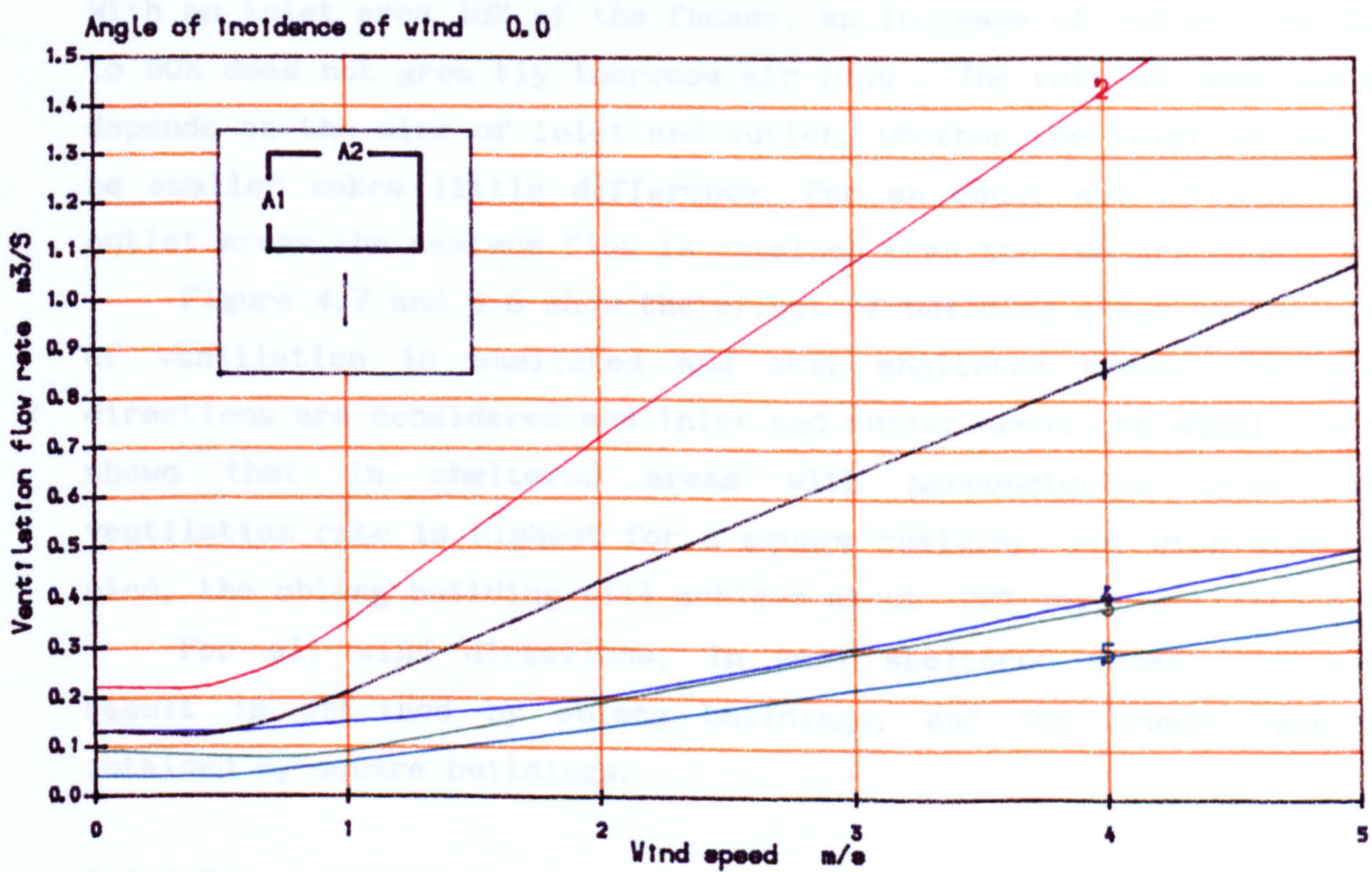
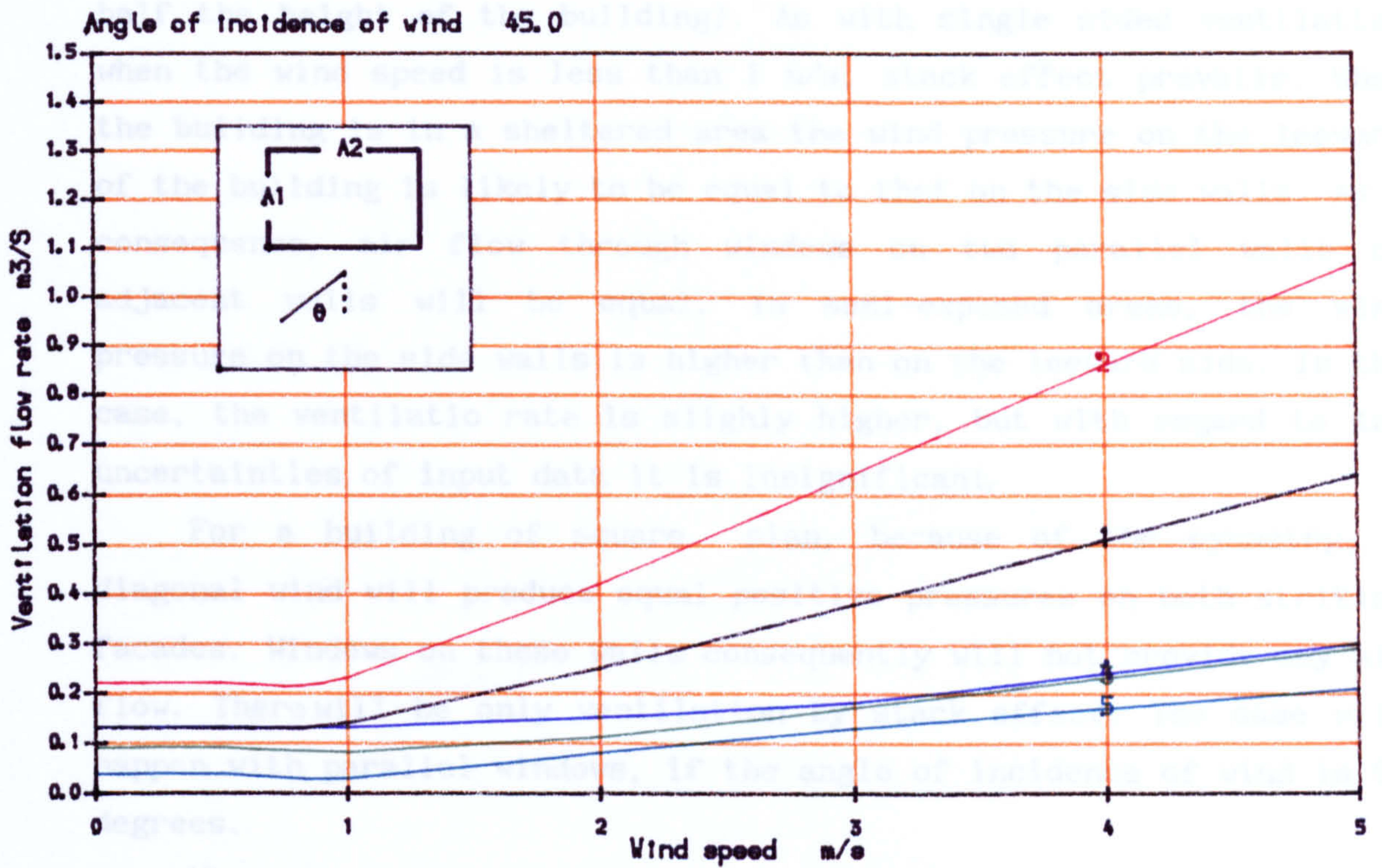
Figure 4.4: Cross flow rate for different opening areas and wind speeds  
 Location: Sheltered  
 Square plan  
 Opening on two adjacent walls or two parallel walls



- |   |                |                |   |                |                |
|---|----------------|----------------|---|----------------|----------------|
| 1 | $A1 = 0.9 m^2$ | $A2 = 0.9 m^2$ | 4 | $A1 = 0.3 m^2$ | $A2 = 1.5 m^2$ |
| 2 | $A1 = 0.5 m^2$ | $A2 = 1.5 m^2$ | 5 | $A1 = 0.3 m^2$ | $A2 = 0.3 m^2$ |
| 3 | $A1 = 0.3 m^2$ | $A2 = 0.9 m^2$ |   |                |                |

Figure 4.5: Cross flow rate for different opening areas and wind speeds

Location: Semi sheltered (surrounded by buildings with 1/2 height of origin)  
 Square plan  
 Opening on parallel walls



- |   |   |   |   |
|---|---|---|---|
| 1 | 0.9 $\text{m}^2$ Inlet & 0.9 $\text{m}^2$ outlet area | 4 | 0.3 $\text{m}^2$ Inlet & 1.5 $\text{m}^2$ outlet area |
| 2 | 1.5 $\text{m}^2$ Inlet & 1.5 $\text{m}^2$ outlet area | 5 | 0.3 $\text{m}^2$ Inlet & 0.3 $\text{m}^2$ outlet area |
| 3 | 0.3 $\text{m}^2$ Inlet & 0.9 $\text{m}^2$ outlet area |   |   |

Figure 4.6: Cross flow rate for different opening areas and wind speeds

Location: Semi sheltered (surrounded by buildings with 1/2 height of origin)  
 Square plan  
 Opening on adjacent walls

half the height of the building). As with single sided ventilation when the wind speed is less than 1 m/s, stack effect prevails. When the building is in a sheltered area the wind pressure on the leeward of the building is likely to be equal to that on the side walls. As a consequence, air flow through windows on two parallel walls or adjacent walls will be equal. In semi-exposed areas, the wind pressure on the side walls is higher than on the leeward side. In the case, the ventilatio rate is slighly higher, but with regard to the uncertainties of input data it is insignificant.

For a building of square plan, because of the symmetry, a diagonal wind will produce equal positive pressures on both striking facades. Windows on these walls consequently will not provide any air flow. There will be only ventilation by stack effect. The same will happen with parallel windows, if the angle of incidence of wind is 90 degrees.

When the inlet and outlet areas are not equal, the ventilation rate is not significantly affected by the increase in outlet area. With an inlet area 10% of the facade, an increase of outlet from 30% to 50% does not greatly increase air flow. The rate of ventilation depends on the size of inlet and outlet, whether the inlet or outlet be smaller makes little difference. For an equal sum of inlet and outlet areas the maximum flow is obtained when the two are equal.

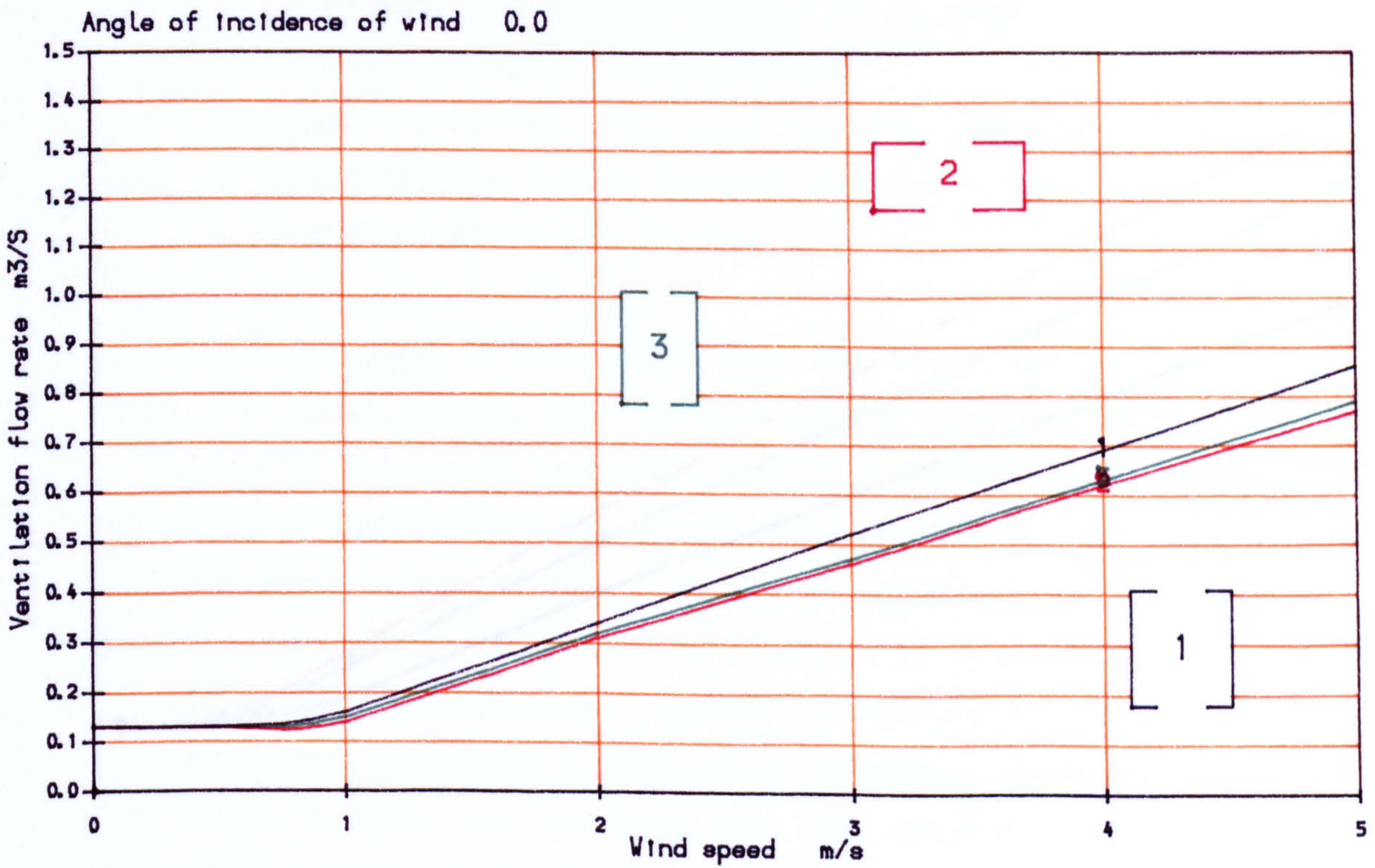
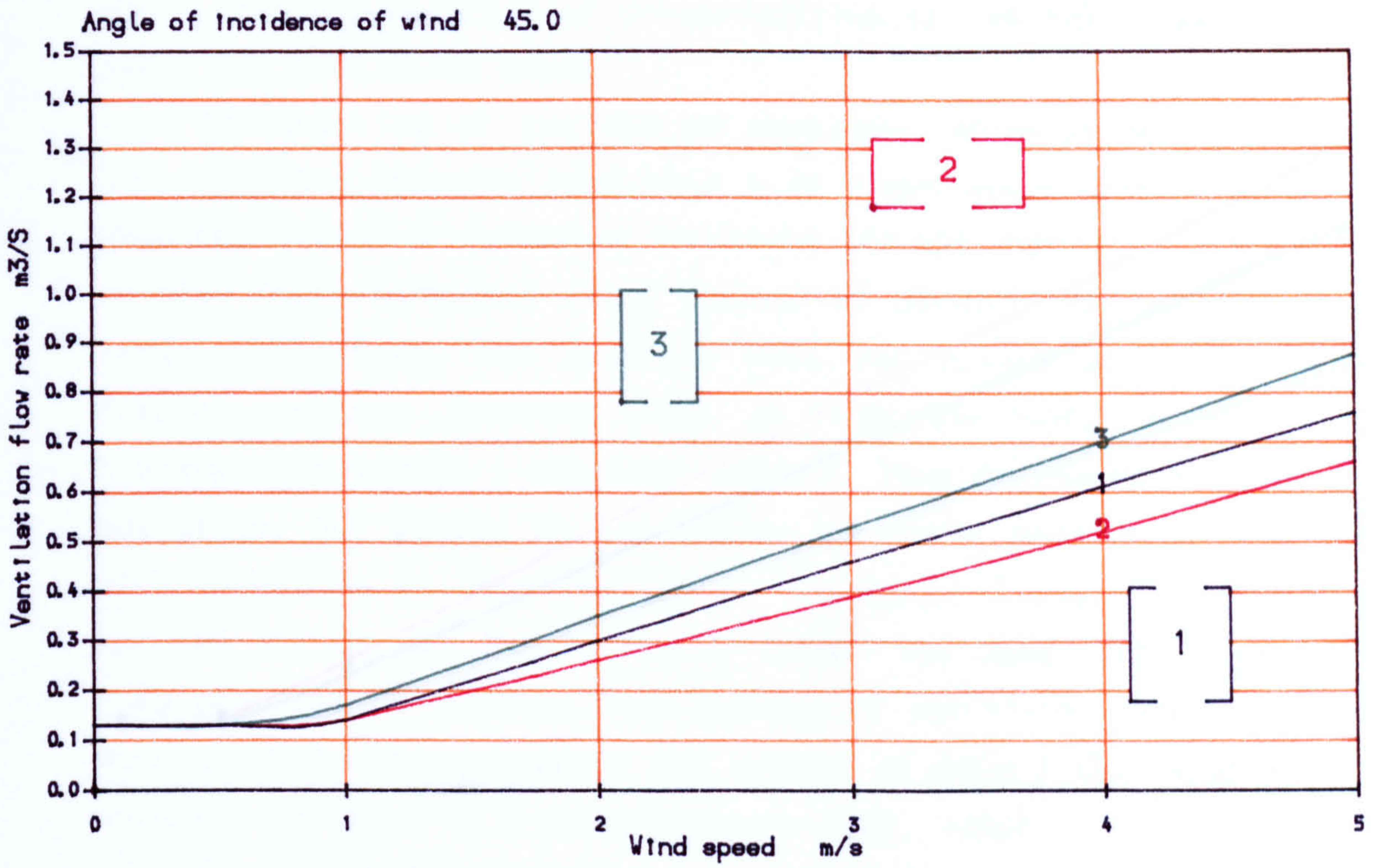
Figure 4.7 and 4.8 show the effect of building shape on the rate of ventilation in sheltered and semi sheltered areas. Two wind directions are considered and inlet and outlet areas are equal. It is shown that in sheltered areas with perpendicular wind, the ventilation rate is highest for a square building, but with diagonal wind, the oblong building will achieve about 20% more ventilation.

For all wind directions, in semi sheltered areas, the best result is obtained by oblong buildings, and the lowest rate is obtained by square buildings.

#### 4.3.3 Cross ventilation in multizone buildings

Achievement of unimpeded cross ventilation, as in buildings without internal divisions, is not easy and usually not feasible. To get complete cross ventilation, a room should either be exposed on more than one wall, or openings in internal partitions should be arranged so that they offer minimum resistance to air flow. For a more realistic view of natural ventilation, a multizone computer model based on the procedure described in (4.2.2) was developed. The

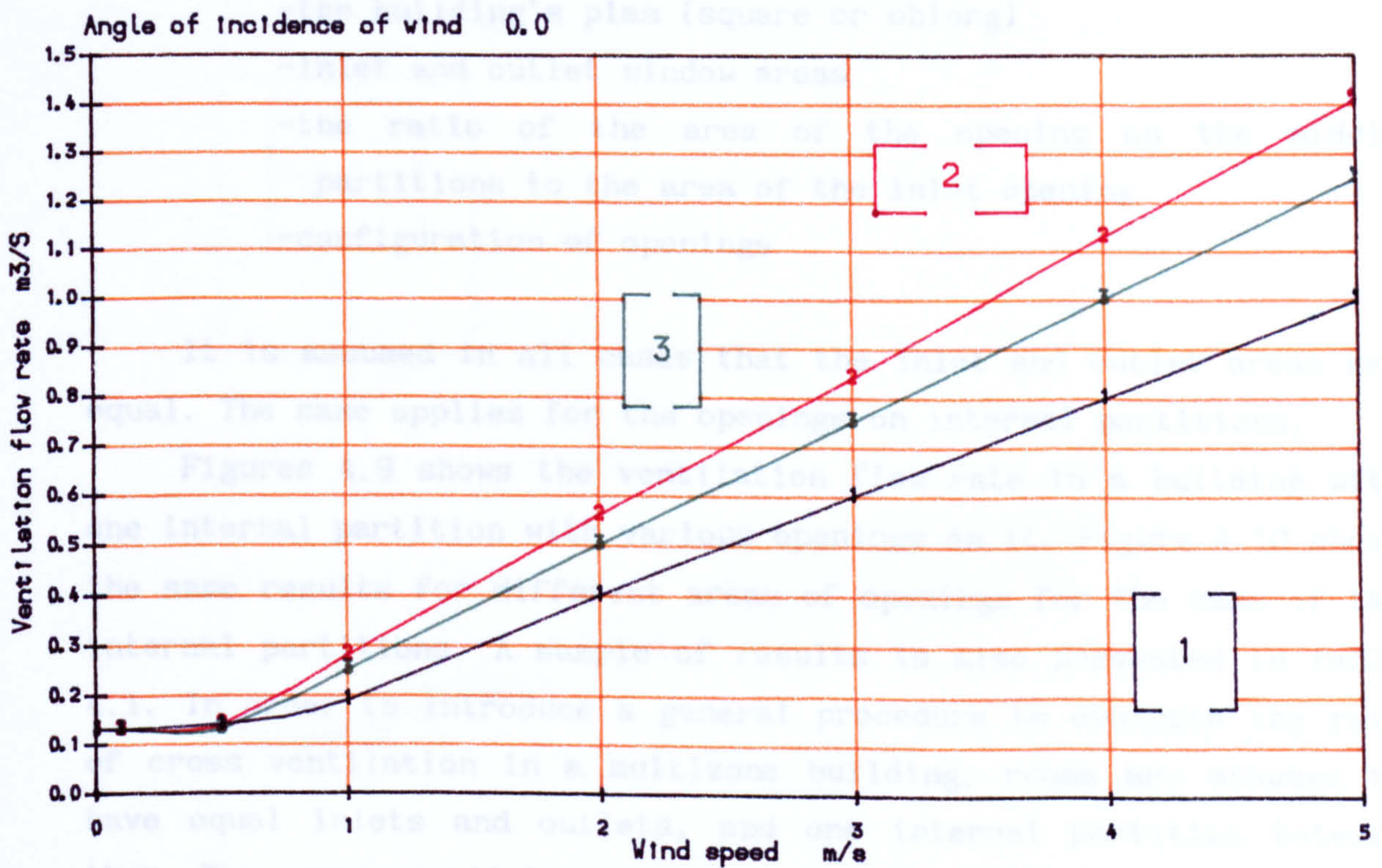
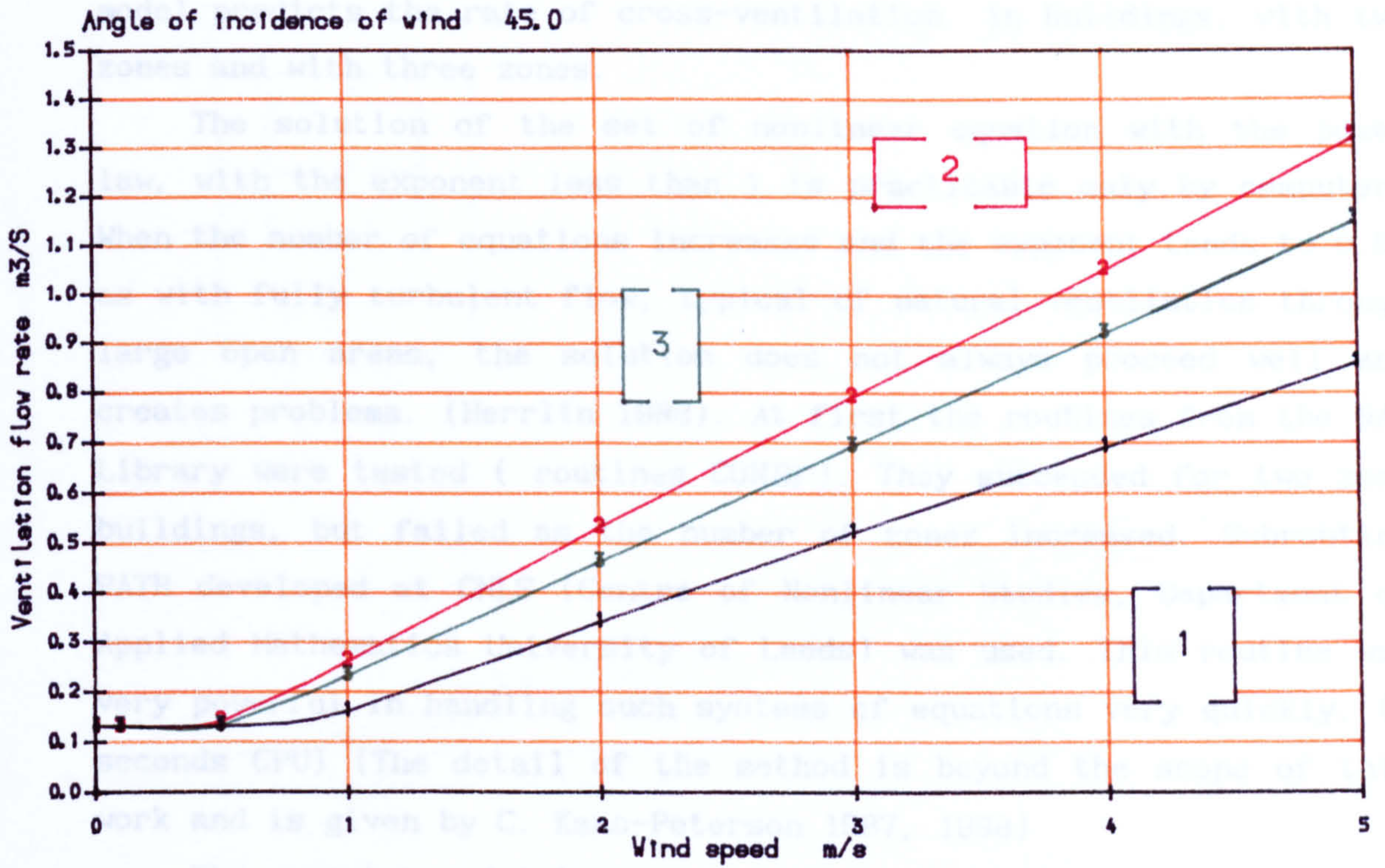




- 1 Square plan
- 2 Oblong plan (L/V = 1/2)
- 3 Oblong plan (L/V = 2)

Figure 4.7: Cross flow rate for different types of building plan

Location: Sheltered areas surrounded by buildings with the same height  
 0.9 m<sup>2</sup> inlet and 0.9 m<sup>2</sup> outlet area



- 1 Square plan
- 2 Oblong plan (L/V = 1/2)
- 3 Oblong plan (L/V = 2)

Figure 4.8: Cross flow rate for different types of building plan

Location: Semi sheltered (surrounded by buildings with 1/2 height of origin)  
0.9 m<sup>2</sup> inlet and 0.9 m<sup>2</sup> outlet area

model predicts the rate of cross-ventilation in buildings, with two zones and with three zones.

The solution of the set of nonlinear equation with the power law, with the exponent less than 1 is practicable only by computer. When the number of equations increases and the exponent tends to 0.5, as with fully turbulent flow, typical of natural ventilation through large open areas, the solution does not always proceed well and creates problems. (Herrlin 1988). At first the routines from the NAG Library were tested ( routines CONBF). They succeeded for two zone buildings, but failed as the number of zones increased. Subroutine PATH developed at CNLS (Centre of Nonlinear Studies, Department of Applied Mathematics University of Leeds) was used. This routine was very powerful in handling such systems of equations very quickly. (2 seconds CPU) (The detail of the method is beyond the scope of this work and is given by C. Kaas-Peterson 1987, 1988)

The computer model is used to explore cross ventilation with the following variables:

- the building's plan (square or oblong)
- inlet and outlet window areas
- the ratio of the area of the opening on the middle partitions to the area of the inlet opening
- configuration of openings

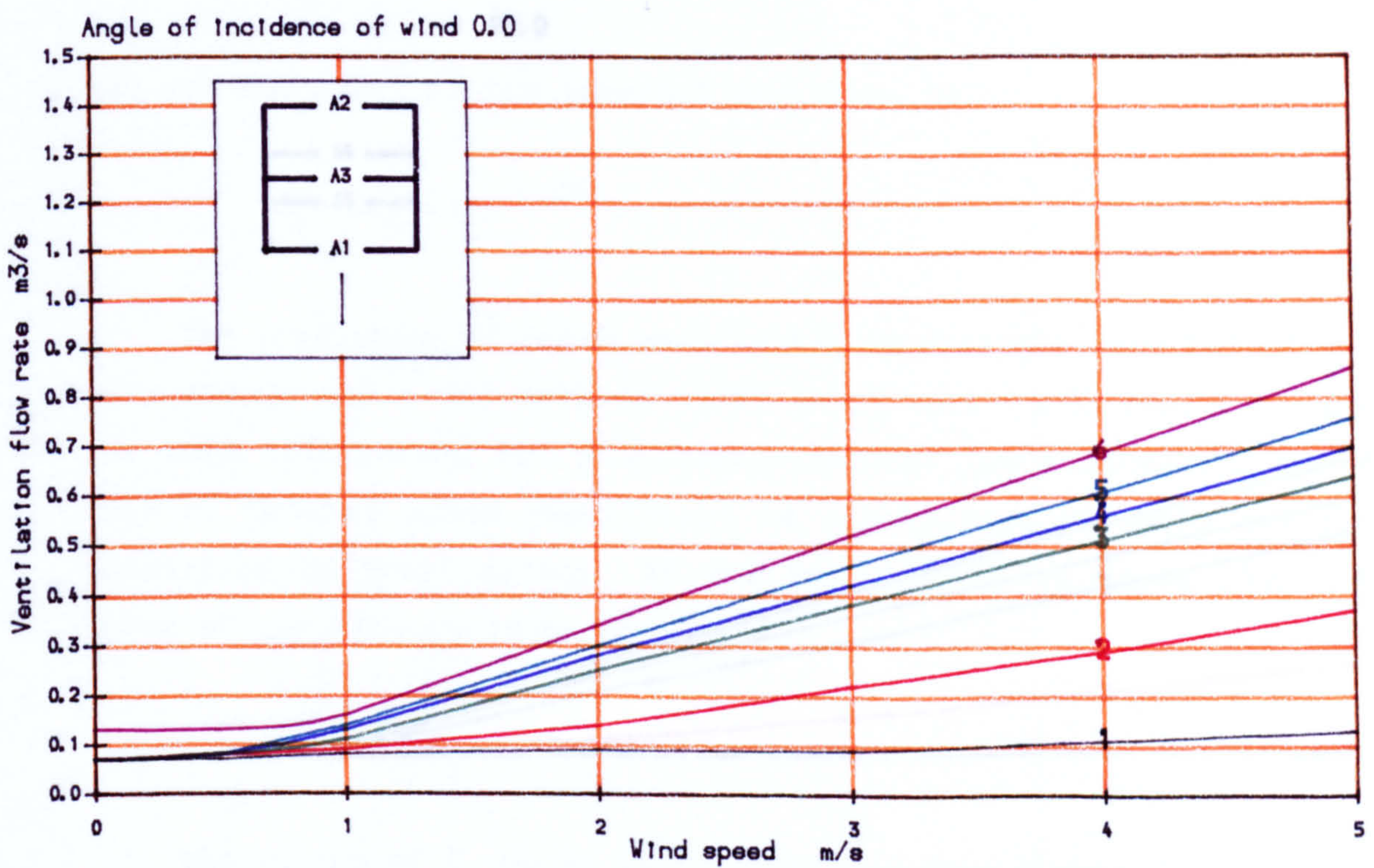
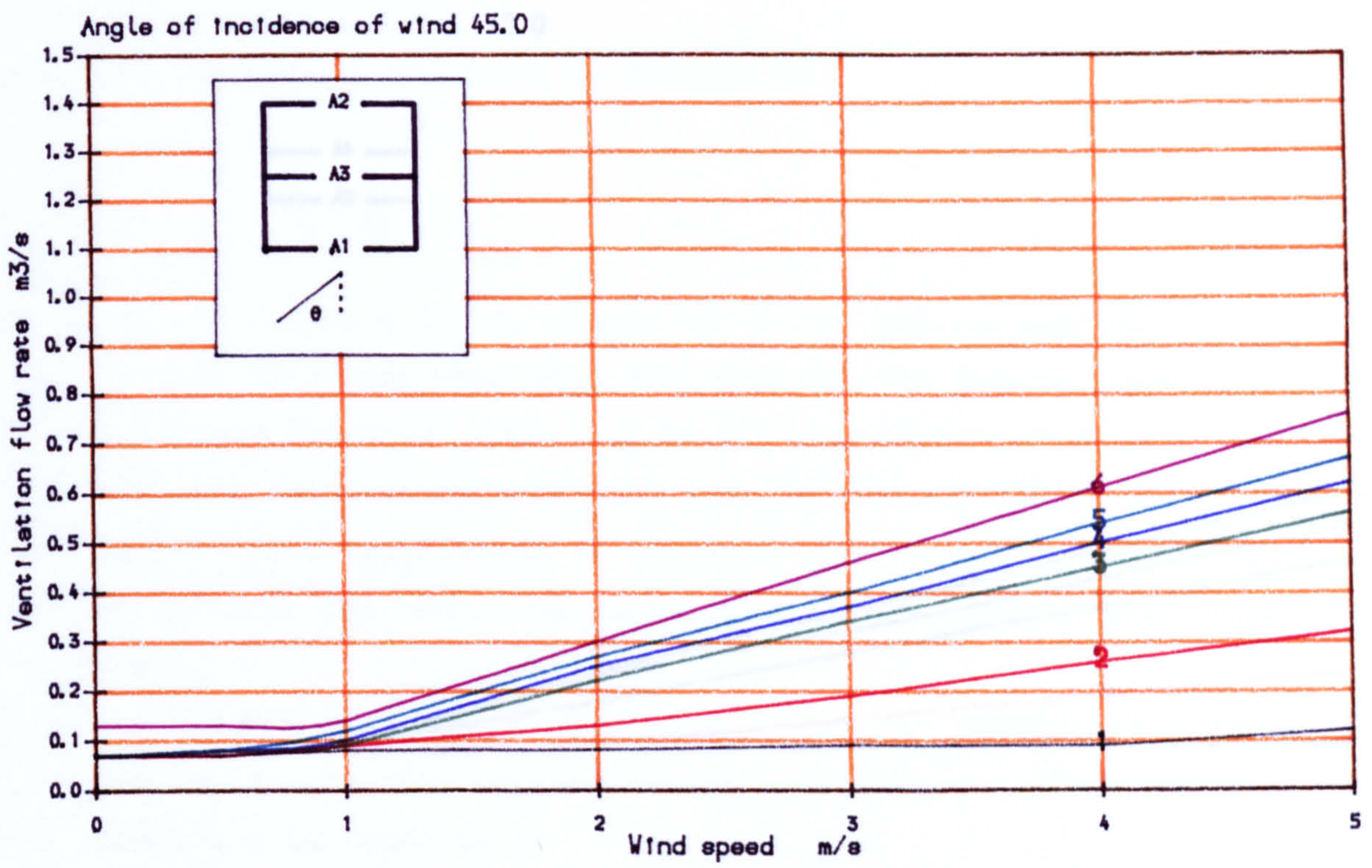
It is assumed in all cases that the inlet and outlet areas are equal. The same applies for the openings on internal partitions.

Figures 4.9 shows the ventilation flow rate in a building with one internal partition with various openings on it. Figure 4.10 shows the same results for different areas of openings for the case of two internal partitions. A sample of results is also presented in table 4.1. In order to introduce a general procedure to evaluate the rate of cross ventilation in a multizone building, rooms are assumed to have equal inlets and outlets, and one internal partition between them. The cross ventilation coefficient is defined by :

$$E_q = \frac{Q_f}{Q_c} \quad (4.11)$$

where

$Q_f$  = cross ventilation with a partitions in the middle  $m^3/s$   
 $Q_c$  = cross ventilation for the same building but with no internal partition  $m^3/s$



1  $A_3=0.1 \text{ m}^2$  1  
 2  $A_3=0.3 \text{ m}^2$  1  
 3  $A_3=0.7 \text{ m}^2$  2

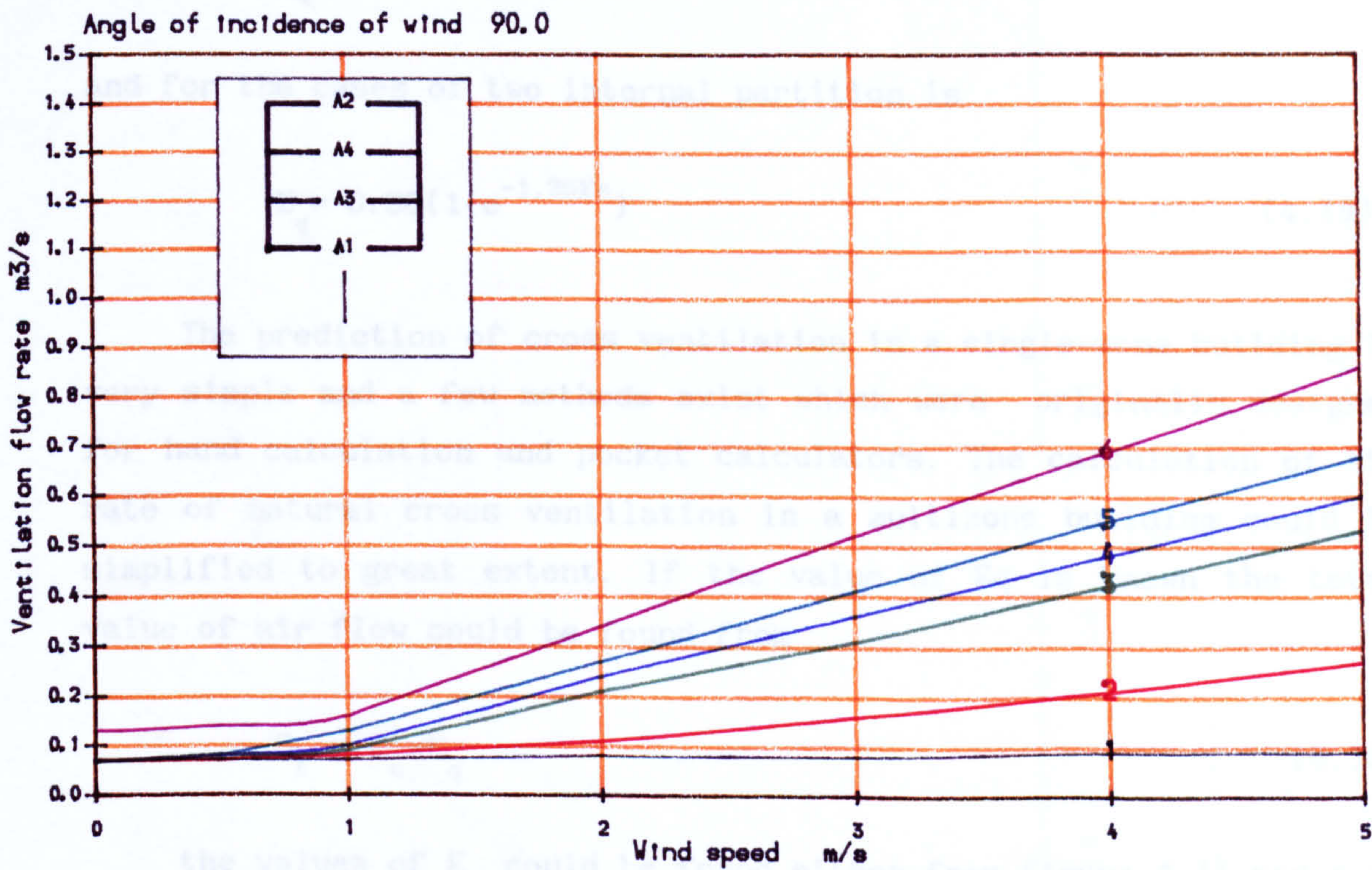
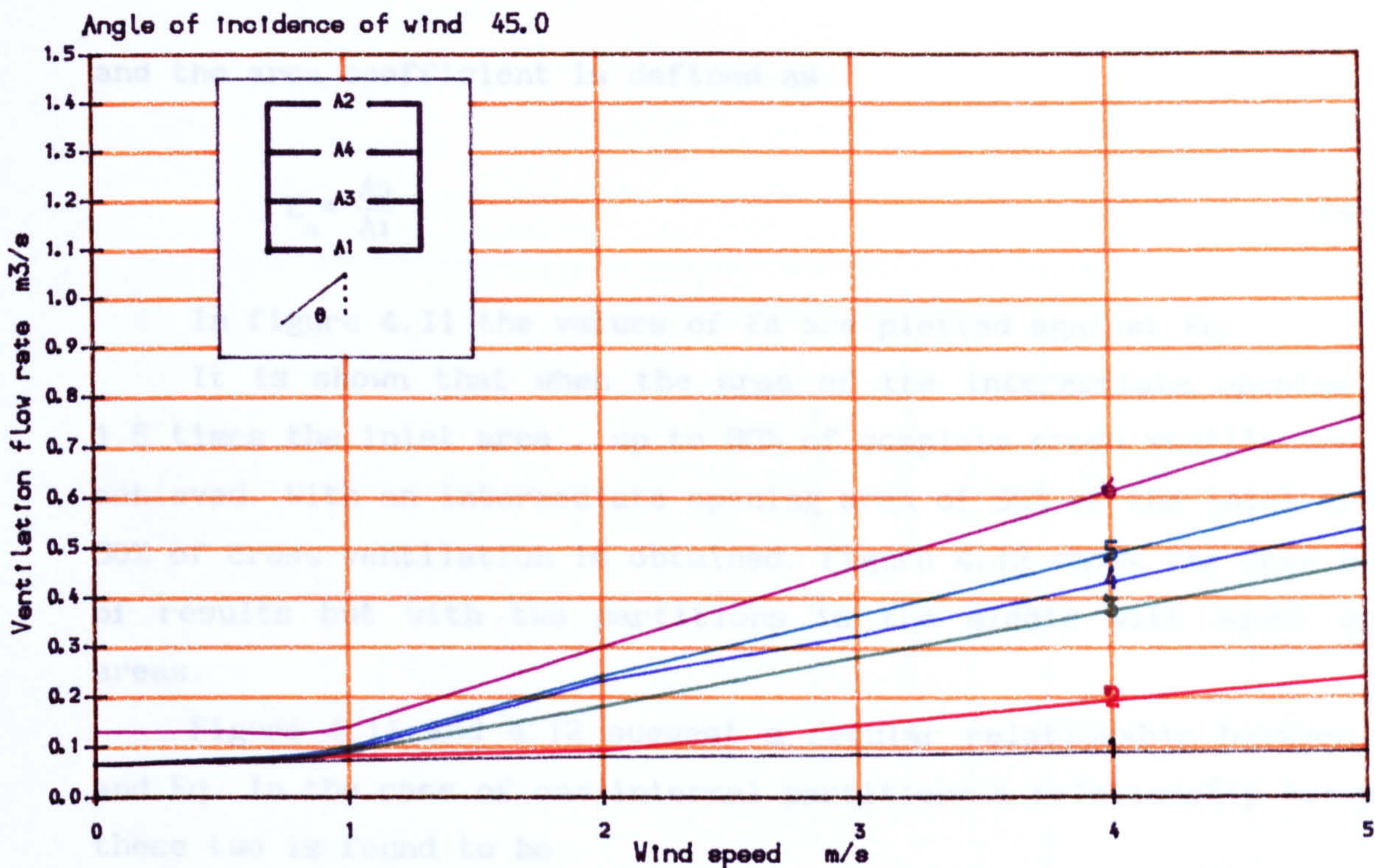
4  $A_3=0.9 \text{ m}^2$  3  
 5  $A_3=1.2 \text{ m}^2$  4  
 No internal partition

Figure 4.9: Cross flow rate for different opening area on internal partition

One internal partition in the middle

Location: Semi sheltered (surrounded by buildings with 1/2 height of origin)

$A_1=0.9 \text{ m}^2$  and  $A_2=0.9 \text{ m}^2$



- |   |               |   |                       |
|---|---------------|---|-----------------------|
| 1 | A3=A4= 0.1 m2 | 4 | A3=A4= 0,9 m2         |
| 2 | A3=A4= 0.3 m2 | 5 | A3=A4= 1.2 m2         |
| 3 | A3=A4= 0.7 m2 |   | No internal partition |

Figure 4.10: Cross flow rate for different opening area on internal partition

One internal partition in the middle  
 Location: Semi sheltered (surrounded by buildings with 1/2 height of origin)  
 A1=0.9 m2 and A2=0.9 m2

and the area coefficient is defined as

$$E_a = \frac{A_3}{A_1} \quad (4-12)$$

In figure 4.11 the values of  $E_a$  are plotted against  $E_q$ .

It is shown that when the area of the intermediate opening is 1.5 times the inlet area, up to 90% of complete cross ventilation is achieved. With an intermediate opening area of 50% of the inlet area, 50% of cross ventilation is obtained. Figure 4.12 shows the same kind of results but with two partitions in the middle with equal open areas.

Figure 4.11 and 4.12 suggest a regular relationship between  $E_a$  and  $E_q$ . In the case of one internal partition a relationship between these two is found to be

$$E_q = 0.98(1 - e^{-1.75E_a}) \quad (4.13)$$

and for the cases of two internal partition is

$$E_q = 0.98(1 - e^{-1.25E_a}) \quad (4.14)$$

The prediction of cross ventilation in a single-zone building is very simple and a few methods exist which were originally designed for hand calculation and pocket calculators. The calculation of the rate of natural cross ventilation in a multizone building could be simplified to great extent. If the value of  $E_q$  is known the total value of air flow could be found from

$$Q_f = Q_c \times E_q \quad (4.15)$$

the values of  $E_q$  could be found either from figure 4.11 and 4.12 directly or from equation 4.13 and 4.14.

#### 4.4 Summary and conclusion

Computer models were developed to predict the rate of natural ventilation through openings in buildings.

These models were used to quantify and identify the significance of design variables in achieving satisfactory ventilation in

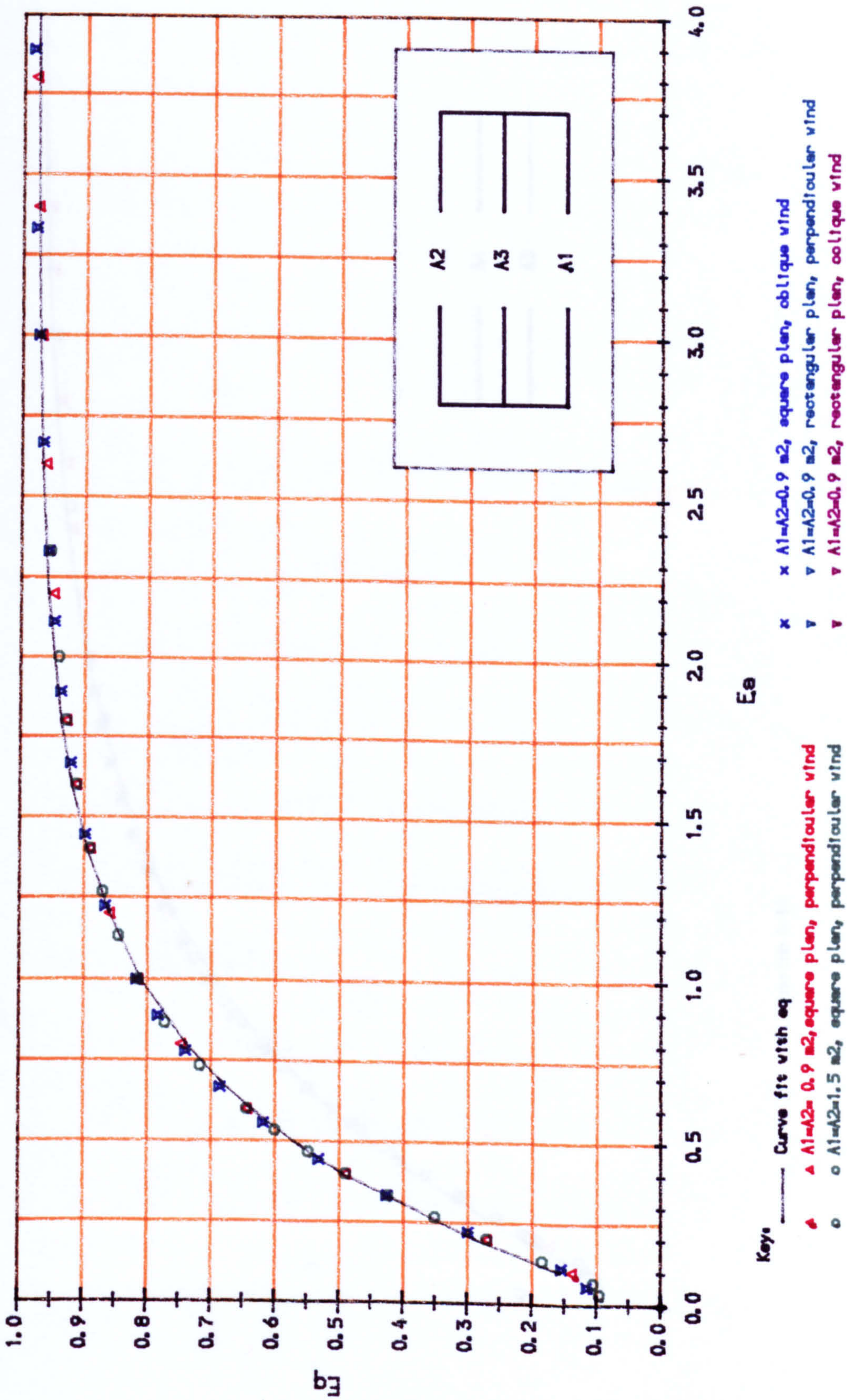


Figure 4.11. Relation between the middle opening coefficient and the flow coefficient  
 One internal partition in the room, equal inlet and outlet area

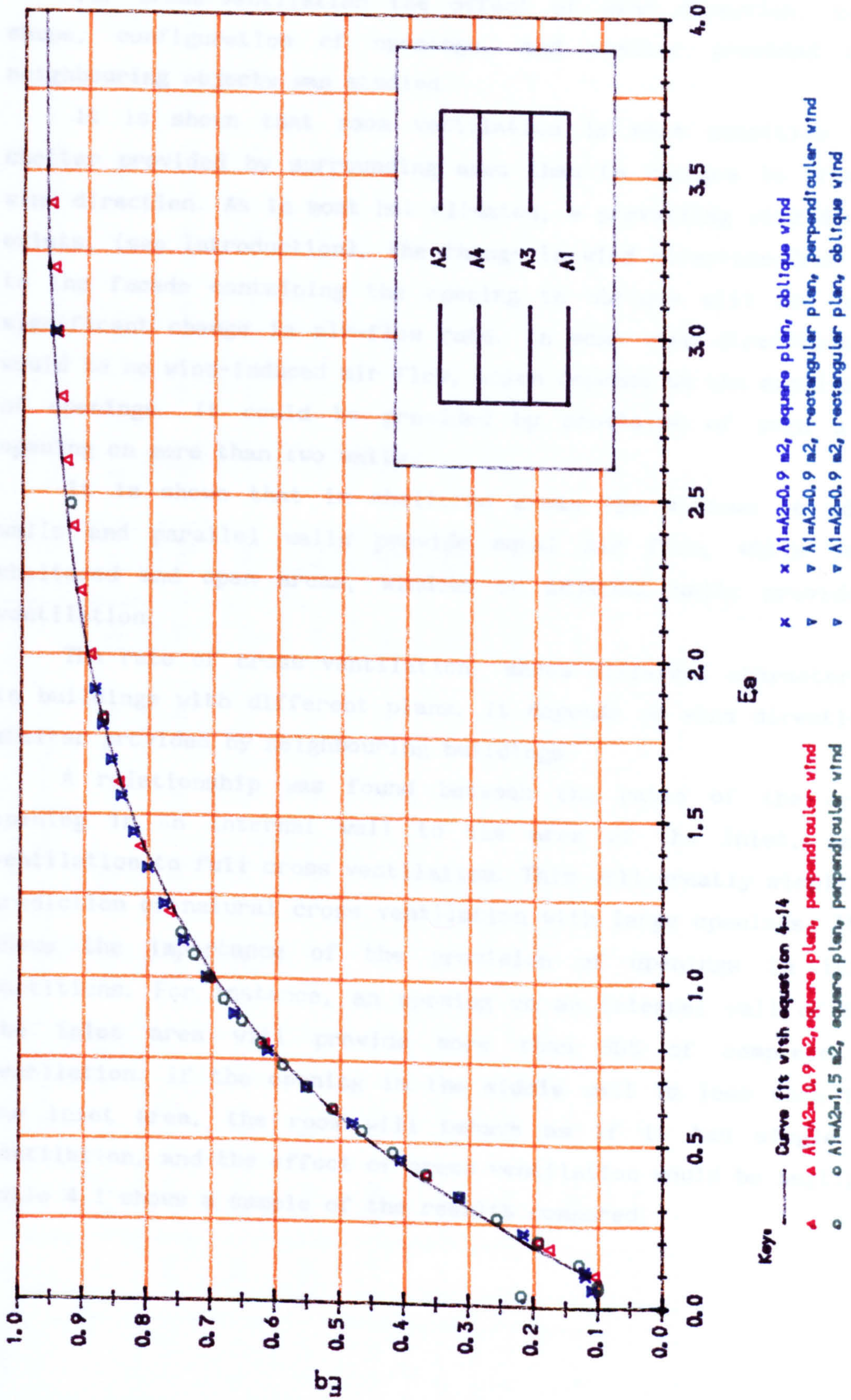


Figure 4.12. Relation between the middle opening coefficient and the flow coefficient  
Two internal partitions in the room, with equal opening areas, equal inlet and outlet areas



buildings in hot climates.

Theoretical examination shows that for single-sided ventilation, the rate of air flow could be increased by up to 50%, by appropriate design.

For cross-ventilation the effect of wind direction, building shape, configuration of openings, and shelter provided by the neighbouring objects was studied.

It is shown that room ventilation is more sensitive to the shelter provided by surrounding area than to changes in prevailing wind direction. As in most hot climates, a prevailing wind direction exists, (see Introduction), the change in wind direction from normal to the facade containing the opening to oblique will not cause a significant change in air-flow rate. In some wind directions there would be no wind-induced air flow, which depends on the configuration of openings. It could be provided by provision of even a small opening on more than two walls.

It is shown that in sheltered areas the windows on adjacent walls and parallel walls provide equal air flow, while in semi sheltered and open areas, windows on adjacent walls provide more ventilation.

The rate of cross ventilation shows different characteristics in buildings with different plans. It depends on wind direction and shelter provided by neighbouring buildings.

A relationship was found between the ratio of the area of opening in an internal wall to the area of the inlet, and the ventilation to full cross ventilation. This will greatly simplify the prediction of natural cross ventilation with large openings. It also shows the importance of the provision of openings in internal partitions. For instance, an opening on an internal wall of 50% of the inlet area will provide more than 50% of complete cross ventilation. If the opening in the middle wall is less than 1/5 of the inlet area, the room will behave as if it had single sided ventilation, and the effect of cross ventilation would be negligible. Table 4.1 shows a sample of the results compared.

Table 4.1: Comparison of the ventilation flow rate in single sided, single-zone and multi-zone cross ventilation  $m^3/s$ 

Wind sp. m/s	Single Sided	One Zone	TWO ZONES										THREE ZONES									
			Area of the opening in the middle ( $m^2$ )										Area of the openings in the middle									
			0.1	0.2	0.3	0.5	0.7	0.9	1.2	1.5	0.1	0.2	0.3	0.5	0.7	0.9	1.2	1.5				
5.0	0.13	0.86	0.13	0.26	0.37	0.53	0.64	0.70	0.76	0.79	0.09	0.18	0.27	0.41	0.53	0.60	0.68	0.70				
4.0	0.12	0.69	0.11	0.21	0.29	0.43	0.51	0.56	0.61	0.63	0.09	0.14	0.21	0.33	0.42	0.48	0.55	0.59				
3.0	0.14	0.52	0.09	0.15	0.22	0.32	0.38	0.42	0.46	0.48	0.08	0.11	0.16	0.25	0.31	0.36	0.41	0.44				
2.0	0.12	0.34	0.08	0.10	0.14	0.21	0.25	0.28	0.30	0.32	0.07	0.09	0.11	0.17	0.21	0.24	0.27	0.29				
1.0	0.11	0.16	0.07	0.08	0.09	0.09	0.11	0.13	0.14	0.15	0.07	0.08	0.08	0.09	0.09	0.10	0.13	0.14				
0.5	0.11	0.13	0.07	0.07	0.08	0.08	0.08	0.08	0.08	0.08	0.07	0.07	0.07	0.07	0.08	0.08	0.08	0.08				
0.1	0.11	0.13	0.07	0.07	0.07	0.07	0.07	0.07	0.07	0.07	0.06	0.07	0.07	0.07	0.07	0.07	0.07	0.07				
0.0	0.11	0.13	0.07	0.07	0.07	0.07	0.07	0.07	0.07	0.07	0.06	0.07	0.07	0.07	0.07	0.07	0.07	0.07				

Inlet area =  $0.9 m^2$ Outlet area =  $0.9 m^2$ Angle of incidence of the wind =  $0.0$ Total area for single sided ventilation =  $0.9 m^2$ 

Square plan

Total area of when single side  $0.9 m^2$

## CHAPTER FIVE

### *MATHEMATICAL MODELS AND COMPUTER PROGRAMS*

#### **5.1 Introduction:**

A thermal model is made up of constituents. First the physical model of a building is presented as a thermal network, where some approximations have to be made. The heat transfer between the elements of the thermal network is then expressed by mathematical equations, where some other assumptions and approximations are also made.

#### **5.2 Thermal models**

In order to evaluate the effect of the approximations made in each model and also to find the importance of each constituent of a thermal model, several thermal models of a room are developed. The results obtained from observations are then compared with those from different models. The effect and importance of each parameter is evaluated.

The models considered in the present study are different in

- the number of nodes in the thermal circuit
- the treatment of unsteady heat conduction
- the treatment of convective heat transfer
- the treatment of ventilation
- the treatment of heat loss through open windows

##### **5.2.1 Number of nodes**

The number of surfaces in a model influences the accuracy of the longwave radiation exchange calculation among internal surfaces and also determines the number of heat flow paths in the thermal model. In the most detailed model each surface should be presented by a single independent node. In a model representing a room similar to the one used in the observation, with two openings, and six surfaces, this will lead to a model of eight convective heat flow paths from

the surface to the air point, and 26 radiative paths among the surfaces, along with eight conductance/capacitances, related to each node. This model will be referred to as the 'nine node model'. The thermal circuit representing such a model is shown in figure 5.1.

Simplification can be introduced by reducing the number of surfaces. If the surface of each opening is combined with the wall containing it as a single node, the number of surfaces will reduce to six. This will simplify the internal heat flow paths and reduce the number of heat flow equations. The physical properties of the common node will be represented by area averaged properties of the two parts. This model will be referred as the 'seven node model', and the thermal circuit is shown in figure 5.2.

In a further simplification all surfaces of the internal walls, the floor and the ceiling, are assumed to be at the same temperature and are represented as a single node. The internal surface of the external wall is shown by another node. These two nodes with the air point will comprise a 'three node model'. The thermal network will be simplified greatly. Figure 5.3 shows the corresponding thermal circuit. If the internal surfaces of the external wall are shown by subscript j and all other surfaces by i the shape factor between these two nodes could be calculated from the general relationship :

$$F_{ij} \cdot A_i = F_{ji} \cdot A_j \quad (5-1)$$

where

$$A = \text{area} \quad \text{m}^2$$

$$F_{ij} = \text{shape factor between surface } i \text{ and } j$$

The shape factor between the internal surface and its surrounding surfaces is unity so that :

$$F_{ij} = \frac{A_i}{A} \quad (5.2)$$

The overall heat transfer coefficient for long wave radiation

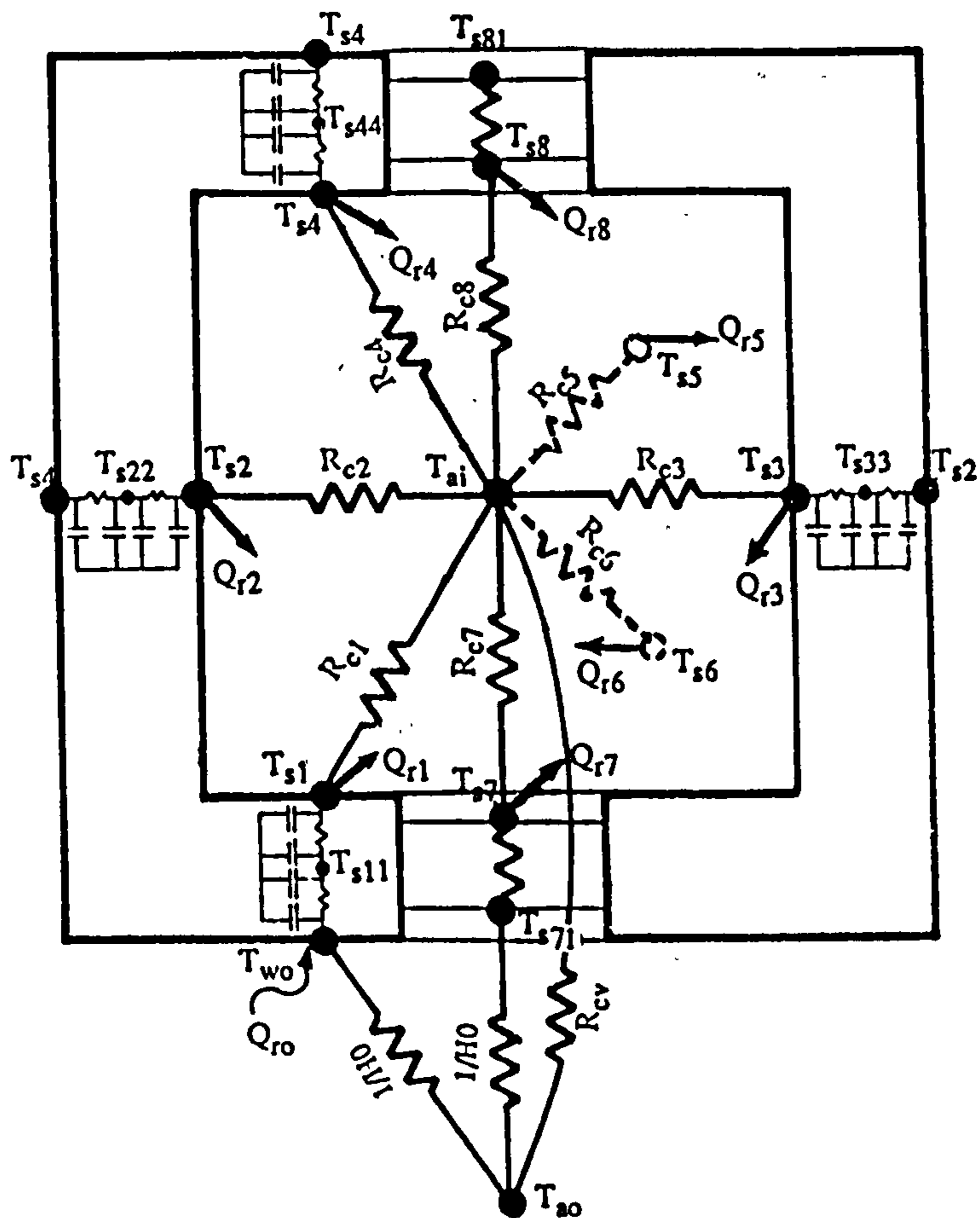


Figure 5.1: Electrical analogue of the test room, nine nodes model.

$Q_r$  = heat flux leaving the surface by radiation

$R_{ci} = 1/hci$

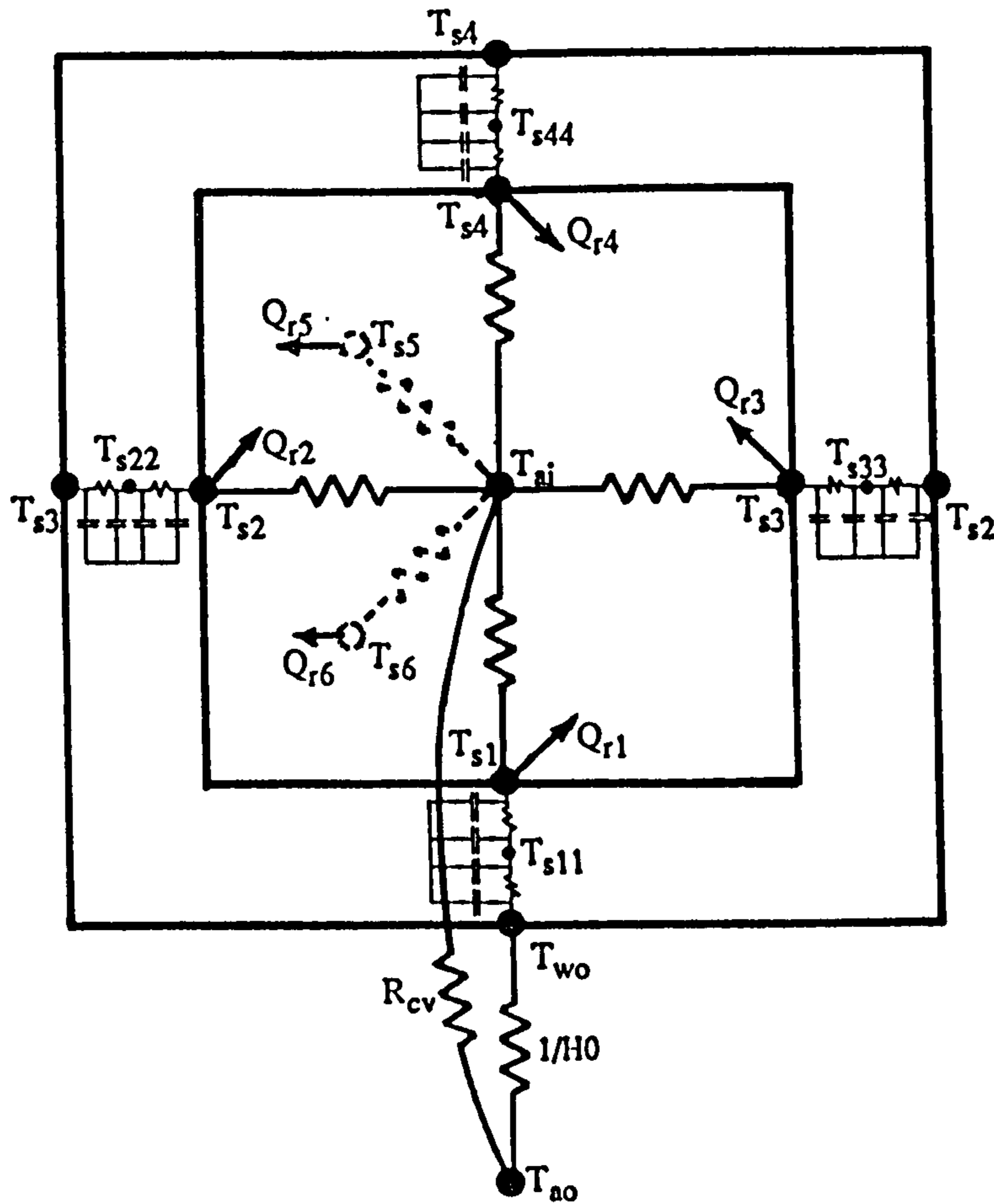


Figure 5.2: Electrical analogue of the test room, seven nodes model.

$Q_r$  = heat flux leaving the surface by radiation

$R_{ci} = 1/hci$



between two nodes representing the surfaces could be found from :

$$h_{r1j} = \sigma \bar{T}^3 \left[ \frac{1-\epsilon_1}{\epsilon_1} + \frac{1}{F_{1j}} + \frac{A_j}{A_1} \left( \frac{1-\epsilon_2}{\epsilon_2} \right) \right]^{-1} \quad (5-3)$$

The physical property of each node in the circuit is the area average of the surfaces combined into the node.

These models are used to investigate the effect of the number of surfaces in a model and treatment of radiation between surfaces.

Another model used is the 'environmental temperature model', which is a simplification of the three nodes model. The environmental temperature model is used in the Admittance Method, of which the detail is given in Chapter Three. The way the method is used in this study is given below when the Harmonic Method is discussed (see 5.5).

### 5.2.2 Unsteady heat conduction:

One of the major constituents of a model is the treatment of unsteady heat conduction. Three different techniques are used ; the Harmonic Method, the Response Factor Method and Finite Difference Method. ( see chapter 2). The Harmonic Methods is only used in the Admittance Method with the environmental temperature model. Finite Difference technique and the Response Factor method are used in the multi-exchange model. The detail of each model is given below.

### 5.2.3 Air ventilation :

When fresh air enters a room three extremes of mixing may occur as shown in figure 5.4 perfect mixing, displacement flow and short circuiting. (LIDDAMENT 1987b).

Perfect mixing takes place if the incoming air continuously and uniformly mixes with all the air present. In this way the room air temperature is considered to be the same throughout the room and the air leaving the room is considered to be at the temperature of the air in the room. The heat loss by ventilation is given by:

$$Q_v = c_p \rho V_o l (T_{ao} - T_{al}) \quad W \quad (5-4)$$

and the ventilation conductance is given by:

$$C_v = c_p \rho V_o l \quad W/K \quad (5.5)$$



Displacement flow occurs when fresh air entering the room displaces the room air without mixing with it. In this way the air temperature is considered to increase along its journey through the room. In this case it is a reasonable assumption to consider the room air temperature to be between that of the air entering the room and that of the air leaving the room. The heat loss by ventilation is then:

$$Q_v = c_p \rho V_{ol} (T_{out} - T_{in}) \quad \text{W} \quad (5-6)$$

where

$$\begin{aligned} T_{in} &= \text{air temperature of the air entering the room} = T_{ao} \quad ^\circ\text{C} \\ T_{out} &= \text{air temperature of the air leaving the room} \quad ^\circ\text{C} \\ T_{al} &= (T_{ao} + T_{out})/2 \quad ^\circ\text{C} \end{aligned}$$

from equation 5.6

$$Q_v = c_p \rho V_{ol} \times 2 (T_{al} - T_{ao}) \quad \text{W} \quad (5-7)$$

and the ventilation conductance as

$$C_v = 2 \rho c_p V_{ol} \quad \text{W/K} \quad (5-8)$$

Short-circuiting is the poorest ventilation condition. Part of the room is ventilated by displacement and part is not ventilated at all. This will often happen with mechanical ventilation.

In practice a combination of these different modes of ventilation may apply, also conditions will be changed by the occupants. In the present study only the first two mechanisms are considered.

#### 5.2.4 Convective heat transfer coefficient:

As discussed in chapter 2, heat transfer between a surface and air depends on the temperature difference between the air and the surfaces, the air velocity and the convection characteristics. Values are given by equations (2.2) to (2.5). In practical analysis, the coefficient might have to be given by a fixed value. In order to investigate its sensitivity and importance, two approaches are used. In the first it is calculated for each time interval as the calculation proceeds, and in the second, fixed values are used as

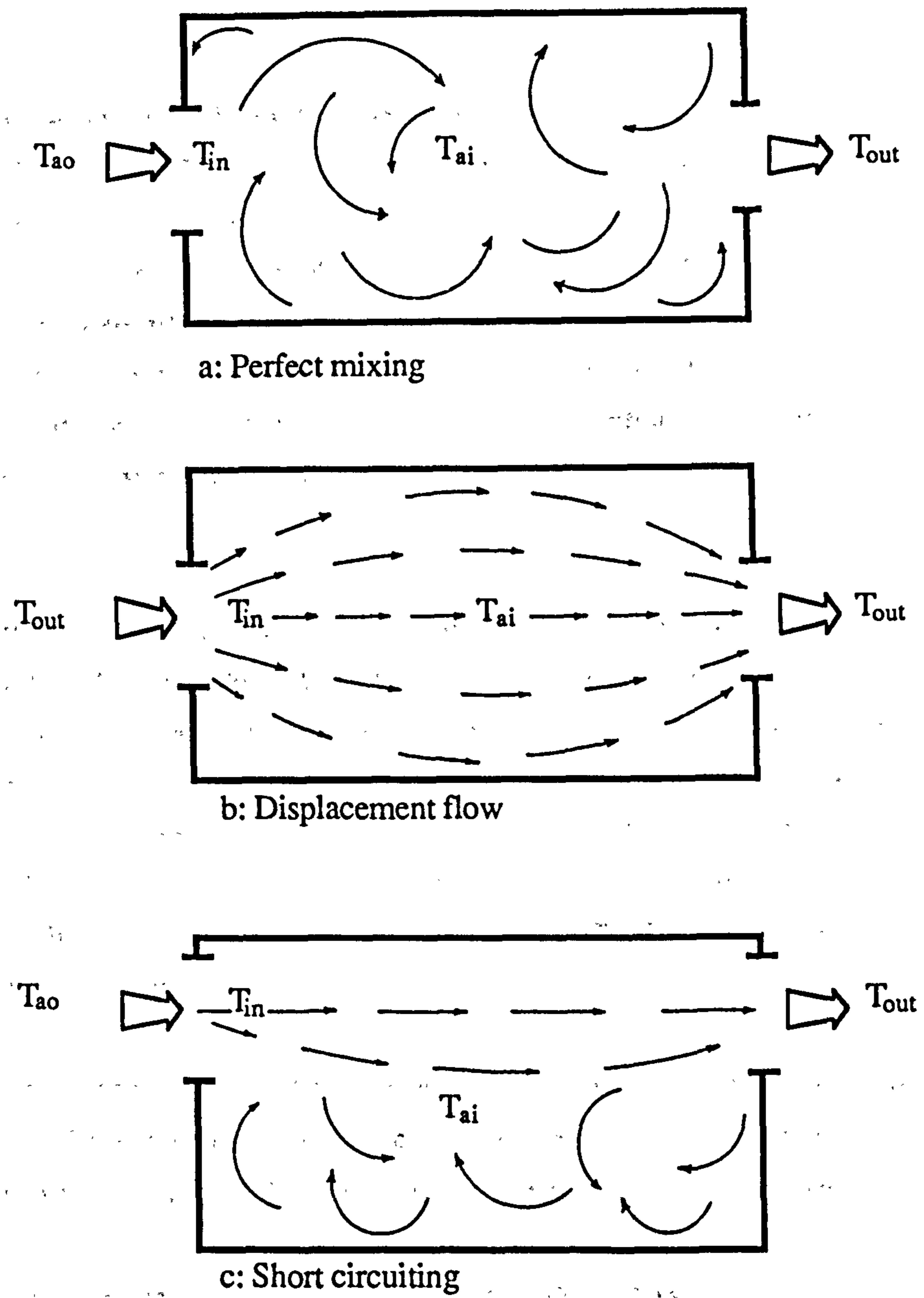


Figure 5.4: Types of ventilation air mixing in a room

suggested by the CIBSE Guide, which gives 3.0, 1.5 and 4.5 W/m<sup>2</sup> K for vertical surfaces, and for horizontal surfaces with the heat flow downward and upward respectively.

#### 5.2.5 Longwave radiation through open windows:

During ventilation, some energy will be lost by longwave radiation through open windows. In order to account for this mechanism of heat transfer, long wave radiation heat transfer is assumed to take place between each surface of the room and the window surface, considered to be at the temperature of the outside air. This is achieved by individual calculations of shape factors between the room surfaces and the opening. This is only possible in the nine node model.

Several models have been developed, combining the variations described, with different methods of solution of the unsteady heat conduction problem. The nomenclature used is that designated at the beginning of each model shows the method of unsteady heat conduction solution, and the number following shows the assumptions made. For example FINIT 9-1 shows the Finit Difference technique and nine node model with the assumptions of group 1. Table 5.1 summarizes these different assumptions.

These assumptions in the multi-exchange model are used in the finite difference and response factor methods. The harmonic methods are applied only to the environmental temperature model. In this case, two different approaches are used. First, the standard admittance procedure as given by CIBSE Guide A-5 is used, and is available in the BRE Package. (BLOOMFIELD 1983) The second method was the same, but the first six harmonics are considered. The following is the description of each technique.

Table 5.1: Different assumptions of multi-exchange model

		9 nodes				7 nodes				3 nodes		
Convective coefficient	Fixed		○						○	○		
	Variable	○		○	○	○	○	○			○	○
Ventilation	Mixed	○	○		○	○	○		○	○	○	
	Not mixed			○				○				○
Radiation through window	Closed	○	○	○		○	○	○	○	○	○	○
	Open				○							
Air thermal capacity	None					○				○	○	○
	Yes	○	○	○	○		○	○	○			
Models		FINIT 9.1	FINIT 9.2	FINIT 9.3	FINIT 9.4	FINIT 7.1	FINIT 7.2	FINIT 7.3	FINIT 7.4	FINIT 3.1	FINIT 3.2	FINIT 3.3

### 5.3 Finite Difference Model:

In building applications the heat flow into slabs can be described by a simple one dimensional heat conduction equation. The general equation of heat flow into a slab is the Fourier equation which, for one directional flow, states that the rate of increase of temperature with time is proportional to the rate of change of the temperature gradient with distance which leads to

$$\frac{\partial T}{\partial t} = \frac{\lambda}{\rho c_p} \frac{\partial^2 T}{\partial x^2} \quad (5.9)$$

Temperature  $T$  is a function of time  $t$  and distance  $x$  from the free space, shown as

$$T = T_{x,t} \quad (5.10)$$

The solution of equation 5.9 is by numerical approximation. As stated above (2-4) either the explicit or the implicit method may be used. In the present study the implicit method is used which has the great advantage of being unconditionally stable, for all time increments and distances. The accuracy of the results is a function of

increments and distances. The accuracy of the results is a function of the time intervals and space increments.

The number of nodes in any homogeneous layer of a slab using a finite difference approximation was studied by Clarke(1978). He has suggested that for the purpose of transient conduction modelling with multilayer composites, a spatial discretisation scheme equal to three nodes for homogeneous elements will give acceptable accuracy in buildings. He has compared the temperature and heat flux variations at the internal and the external boundary surfaces of two similar slabs, one divided into three, and the other into fifteen nodes. The difference was found to be negligible.

For the present models, three nodes are allocated for each homogenous layer in the slab, one to each boundary and one in the middle. A thermal network similar to figure 5.1 is used for the heat balance equation for each surface.

In general, any node at the boundary between different homogeneous elements will represent mixed thermal property regions. Nodes at the extreme surfaces undergoing convective, radiative and conductive heat exchange will have associated with them thermal capacity equal to some fraction of the capacity of the "next to the surface node".

### 5.3.1 Heat balance equation for different nodes in the model:

The first boundary condition will be obtained from the heat balance at the outer face of the external wall. The energy input at this point is partly conducted deeper into the wall and partly lost to the outside by convection and longwave radiation, therefore the heat balance for the external surface (shown by subscript  $s_o$ ) would be

$$Q_o = A_w H (T_{s_o,t} - T_{a_o,t}) - A_w \lambda \frac{\partial T}{\partial X} \Big|_{x=0} \quad (5.11)$$

where

$$\begin{aligned} A_w &= \text{Area of the wall} && \text{m}^2 \\ \lambda_w &= \text{Thermal conductivity} && \text{W/m K} \\ T_{a_o} &= \text{Outside air temperature} && \text{°C} \end{aligned}$$

and  $Q_o$  is the energy input at the outside surface of the external wall. If solar energy is absorbed by the external surface it is equal to

$$Q_o = A I_s \alpha_s \quad (5.12)$$

$\alpha_s$  = the solar absorptivity of the external wall

$I_s$  = total solar intensity  $W/m^2$

$H_o$  is the total coefficient for convective and radiative heat transfer of the outside wall and is based on the assumption that the heat flow by both radiation and convection is proportional to the temperature difference of outside air and the surface. It is valid only for the radiative contribution if the relevant temperature difference be small. (MITALAS 1965)

$$H_o = \epsilon h_r + h_{co} \quad (5.13)$$

where

$\epsilon$  = emissivity of the external wall

$h_r$  = radiative conductance coefficient  $W/m^2K$

In the case of window glass, the above equation will be used the same way but the absorptivity of glass is very low ( $\gamma = 0.05$ )

The finite difference approximation of the above equation, using the unknown temperatures in the future time row, will result in:

$$(T_{so,t+dt} - T_{so,t}) A_w \frac{c_p \rho dx}{2dt} + A_w \frac{T_{so,t+dt} - T_{s11,t+dt}}{\frac{dx}{\lambda_w}} + A_w \frac{T_{so,t+dt} - T_{s11,t+dt}}{\frac{dx}{\lambda_w}} = Q_{o,t+dt} \quad (5-14)$$

$T_{s11}$  is the temperature in the middle of the external wall

Assuming the temperature at time  $t$  known, and arranging the equation gives

$$T_{so,t+dt} \left( 1 + \frac{2\lambda dt}{c_p \rho dx^2} + H_o \frac{2dt}{c_p \rho dx^2} \right) + T_{s11,t+dt} \left( \frac{-2\lambda dt}{c_p \rho dx^2} \right) = T_{ao,t+dt} \left( H_o \frac{2dt}{c_p \rho dx^2} \right) + T_{so,t} + Q_{o,t+dt} \quad (5.15)$$

The heat balance equation for the internal node at the middle of the external wall in the same way will be:

$$(T_{s11,t+dt} - T_{s11,t}) \frac{c_p \rho dx}{dt} + \frac{T_{s11,t+dt} - T_{so,t+dt}}{\frac{dx}{\lambda_w}} + \frac{T_{s11,t+dt} - T_{s1,t+dt}}{\frac{dx}{\lambda_w}} = 0 \quad (5.16)$$

and the same way rearrangement of equation 5.16 gives

$$T_{so,t+dt} \left( \frac{-\lambda dt}{c_p \rho dx^2} \right) + T_{s11,t+dt} \left( 1 + \frac{2\lambda dt}{c_p \rho dx^2} \right) + T_{s1,t+dt} \left( \frac{-\lambda dt}{c_p \rho dx^2} \right) = T_{s11,t} \quad (5.17)$$

The second boundary condition is obtained from the heat balance at the internal surfaces of the enclosure. The algebraic sum of the energy input and the heat transfer component resulting from the three heat transfer mechanisms, (conduction, convection and radiation is zero. This is the basis of the heat transfer equation and boundary condition for all internal surfaces. Therefore the heat conducted and heat input to the surface is balanced by the heat lost by convection to the inside air, and by longwave radiation between the room's surfaces each presented by single separate nodes the resulting equation is

$$A_i h_{ci} (T_{ai} - T_i) + A_i \sum_{j=1}^J h_{r1j} (T_j - T_i) - A_i \lambda_i \left. \frac{\partial T}{\partial x} \right|_{x=1} = Q_i \quad (5-18)$$

where

$h_{r1j}$  = Configuration factor between surface  $i$  and  $j$

$Q_i$  = energy input to the surface  $i$  W

$h_{ci}$  = convective heat transfer coefficient  $W/m^2K$

This is the general equation for the heat balance at the internal surfaces.  $J$  shows the number of surfaces in the room and depends on the number of nodes representing the room surfaces. The implicit finite difference representation of equation 5.18 for surfaces at time  $t+dt$  shown as  $T_{s1,t+dt}$  is

$$\begin{aligned}
& (T_{si,t+dt} - T_{si,t}) A_1 \frac{c_p \rho dx}{2dt} + A_1 h_{ci} (T_{ai,t+dt}) + \sum_1^J h_{rij} (T_{sj,t+dt} - T_{si,t+dt}) \\
& + A_1 \frac{T_{si,t+dt} - T_{si-dx,t+dt}}{\frac{dx}{\lambda_s}} = Q_{i,t+dt} \quad (5-19)
\end{aligned}$$

and rearrangement in the same way for the external surface will result

$$\begin{aligned}
& T_{si-dx,t+dt} \left( \frac{-2\lambda dt}{c_p \rho dx^2} \right) + T_{si,t+dt} \left( 1 + \frac{2\lambda dt}{c_p \rho dx^2} + \frac{2dt}{c_p \rho dx} h_{ci} + \frac{2dt}{c_p \rho dx} \sum_{j=1}^J h_{rij} \right) + \\
& \sum_{j=1}^J \left( \frac{-2dt}{c_p \rho dx} h_{rij} T_{sj,t+dt} \right) + T_{ai,t+dt} \left( -h_c \frac{2dt}{c_p \rho dx} \right) = T_{si,t} - Q_{i,t+dt} \quad (5.20)
\end{aligned}$$

The next boundary condition is obtained from the heat balance at the air point. The heat loads at the air point are: the cooling or heating of the ventilating air, and the heat loss or gain by convection to the inside surfaces. The heat balance of the inside air is:

$$\frac{\partial T_{ai}}{\partial t} = \frac{1}{B} (Q_c + Q_v + Q_{ai}) \quad (5.21)$$

where

$Q_c$  = the rate of heat gain or loss by room air from the room envelope by convection

$$= \sum_{j=1}^J A_j h_{cj} (T_j - T_{ai}) \quad W$$

$Q_{ai}$  = the energy input directly to the air eg. by the plant

$Q_v$  = the heat input component to the air by entilation

$$= C_v (T_{ao} - T_{ai}) \quad W$$

$$C_v = N \rho_a c_p Vol \quad W/K$$

$C_p$  = specific heat capacity of air  $J/kgK$

$\rho_a$  = density of air  $kg/m^3$

$Vol$  = Volume of the room  $m^3$

$N$  = number of air changes  $h^{-1}$



$B$  = heat storage capacity of the room air J/K

The above equation could be approximated by

$$\frac{T_{al,t+dt} - T_{al,t}}{dt} = \frac{1}{c_{p_a} \rho_a Vol} \left( \sum_{j=1}^J A_{s_j} h_{c_j} (T_{s_j,t+dt} - T_{al,t+dt}) \right) + C_v T_{ao,t+dt} - T_{al,t+dt} + Q_{i,t+dt} \quad (5.22)$$

rearrangement of equation 5.14 gives

$$\sum_{j=1}^J \left( \frac{-dt}{c_{p_a} \rho_a Vol} A_{s_j} h_{c_j} T_{s_j,t+dt} \right) + T_{al,t+dt} \left( 1 + \sum_{j=1}^J A_{s_j} h_{c_j} + \frac{C_v dt}{c_{p_a} \rho_a Vol} \right) = \frac{C_v dt}{c_{p_a} \rho_a Vol} T_{ao,t+dt} + T_{al,t} + Q_{i,t+dt} \quad (5.23)$$

It is reasonable to ignore the thermal capacity of the air inside the room. This will simplify equation 5.23 to

$$\sum_{j=1}^J A_{s_j} h_{c_j} (T_{s_j,t+dt}) + T_{al,t+dt} \left( \sum_{j=1}^J A_{s_j} h_{c_j} + C_{v,t+dt} \right) = Q_{i,t+dt} \quad (5-24)$$

Using the heat balance equation for the nodes in question, (similar to eq 5.14, 5.17, 5.20), and for the air will result in a set of simultaneous equations. The solution of this system of equations could be achieved by different methods, of which details can be found in the literature. In the present study the simultaneous equations are solved by matrix algebra of the form

$$|T| \cdot |B| = |Q| \quad (5.25)$$

where  $|T|$  represents the temperature at the time in question for the different nodes. This could be achieved by multiplication of  $|B|^{-1}$  by  $|Q|$  assuming the temperature at time  $t$  as known.

To avoid repetition the seven node model only is presented. The matrix representation of the set of heat balance equation for the experimental room, the thermal network shown in figure 5.1) is given in table 5.2. where



$$Fo = \frac{2dt\lambda}{c_p \rho dx^2} \quad (5.26)$$

$$C = \frac{2dt}{c_p \lambda dx} \quad (5.27)$$

$$Ca = \frac{dt}{c_{p_a} \rho_a Vol_{air}} \quad (5.28)$$

### 5.3.3 Finite difference computer program

A Fortran 77 computer program is written which calculates the temperature distribution at different nodes. The program FINIT consists of a source program and several subroutines.

The first subroutine INTERP reads the climatic data usually as hourly values, and creates new values by interpolation according to the chosen time interval. The interpolation of data is done by nonlinear interpolation employing two routines from the NAG library.

The second subroutine "SHAPE" calculates the configuration factors  $E_{ij}$ , between the surfaces of a room. The general algorithm for any configuration of a rectangular surface in a room is given by Clarke (1983). Appendix A gives a general computer based procedure for view factor calculations, for windows and walls in parallel and perpendicular. The detailed procedure is discussed in chapter two (2-3).

The third subroutine calculates the coefficient of heat transfer by convection; it uses the ventilation rate, assuming a uniform distribution of air over the cross section of the room and temperature of the room air and surface, calculates  $h_c$  for different cases of convection (forced, natural or mixed). The formulae are discussed in chapter two(2-3).

The fourth subroutine HH inverts the matrix [B] and by multiplication with [Q] creates the row dimension [T] which consists of the temperature of different surfaces and air of the room. The (F01AAF) routine of the NAG library is used to invert the matrix and (F01CKF) routine is used for multiplication of matrices.

The program starts by assuming the time interval, according to which interpolation is being done. An initial value for all temperatures is assumed and based on these values  $h_c$  is calculated. Matrix [B] with [Q] are set based on the calculated values of  $h_c$  and the present ventilation rate. The new temperatures are calculated by

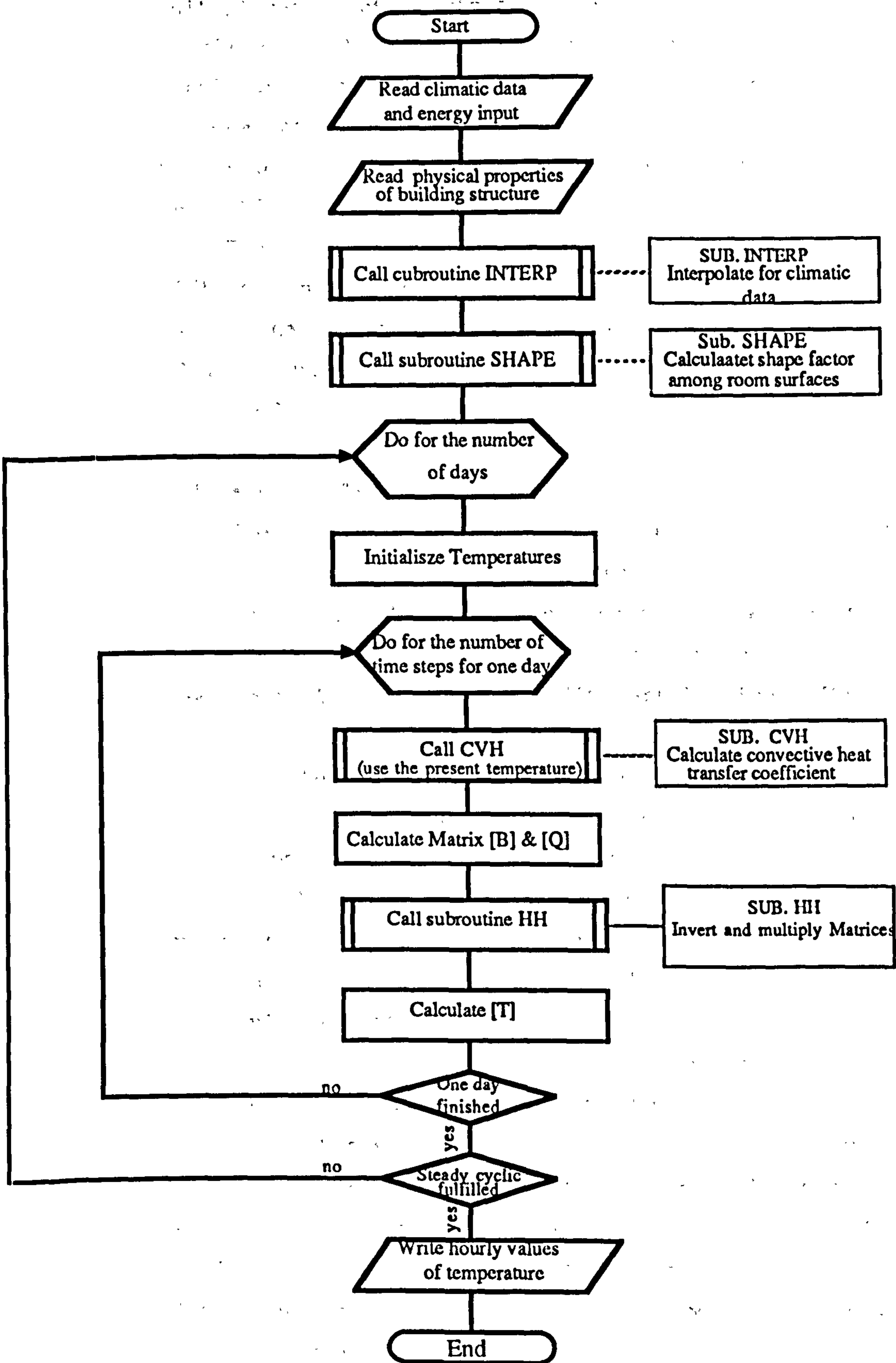


Figure 5.5: Flowchart of Finite Difference program

multiplication of matrices. The procedure is repeated until the end of the day. The whole procedure is repeated until a steady cyclic condition is reached. This could be done by checking that the temperature at the beginning and the end of a cycle are nearly within a chosen allowable limit. Figure 5.5 shows the flowchart of the FINIT program.

The FINIT program is used to investigate the assumptions of different models as discussed in (5.1.2). Three thermal models are used, nine, seven, and three nodes network. The physical properties of nodes representing more than one surface are the area weighted values of its constituents.

#### 5.4 Response factor program :

The response factor method is essentially a numerical method, but its application is restricted to both linear and invariable systems, while the finite difference technique can deal with both linear and non-linear systems. The restriction does not usually limit the use of the method in building applications. The only significant difference compared with the finite difference method is the way the transient heat conduction through a slab is dealt with. It can deal with periodic and non periodic situations, and for this reason has wider application than the harmonic method. It is essentially a computer based method, although the computation time and the programming is less than for the finite difference method.

The basic strategy is to establish the response of a system to some unit excitation applied under boundary conditions similar to the actual excitation. The overall response of a system could be obtained by the sum of the responses to a train of excitations. To achieve such response, the excitation function should be represented by simple individual component elements. This is done by dividing the excitation function into triangular pulses. (MILBANK & STEPHENSON 1967) The response of the system to these individual excitation functions should be added to get the overall response. This is done by the appropriate pre-calculated response factors. Response factors are independent of climatic factors, and need to be calculated only once for any given structural system. This is the main attraction of the method compared with the finite differences method where for each time step the calculation have to be repeated. The detail and definitions related to conductive heat transfer calculations using the response factor method are given in chapter two.

#### 5.4.1 Room thermal response factor:

A room could be considered as an integrated system, and a unit response function under any excitation may be determined. This is achieved by the energy balance equations for each surface and the air in an enclosure. The subsequent simultaneous solutions of this set of equations under any applied unit excitation gives the corresponding unit response function. Repetition of this procedure for each separate unit excitation gives all the unit response function from which the total response of the system, to actual temperature and energy, can be found.

#### 5.4.2 Heat balance equation :

The heat balance for any enclosure surface at any time  $t$  is given by :

$$Q_{cv,t} + Q_{rd,t} + Q_{cd,t} + Q_{i,t} = 0 \quad (5.29)$$

where

$Q_{cv,t}$  is the heat gain by convection at time  $t$

$Q_{rd,t}$  is the heat gain by long wave radiation at time  $t$

$Q_{cd,t}$  is the heat flux by conduction towards the surface

$Q_{i,t}$  is the energy input to the surface (eg. solar energy falling on the surface)

and

$$Q_{cv,t} = h_c A (T_{ai,t} - T_{si,t}) \quad (5.30)$$

$$Q_{rd,t} = \sum^J E_{i,j} A_i h_r (T_{sj,t} - T_{si,t}) \quad (5.31)$$

$$Q_{cd,t} = -T_{si,t} X + T_{sk,t} Y \quad (5.32)$$

$X, Y$  = response factors for the slab

(subscript  $sk$  indicates the other surface of the wall.)

Using the above equation for the heat flux by conduction, the heat conduction through a wall surface for unit area at time  $t$  is given by

$$Q_{cd,t} = -\sum_{p=0}^{\infty} T_{sl,(t-p)} \cdot x_p + \sum_{p=0}^{\infty} T_{sk,(t-p)} \cdot y_p \quad (5.33)$$

substitution for  $Q_{cd,t}$ ,  $Q_{cv,t}$  and  $Q_{rd,t}$  gives

$$\begin{aligned} & -T_{sl,t} \left[ h_{cs} + \sum_{j=1}^J E_{1j} h_r + x_0 \right] + T_{sk,t} \cdot y_0 + \sum_{j=1}^J E_{1j} h_r T_{sj,t} \\ & = -Q_{1,t} - T_{1,t} + \sum_{p=1}^{\infty} T_{sl,(t-p)} \cdot x_p - \sum_{p=1}^{\infty} T_{sk,(t-p)} \cdot y_p \end{aligned} \quad (5.34)$$

Using the heat balance equation for the outside surface and air will result in a set of equations for an unknown point.

The heat balance at the outside surface is simplified by using a combined heat transfer coefficient for radiation and convection :

$$H_1 (T_{ao,t} - T_{so,t}) - \sum_{p=0}^{\infty} T_{so,(t-p)} \cdot x_p + \sum_{p=0}^{\infty} T_{sl,(t-p)} \cdot y_p + Q_{1,t} = 0 \quad (5.35)$$

or

$$T_{so,t} (-H_1 - x_0) + T_{sl,t} (H_1 + y_0) = \sum_{p=1}^{\infty} T_{so,(t-p)} \cdot x_p - \sum_{p=1}^{\infty} T_{sl,(t-p)} \cdot y_p - Q_{1,t} \quad (5.36)$$

The heat balance for the room air is given by the sum of the energy input to the air by convection from all surfaces, by ventilation between inside air and outside air and any energy input directly to the air. This yields

$$\sum_{j=1}^J A_j h_{cj} (T_{sl,t} - T_{al,t}) + C_{v,t} (T_{ao,t} - T_{al,t}) + Q_{al,t} = \frac{(T_{al,t-dt} - T_{al,t})}{B/dt} \quad (5.37)$$

where

$B$  = heat storage capacity of the air

$dt$  = selected calculation time interval

whence:

$$\sum_{j=1}^J A_{j,cj} h_{cj} T_{sj} + (C_{v,t} - \sum_{j=1}^J A_{j,cj} h_{cj} + \frac{\rho c_p \text{Vol}}{dt}) T_{ai,t} = -C_{v,t} T_{ao,t} + \frac{\rho c_p \text{Vol}}{dt} T_{ai,t-dt} \quad (5.38)$$

The heat balance equation for each unknown node and the air in the thermal circuit can be derived from equations 5.34 and 5.36 and 5.38. The complete set is represented by

$$|T| \times |M| = |Q| \quad (5.39)$$

where

$|T|$  = column matrix containing the values of the unknown temperatures at time  $t$

$|M|$  = matrix of temperature coefficients as given by the heat balance equations

$|Q|$  = column matrix includes values from equations (5-34) (5-36) and (5-38), which depend on the excitation component at time  $t$  and the complete history from time zero to  $t-dt$

The solution of equation 5.39 is given by

$$|T| = |M|^{-1} \times |Q|$$

The inverted matrix  $|M|$  is unchanged. If the ventilation changes during the day,  $|M|$  should be calculated for each value of the ventilation rate, and the inversion should be repeated for each matrix. As the ventilation is usually one rate during the day and another at night, this will not cause a serious problem. The value of the convection heat transfer coefficient  $h_c$  is considered to be constant during the day. The method is capable of allowing  $h_c$  to be variable but only at the cost of analytical rigour. This could be done by calculating  $h_c$  based on the previous temperature difference between air and surface and consequently recalculating  $|M|$  for each time interval.

#### 5.4.2 Response factor computer program;

The thermal response factors for a homogeneous slab can be expressed in terms of its thermal properties and thickness and the time interval.

Fortran program RESFAC is designed to calculate the temperatures



Table 5.3: The matrix representation of the Response Factor Program

$T_{wo}$	$H_o - X_0$	$Y_0$								$H_0 T_{ao,t} + \sum T_{sw,(t-p)} X_p - \sum T_{s1,(t-p)} Y_p - Q_e$
$T_{s1}$	$Y_0$	$-h_{c1} - \sum E_{1,j} h_r - X_0$	$h_r E_{1,2}$	$h_r E_{1,3}$	$h_r E_{1,4}$	$h_r E_{1,5}$	$h_r E_{1,6}$	$h_{c1}$		$+ \sum T_{s1,(t-p)} X_p - \sum T_{sw,(t-p)} Y_p - Q_e$
$T_{s2}$		$h_r E_{2,1}$	$h_{c2} - \sum E_{2,j} h_r - X_0$	$h_r E_{2,3} + Y_0$	$h_r E_{2,4}$	$h_r E_{2,5}$	$h_r E_{2,6}$	$h_{c2}$		$+ \sum T_{s2,(t-p)} X_p - \sum T_{s3,(t-p)} Y_p - Q_e$
$T_{s3}$		$h_r E_{3,1}$	$h_r E_{3,2} Y_0$	$-h_{c3} - \sum E_{3,j} h_r - X_0$	$h_r E_{3,4}$	$h_r E_{3,5}$	$h_r E_{3,6}$	$h_{c3}$		$+ \sum T_{s3,(t-p)} X_p - \sum T_{s2,(t-p)} Y_p - Q_e$
$T_{s4}$		$h_r E_{4,1}$	$h_r E_{4,2}$	$h_r E_{4,3}$	$-h_{c4} - \sum E_{4,j} h_r - X_0 + Y_0$	$h_r E_{4,5}$	$h_r E_{4,6}$	$h_{c4}$		$+ \sum T_{s4,(t-p)} X_p - \sum T_{s4,(t-p)} Y_p - Q_e$
$T_{s5}$		$h_r E_{5,1}$	$h_r E_{5,2}$	$h_r E_{5,3}$	$h_r E_{5,4}$	$-h_{c5} - \sum E_{5,j} h_r - X_0$	$h_r E_{5,6} + Y_0$	$h_{c5}$		$+ \sum T_{s5,(t-p)} X_p - \sum T_{s6,(t-p)} Y_p - Q_e$
$T_{s6}$		$h_r E_{6,1}$	$h_r E_{6,2}$	$h_r E_{6,3}$	$h_r E_{6,4}$	$h_r E_{6,5} + Y_0$	$-h_{c6} - \sum E_{6,j} h_r - X_0$	$h_{c6}$		$+ \sum T_{s6,(t-p)} X_p - \sum T_{s2,(t-p)} Y_p - Q_e$
$T_{ai}$		$A_1 h_{c1}$	$A_2 h_{c2}$	$A_3 h_{c3}$	$A_4 h_{c4}$	$A_5 h_{c5}$	$A_6 h_{c6}$	$-\sum \Delta_i h_{c,i}$		$-C_{v,i} T_{ao,t} + F_{air,i}(cprv/dt)$

X

of surfaces and the air in a room. The program starts by calculating the thermal response factors for the outside wall, the inside partitions, the floor and the ceiling. The values of  $|M|$  and column matrix  $|Q|$  are based on previously calculated thermal response factors. The calculation must start of course, at time  $t=1$  for which the internal temperatures at  $t=0$  are assumed to be known. Using  $|Q|$  at time  $t=0$  the temperatures for  $t=1$  are calculated by multiplication of  $|M|$  by  $|Q|$ . The calculations are repeated for successive values of  $t$  until the complete daily cycle of 24 hours is completed. The time step chosen for calculation is assumed to be one hour.

The RESFAC Fortran program consists of a source program and subroutines. The subroutine SHAPE which calculates the configuration factor among surfaces and HH1 for inversion and multiplication is the same as used in the finite difference program.

Subroutine RESFAC calculates the response factors for each structural element. The number of factors is dependent on the structure and the thermal properties of the slab as the factors tend to zero after a while. The subroutine HFLUX calculates the energy input to any surface by conduction using the response factors obtained from RSFAC.

### 5.5 Harmonic Method:

The harmonic method of solution of the problem of heat transfer has a widespread use in buildings. Different researchers have used the method in buildings with different complexities and applications. A short review is given above. (chapter 3 3-3).

In this comparative study, the method is used in its specific form as applied to the environmental temperature model; the Admittance Method (CIBSE 1985) (chapter three 3-4-4). The following is the algorithm used in the present study, based on a thermal network as shown in figure 5.6.

#### 5.5.1 The Admittance Method :

As stated above the Admittance Method uses factors obtained from the harmonic method of solution to the unsteady heat conduction equation, namely the admittance, the decrement, and the surface factor and their associated time lags.

To estimate the total energy transfer and the total temperature response under steady cyclic or periodic conditions where the energy and temperature variations are repeated over a period of time, first

the temperature cycles are approximated by a Fourier series of sine and cosine wave harmonics about a constant term, the mean value. Then associated dynamic thermal factors are calculated for each harmonic. The response of each energy and temperature cycle is calculated, using the precalculated factors and associated time lags for its harmonics. The final temperature or energy load prediction is obtained by summing the contributions from each of the harmonics and expressing this result with respect to the contribution made by the steady state term.

If the environmental temperature model shown in figure 5.6 is considered, the daily means of the internal air and the environmental temperatures are found from the daily mean heat input to the enclosure. The mean, steady state, balance at air point is given by ;

$$\bar{Q}_a = \frac{1}{24} \sum C_{v,t} (T_{ai,t} - T_{ao,t}) - h_a \sum (A) (\bar{T}_{ai} - \bar{T}_{ei}) \quad (5.41)$$

and at the environmental point:

$$\bar{Q}_e = \sum (AU) (\bar{T}_{ei} - \bar{T}_{ao}) + h_a \sum (A) (\bar{T}_{ei} - \bar{T}_{ai}) \quad (5.42)$$

The contribution of each cycle of energy and temperature to the swing (i.e. fluctuation about the mean at some time) in internal temperature value could be obtained by the heat balance equation for cyclic energy inputs and factors appropriate to their frequencies. at the air and environmental points:

at the air point:

$$\tilde{Q}_{a,t} = C_{v,t} (\tilde{T}_{ai,t} - \tilde{T}_{ei,t}) - h_a \sum (A) (\tilde{T}_{ei,t} - \tilde{T}_{ai,t}) \quad (5.43)$$

and at the environmental point:

$$\tilde{Q}_{e,t} = \sum (A.Y) \tilde{T}_{ei,t+\omega} + h_a (\tilde{T}_{ei,t} - \tilde{T}_{ai,t}) \quad (5.44)$$

where  $\tilde{T}_{ei,t}$  and  $\tilde{T}_{ai,t}$  are the swing of internal environmental and air temperature at some time  $t$ , and  $Q_{a,t}$  and  $Q_{e,t}$  are the total load at

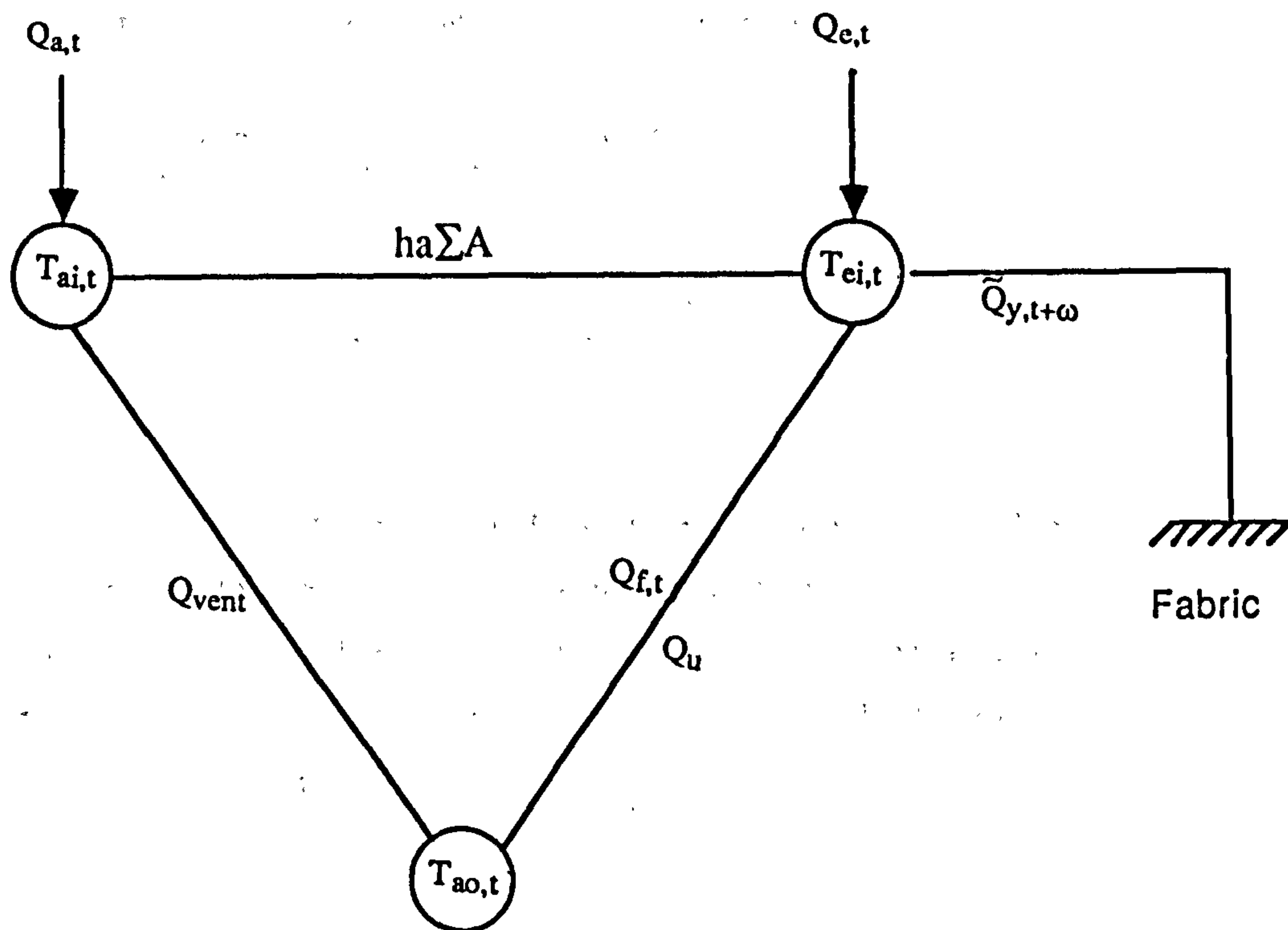


Figure 5.6: The heat transfer triangle in the Admittance Method

sum of a daily mean value and the sum of the cyclic component for different periods 24,12,6,.... hours.

Equations 5.41 and 5.43 ,and,5.42 and 5.44 could be added together to find the instantaneous temperature at the air and the environmental point due to each cycle and appropriate harmonics

$$Q_{a,t} = C_{cv,t} (T_{ai,t} - T_{ao,t}) - h_a \sum (A) - h_a (T_{ei,t} - T_{ai,t}) \quad (5.45)$$

and

$$Q_{e,t} = \sum (A.U) (T_{ei,t} - T_{ao,t}) + h_a \sum (A) (T_{ei,t} - T_{ai,t}) + \sum (A.Y) T_{ei,t+\omega} \quad (5.46)$$

These equations could be used to calculate the overall response of the building to some energy input at some time t and due to any number of harmonics . It is convenient to give the swing temperature at time (t) in the term  $T_{ei,t+\omega}$  as the difference between the mean and the temperature at time t

$$\bar{T}_{ei,t+\omega} = T_{ei,t+\omega} - \bar{T}_{ei} \quad (5.47)$$

Rearrangement of equations 5.45, 5.46 and 5.47, will result in:

$$T_{ai,t} (h_a \sum (A) + C_{v,t}) + T_{ei,t} (-h_a \sum (A)) = Q_{a,t} + C_{v,t} T_{ao,t} \quad (5.48)$$

$$\begin{aligned} T_{ai,t} (-h_a \sum (A)) + T_{ei,t+\omega} (h_a \sum (A) + \sum (A.Y)) + \bar{T}_{ei} (\sum (A.U) - \sum (A.Y)) \\ = Q_{e,t} + T_{ao,t} \sum (A.U) \end{aligned} \quad (5.49)$$

Equations 5.48 and (5.49) are the fundamental equations of the heat transfer triangle shown in figure 5.6.

The total energy input at the environmental point, at any time t is divided into two parts ; the mean, and the fluctuation due to the contribution by each harmonic to the swing in internal environmental temperature about the mean value

$$Q_{e,t} = \bar{Q}_e + \tilde{Q}_{e,t} \quad (5.50)$$

$$\bar{Q}_e = \bar{Q}_f + \bar{Q}_{se} + \bar{Q}_{ce} + \bar{Q}_{pe} \quad (5.51)$$

$$\tilde{Q}_{e,t} = \tilde{Q}_{fs,t} + \tilde{Q}_{se,t} + \tilde{Q}_{ce,t} + \tilde{Q}_{fc,t} + \tilde{Q}_{pe,t} \quad (5.52)$$

where

$Q_{fs}$  = solar gain through opaque surfaces

$Q_{se}$  = solar gain through transparent surfaces

$Q_c$  = casual gain released at environmental point

$Q_{pe}$  = energy input from the plant to the environmental point

$Q_{fc,t}$  = energy gain through the opaque surfaces due to fluctuation of external conditions

These energy inputs are given as follows .

The calculation of solar gain through the transparent surfaces is lengthy and time consuming. The use of the solar gain factor as proposed by Loudon (1968) is given in the CIBSE Guide. The detailed discussion is given in (3-4-2).

The swing and mean solar gain through a transparent area is given by :

$$\bar{Q}_{se} = A_g \bar{S}_e \bar{I}_s \quad W \quad (5.53)$$

$$\tilde{Q}_{se,t} = A \tilde{S}_e \tilde{I}_{s,t} \quad W \quad (5.54)$$

where

$\bar{S}_e$  = solar gain factor

$\tilde{S}_e$  = alternating solar gain factor

$I$  = total solar intensity  $W/m^2$

The alternating solar gain factor includes the effect of the surface factor. For higher harmonics, this may be corrected by the use of an appropriate surface factor. (CLARKE 1983) Solar gain through each opaque surface is given by:

$$\bar{Q}_{fs} = AUR_{so} (\alpha I_s - \epsilon \bar{I}_o) \quad W \quad (5.55)$$

$$\tilde{Q}_{fs,t} = AUR_{so} f_i \alpha \tilde{I}_{s(t-\phi)} \quad W \quad (5.55)$$

where

$f_i$  = decrement factor corresponding to the frequency

$\phi$  = time lag associated with the decrement factor h

$\alpha$  = solar absorptivity

$I_o$  = radiation loss to the outside

The fluctuating energy gain through each external wall by

conduction due to any particular harmonic and energy input is given by :

$$Q_{fc,t} = AUf\tilde{T}_{ao,(t-\Phi)} \quad W \quad (5.57)$$

The total energy input at the air point includes the convective input from any plant or casual energy source to the air and the part of solar radiation input to the room , which is released at the air point by convection in the presence of internal blinds

$$Q_{al,t} = Q_{pa,t} + Q_{ca,t} + Q_{sa,t} \quad W \quad (5.58)$$

where

$$\begin{aligned} Q_{pa,t} &= \text{heat input from the plant to the air point} & W \\ Q_{ca,t} &= \text{convective part of casual energy input} & W \\ Q_{sa,t} &= \text{convective part of solar input} & W \end{aligned}$$

The solar gain at the air point could be calculated by means of the solar gain factors at the air point  $S_a, \tilde{S}_a$ , in the same way as the energy input to the environmental point.

Eliminating  $T_{ei}$  in equations 5.48 and 5.49 will enable the set of equations to be solved for hourly calculation of the environmental temperature. The resulting equation after some manipulation is :

$$\begin{aligned} T_{ei,t}(-F_{v,t}) + T_{ei,t+\omega}(h_a \sum(A) + \sum(A.Y)) + \bar{T}_{ei}(\sum(A.U) - \sum(A.Y)) = \\ = Q_{e,t} + T_{ao} \sum(A.U) + Q_{a,t} F_{vt} + T_{ao,t} C_{v,t} F_{v,t} \end{aligned} \quad (5.59)$$

where

$$F_{v,t} = \frac{h_a \sum(A)}{h_a \sum(A) + C_{v,t}} \quad (5.60)$$

$$T_{ei} = \sum_{24} \frac{1}{24} T_{ei,t}$$

The solution to this set of equations could be achieved by:

$$|T| \times |A| = |B| \quad (5.61)$$

$$\begin{array}{c|c}
 \begin{array}{c} T_1 \\ T_2 \\ T_3 \\ \dots \\ T_{24} \end{array} & \times \begin{array}{c} a_{1,1} \quad a_{1,2} \quad a_{1,3} \quad \dots \quad a_{1,24} \\ a_{2,1} \quad a_{2,2} \quad a_{2,3} \quad \dots \quad a_{2,24} \\ a_{3,1} \quad a_{3,2} \quad a_{3,3} \quad \dots \quad a_{3,24} \\ \dots \\ a_{24,1} \quad a_{24,2} \quad a_{24,3} \quad \dots \quad a_{24,24} \end{array} & - \begin{array}{c} b_1 \\ b_2 \\ b_3 \\ \dots \\ b_{24} \end{array} & (5.62)
 \end{array}$$

where

$T_1$  = environmental temperature at time  $t$

$A_{1,1} = -F_{v,t} + 1/24 \sum (A.U) - \sum (A.Y)$

$A_{1,j}$  when  $i \neq j = 1/24 (\sum (A.U) - \sum (A.Y))$

$A_{1,1+\omega} = h_a \sum (A) + \sum (A.Y) + 1/24 (\sum (A.U) - \sum (A.Y))$

$B_1 = Q_{e,t} + Q_{e,t} + T_{ao} \sum (A.U) + Q_a - F_{v,t} + Q_{a,t} F_{v,t}$   
 $+ T_{ao}.C_{v,t}.F_{v,t}$

### 5.5.2 Harmonic method computer program:

The solution to the equation 5.62 starts with analysing of temperature and energy cycles into a mean and the different harmonics, with periods of (24, 12, 6, h) and column matrix [B] is calculated. The square matrix [A] is calculated using the values of dynamic thermal factors (Y f and s and their associated time lag) based on the corresponding harmonics. First the response of the system to the sum of mean and the first harmonic, and then the response to the next harmonics is calculated. The final result is obtained by the summation of the response to the different harmonics and the mean and the first one. It is worth noting that the mean value on the right of equation 5.59 will be zero for all harmonics other than the first.

A Fortran computer program ADMHAR is designed to calculate the internal temperature in a room using the above procedure. Figure 5.7 shows the flow chart of the computer program.



Do N= number of harmonics

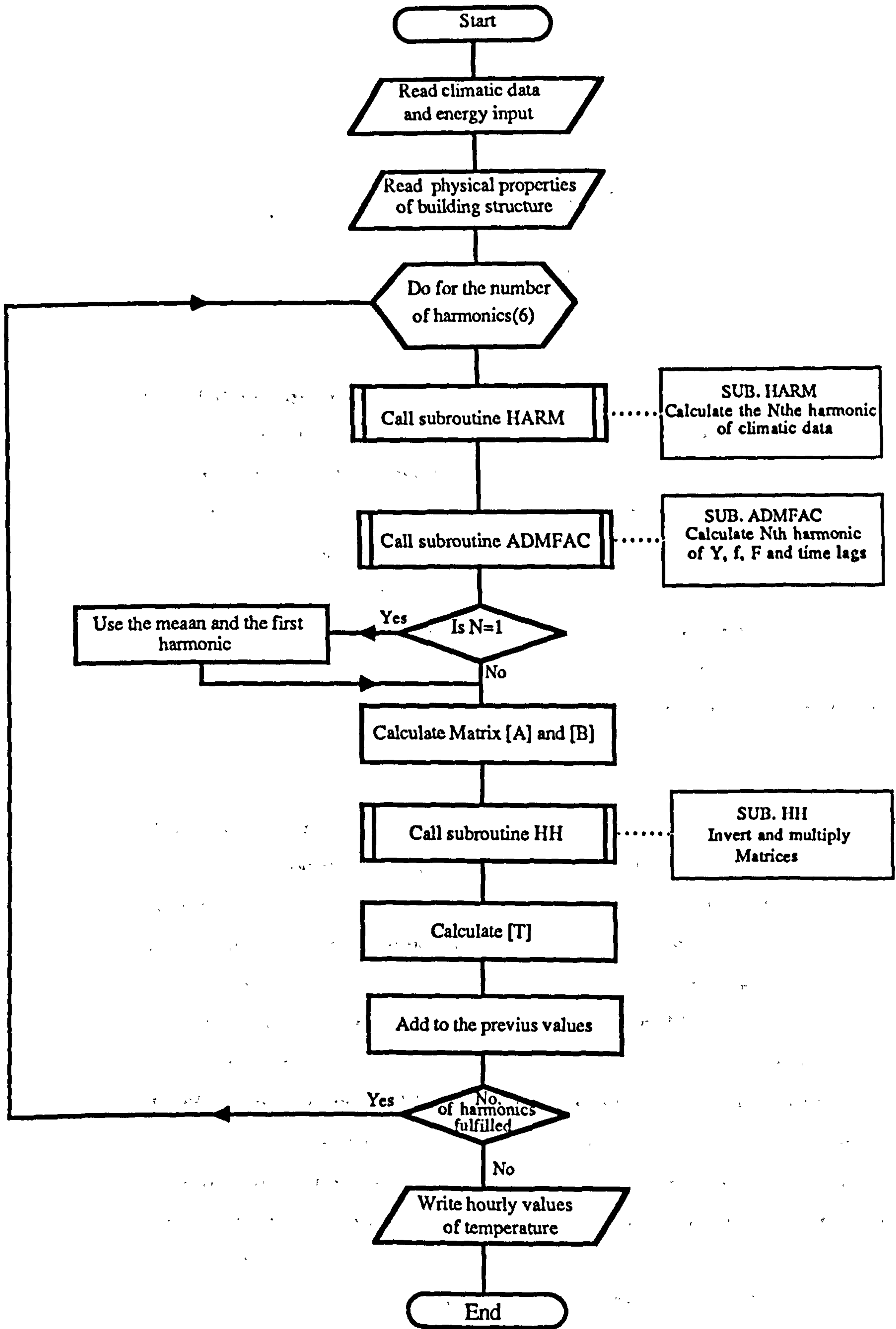


Figure 5.7: Flowchart of harmonic program

## CHAPTER SIX

### OBSERVATIONS

#### 6.1 Introduction

To determine whether the thermal simulation programs are capable of predicting the passive behaviour of buildings under particular conditions, including variable ventilation, with satisfactory accuracy, comparison of predictions with measured data is necessary. Data obtained from the observations are also used to evaluate the importance of the parameters involved in different models, discussed in this study. At first attempts were made to provide the required data from published work but no data with controlled variable ventilation were found.

#### 6.2 Background

Experimental evidence on real buildings for comparison with predictions is sparse. The empirical validations of models varies; ranging from measurements on a small test box in the laboratory to real field measurements. Neither laboratory nor field tests covered the case of buildings with variable ventilation.

In one of the early studies of dynamic thermal models, Muncey (1953) made observations under laboratory conditions, using a scaled model. The results were used to evaluate the thermal simulation technique. The method is based on the harmonic solution to the unsteady heat conduction equation and is known as the matrix method. Good agreement is reported.

Gupta (1964) made observations in a test room specially constructed in an open space. The test room had no windows and no ventilation, and was only subjected to the variations of outside air temperature and insolation. Muncey's method was extended to include the effect of internal heat exchange by long wave radiation between surfaces. Improvements were shown.

Milbank and Harrington-Lynn (1970) published results on two offices. Comparison is made with the predictions of an electrical

analogue. The results of the Admittance Method are also compared with the electrical analogue. Because of good agreement, it was thought to validate the Admittance Method.

Loudon (1968) has published results comparing the Admittance Method and measurement in an unoccupied and unventilated room, over a period of three days. No descriptions of any kind are given. The agreement between measurements and calculations is not particularly good and discrepancies of up to 5 degrees at certain times of the day are reported.

Detailed measurements to test the validity of the Response Factor method have been carried out by Peavy et al.(1974). The measurements were carried out on an experimental building (6 by 6 by 3 m.) under laboratory conditions, constructed in a large environmental chamber. Outside air temperature changes were simulated on a 24 hours cycle, ranging from 4 to 38 °C. The rate of infiltration was also measured. Good agreement is reported between the measurements and the calculations performed by the Response Factor method.

### 6.3 Physical description and measurement technique

In the present study two options were considered : to use an existing room or to build a scaled model room and conduct the measurement under laboratory conditions. Because the rate of ventilation plays an important role in the thermal performance of buildings and is the main subject of this study, the first option was rejected , as an accurate measurement of the ventilation rate in an existing room is very difficult and not practicable with the available equipment . It was decided to make measurements on a small-scale model under laboratory conditions.

One of the main points of concern, in using a scale model is heat transfer by convection. The convective heat transfer coefficient is a function of the size of the surfaces and the temperature difference and air velocity. Using the procedure above, (chapter two 2-2), it was found that the difference between the coefficient of a full scale model and a 2/3 scaled model is negligible for the purposes of the present study. A comparison was made between a cubic room of 3 metre length and of 2 metre length. The variations in the heat transfer coefficient for convection with a range of temperatures difference ,similar to those used in the observations, between air and surfaces was found to be very small,

i.e. less than 5% for a temperature difference greater than 2 K. Higher temperature difference would result in smaller deviations while the uncertainty in the convective heat transfer coefficient used in buildings is far greater than that. Alamdari et al. (1986) have compared different values calculated with simulation methods and reported greater differences between them and the standard values given by CIBSE.

### 6.3.1 Test room

The room designed to represent a room surrounded by similar rooms experiencing the same thermal circumstances, all with one external wall and window. The outside dimensions of the room were 2.2 by 2.2 m and 1.9 m. high.

The floor was made of five 0.21 m wide reinforced concrete slabs, 50 mm thick. The roof was of insulation board commercially available as "Purideck", of 6.5 mm exterior grade plywood facing downward into the test room and 55 mm expanded polyurethane with aluminum foil laminated facing upward. This was chosen because of technical difficulties with using concrete for the roof, and it was found not to be far from the reality, where there is a false ceiling exist. The walls were 0.1 m thick and made of concrete blocks 0.1 by 0.2 by 0.4 m. , joined with fully bedded mortar joints. The concrete blocks were of a nominal density  $2100 \text{ kg/m}^3$ .

Two openings 0.6 by 0.6 m were in the middle of the walls , one on the external wall and one on the opposite wall in parallel in order to allow cross ventilation. The frames of the openings were made of wood . Each opening had a sliding removable shutter of plywood. The cracks around the wooden frame were first filled with expanded foam and later taped with aluminium tape to reduce infiltration. A fan was fixed 0.7 m. from and parallel to the external wall of the room to create ventilation. The air flow rate was controlled by a speed controller connected to the fan.

The floor was about 0.3 m. above ground level and open from two side walls , to let the air around the room move below the floor. It was covered with insulation board with polished aluminium facing the ground, to reduce the radiation exchange between the ground and the floor. Figure 6.1 and 6.2 shows the plan and section of the test room.

All surfaces of the room were covered with commercially available "Celtex double-R2" insulation on the outside. This consists

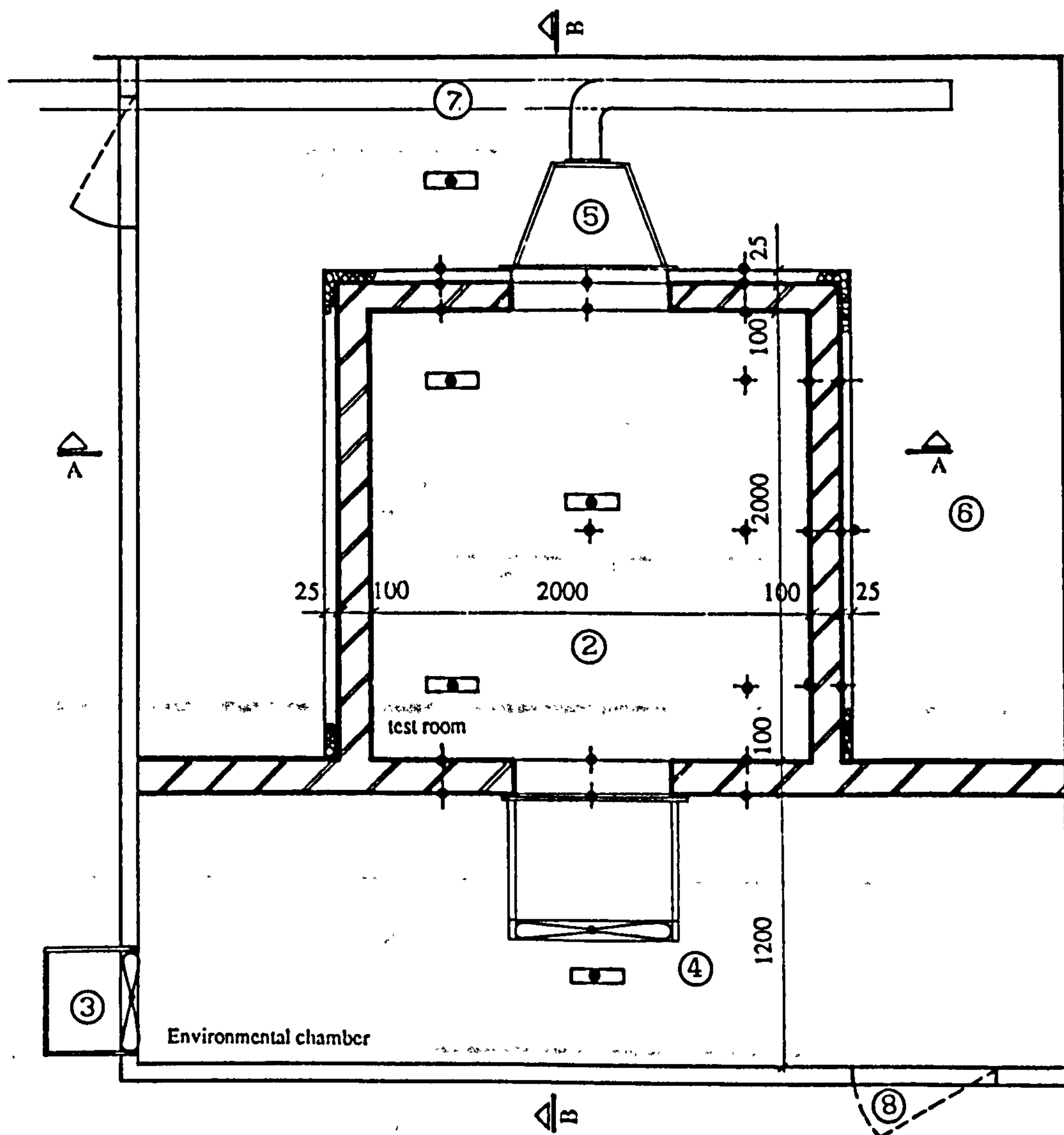


Figure 6.1: Plan of the test room and thermocouple locations.

1: Environmental chamber

2: Test room

3: Hot air furnace

4: Fan on the front wall

5: Air collector cone

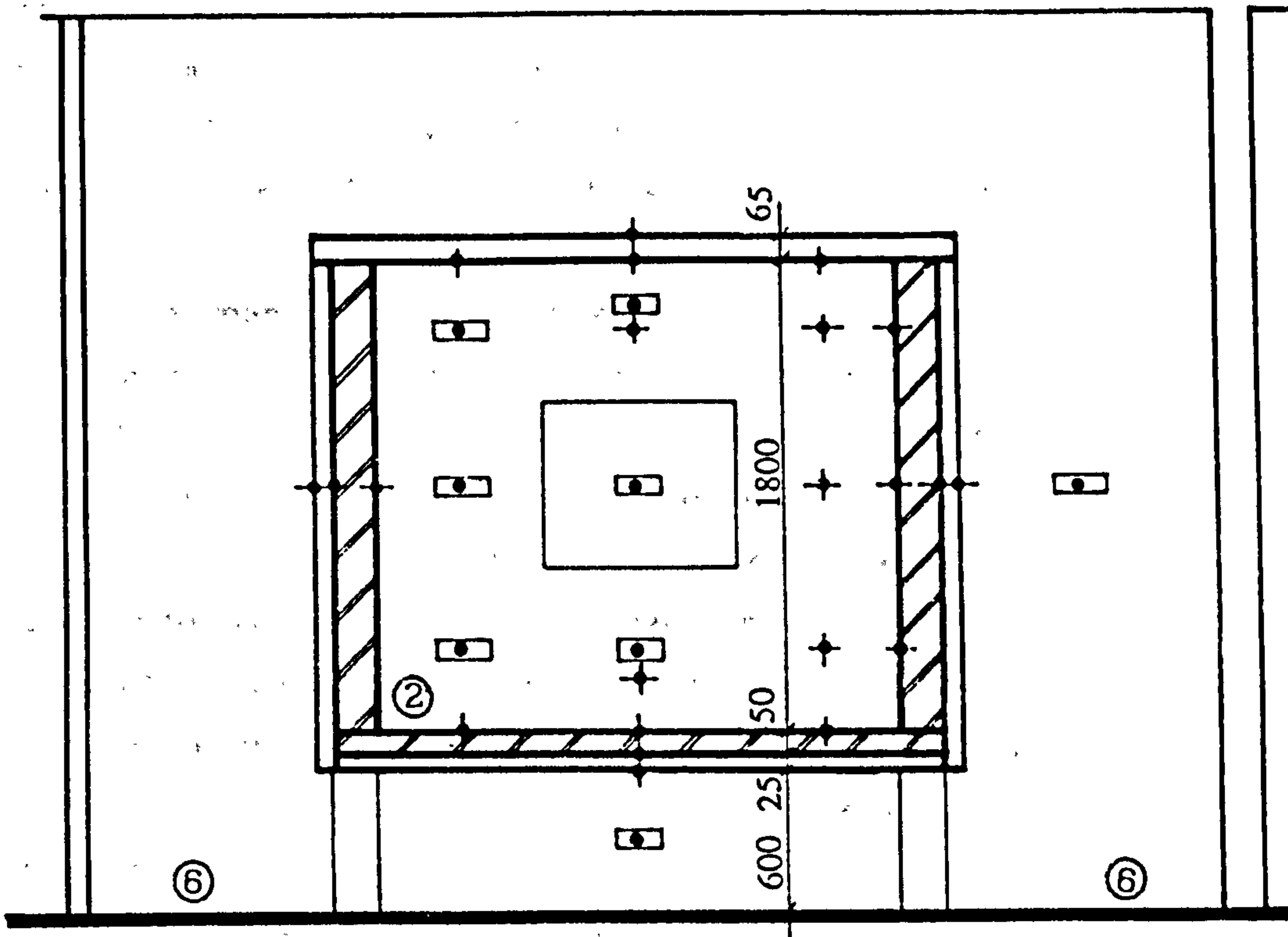
6: Open space around the room

7: Orifice plate device

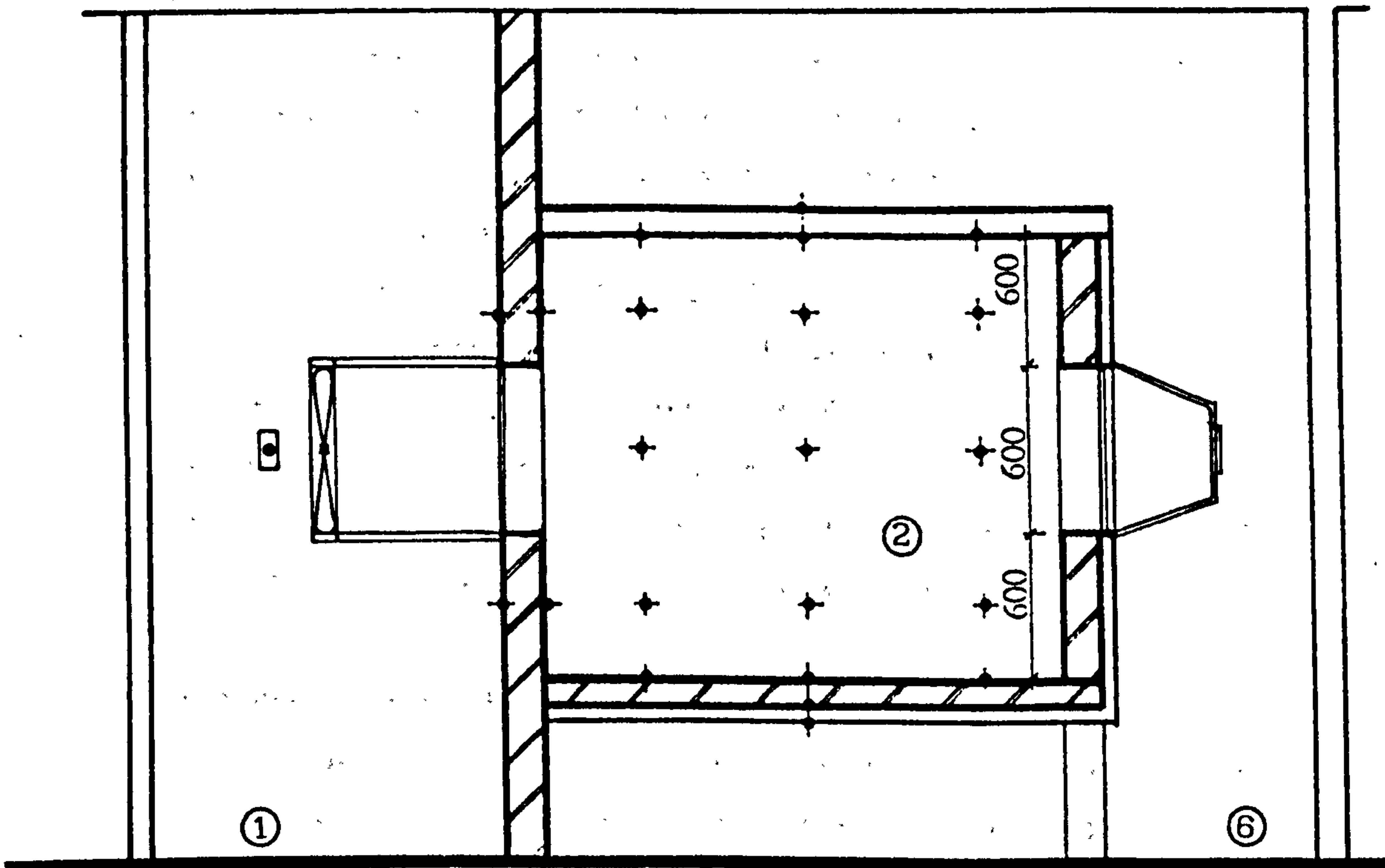
8: Access to the chamber

⊕ Surface temperature thermocouple

▣ Air temperature thermocouple



SECTION A\_A



SECTION B\_B

Figure 6.2: Sections of the test room.

of 25 mm rigid polyisocyanurate foam reinforced throughout with long strand glass fibres. It was covered on one sides with a white embossed aluminium foil, and with highly reflective polished aluminium foil on the other side.

The test room was designed to represent a room in a facade of similar rooms. To achieve this, the test room was enclosed in a larger space 1.2 m. from each side. The air temperature around the room, between the test room's surfaces and the outer envelope, shown in figure 6.1 was kept the same as the air temperature in the middle of the test room. This was done by a differential temperature controller connected to a fan heater to heat the space around the room to the same temperature as the room. When the temperature around the room was higher than that of the room a fan on the laboratory wall was turned on to lead the cooler air to the space around the room. This rarely happened during the measurements.

Although the space around the room was kept at the same air temperature as the inside air, it was impracticable to achieve a 100% success in keeping the two temperatures equal, and some heat might be transferred by conduction through the internal walls. Internal walls were considered so that there would be no heat flow across them. The insulation on all surfaces would increase the overall thermal resistance of the surfaces, and decrease the heat transfer across them. A thermocouple was fixed on each side of the insulation board, one between the outside surface of the wall and insulation board, and another on the outside face of the insulation. As the thermal capacity of the insulation was negligible and temperature differences across it were also not large, this would allow the calculation of any heat flux through internal walls. The aluminum face of the insulation would also reduce any radiation exchange between the envelope and the walls. As a result of these precautions, the heat flux, was found to be small.

### 6.3.2 Environmental Chamber

To simulate the outside environmental temperature a space of 1.4 m. wide was enclosed outside the external wall side of the test room, as an "environmental chamber".

The air temperature in the environmental chamber was controlled by a cam controller, series QG of West Instrument Co. A complete revolution of the appropriately shaped cam during twenty four hours of the day represented the sol-air temperature in the hot dry climate

during the day . It was first decided to warm the air in the environmental chamber by commercially available fan heaters, but after a few days they caught fire and failed. A appropriate system of air heaters was designed and built. It consisted of six, 1 kW rod heaters, it was connected to the chamber's wall. The heaters of the air heater system were connected to the cam controller so that when the temperature in the chamber fell below the required temperature of the cam , the heaters would switch on. A fan was fixed at the opening of the heater to circulate the air into the chamber through the heater as well as circulating the air in the chamber to avoid a temperature build up near the top of the wall.

### 6.3.3 Temperature measurement

All temperatures were measured using welded copper constantan type 'k', thermocouples to British Standard 1041 (1966) with plastic insulation. The junctions were first twisted and then welded together. For surface temperatures, the junctions were first fixed on the surface of the concrete wall , and then covered with a thin layer of cement paste to make them subject to same radiation regime as the wall itself. For air temperature measurement all thermocouples were suspended in a polished aluminium shield to minimize the effect of radiation on the thermocouple .

Each surface of the room was divided into equal areas and the overall surface temperature was averaged over the surface. The air temperature was also measured at three different heights and three locations within the room. Figures 6.1 and 6.2 show the location of the thermocouples.

All thermocouples were connected to a CD284 Christie Data Logger with 64 channels. A cassette recorder module was coupled directly to the data logger. The data logger registered all temperatures in degree C with a cold junction reference compensation , by means of a P.R.T. sensor utilizing input to channel 1. The P.R.T. sensor was first installed on the inside surface of the panel at the rear of the data logger . This was found to result in random errors up to 3 degrees , due to the temperature difference between the ambient in the laboratory and the inside surface of the data logger's panel, where the thermocouples are connected to the logger. The data logger was sent to the manufacturer and this discrepancy was corrected by fixing the P.R.T. sensor on the outside surface of the panel. All observations were then repeated.



#### 6.3.4 Air flow measurement

At first it was decided to use a low velocity heated thermistor anemometer to monitor air flow, but this was rejected as the accuracy obtained from the available instrument was not sufficient. The orifice plate technique to B.S. 1042 (1982) was finally used for the measurement of air flow.

A rectangular base pyramid was fixed to the back opening to collect the ventilated air from the room. It was connected by a plastic flexible pipe to a long pipe with the orifice plate in the middle of the pipe. The orifice plate, the upstream and downstream length of the pipe were designed to comply with British Standard BS 1042 part 1.(1982) Pressure tapings were positioned close to the surfaces of the orifice plate and pressure difference was measured with a Furnace micro manometer, capable of reading a maximum of 100 Pa. The flow rate is computed according to BS 1042 section 1.4 part two(1982). The details of the orifice plate technique used are described by Lee.(1979)

The measurements were conducted in a range from three air changes per hour to 30 air changes per hour (55 to 3.7 litres/second) In order to achieve such a wide range it was necessary to use pipes of 100 mm. and 150 mm. diameter with appropriate orifice plates.

#### 6.4 Measurement procedure

Figure 6.3 represents the outside air temperature wave-form and resulting outside surface temperature imposed on the experimental room for each 24-hour period. The air temperature cycle of figure 6.3 was derived from the solair temperature pattern appropriate to a hot climate.

The temperature variations as shown were maintained for a period of about three weeks before observations were made and the system reached steady cyclic conditions, i.e. the temperature cycle repeating itself over the 24 hour period. Two sets of measurements were made: one with 10 hours of ventilation, and the other with 4 hours of ventilation each with different rates of air flow.

In the cases with 10 hours of ventilation the shutters over the windows were removed at 2000 hours and were replaced at 0600 hours. In the cases of 4 hours of ventilation, the windows were open between 2000 hours and 2400 hours. Each observation was repeated on two consecutive days and the results of the second day were used for the

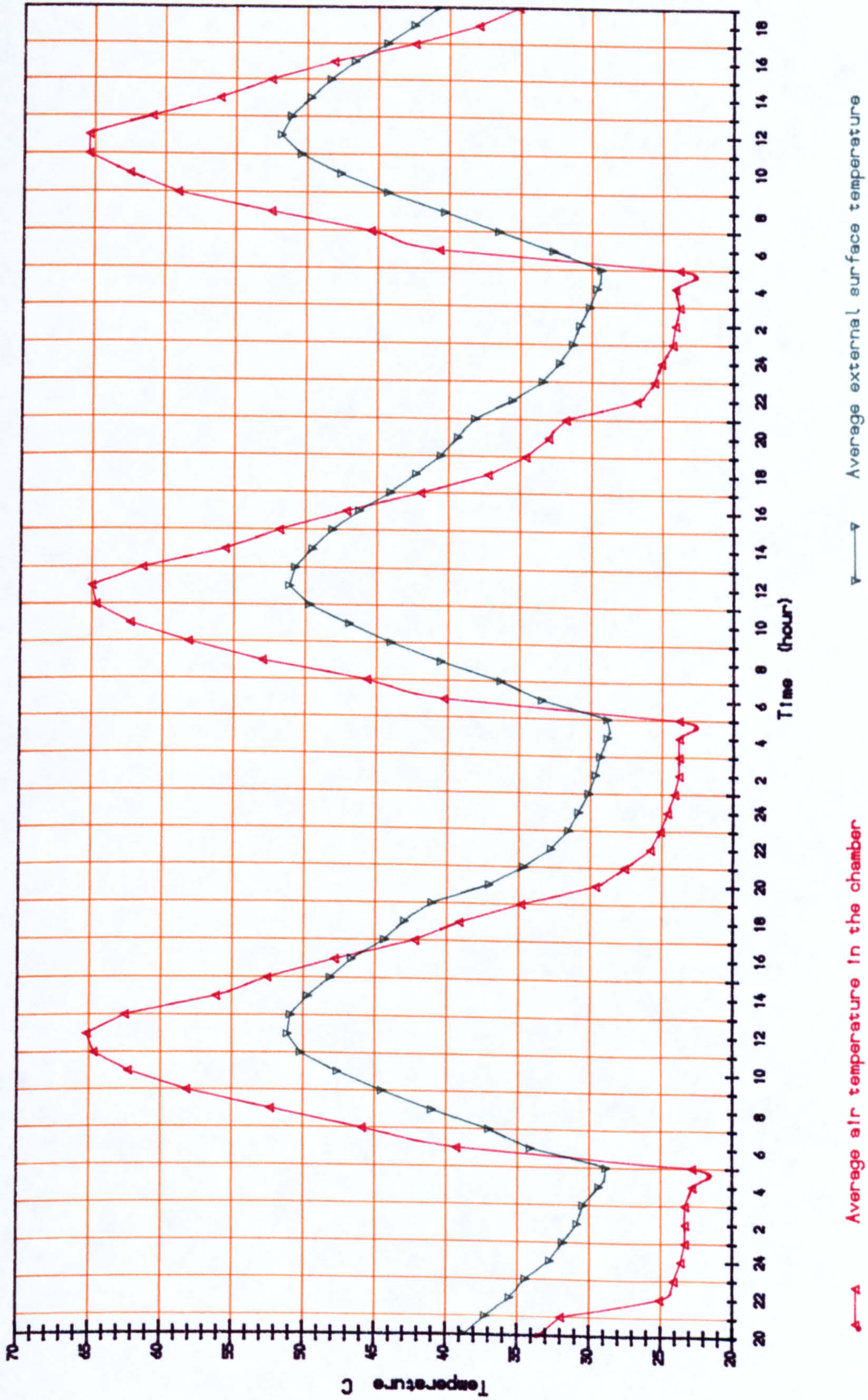


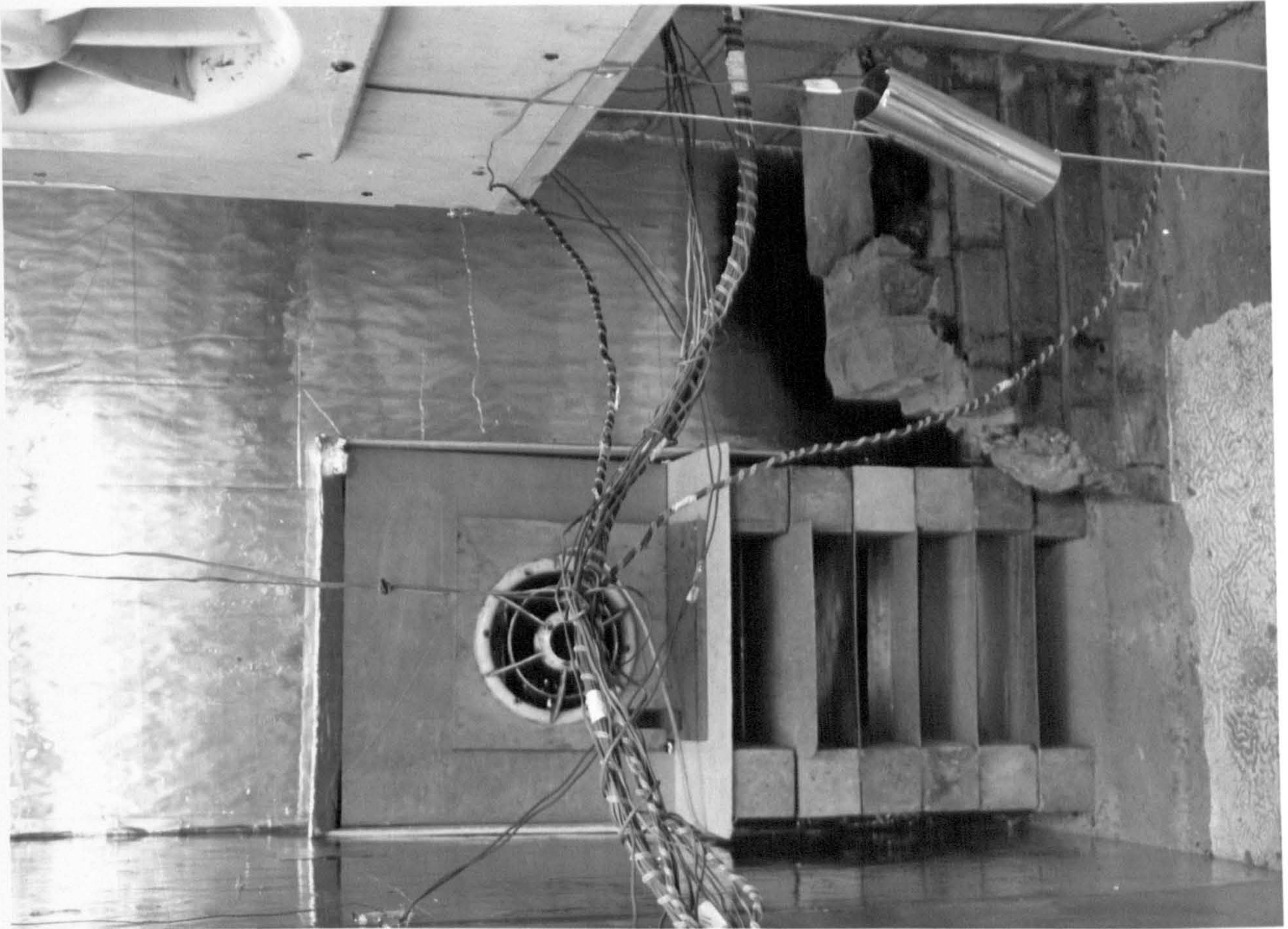
Figure 6.3. Variations of temperature in the environmental chamber for three days

**Plate 6.1: The environmental chamber and the air flow measurement device**

114

The louvers (which obscure the air heater), reduces heat exchange with surrounding surfaces to avoid local temperature increase

The air is collected by the cone, and passes through a flexible duct to the pipe containing an orifice plate to B.S. 1042 (1982)



analysis, although the result of the first and second day were found to be very similar.

After each measurement the system was left for at least 24 hours without ventilation before the next measurements were made.

A complete set of data for each test consisted of the recorded temperatures and the digital output from the micromanometer for every 15 minutes. The hourly values of the temperatures were averages based on 15 minute measurements.

The physical properties of the materials used in the building and used in the computer program and analysis are given in table 6.1. Thermal conductivity and specific heat capacity of the material used in the observations are obtained from the CIBSE Guide chapter A-3 and from the relevant literature. The thermal conductivity of the concrete used in the experiment was corrected according to the moisture content of the material obtained from oven dried samples and determined according to Stuckes et al. (1986).

Table 6.1 Physical specifications of the test room

	$\lambda$ W/m K	$l$ m	$\rho$ kg/m <sup>3</sup>	$c_p$ J/kg K
Outside wall concrete	1.35	0.10	2100	1000
Ceiling plywood foam	0.14 0.022	0.0065 0.055	530 32	1200 1400
Floor concrete	1.35	0.05	2100	1000
Inside Wall concrete	1.35	0.10	2100	1000
Insulation "Celotex"	0.020	0.03	35	1400

### 6.5 Measurements accuracy and uncertainty

The uncertainty and errors associated with the measurements are the followings :

- accuracy of the thermocouples and temperature measurements
- accuracy of air flow measurements
- uncertainty in the physical properties

A number of thermocouples were selected from each reel of wires used in the work. The thermocouples were connected to the data logger and the junctions were put in a bath of well stirred iced distilled water. The water was warmed, and a range of readings between ice point and boiling water was compared with a mercury thermometer with 0.1 K resolution. The data logger could be linearized with a typical resolution of 0.25 K for copper constantan thermocouples. The uncertainty in the temperature measurement was found to be about  $\pm 0.50$  K.

Different parameters influence the uncertainty of air flow measurement. British Standard 1042 (1982) suggests a formula for practical calculation of the uncertainty of the flow measurement. As in the design of the orifice plate, the upstream and downstream length of the pipe was fully in accordance with the B.S., it was not necessary to consider additional uncertainty.

Air density varies with temperature. Using different air densities according to temperature was not practicable. A fixed value from the appropriate charts at 30 C was used. This was found not to cause a great error as air density changes less than 6 % with 20 K difference in temperature. The accuracy of the pressure difference measurement was assumed to be 10 %. Using the B.S. procedure to calculate the overall accuracy of air flow, it was found that the maximum error in the flow, in the range used in the measurements, was less than 5%.

The physical properties of the building material can be a significant problem. The specific heat capacity and thermal conductivity of the concrete blocks are taken from the CIBSE Guide, and the insulation board and the ceiling board from the manufacturer's specification. The uncertainty of the conductivity of the material is considered to be 5% after the appropriate correction for the moisture content.

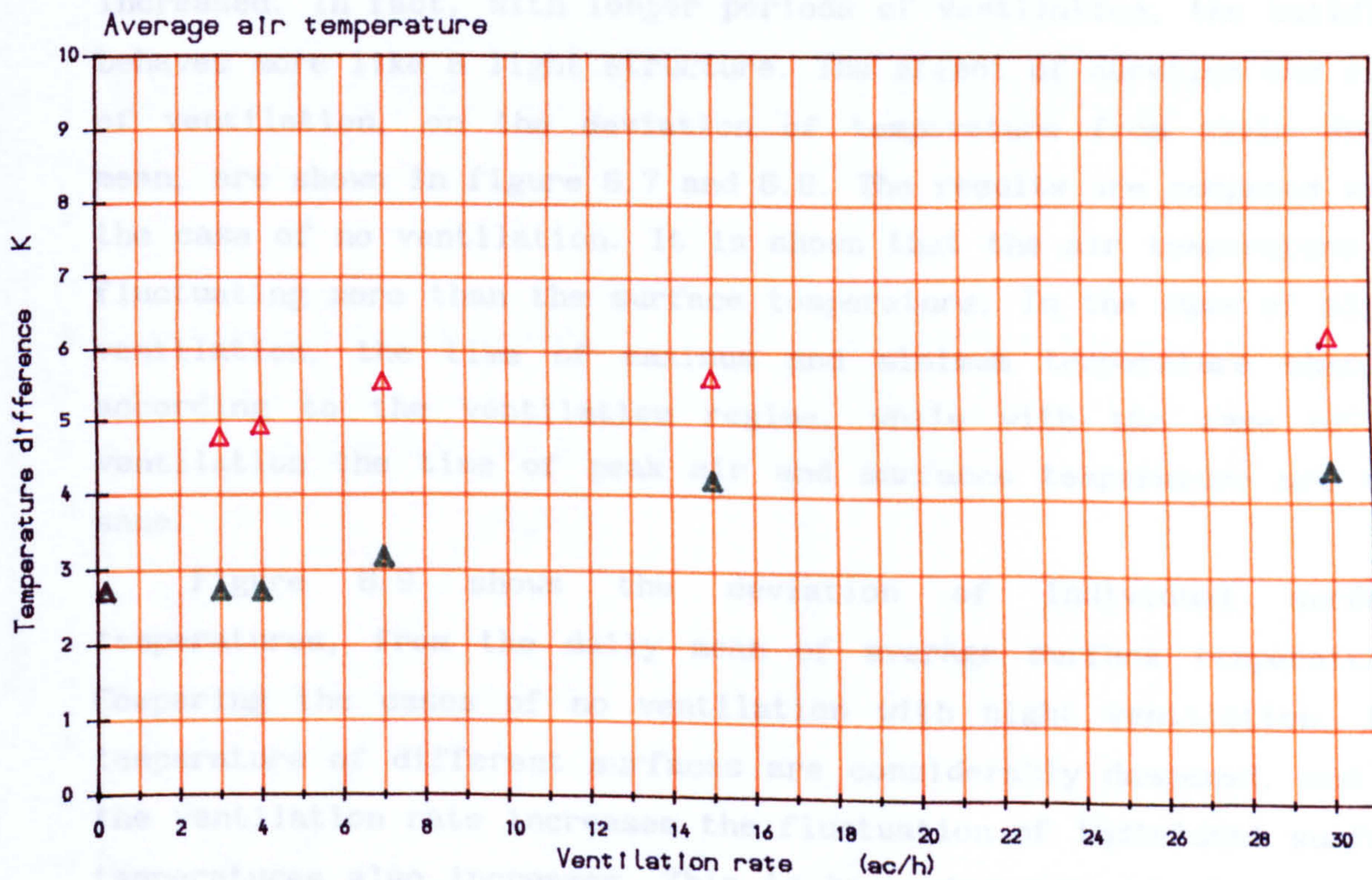
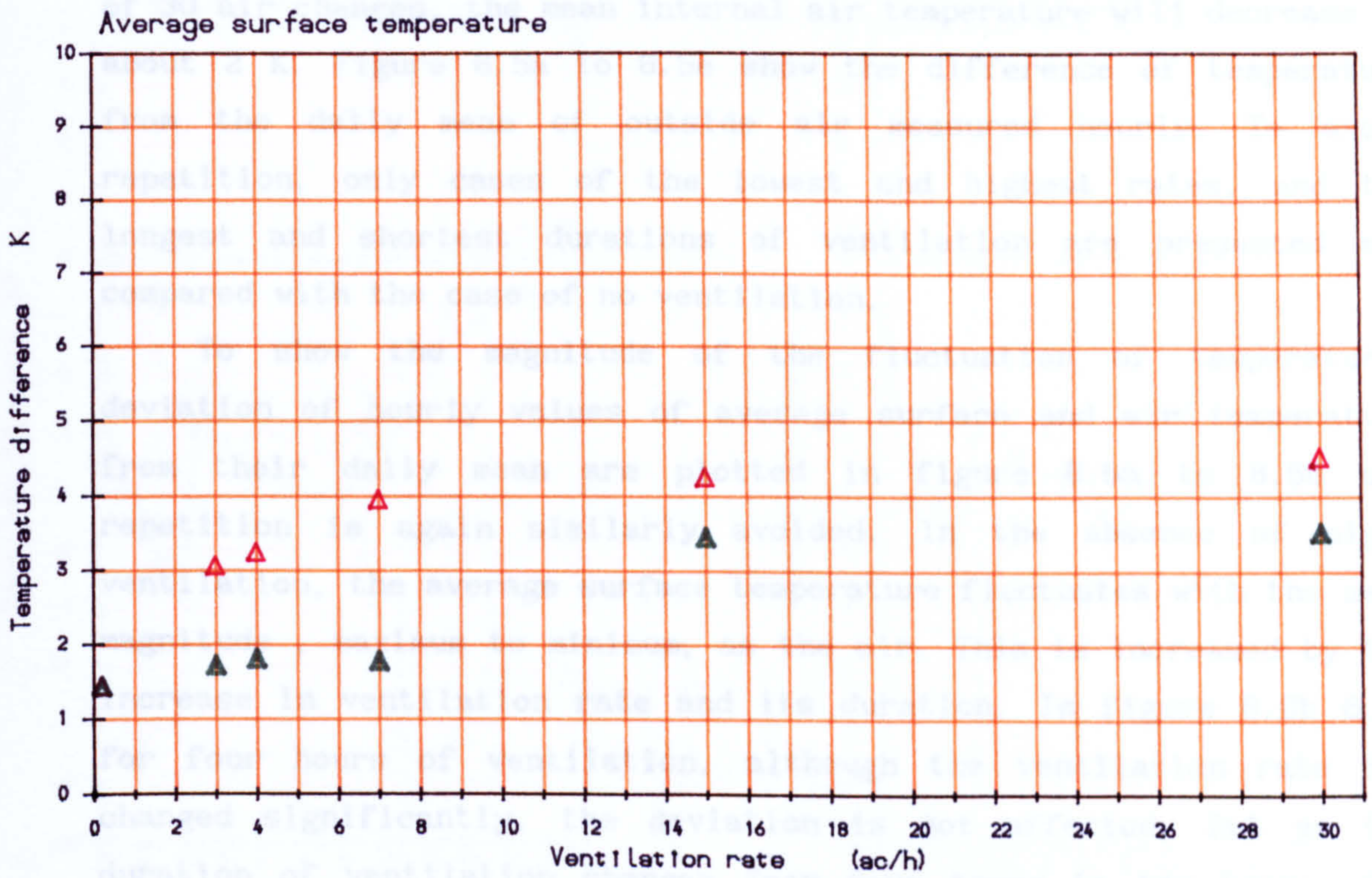
The dynamic physical factors of the structures used in the admittance method, the admittance, decrement factor and surface factor, are related to the outside surface resistance,  $R_{so}$ . The standard values are not applicable, because the conditions are totally different. The overall value is calculated by a surface energy balance at the outside surface and with the finite difference approximation for transient one dimensional heat conduction. A daily mean value of  $R_{so}=0.15 \text{ Km}^2/\text{W}$  was chosen.

## 6.6 Results and discussion

The measurements were performed primarily for the evaluation, and comparison of the models under consideration in this study, but through the analysis of the data obtained from the measurements, some useful points may be noticed. In addition the analysis of the response of the test room to night-ventilation determines the importance of the factors influencing the development of the mathematical models. The observations also show trends in which the buildings behave under different regimes of ventilation. It should be mentioned that because the measurements were not identical, and slight uncontrollable variation in the observation, were unavoidable, direct comparison of the results is not possible. Instead the relation between them is discussed.

Figure 6.4 shows the difference between the daily mean of internal air and the average surface temperature from daily mean of the outside air, for ten and four hours of ventilation. When the room is not ventilated and no energy is put into the room, the daily mean temperature of inside air and outside air would be expected to be the same. The inside air and average surface temperature are then also expected to be equal. The graph shows some differences. This might be accounted for by two sources: heat loss through the internal surfaces, and infiltration into the room. The room internal surfaces were covered with insulation board. Because the overall thermal capacity of the insulation board is negligible, this makes it possible to calculate the heat loss through them, and is accounted for in the calculations as discussed above (6.3.1), but for the present comparison it is not possible to take it into consideration. The infiltration rate is also not measured. Air moves between the environmental chamber and the test room, through the cracks around the front opening and even the plywood shutter. It also moves to the space around the test room, although precautions were taken to keep its temperature the same as that of the test room. For the calculations a fixed value for the infiltration is allowed for in all observations. These are a source of systematic errors and will not affect the comparison of different observations.

Figure 6.4 shows that, the duration of ventilation is more important than its rate. For example, when the room is ventilated by 30 air changes per hour for four hours, total of 120 air changes, the difference between the mean inside air and mean of outside air will not significantly change, But with 3 ac/h for ten hours, at a total



▲ ▲ Ten hours of ventilation      ▲ ▲ Four hours of ventilation

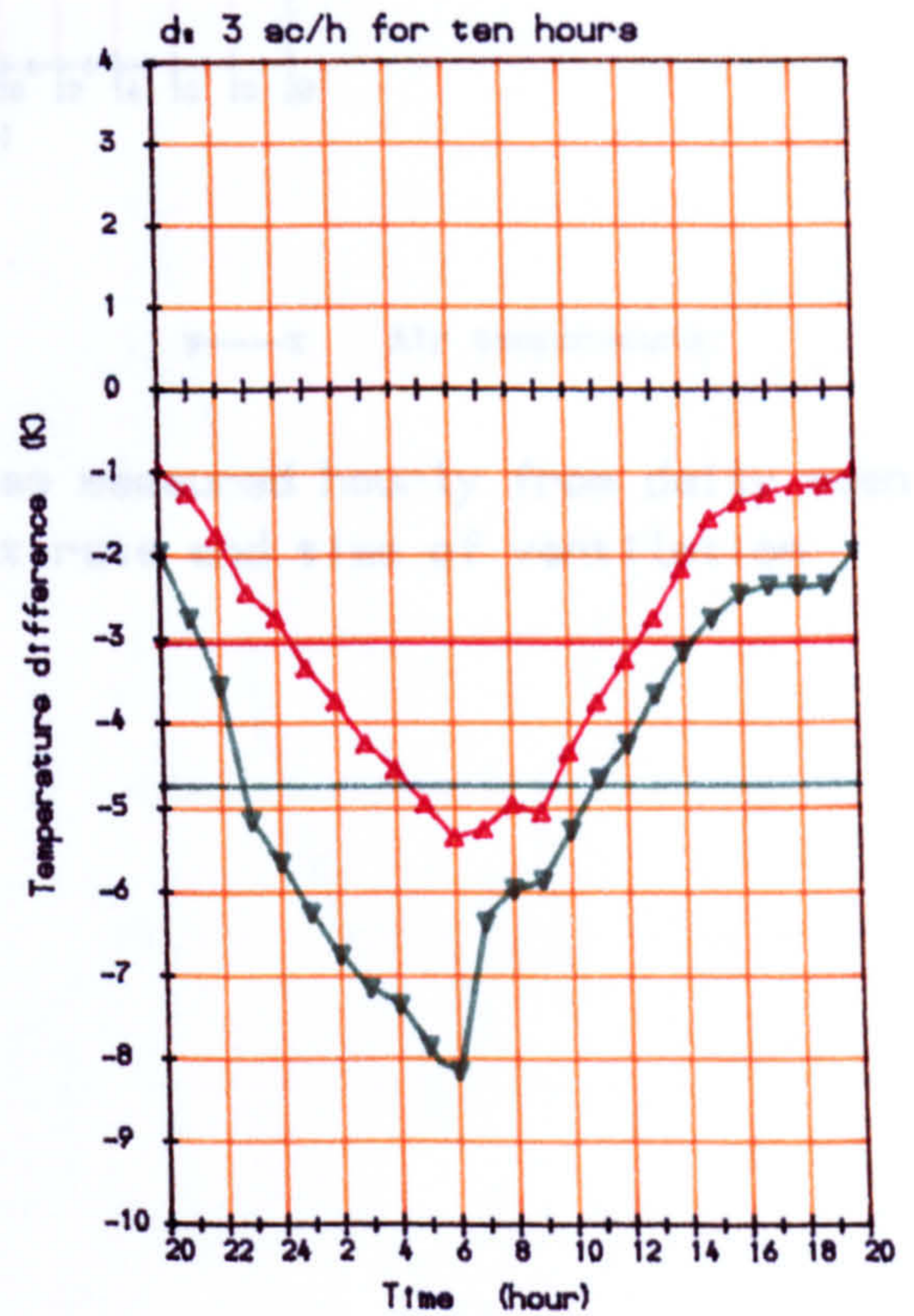
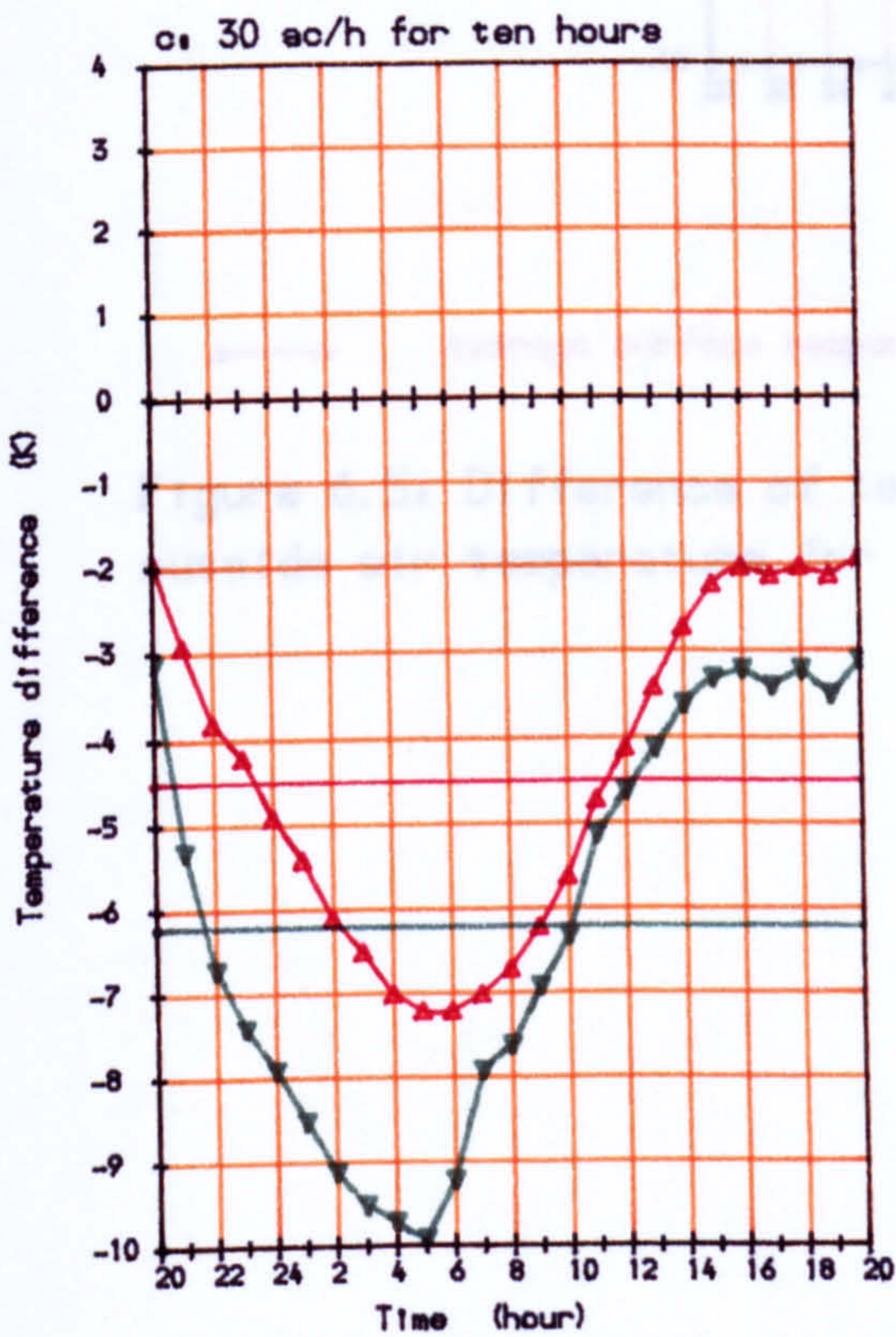
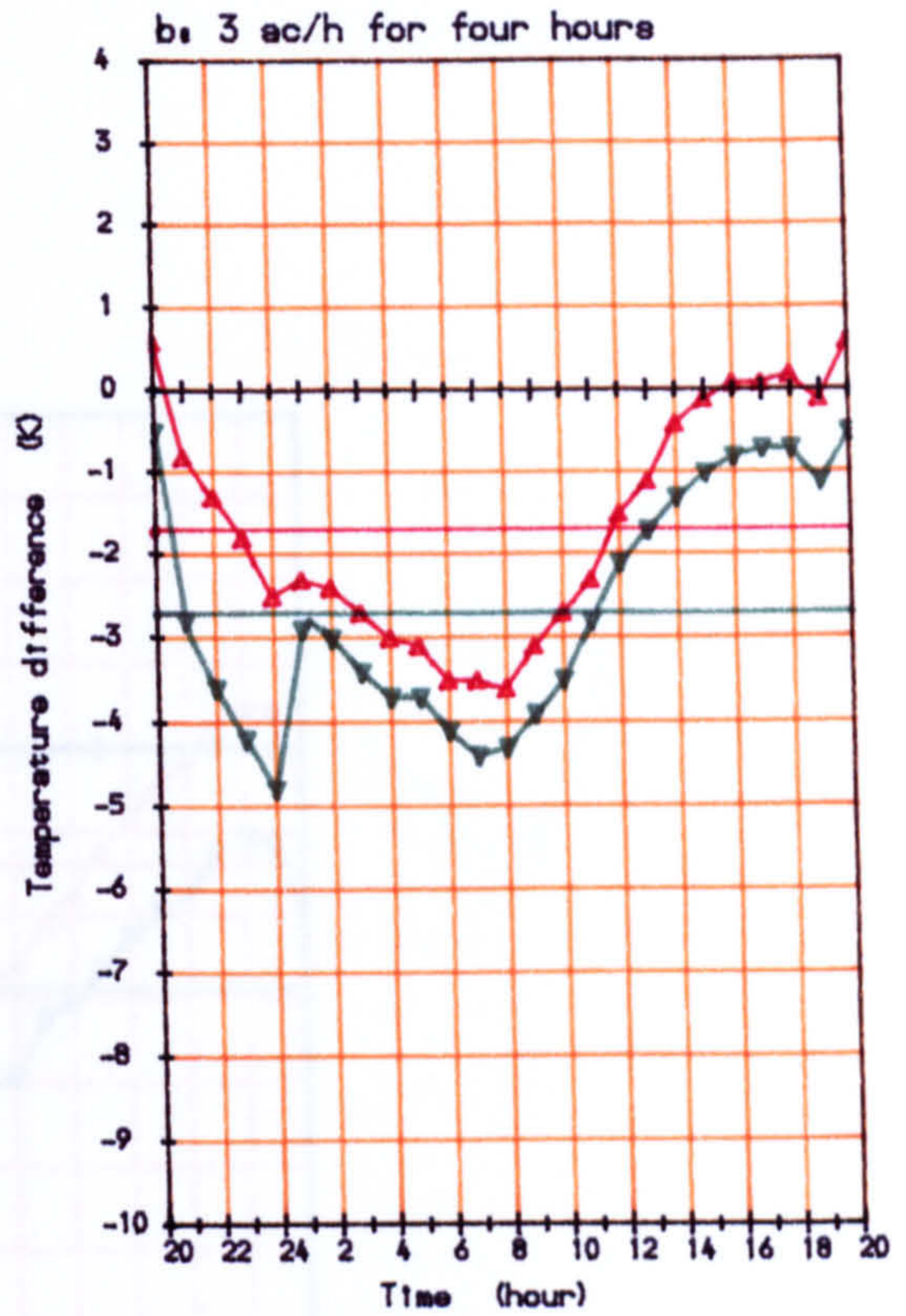
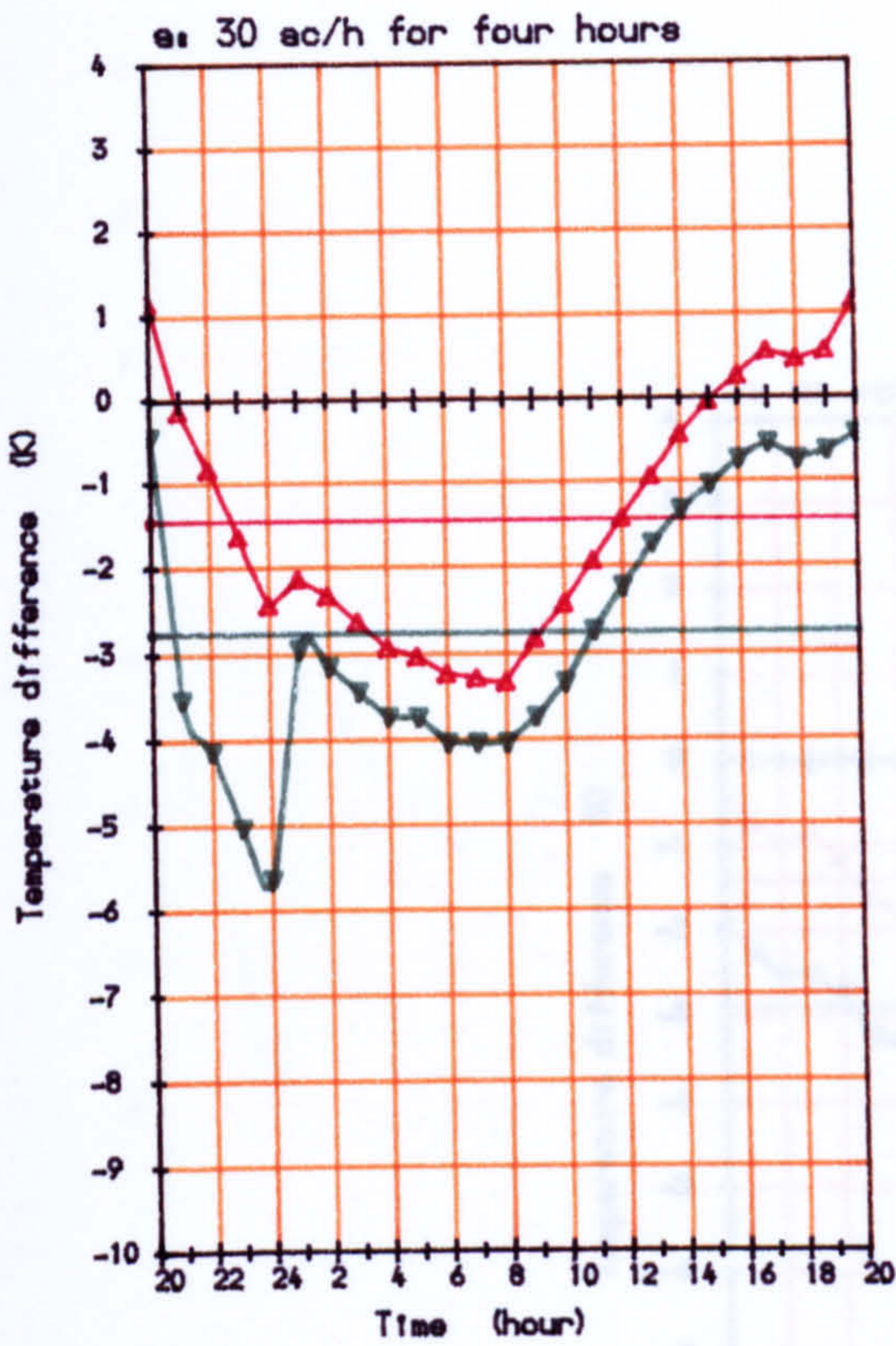
Figure 6.4: Deviation of daily mean air and average surface temperature from daily mean of outside air



of 30 air changes, the mean internal air temperature will decrease by about 2 K. Figure 6.5a to 6.5e show the difference of temperature from the daily mean of outside air measured hourly. To avoid repetition, only cases of the lowest and highest rates, and the longest and shortest durations of ventilation are presented and compared with the case of no ventilation.

To show the magnitude of the fluctuation of temperature, deviation of hourly values of average surface and air temperature from their daily mean are plotted in figure 6.6a to 6.6e and repetition is again similarly avoided. In the absence of night ventilation, the average surface temperature fluctuates with the same magnitude, maximum to minimum, as the air. This is increased by the increase in ventilation rate and its duration. In figure 6.6b 6.6c for four hours of ventilation, although the ventilation rate has changed significantly, the deviation is not affected. But as the duration of ventilation changes from four hours to ten hours, the deviation of both average surface and air temperature is also increased. In fact, with longer periods of ventilation, the building behaves more like a light structure. The effect of duration and rate of ventilation, on the deviation of temperature from their daily mean, are shown in figure 6.7 and 6.8. The results are compared with the case of no ventilation. It is shown that the air temperature is fluctuating more than the surface temperature. In the case of night ventilation, the time of maximum and minimum temperature changes according to the ventilation regime, while with the case of no ventilation the time of peak air and surfaces temperature are the same.

Figure 6.9 shows the deviation of individual surface temperatures, from the daily mean of average surface temperature. Comparing the cases of no ventilation with night ventilation, the temperature of different surfaces are considerably dampened, and as the ventilation rate increases the fluctuation of individual surface temperatures also increases. This is happening more at the internal surface of the external wall. This is because the surface is less cooled with night ventilation, than other surfaces. The temperature difference between surfaces is also affected by the change in the ventilation rate. In comparison of figure(6.9a) and (6.9e), (no ventilation and 30 ac/h for 10 hours), the temperature difference between the internal face of the external wall and other surfaces increased by about 2 K. The temperature of the ceiling is also

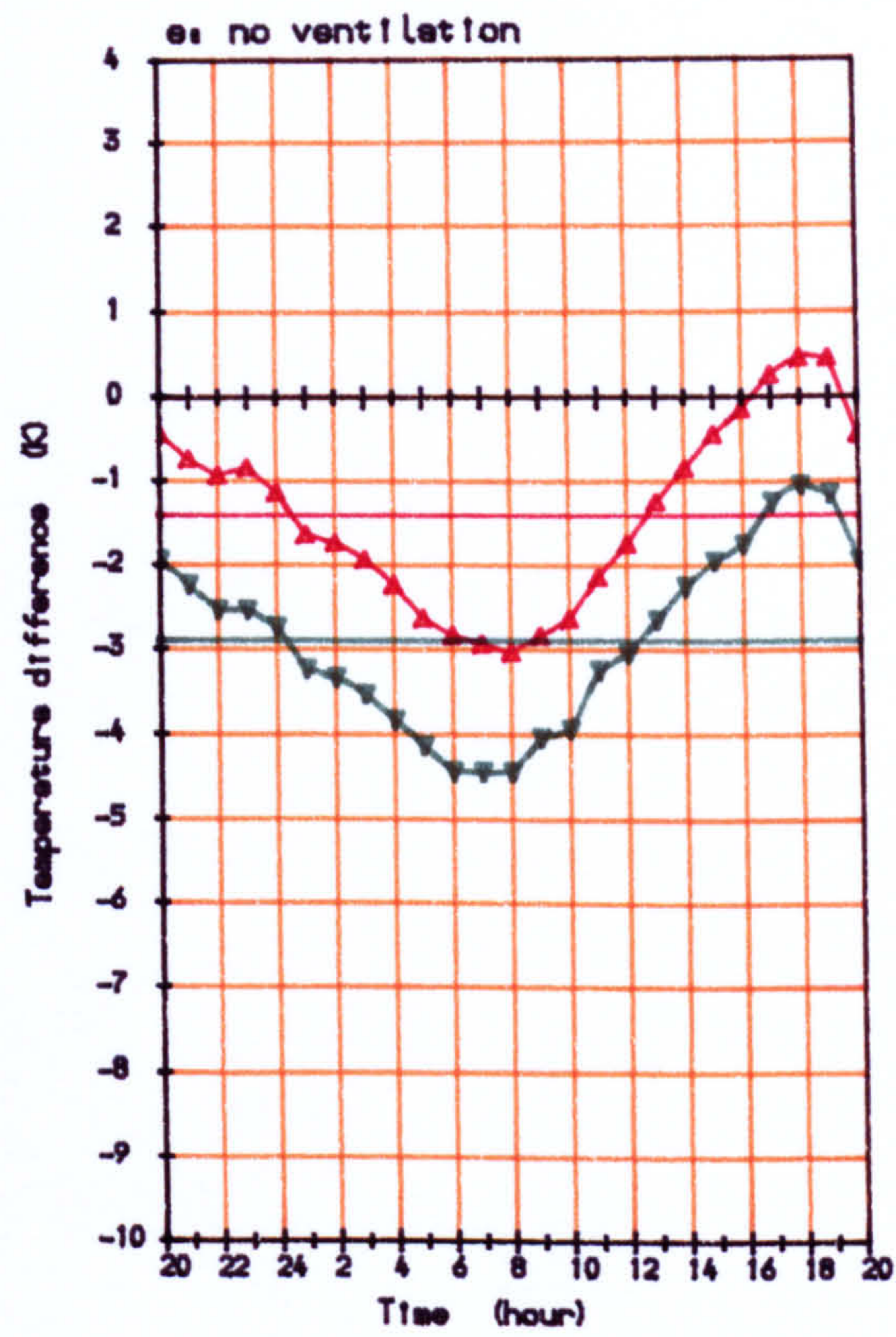


▲—▲ Average surface temperature

▼—▼ Air temperature

Figure 6.5: Difference of temperatures measured hourly from daily mean of outside air temperature for different rate and time of ventilation

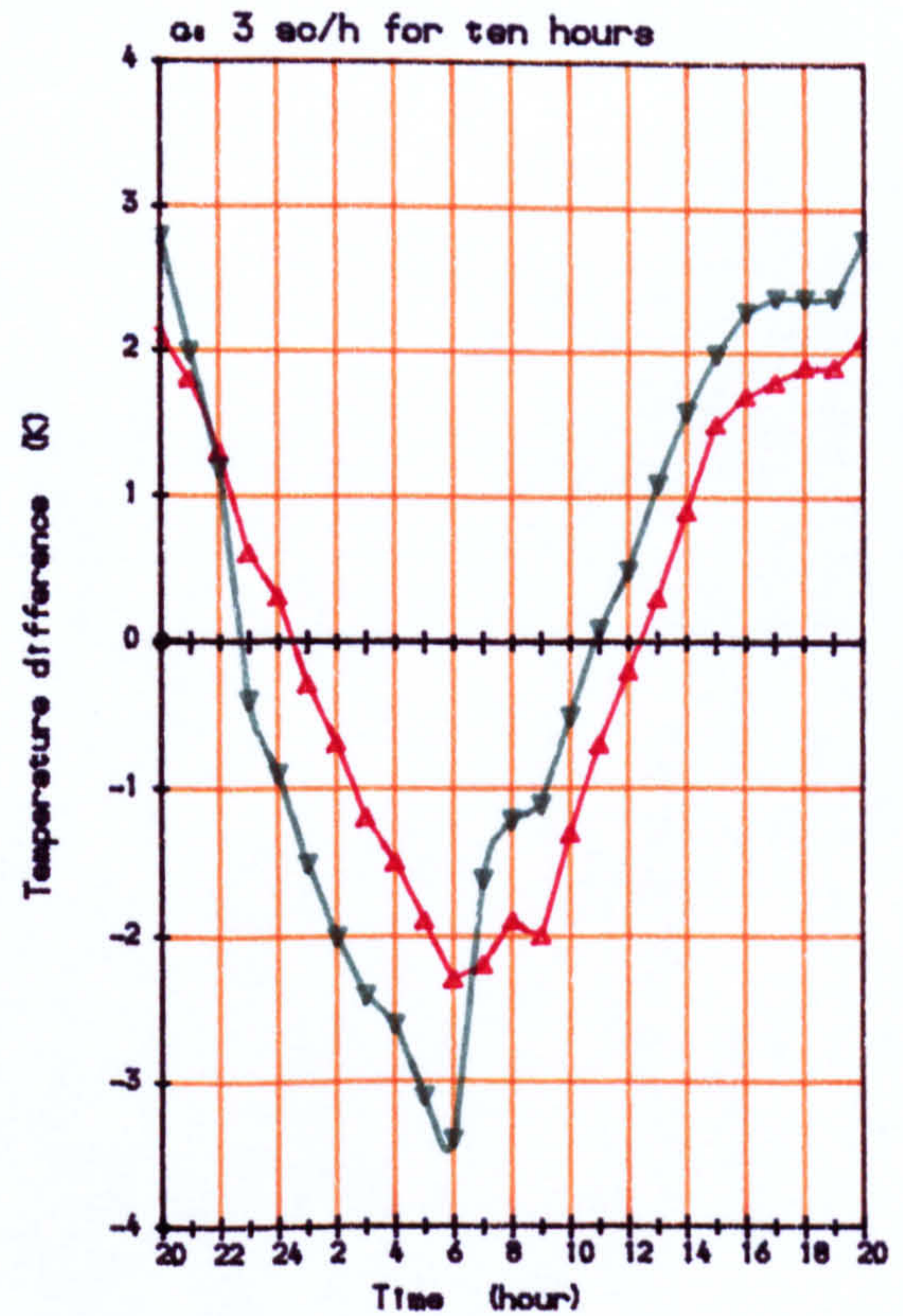
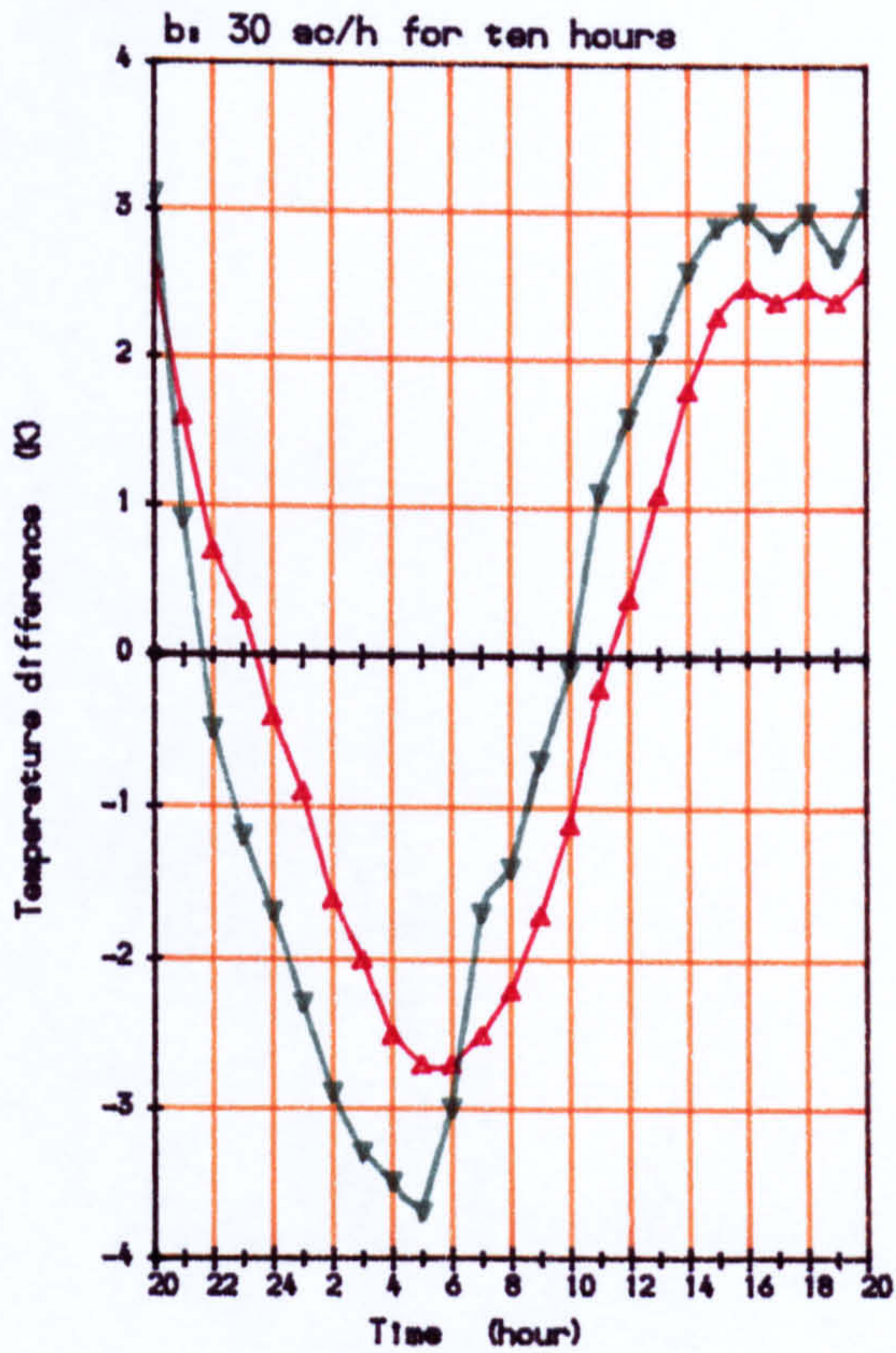
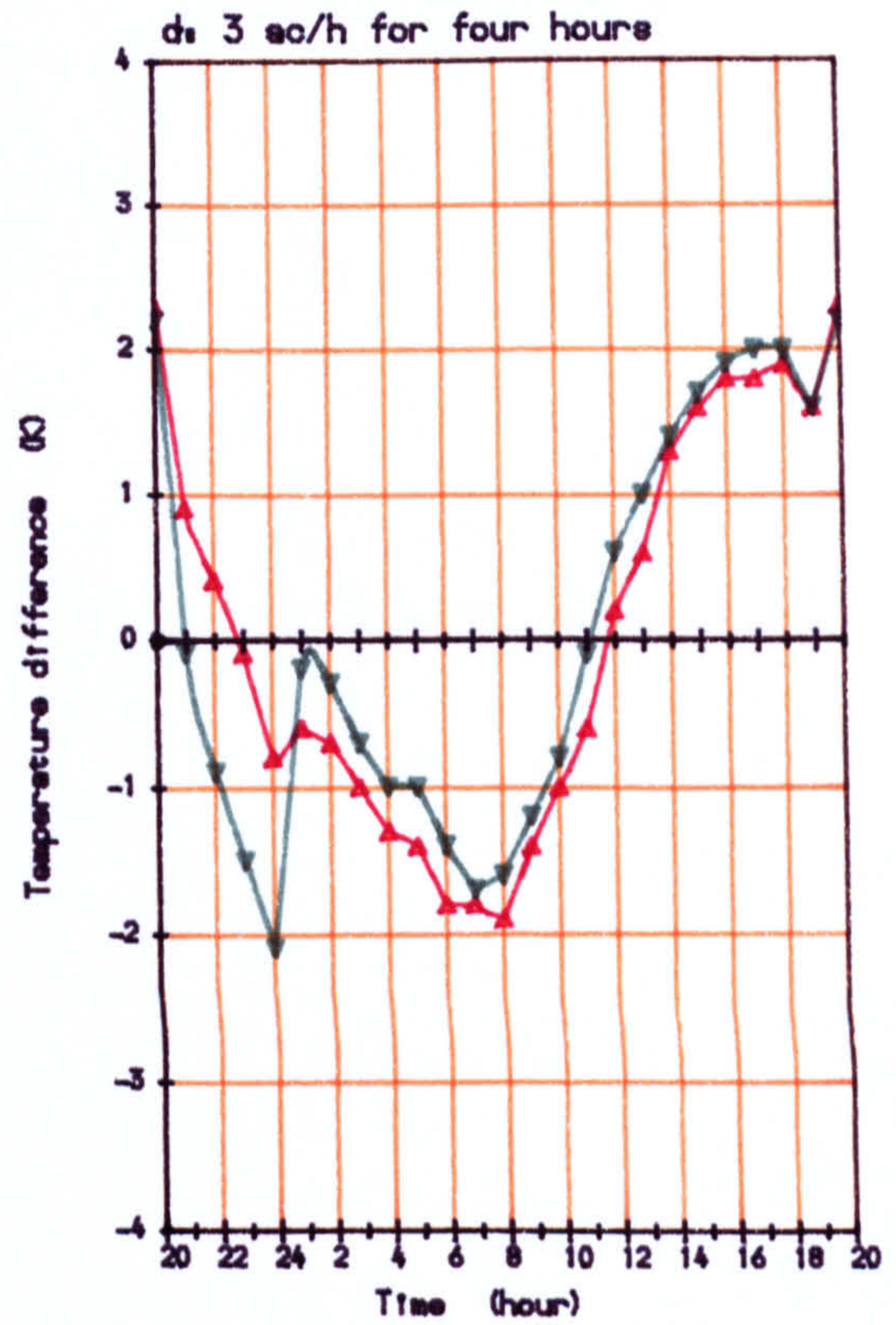
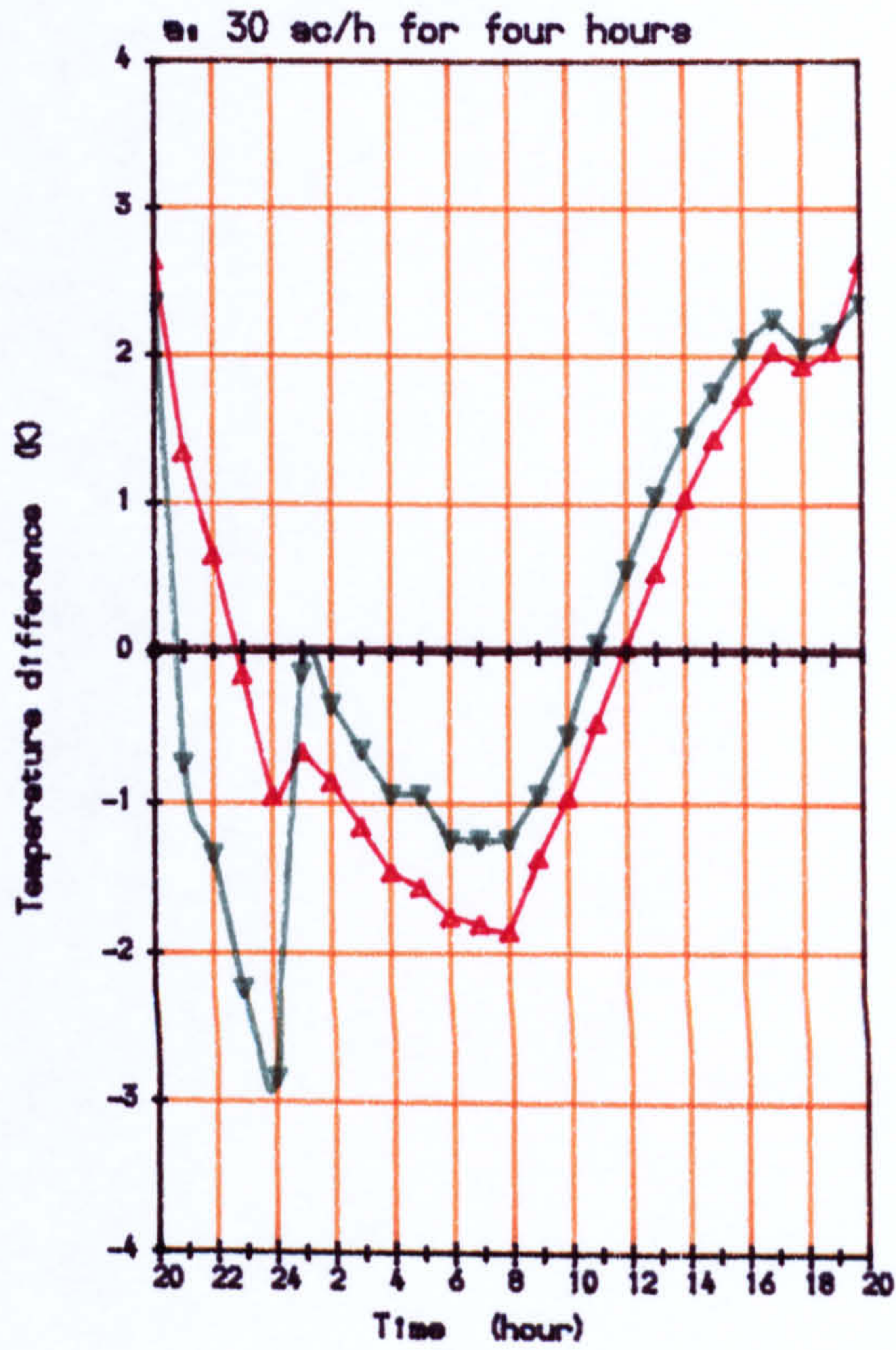
(Cont. next page)



▲—▲ Average surface temperature

▼—▼ Air temperature

Figure 6.5: Difference of temperatures measured hourly from daily mean of outside air temperature for different rate and time of ventilation

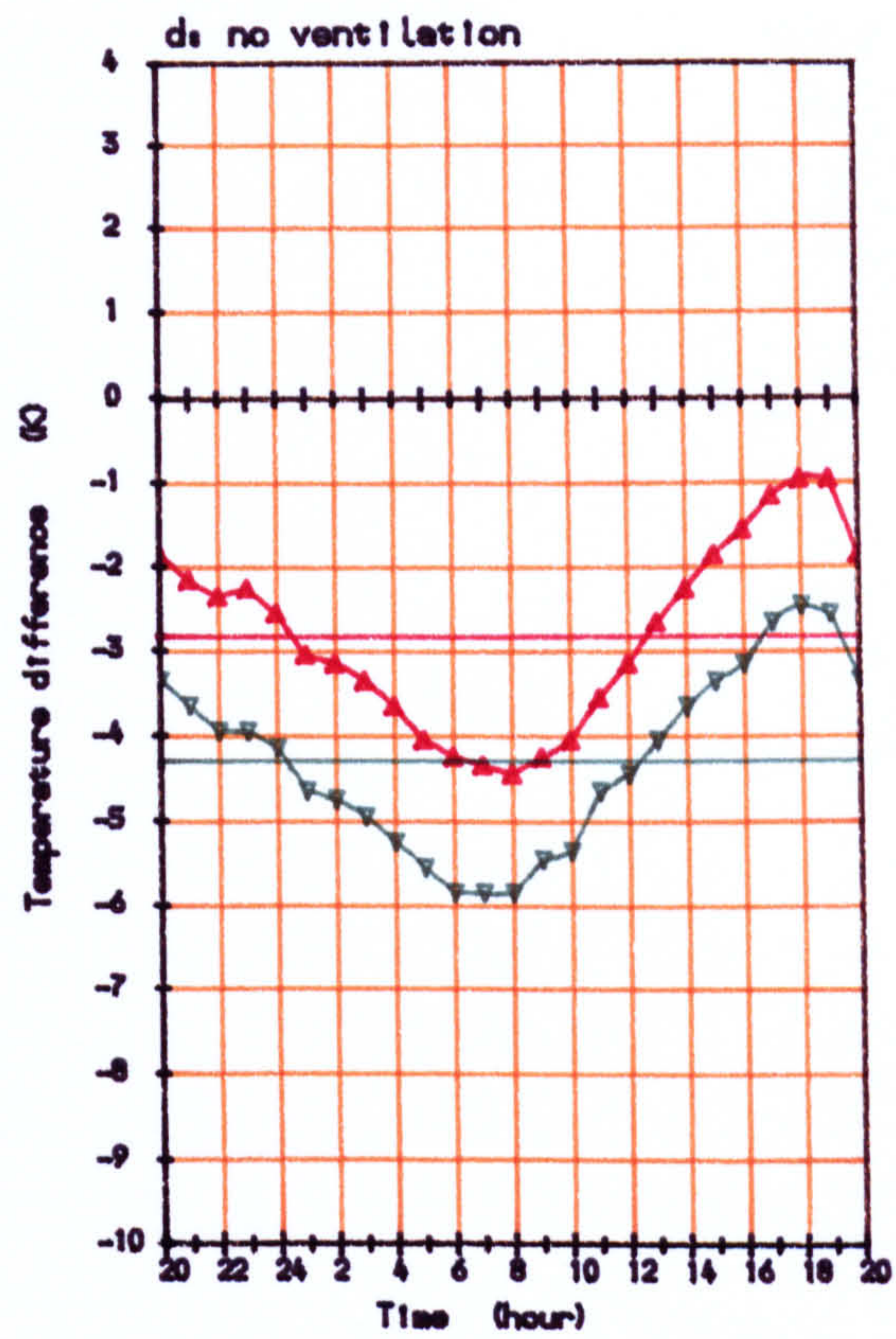


▲—▲ Average surface temperature

▼—▼ Air temperature

Figure 6.6: Difference of temperatures measured hourly from their daily mean for different rates and time of ventilation

(Cont. next page)



▲ Average surface temperature

▼ Air temperature

Figure 6.6: Difference of temperatures measured hourly from their daily mean for different rate and time of ventilation

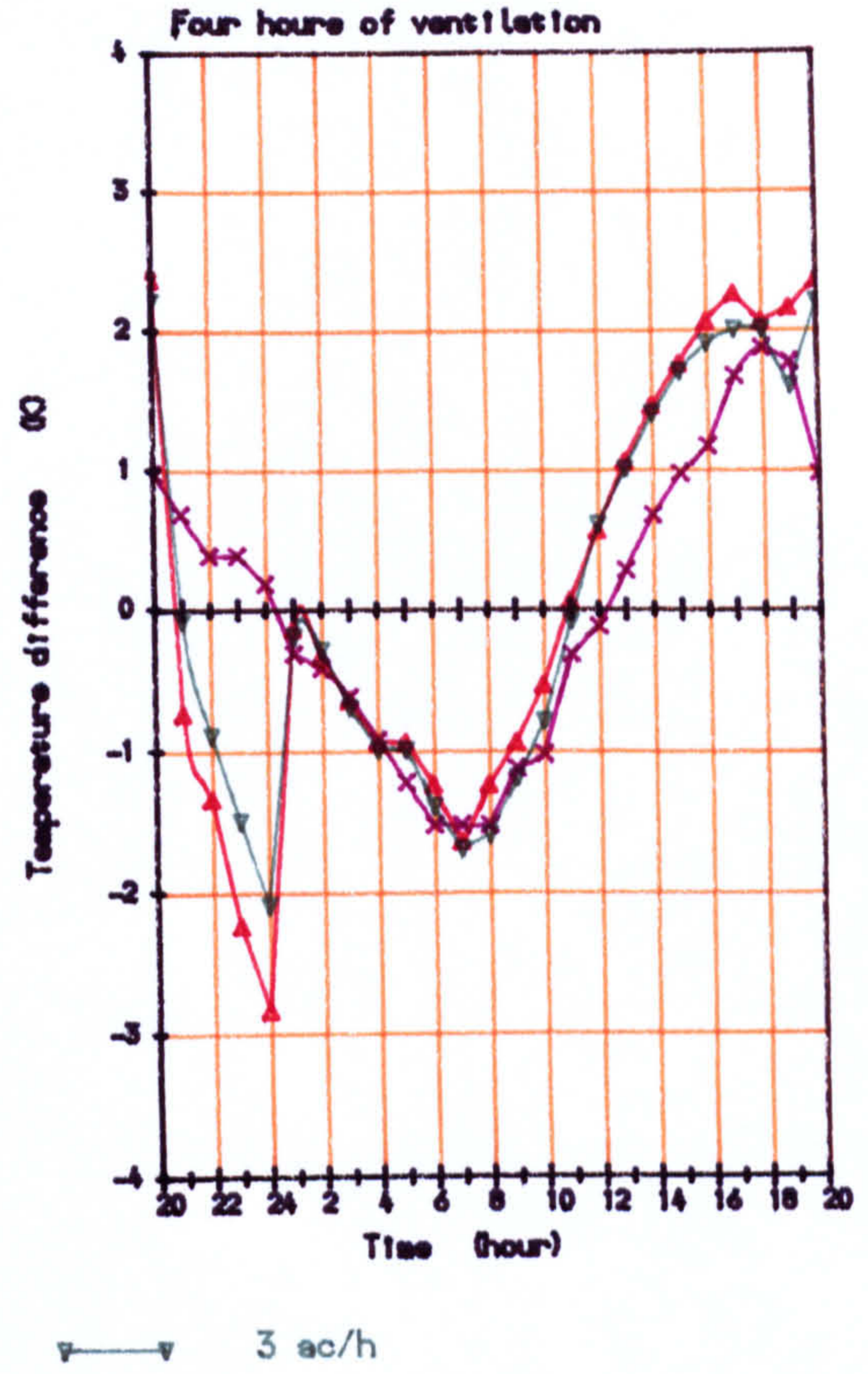
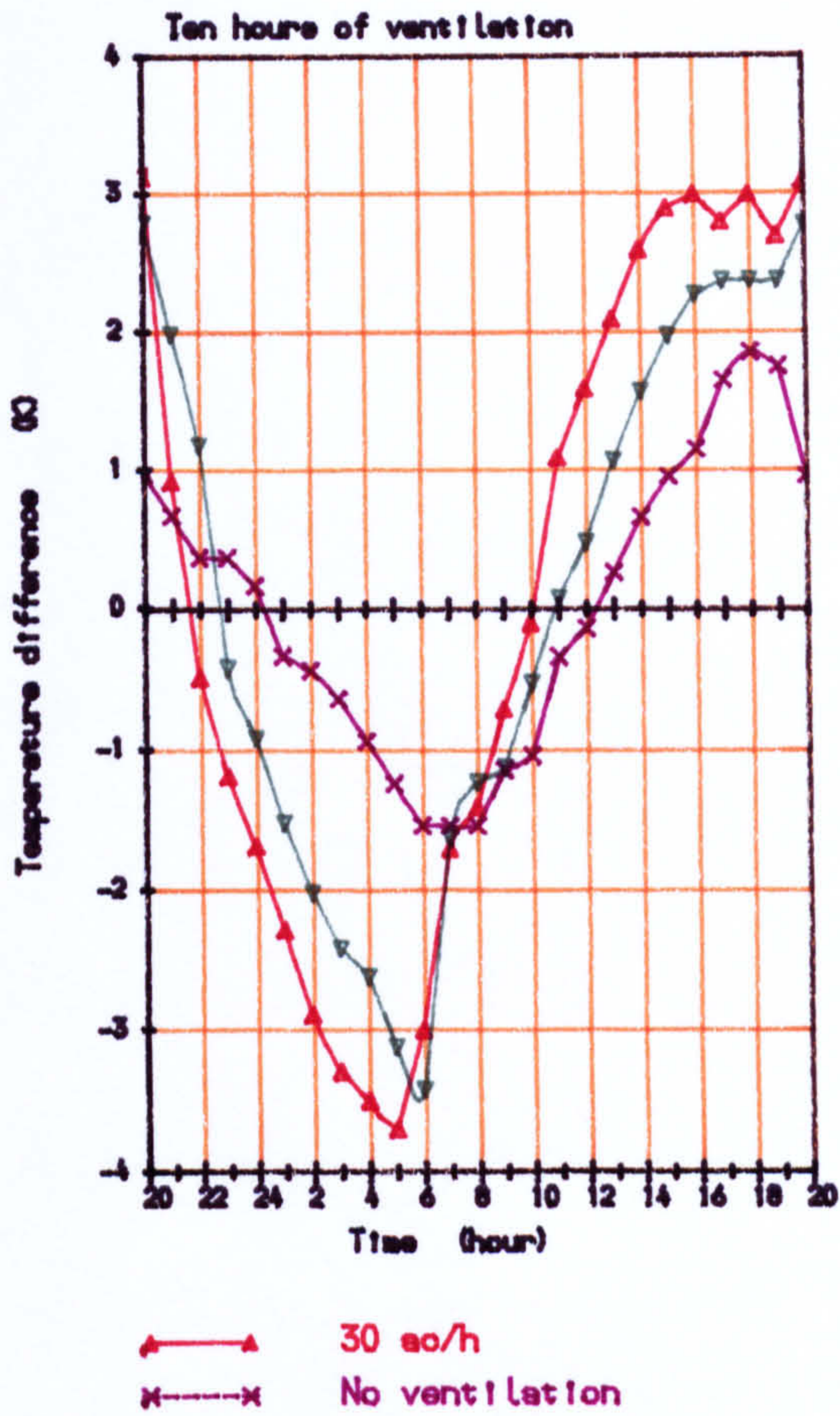


Figure 6.7: Deviation of air temperature measured hourly from their daily mean for different ventilation time

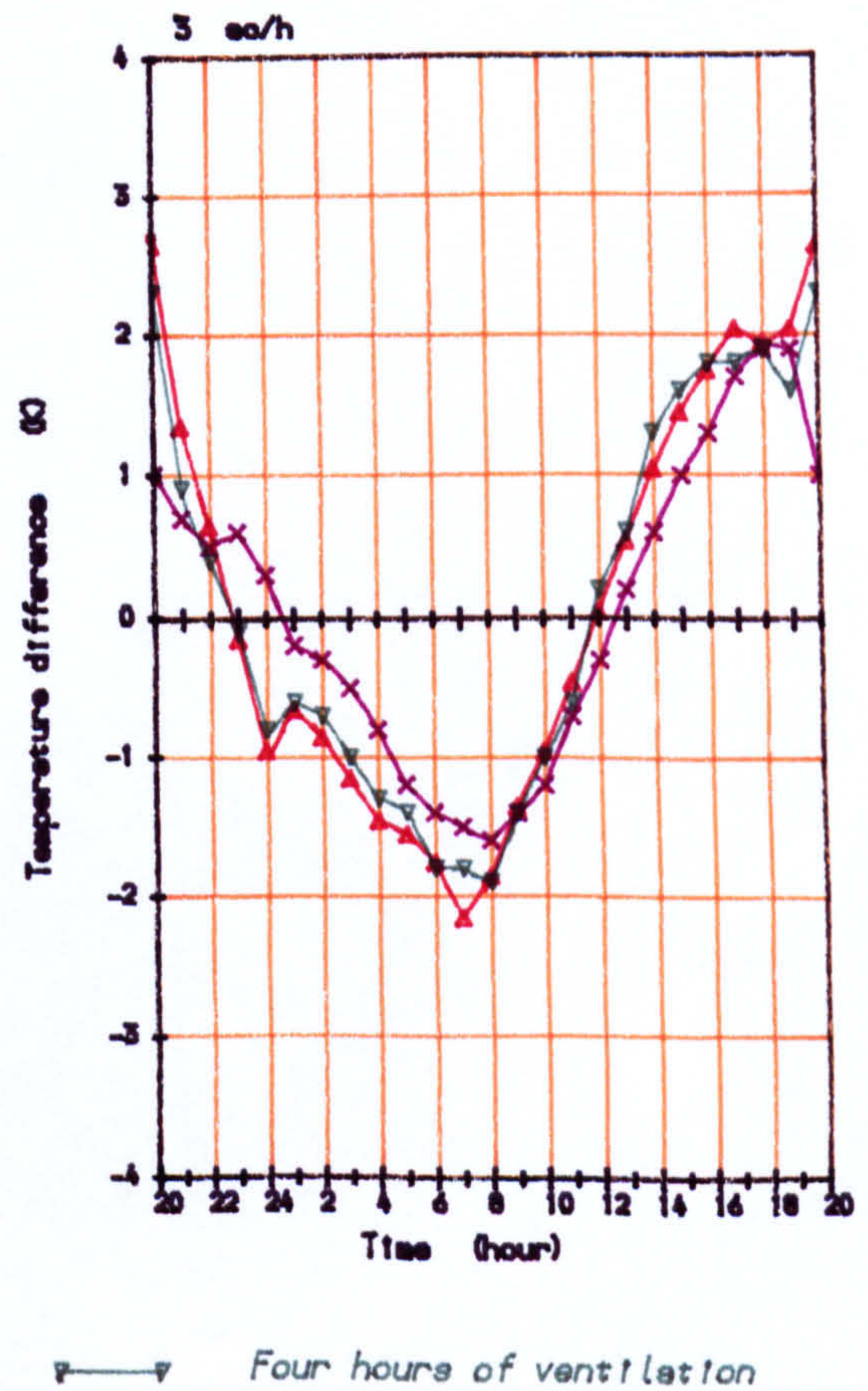
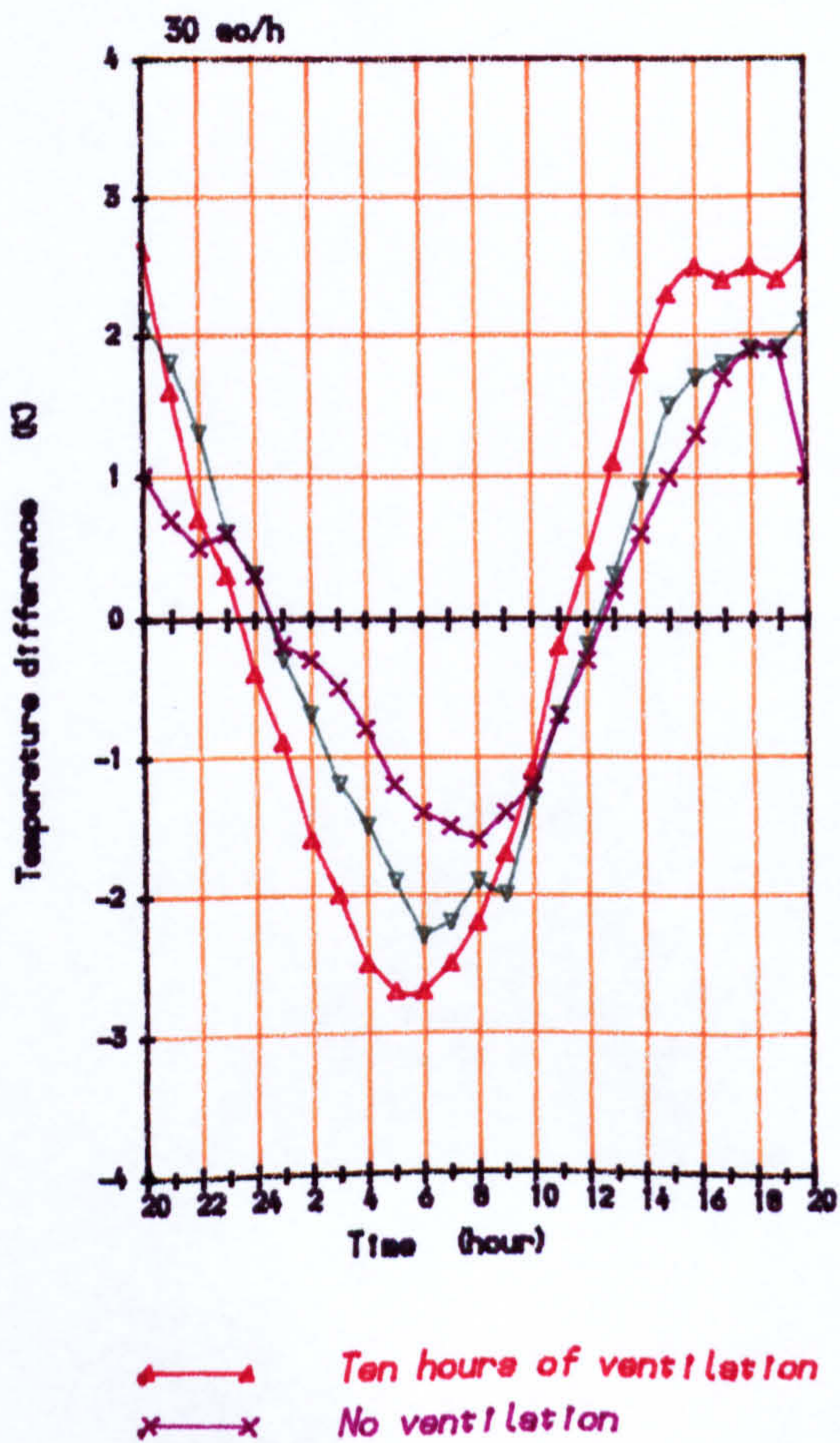


Figure 6.8: Deviation of average surface temperature measured hourly from their daily mean for different ventilation rates

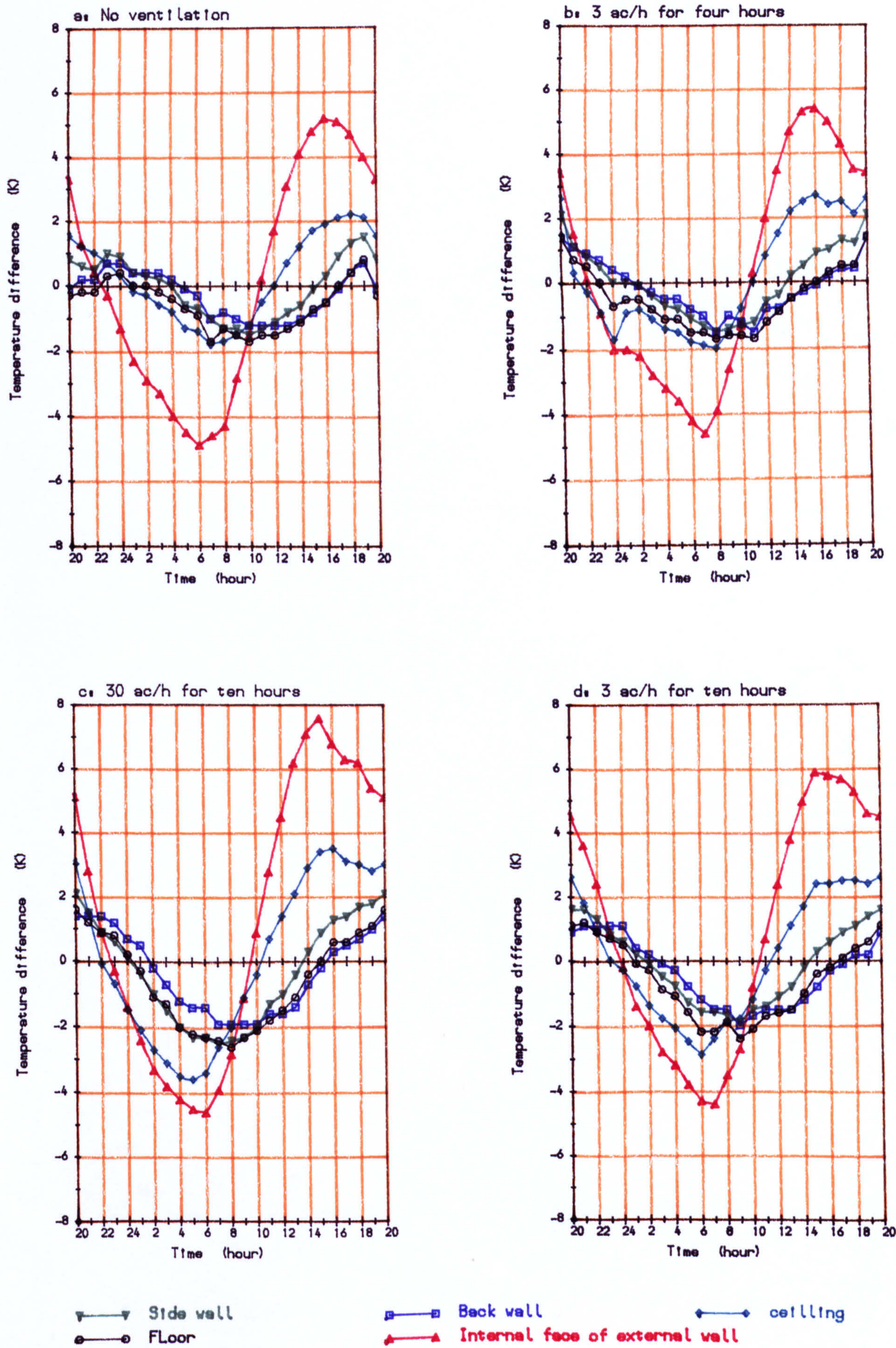


Figure 6.9: Deviation of surface temperatures from daily mean of average surface temperature for different rate and time of ventilation

responding more quickly to the ventilation rate. This is believed to be caused by the fact that the ceiling was made of light-weight material. The rest of the surfaces follow the same pattern of variations.

One must conclude that the indoor convection pattern is continuously changing and is also affected by the rate of ventilation. This is more important for the ceiling and the front wall. The time of minimum and maximum of individual surface temperatures (e.g. external wall and ceiling) is also changed by the ventilation regime.

To show the temperature difference between individual surfaces, in figure 6.10 the individual surface temperatures from instantaneous average surface temperature are plotted against time. Positive deviation signify that the temperature of the surface was higher than the average surface temperature at the time. Although most of the surfaces are in equilibrium, the plot suggests that the radiation exchange between the surfaces is slightly affected by the ventilation regime.

Figure 6.11 shows the variations of temperature at different points on the internal face of the external wall along a vertical axis. The figure shows that the pattern of temperature gradient over the wall is the same for different regimes of ventilation. This suggests that the assumption of one dimensional heat flow across the external wall is not affected by the variations in the ventilation regime.

Similarly figure 6.12 shows the temperature variations for different thermocouple positions on the side wall, along a vertical and horizontal axis. As for the external wall, the temperatures were not greatly affected by the variation in the ventilation rate and its duration.

In figure 6.13 the deviations of inside air temperature from instantaneous average air temperature at different thermocouple locations for different rates and duration of ventilation are plotted against time. The graph suggests that the temperature difference between thermocouple locations is affected by the changes in the ventilation regime. This is believed to be caused by the way the new air entering the room mixes with the room air.

Experimental data indicate a few points to be considered in the development and evaluations of thermal models, which may be summarized thus:



The variation of time of maximum and minimum temperature in treatment of time lag in some models, , convection and radiation treatment in the room, the temperature fluctuation due to variations in ventilation regime and the way the air mixes in the room. The way these points are investigated are discussed in more detail in Chapter 5 in development of the models.

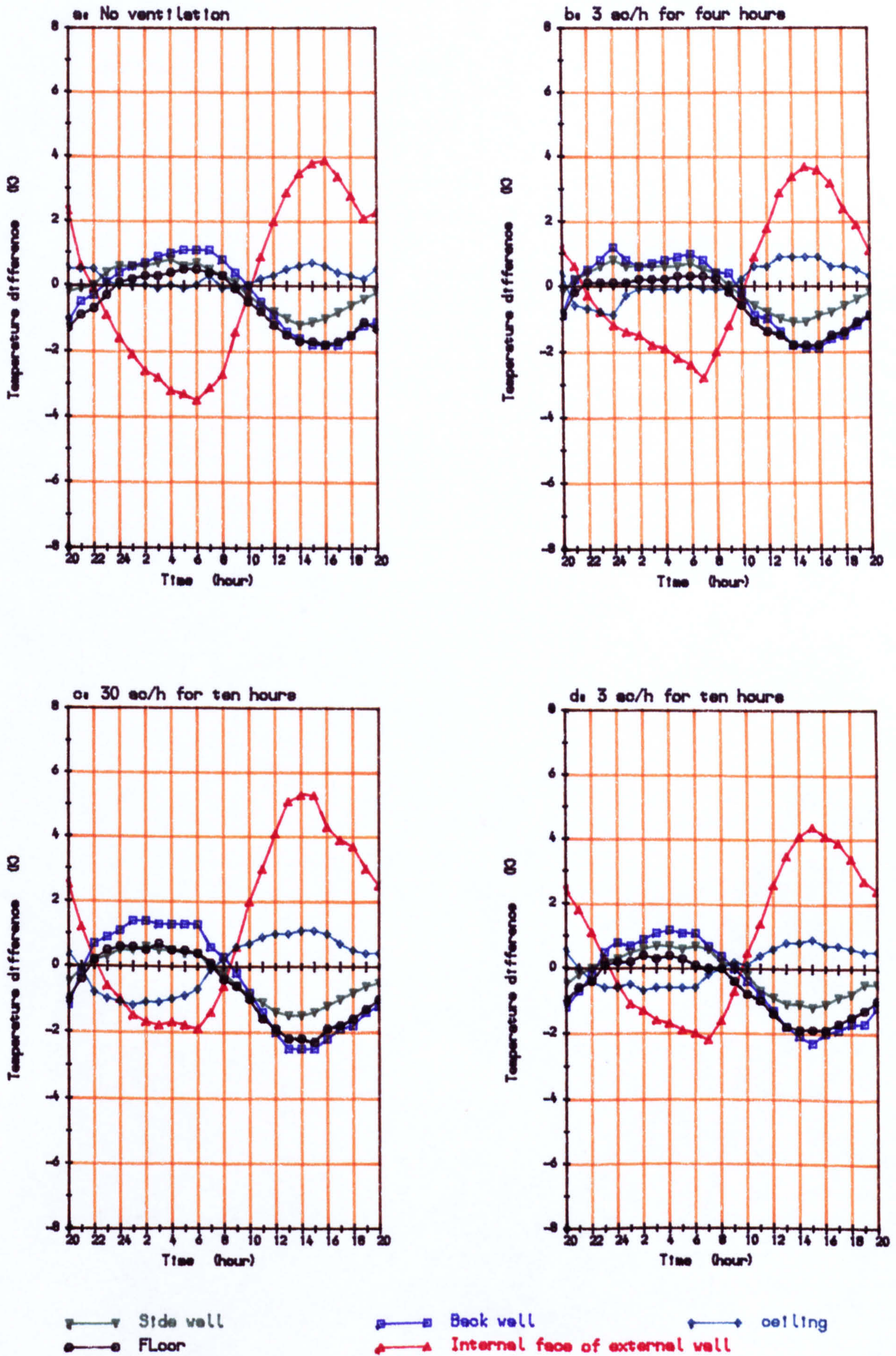
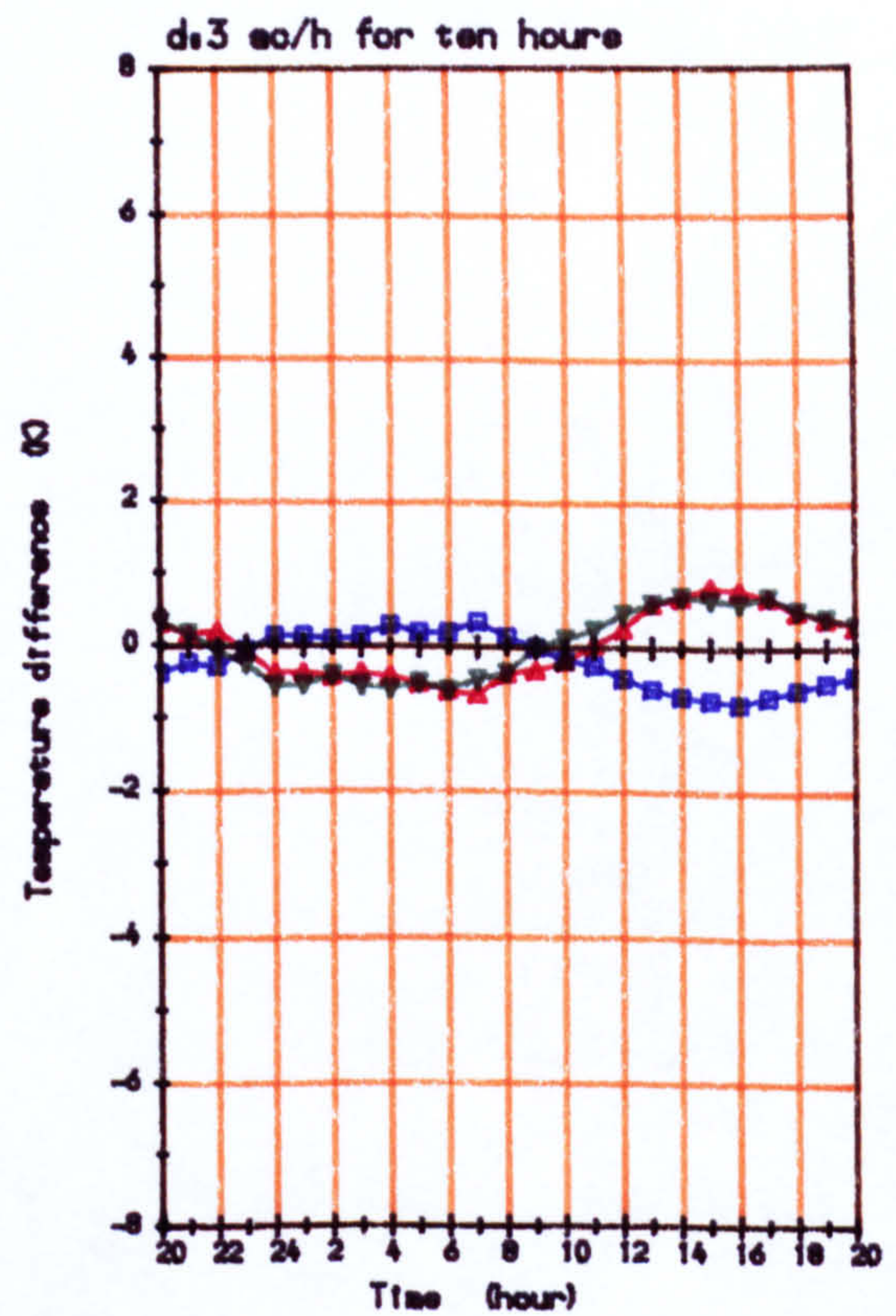
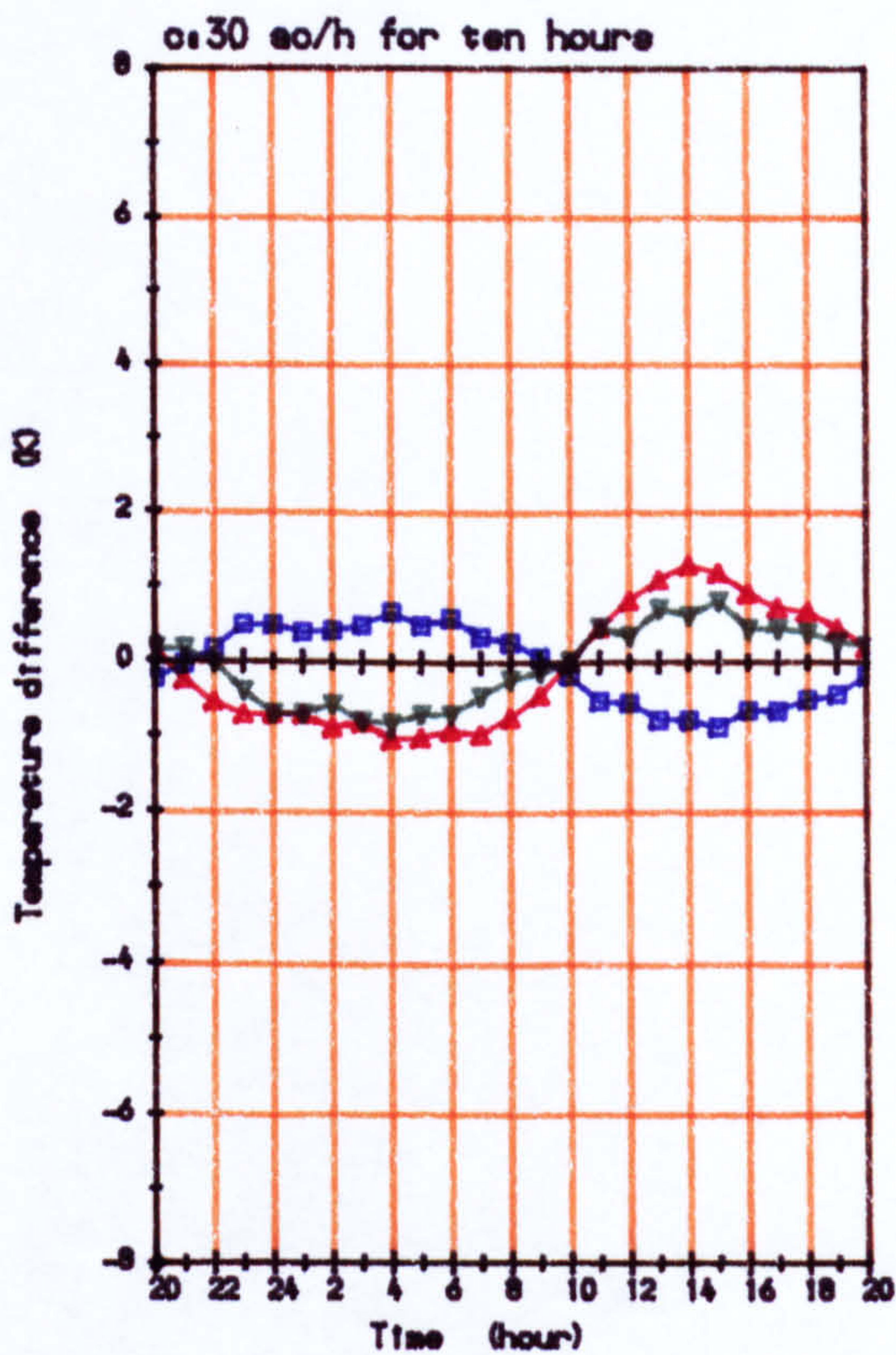
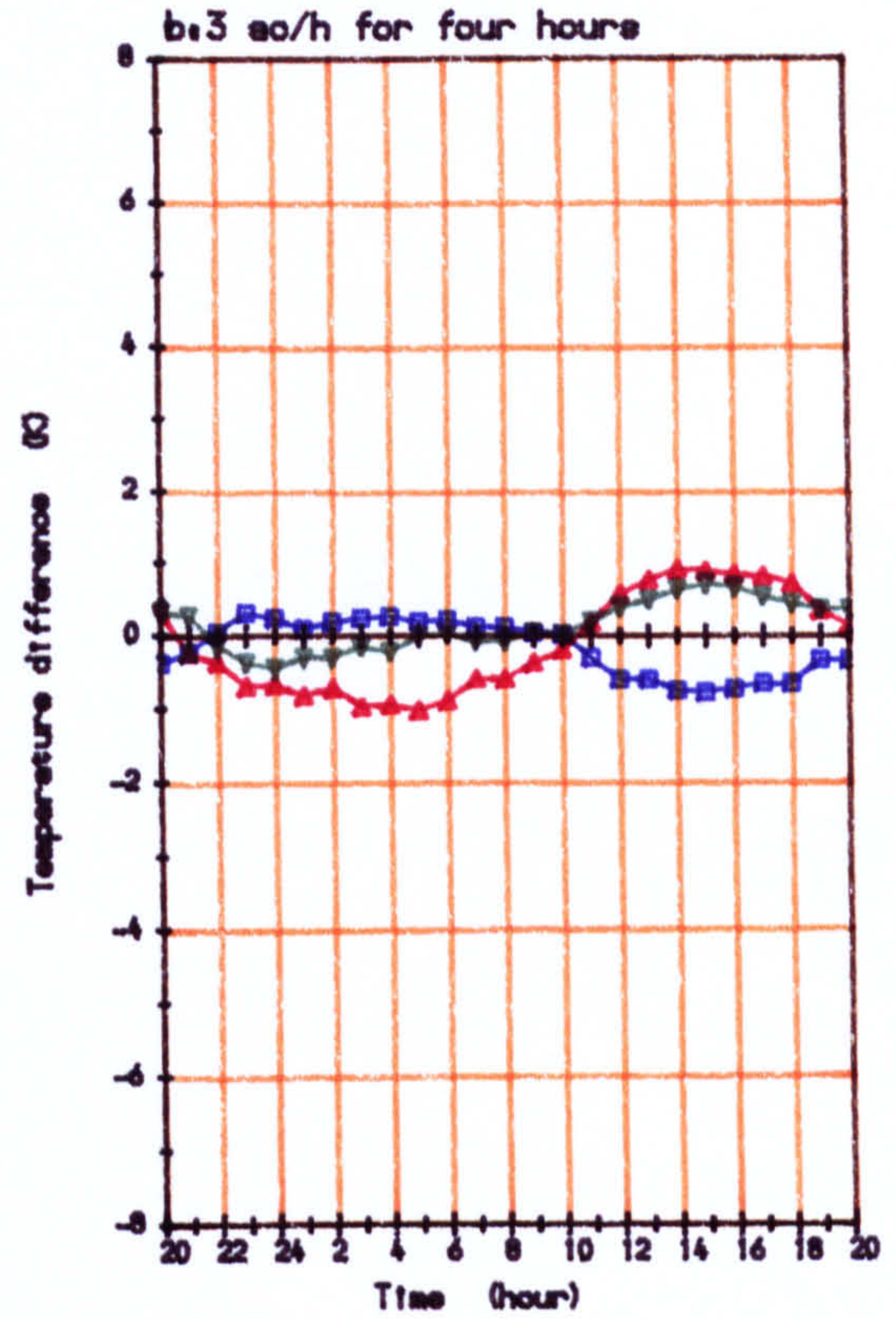
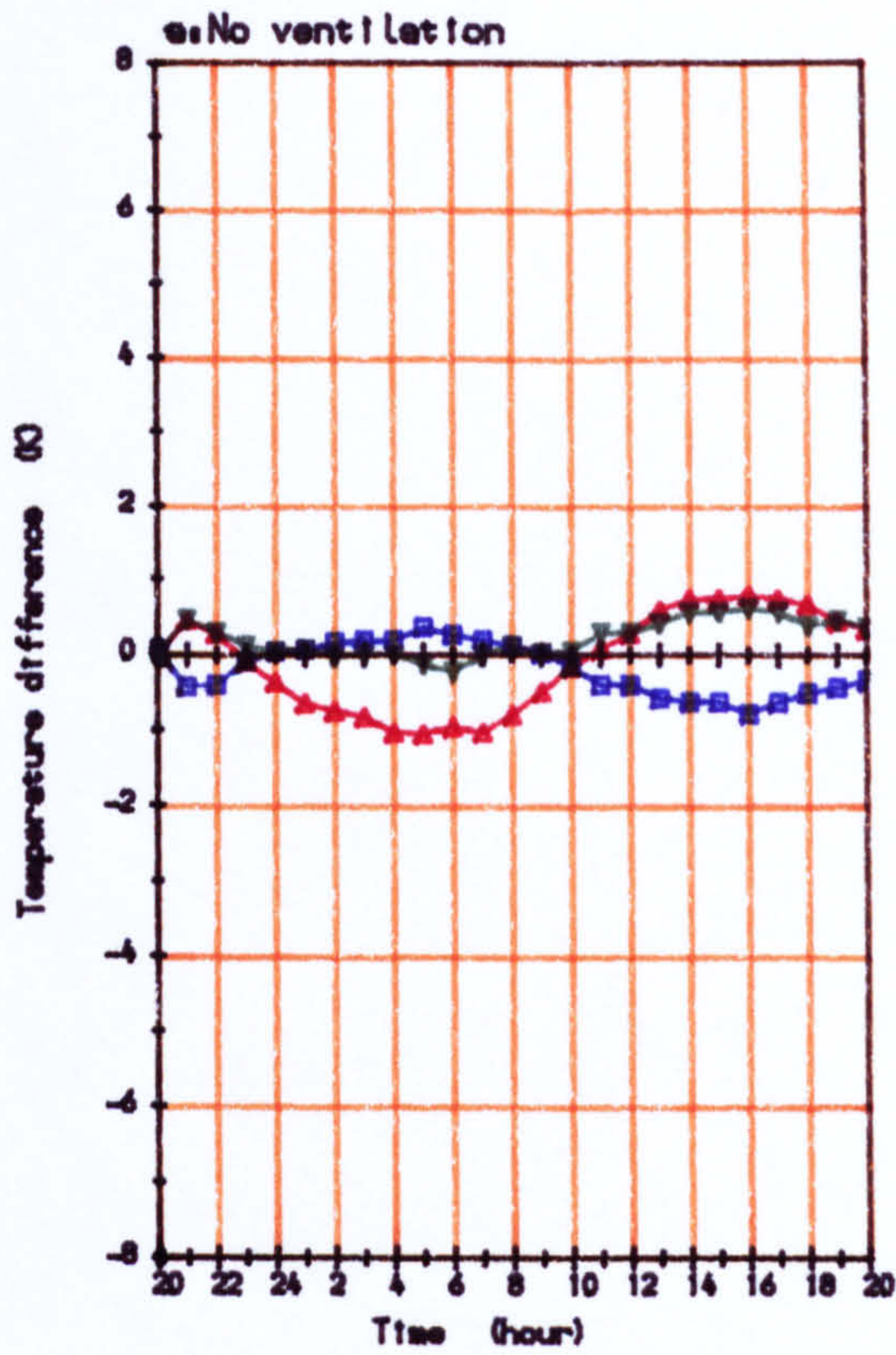


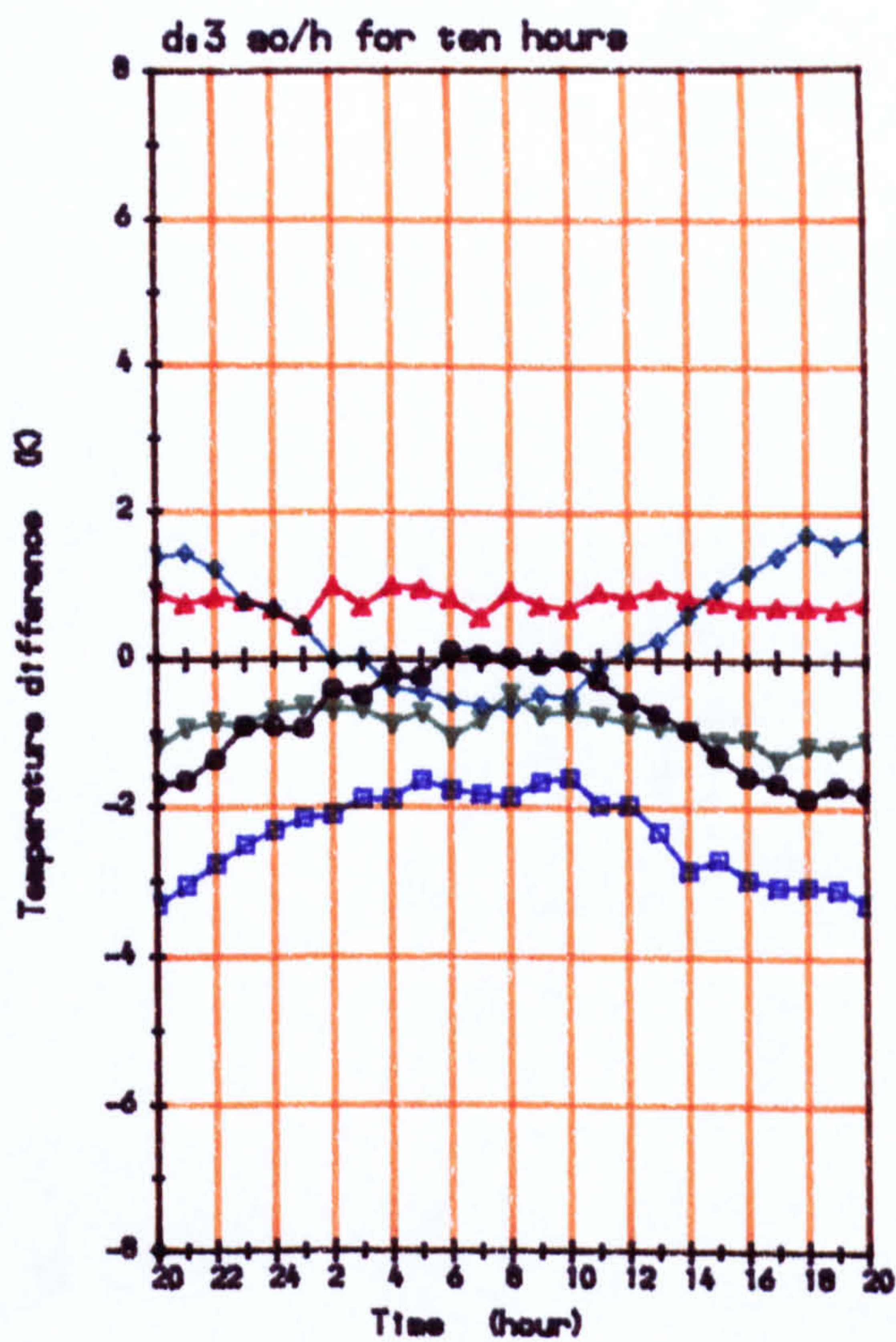
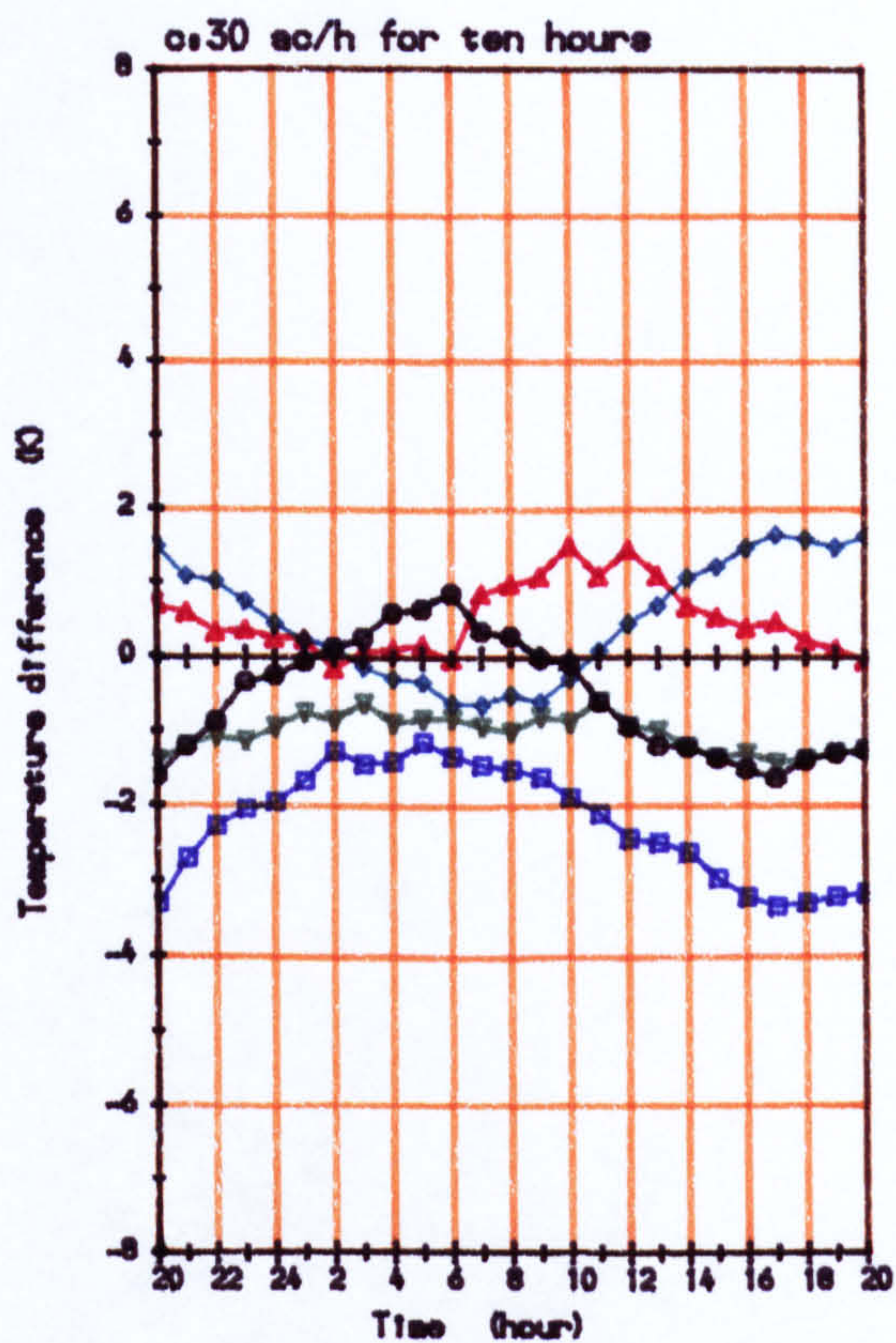
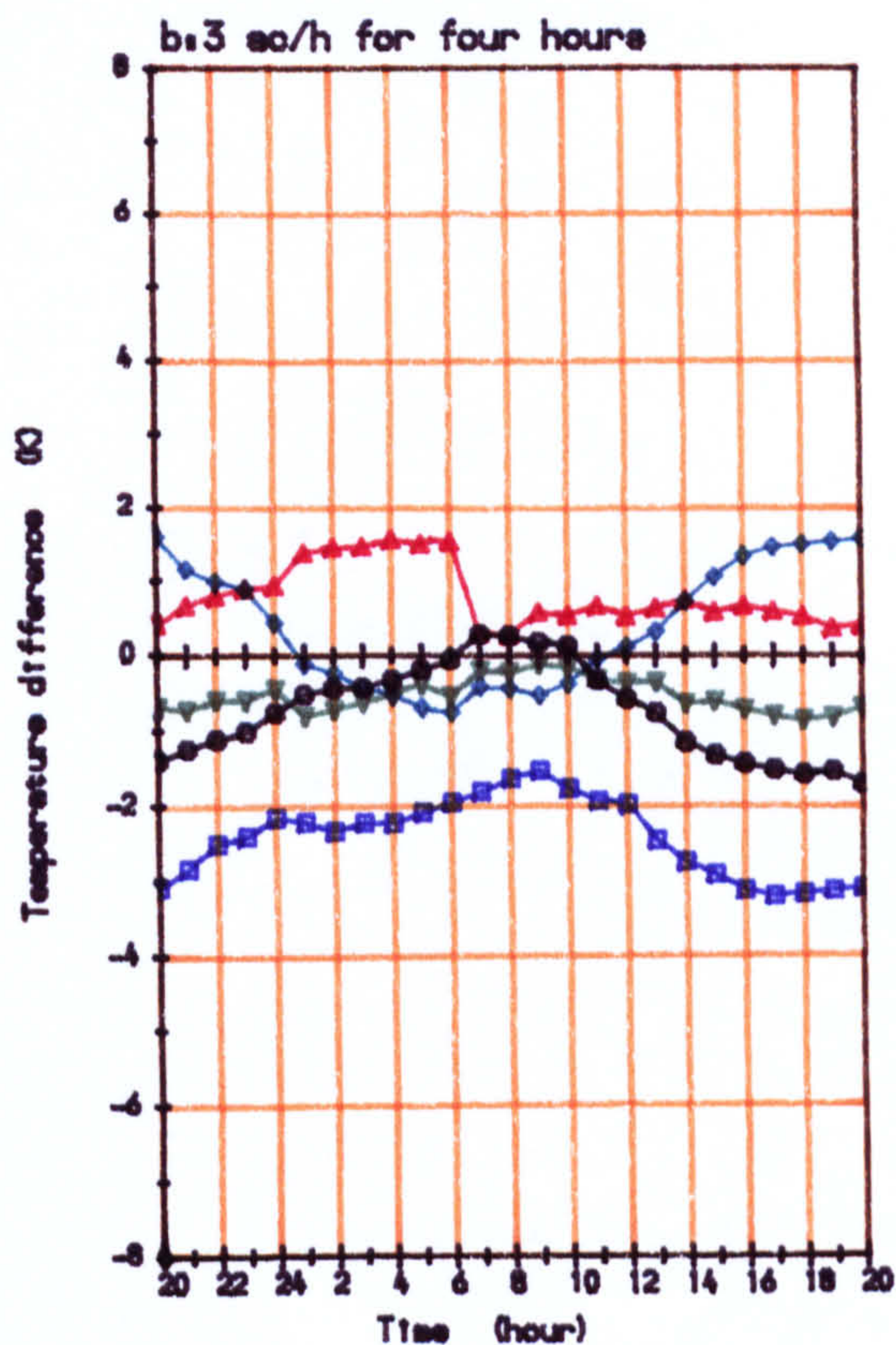
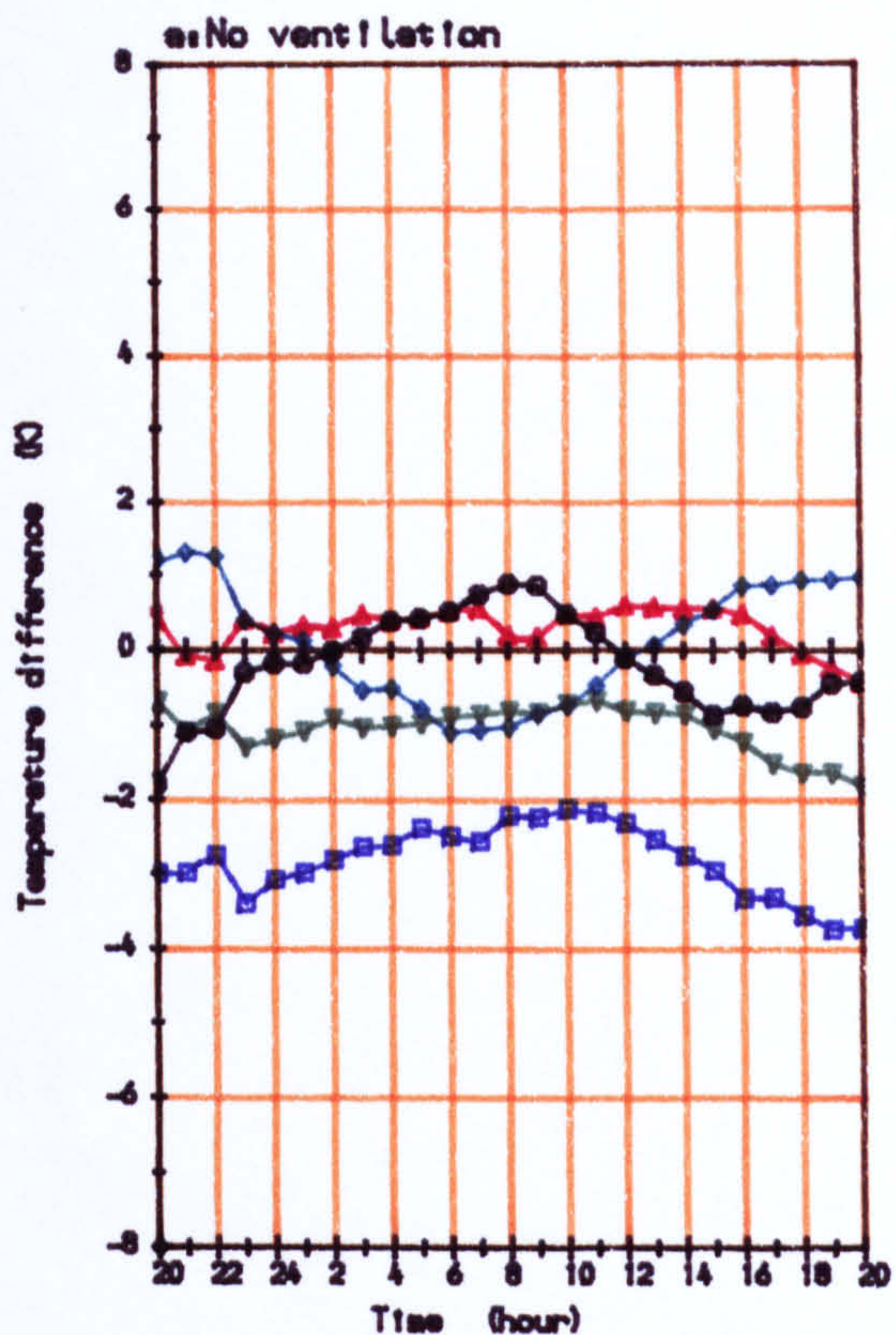
Figure 6.10: Deviation of surface temperatures from instantaneous average surface temperature for different rate and time of ventilation



▲—▲ 5 cm. above the floor  
 ■—■ 5 cm. below the ceiling

▼—▼ In the middle

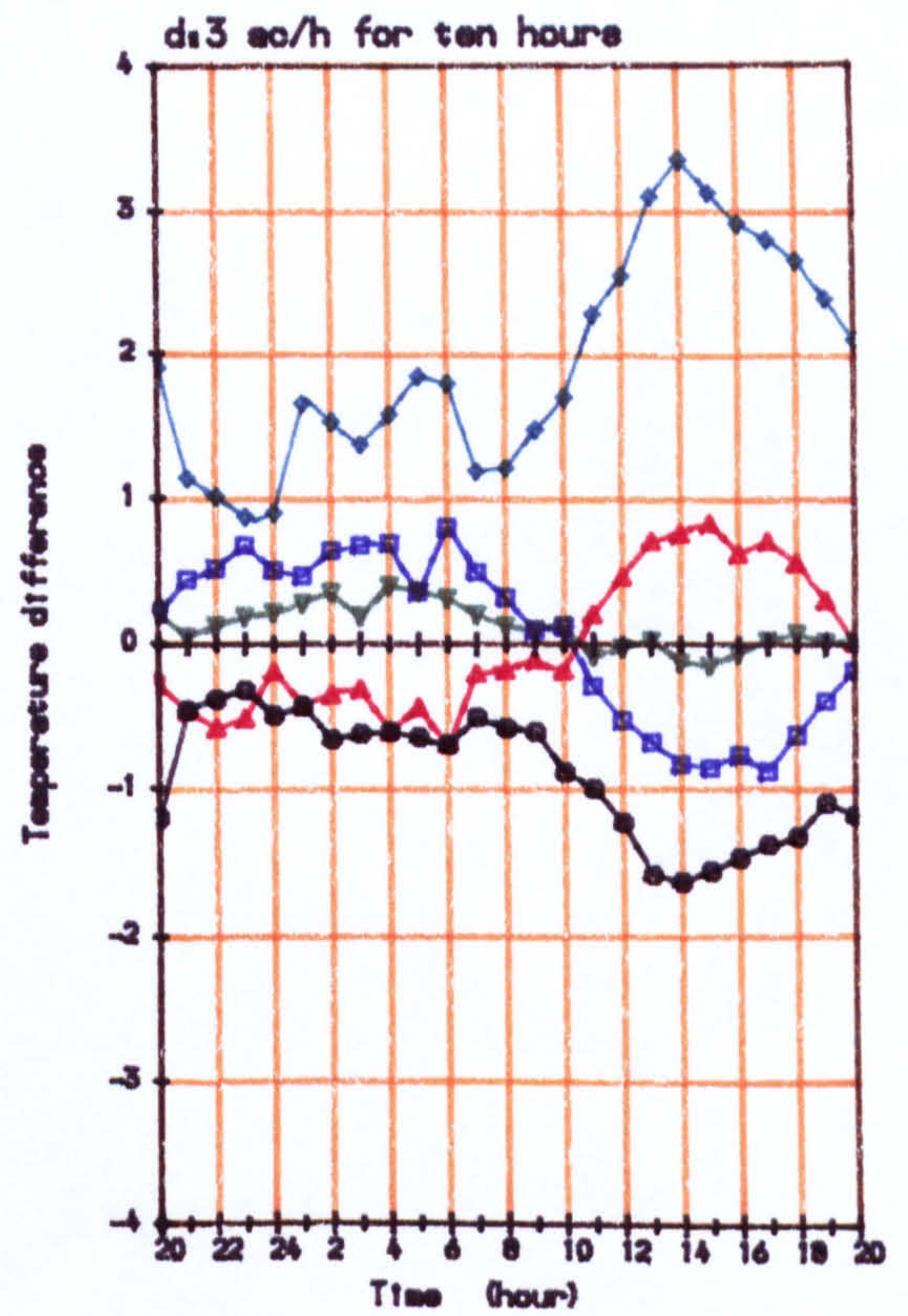
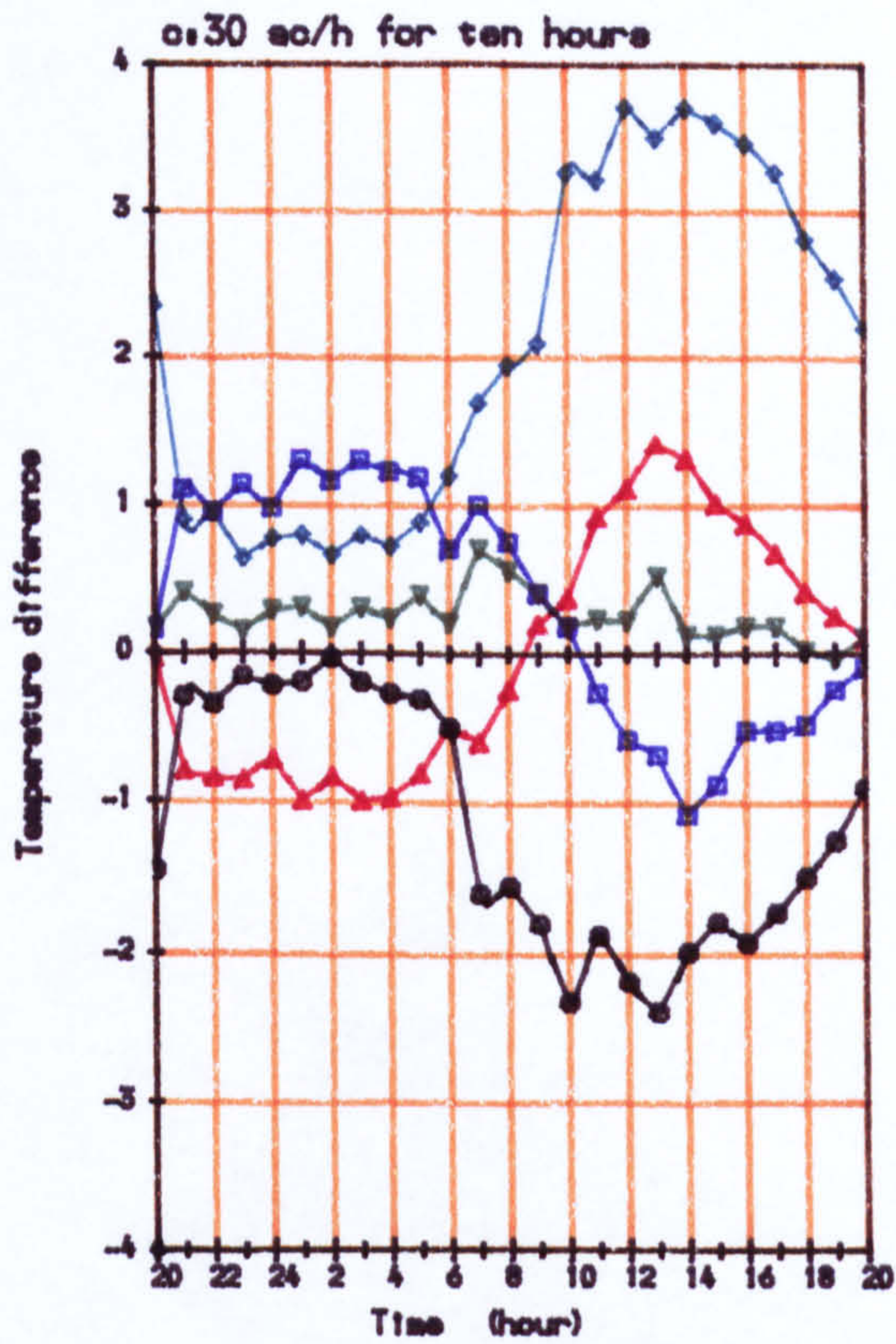
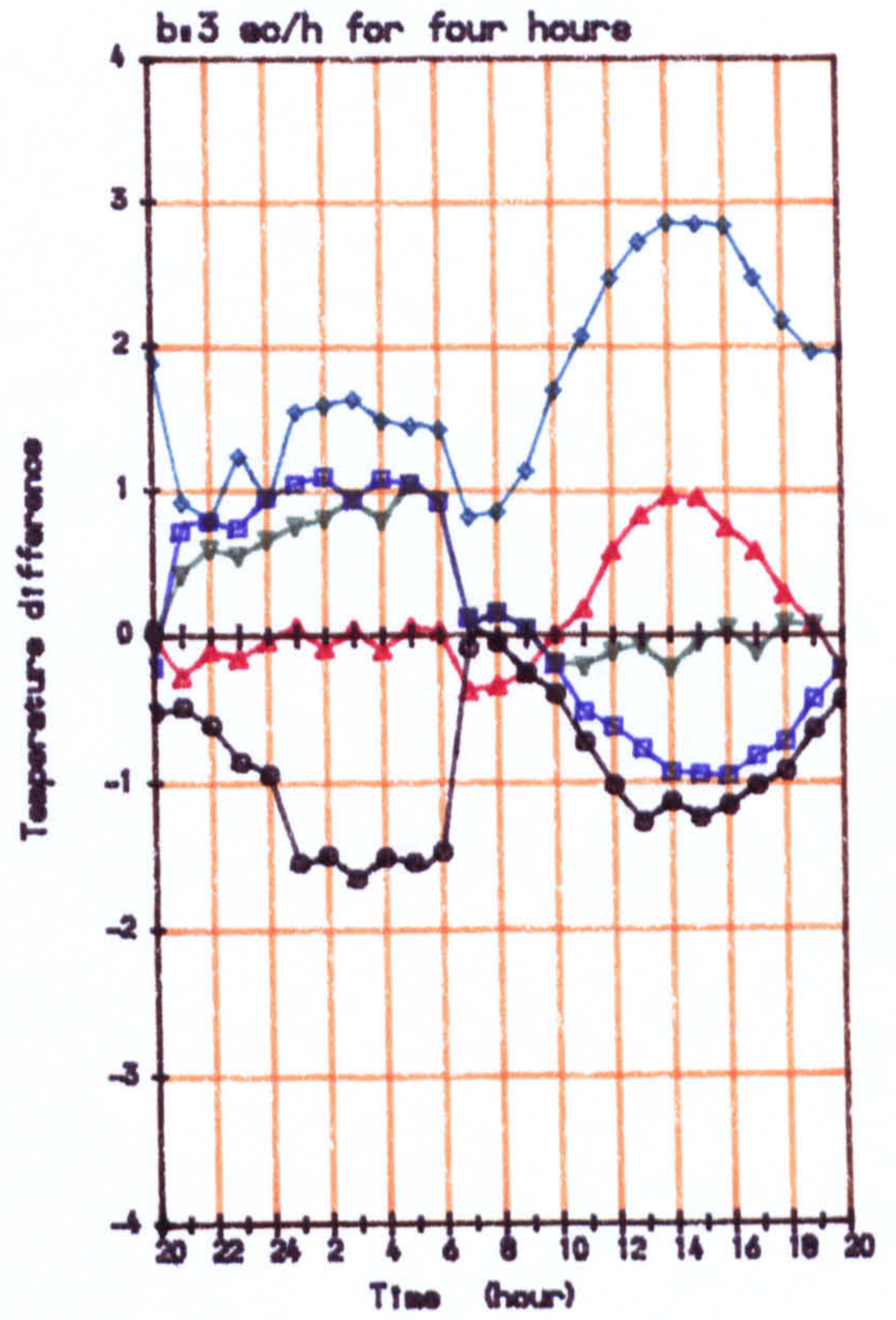
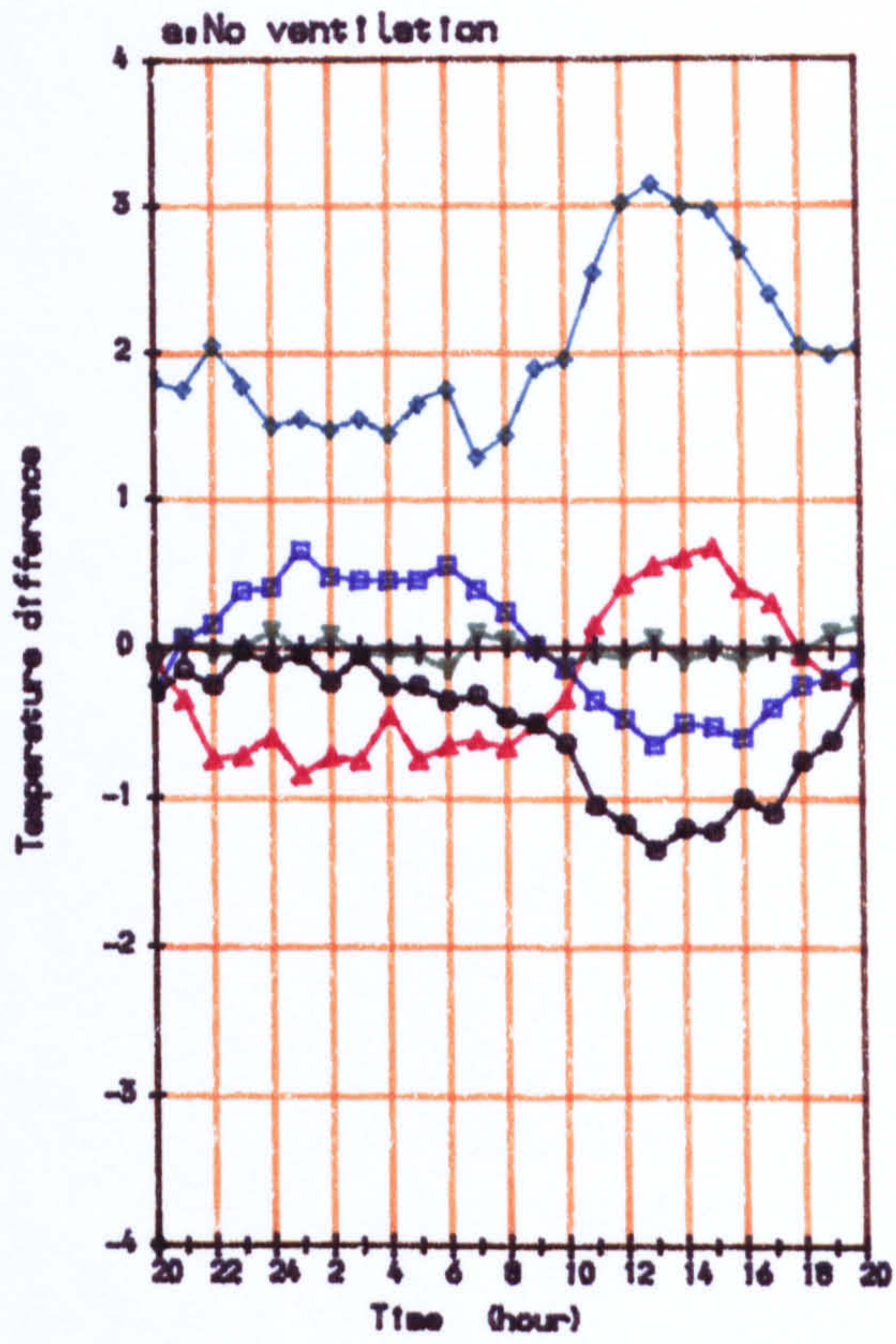
Figure 6.11: Deviation of temperature at different points on internal face of external wall from instantaneous average



▲ 5 m. below the ceiling  
 ■ 5 m. above the floor  
 ● near the back wall

▼ At the middle  
 ◆ Near the front wall

Figure 6.12: Deviation of temperature at different points on the side wall from instantaneous average



▲ 5 cm. below the ceiling  
■ 5 cm. above the floor  
● Near the front wall

▼ At the middle  
◆ Near the back wall

Figure 6.13: Deviation of air temperature at different points in the room from instantaneous average

## CHAPTER SEVEN

### *COMPARISON BETWEEN MEASUREMENTS AND CALCULATIONS*

#### 7.1 Introduction

Several dynamic thermal calculation models have been used to predict the thermal response of a room with varying rate and duration of ventilation. The experimental results are used to find and compare the correctness and accuracy of each model.

The methodology of evaluation and verification of thermal calculation techniques is the subject of recent research (BOWEN & LOMAS 1981 BLOOMFIELD 1985 IRVING 1988). Three major steps are proposed: analytical verification, inter model comparison, and experimental verification. Empirical verification of a model is the most powerful technique as it provides a direct comparison with reality. In the present study two methods are used. The results of different models are compared, and the measured data are used as an indication of their accuracy. Throughout the inter-model and experimental comparison a compromise between precision and simplification is sought.

#### 7.2 Errors and uncertainties

In order to give better understanding and evaluation of the real meaning of a comparison between observed and theoretical results, an analysis of the uncertainties is necessary. A detailed analysis of uncertainties will also allow the evaluation of the importance and sensitivity of each parameter in the simulation model.

The measured parameters of the observations are used as input to the models. They include the outside air temperature and the ventilation flow rate. The error of the temperature measurement is  $\pm 0.5$  K, and of the air flow rate, 5%. (See Ch. 6) The parameters used in the models are:

- dimensions of the room
- thermal properties of the room components
- ventilation rate based on measurement

- infiltration rate based on estimation and
- measured outside air temperature.

There are some internal parameters in each simulation technique, which will affect the final results. The most important is the convection heat transfer coefficient. In the finite difference and response factor models it is used directly to calculate the convective heat transfer between the surfaces and the air. In the harmonic models it will appear as a part of the inside surface resistance,  $R_{si}$ . Each variable in the model has an error associated with it. In table 7.1 the uncertainties associated with each parameter are shown.

Table 7.1: The uncertainty of parameters in the models

Parameter	Uncertainty
Thermal conductivity $\lambda$	$\pm 5\%$
Specific heat $c_p$	$\pm 5\%$
Density $\rho$	$\pm 5\%$
Thickness $l$	$\pm 1\%$
Volume $Vol$	$\pm 2\%$
Ventilation rate $V$	$\pm 5\%$
Infiltration rate $V_{inf}$	$\pm 0.5$ ac/h
Convective heat transfer coefficient $h_c$	$\pm 1.5$ W/m <sup>2</sup> K
Outside air temperature $T_{ao}$	$\pm 0.5$ °C
Outside surface resistance $R_{so}$	$\pm 0.06$ m <sup>2</sup> K/W
Inside surface resistance $R_{si}$	$\pm 0.06$ m <sup>2</sup> K/W

### 7.2.1 Methods of uncertainty analysis

If  $q$  is defined as:

$$q = f(u, x, \dots, z) \quad (7.1)$$

and each variable is measured with uncertainties  $du$ ,  $dx$ , ...,  $dz$  then the uncertainty in  $q$  is given by

$$dq = \left[ \left( \frac{\partial q}{\partial u} du \right)^2 + \left( \frac{\partial q}{\partial x} dx \right)^2 + \left( \frac{\partial q}{\partial z} dz \right)^2 \right]^{0.5} \quad (7.2)$$

provided the uncertainties in  $u, x, \dots, z$  are random and independent. (TAYLOR 1982).

As in the case of the prediction of the thermal response of buildings, the final answer results from the solution of a system of complicated equations. The analytical solution using equation 7.2 to find the uncertainties is complicated. To simplify it, the derivative of the functions are calculated numerically. The following approximation is used to represent the derivative:

$$\frac{\partial q}{\partial x} = \frac{q_{x+h_0} - q_x}{h_0} \quad (7.3)$$

Where  $h_0$  has to be small enough to give reasonably accurate results.

The models will produce hourly temperatures for different nodes; air and surfaces. It is difficult to present and evaluate the uncertainty in hour by hour sequences. To give a sound basis two different sets of data are evaluated : the mean air and surface temperature , and the temperature difference between calculation and observation. In order to give a single value for temperature difference for a whole day a function  $\phi$  is defined as

$$\phi_{tai} = \left[ 1/24 \sum (T_c - T_o)^2 \right]^{0.5} \quad (7-4)$$

where

$T_c$  is the calculated temperature  $^{\circ}\text{C}$

$T_o$  is the Observed temperature  $^{\circ}\text{C}$

To find the best values for the derivatives a computer program is loaded for each different parameter several times. For each run the parameter is slightly changed. This small change is decreased at each step. The corresponding value of the derivative is found in the regions where the results are not changing significantly . It is believed that in further steps decreasing the increments, the error of calculation will become great and will affect the final results.



The uncertainties of each parameter should, to satisfy the limitations of equation 7.2, be independent and random. A large uncertainty in some of the parameters will affect these restrictions. For instance, if the density is increased the thermal conductivity and specific heat capacity also change and so the independence condition will not be fulfilled. With large numerical uncertainties in some parameters the error may not be normally distributed. In such a case if  $q$  is a function of  $x_1, x_2, \dots, x_i, \dots, x_n$  the uncertainty in  $q$  is found from

$$dq = \left[ \sum_{i=1}^n \left( \frac{\partial q}{\partial x_i} dx_i \right)^2 + \sum_{i=1}^n \sum_{j=1, j \neq i}^n \frac{\partial q}{\partial x_i} \frac{\partial q}{\partial x_j} dx_i dx_j \right]^{0.5}$$

Where  $dx_i dx_j$  is the co-variance between parameters. This equation is valid whether the parameters are independent or the variations are normally distributed.

If the response of a building to the degree of variations of each parameter is not linear,  $dq$  may not be calculated by equation 7.2. The derivative obtained for each point is a local value and should be used with caution. It should only be used where the response of the building to the changes of the derivative is assumed to be linear. To investigate the effect of larger uncertainties, within each parameter, an analysis of the sensitivity of the overall response of the building is required. The analysis of the distribution of the derivatives using such variations will show the importance of the magnitudes of uncertainties associated with each parameter.

Buildings subjected to variable ventilation will respond differently accordingly to the time of the day. The effect of the uncertainties of each parameter might also be different at different times of the day. An hourly investigation is appropriate. Such thorough sensitivity analysis to the changes of a thermal model's constituents is beyond the scope of this study. In this research a general investigation into the effect of uncertainties of the parameters of a thermal model seemed to be enough for the purpose of the comparisons among different models. In table 7.1 modest values of error are chosen to satisfy the above conditions.

It should be noted that the models are only as robust as the accuracy of the input data.

### 7.2.2 Results of error analysis

Table 7.2 to 7.4 show the results of the analysis and the derivatives of the air and average surface temperatures, and the temperature difference cause by the errors in the parameters of the models.

It is shown from the analysis that from the sort of errors expected, some parameters such as specific heat capacity, density and thickness of the slabs etc., do not significantly affect the overall uncertainty.

In the Finite Difference model the effect of the error caused by the uncertainty in  $hc$  is greater for higher rates of ventilation. With lower rates of ventilation the uncertainty in ventilation rate is more significant than with higher ventilation rates.

It was expected that  $R_{s1}$  would play an important role in the final results, because the convection coefficient is subjected to constant change. It is shown with the range of errors expected in  $R_{s1}$  that the final result is not affected to a significant extent by the errors in  $R_{s1}$ . The effect of  $R_{s0}$  is more important.

With lower rates of ventilation, the uncertainty in the ventilation rate has a more important role in the final result.

In general, the uncertainty associated with the prediction of air and average surface temperatures is mostly affected by the errors in outside air temperature and infiltration rate. Outside surface resistance,  $R_{s0}$ , ventilation rate and inside surface resistance also affect the overall results, but to a lesser extent. The average general uncertainty caused by the errors in the parameters of the Harmonic models, under applied conditions, is  $\pm 1.0$  K, with a maximum of  $\pm 2.5$  K and in the Finite Difference Method are  $\pm 1.1$  K with maximum of  $\pm 2.5$  K.

### 7.3 Results and comparison of the models

The Response Factor method and Finite Difference method are both numerical solutions and give accurate and similar results. The results from these two were generally in good agreement with each other. To avoid repetition, the results from the response factor method only are shown for model 7.1, and the evaluation of different parameters, appearing in different models, is only presented for the finite difference technique.

Using the multi exchange model enables the temperature of

**Table 7.2: Error analysis of the daily mean of air and average surfaces temperature calculated by the Finite Difference Method**

Parameter	30 ac/h for ten hours				3 ac/h for four hours			
	Tai		Ts		Tai		Ts	
	$\frac{\partial T_{ai}}{\partial x}$	$\frac{\partial T_{ai}}{\partial x} dx$	$\frac{\partial T_s}{\partial x}$	$\frac{\partial T_s}{\partial x} dx$	$\frac{\partial T_{ai}}{\partial x}$	$\frac{\partial T_{ai}}{\partial x} dx$	$\frac{\partial T_s}{\partial x}$	$\frac{\partial T_s}{\partial x} dx$
Conductivity	0.6	0.04	0.4	0.02	0.33	0.02	0.3	0.2
Specific heat	0.001	0.05	0.001	0.05	0.001	0.05	0.001	0.05
Density	0.001	0.01	0.001	0.01	0.001	0.01	0.001	0.01
Thickness	21.0	0.21	18.0	0.18	26.2	0.26	24.0	0.24
Surface resistance (outside)	9.4	0.6	7.5	0.45	5.6	0.3	5.1	0.3
Ventilation rate	0.07	0.11	0.1	0.15	0.45	0.05	0.5	0.05
Infiltration rate	0.8	0.4	1.0	0.5	0.8	0.4	1.0	0.5
Outside air temperature	0.8	0.4	0.9	0.45	0.8	0.4	0.75	0.37
Conv. heat transfer coefficie	0.45	0.7	0.2	0.3	0.1	0.15	0.1	0.15
Volume	0.2	0.02	0.18	0.02	0.15	0.015	0.18	0.02
Standard error °C	±1.1		±0.9		±0.7		±0.8	
Maximum error °C	±2.5		±2.1		±1.6		±1.5	

**TEXT BOUND INTO  
THE SPINE**

**Table 7.3: Error analysis of the daily mean of temperature difference between measurements and calculations by the Finite Difference Method**

Parameter	30 ac/h for ten hours				3 ac/h for four hours			
	Tai		Ts		Tai		Ts	
	$\frac{\partial T_{ai}}{\partial x}$	$\frac{\partial T_{ai}}{\partial x} dx$	$\frac{\partial T_s}{\partial x}$	$\frac{\partial T_s}{\partial x} dx$	$\frac{\partial T_{ai}}{\partial x}$	$\frac{\partial T_{ai}}{\partial x} dx$	$\frac{\partial T_s}{\partial x}$	$\frac{\partial T_s}{\partial x} dx$
Conductivity	0.5	0.04	0.5	0.04	0.3	0.02	0.3	0.02
Specific heat	0.001	0.05	0.001	0.05	0.001	0.05	0.001	0.05
Density	0.001	0.01	0.001	0.01	0.001	0.01	0.001	0.01
Thickness	25.0	0.25	25.0	0.25	22.2	0.22	27.0	0.27
Surface resistance (outside)	8.5	0.5	9.2	0.55	4.8	0.28	6.0	0.35
Ventilation rate	0.1	0.15	0.1	0.15	0.55	0.06	0.4	0.04
Infiltration rate	1.0	0.4	1.0	0.5	0.95	0.45	0.8	0.4
Outside air temperature	0.8	0.4	0.8	0.4	0.75	0.37	0.75	0.37
Conv. heat transfer coefficient	0.4	0.6	0.4	0.6	0.11	0.16	0.1	0.16
Volume	0.1	0.01	0.15	0.01	0.19	0.02	0.14	0.01
Standard error ° C	±1.1		±1.1		±0.7		±0.7	
Maximum error ° C	±2.5		±3.0		±1.4		±1.2	

**Table 7.4: Error analysis of the daily mean of air and average surfaces temperature calculated by the Harmonic Method..**

Parameter	30 ac/h for ten hours				3 ac/h for four hours			
	Tai		Ts		Tai		Ts	
	$\frac{\partial T_{ai}}{\partial x}$	$\frac{\partial T_{ai}}{\partial x} dx$	$\frac{\partial T_s}{\partial x}$	$\frac{\partial T_s}{\partial x} dx$	$\frac{\partial T_{ai}}{\partial x}$	$\frac{\partial T_{ai}}{\partial x} dx$	$\frac{\partial T_s}{\partial x}$	$\frac{\partial T_s}{\partial x} dx$
Conductivity	0.4	0.03	0.5	0.03	0.3	0.02	0.28	0.02
Specific heat	0.001	0.05	0.001	0.05	0.001	0.05	0.001	0.05
Density	0.001	0.01	0.001	0.01	0.001	0.01	0.001	0.01
Thickness	16.0	0.1	18.0	0.2	7.5	0.07	8.0	0.08
Surface resistance (outside)	7.9	0.5	9.7	0.6	5.0	0.3	5.2	0.3
Ventilation rate	0.1	0.15	0.1	0.15	0.7	0.1	0.6	0.09
Infiltration rate	1.1	0.66	1.0	0.5	1.3	0.65	1.2	1.2
Outside air temperature	1.0	0.5	1.0	0.5	1.0	0.5	1.0	0.5
Surface resistance (inside)	2.8	0.18	4.6	0.28	3.7	0.22	3.9	0.23
Volume	0.2	0.02	0.18	0.02	0.25	0.02	0.22	0.02
Standard error °C	±1.0		±1.0		±0.75		±0.9	
Maximum error °C	±2.2		±2.3		+1.9		±2.1	

different surfaces of the room to be predicted individually . Figures 7.1 7.3 7.5 and 7.7 show the surface temperatures predicted by these two methods against similar data obtained from measurements. In figures 7.2 7.4 7.6 and 7.8 the average surface temperatures and air temperatures are shown. As assessment of comfort is one of the major points of interest , dry resultant temperatures ( the mean of air and average surface temperature) are also shown.

The general agreement between the response factor and the finite difference method with the measurements is good. There is some disagreement between observations and predictions for inner and outer surface temperatures of the external wall. This is thought to be caused by the use in the calculation of a fixed value for the external surface resistance, for a whole day. The external surface resistance includes both radiation and convection. The rate of heat transfer by convection on the outside surface of a wall is a function of temperature difference between the surface and the outside air. Each is subjected to continuous change during the course of the day. So the surface resistance variation caused only by changes in the convection part may well be between (0.07 to 0.2  $m^2K/W$  ). A fixed value may cause, at least for parts of the day , an overestimation of the surface temperature and consequently will affect the internal surface temperatures.

It is shown in figures 7.1 and 7.3 that the ceiling temperature responds quickly to the rate of ventilation. The ceiling was made of light material, and as the cooler air enters the room, the exchange of heat by convection results in a rapid drop of surface temperature. This drop is a function of the ventilation rate and will continue during ventilation. As soon as ventilation stops, the temperature will recover. Neither of the models is able to follow this variation accurately. The reason might be the inaccurate estimation of the convection coefficient at the time of change.

The results of the finite difference and response factor methods are in good agreement . The difference between these two is only in the way the unsteady heat conduction through the slab is dealt with. In the response factor method a time step of one hour is used while in finite difference method, a five minute time interval is chosen. This is not found to be advantageous.

The air temperature is the most difficult to predict. The behaviour of air entering the room is complicated and will change with the rate of ventilation and infiltration, the type, position and

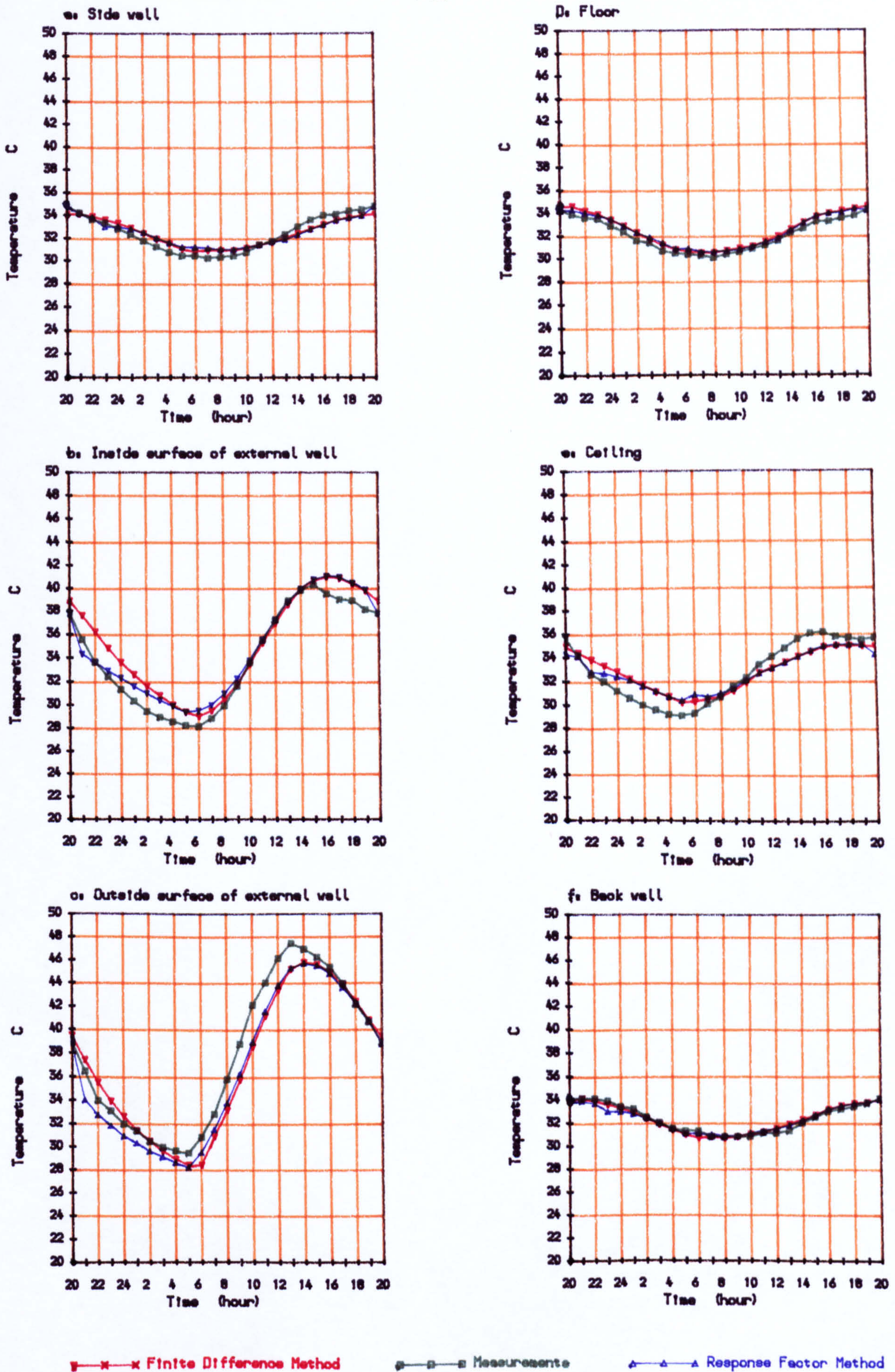


Figure 7.1: Comparison of measurements and predictions of the Finite Difference and the Response Factor Method  
 30 air changes per hour for ten hours (from 2000 to 0600 hours)



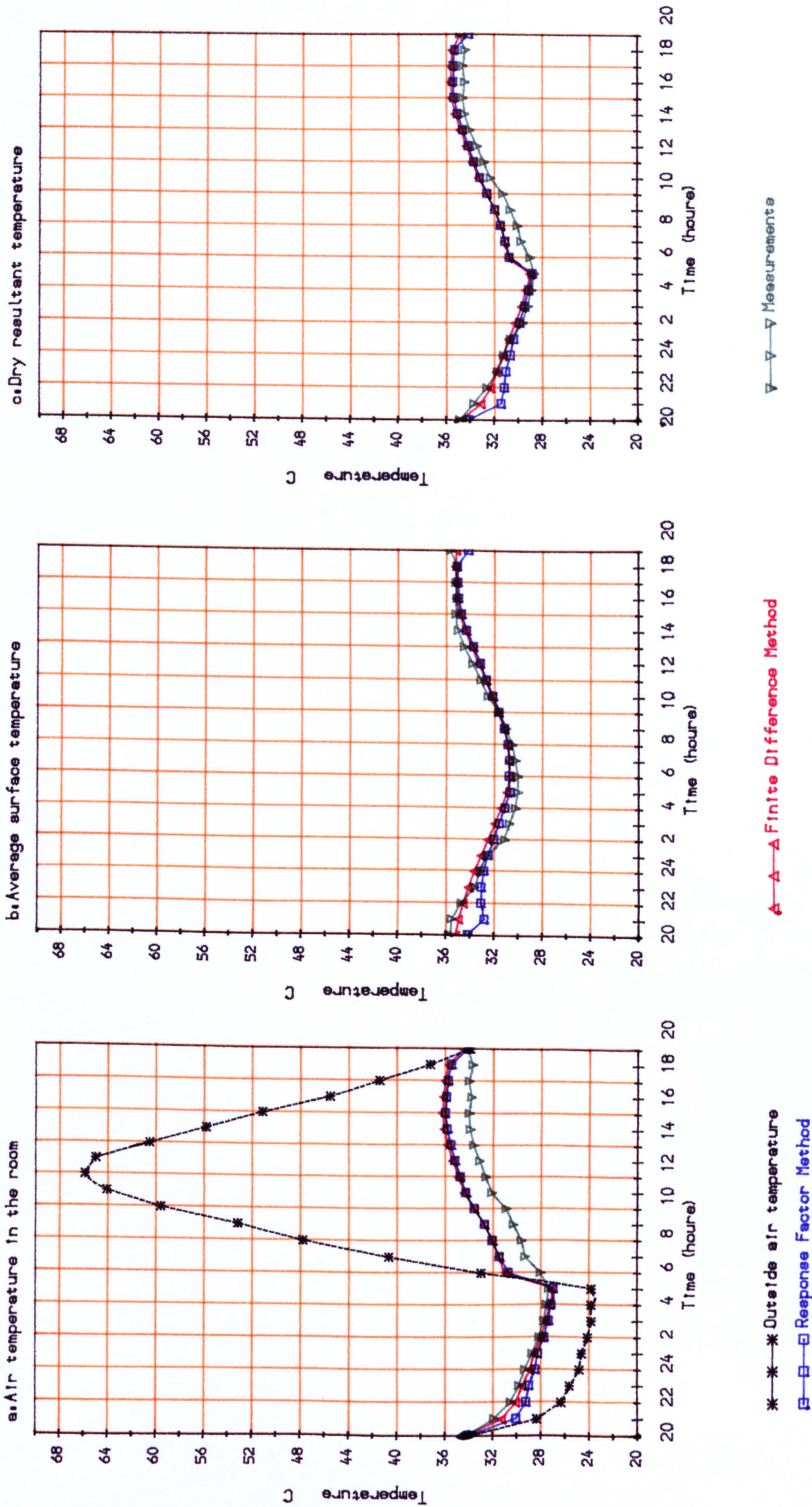


Figure 7.2. Comparison of measurements and predictions of the Finite Difference and the Response Factor Method  
 30 air changes per hour for ten hours (from 2000 to 0600 hours)

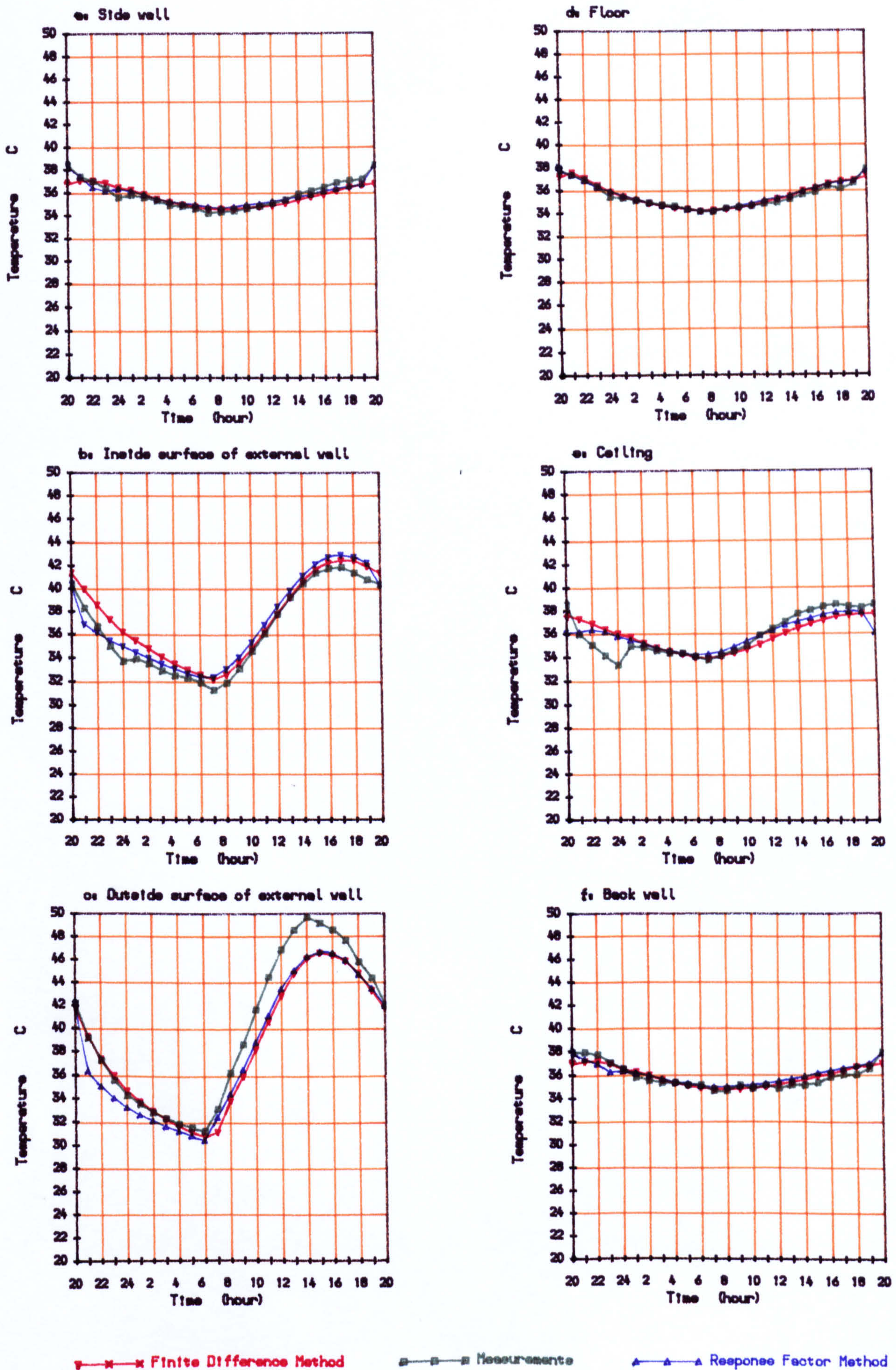


Figure 7.3: Comparison of measurements and predictions of the Finite Difference and the Response Factor Method

30 air changes per hour for four hours (from 2000 to 2400 hours)

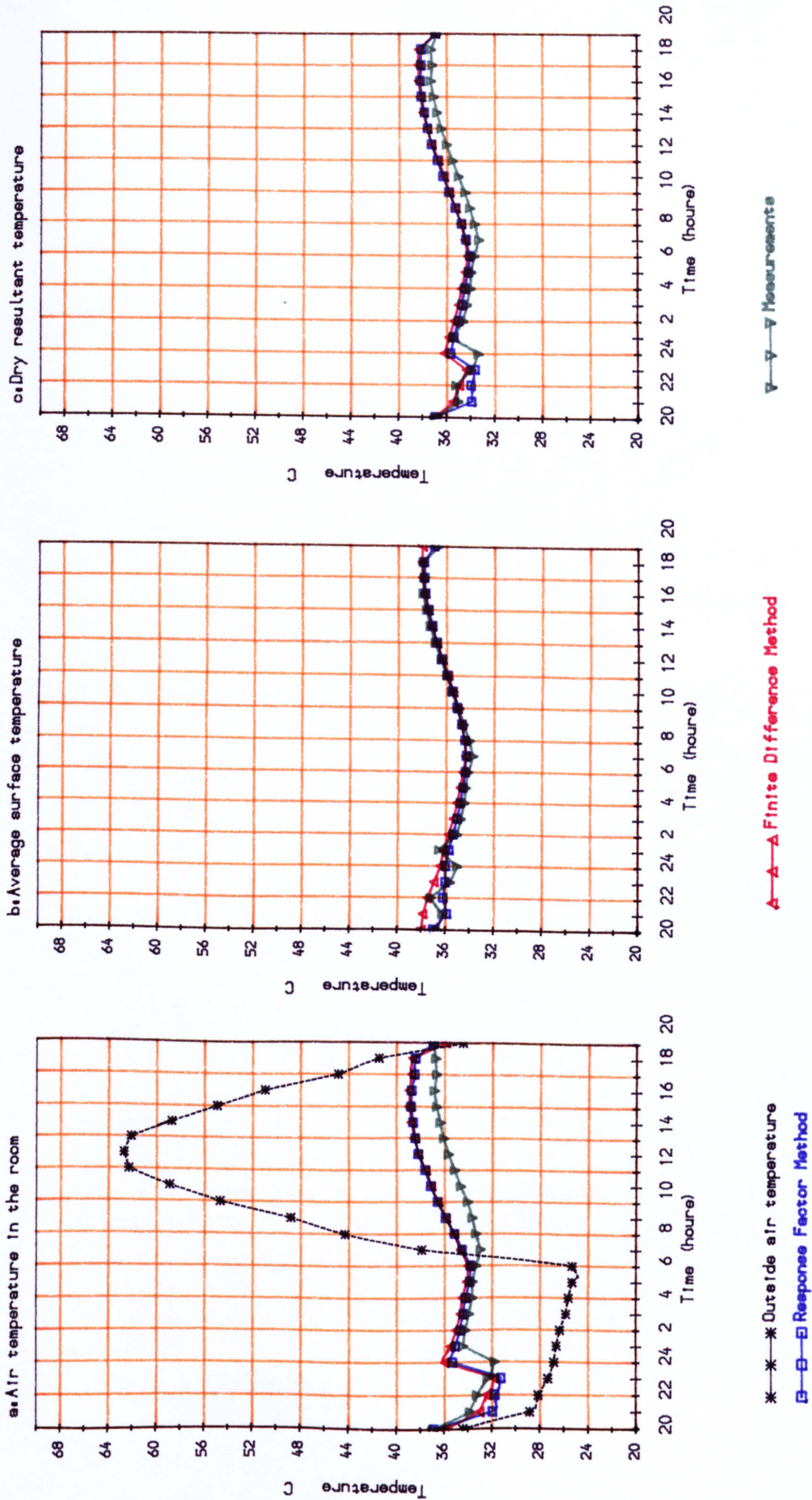
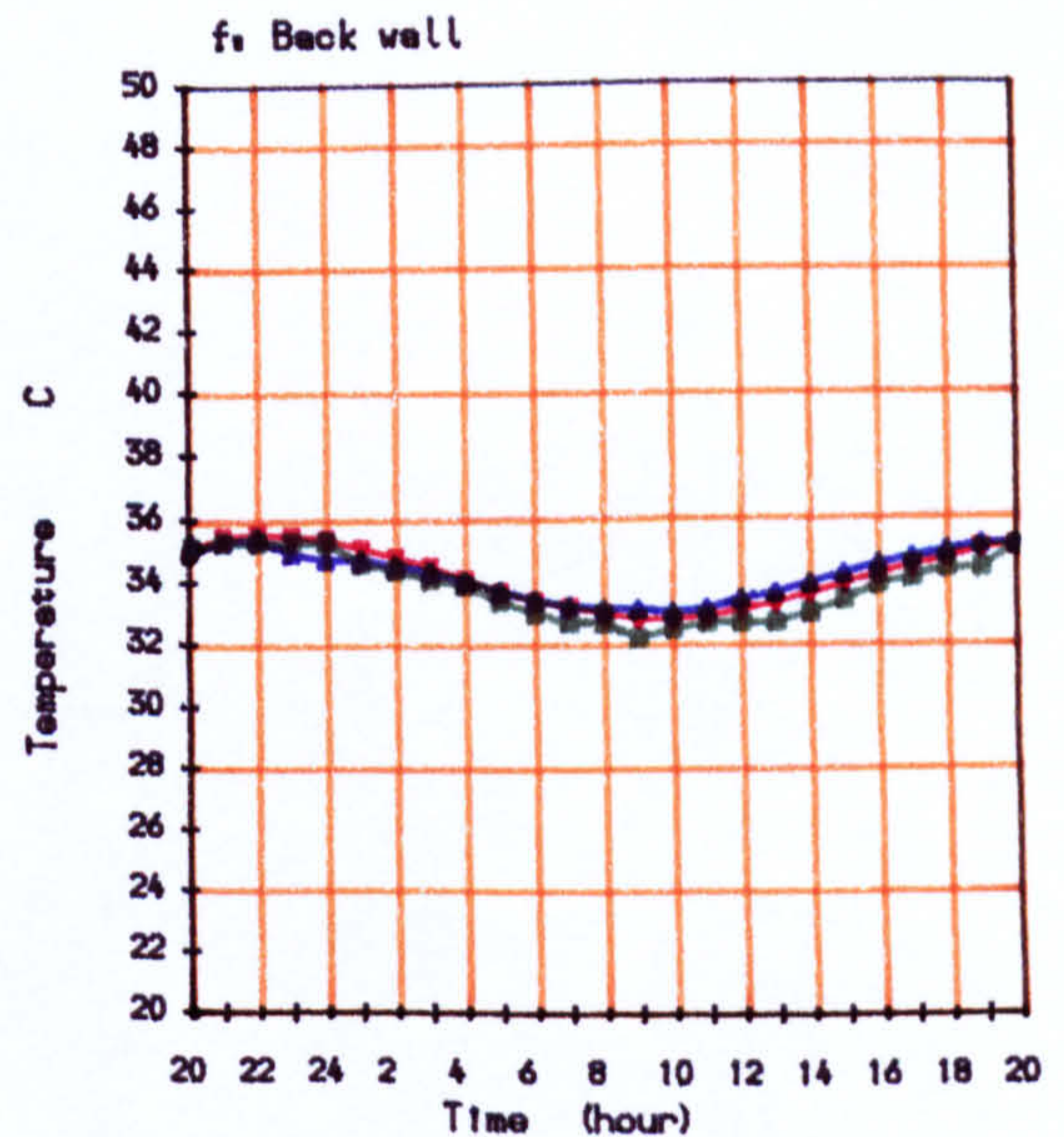
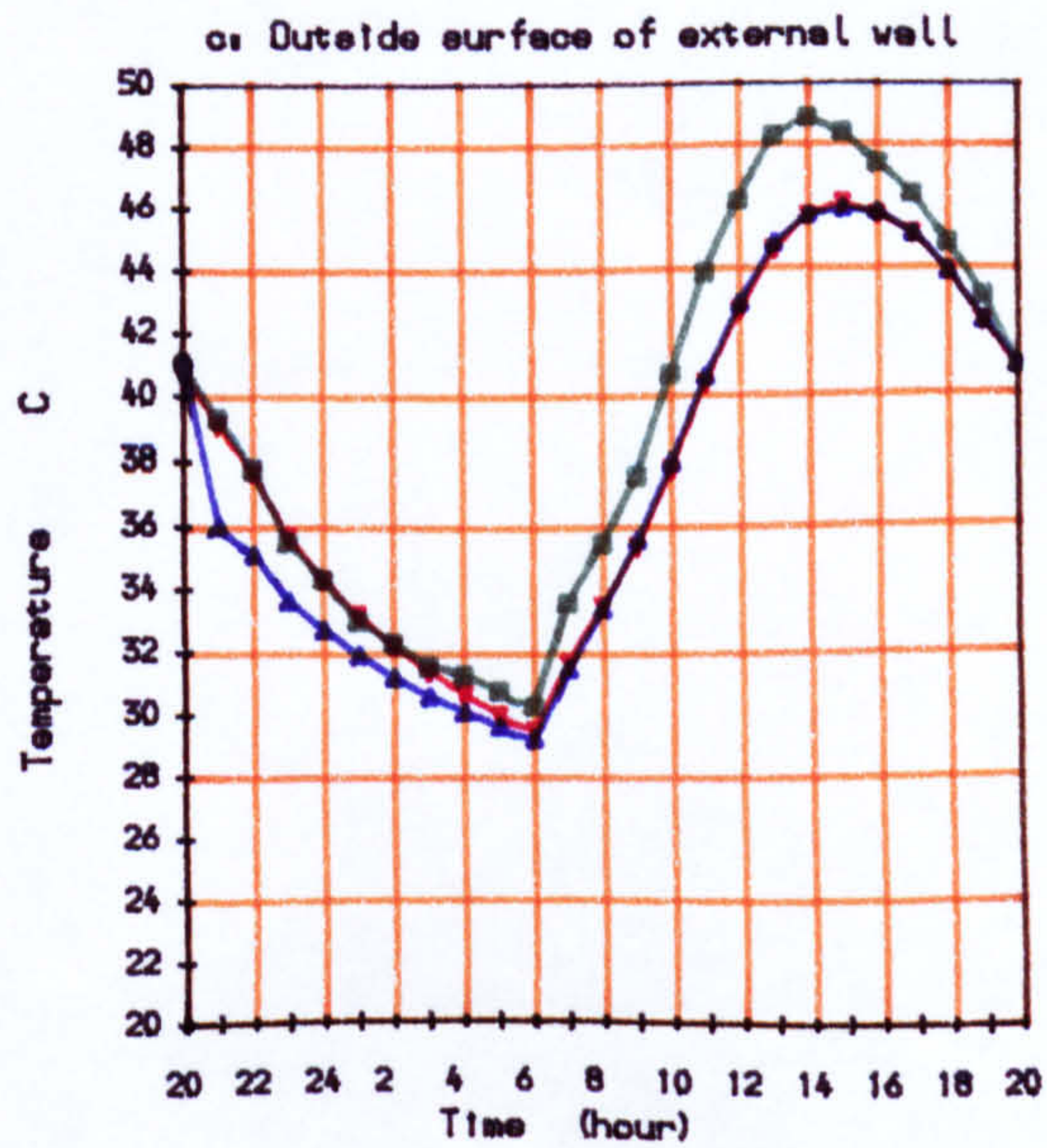
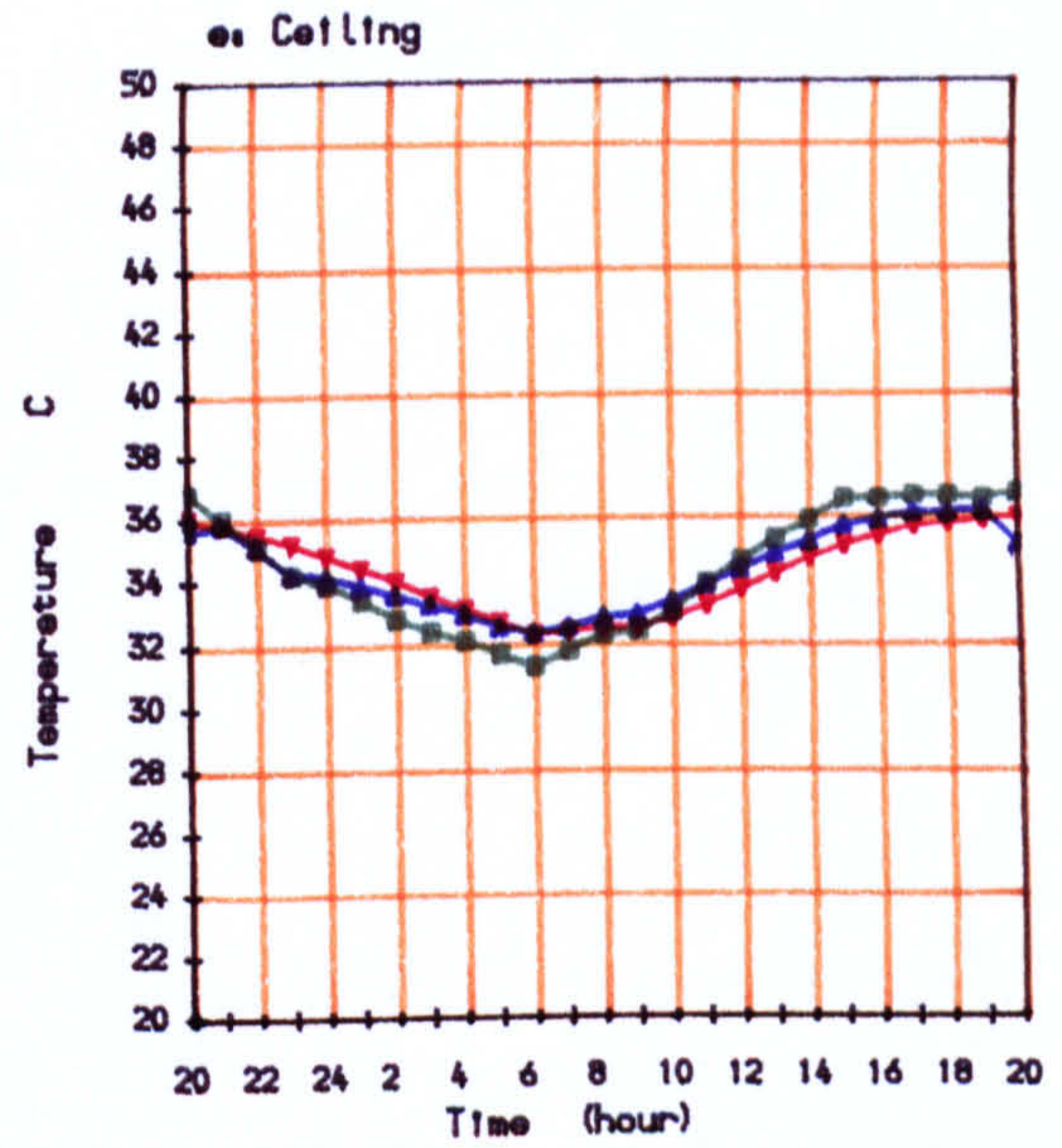
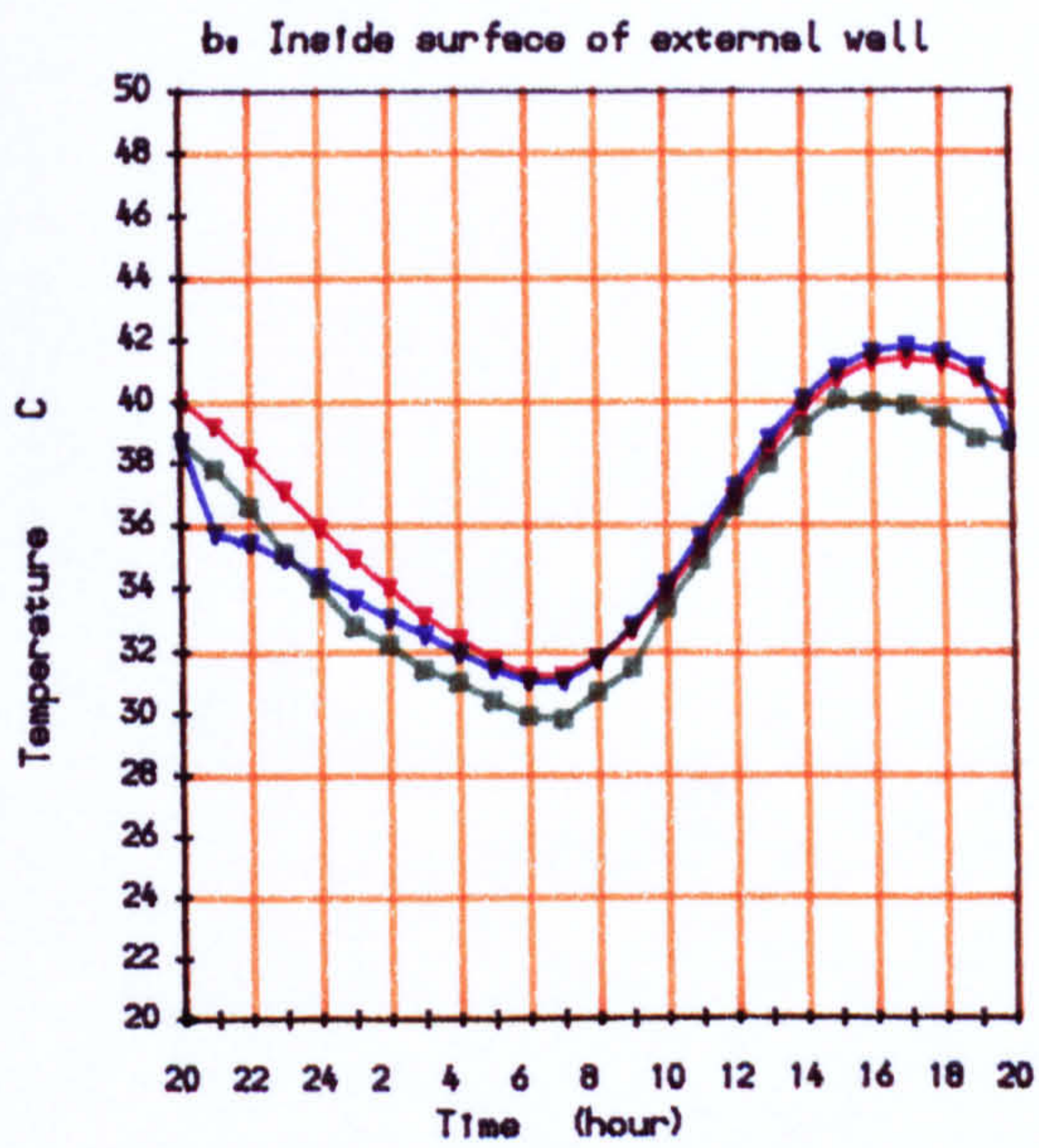
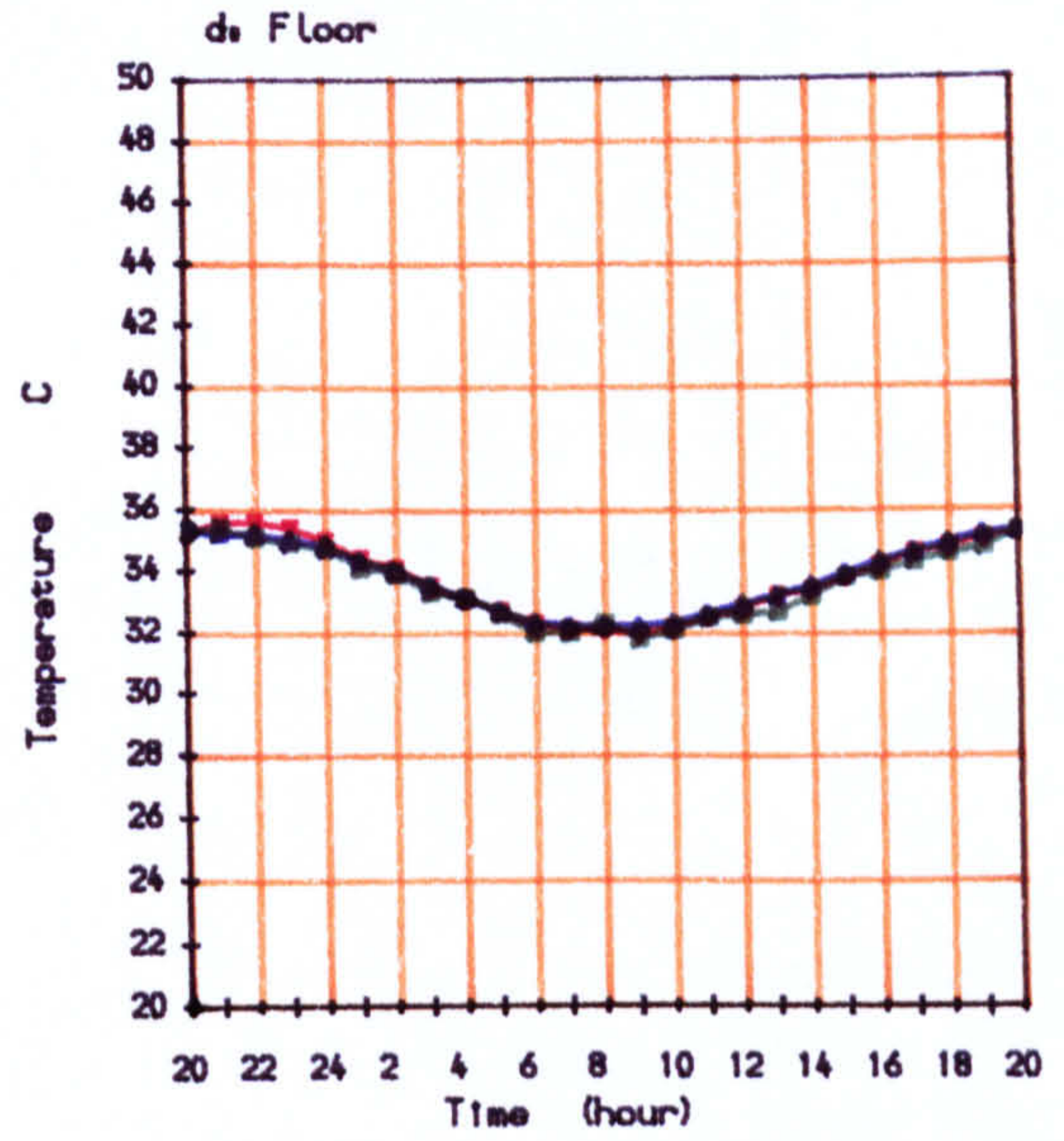
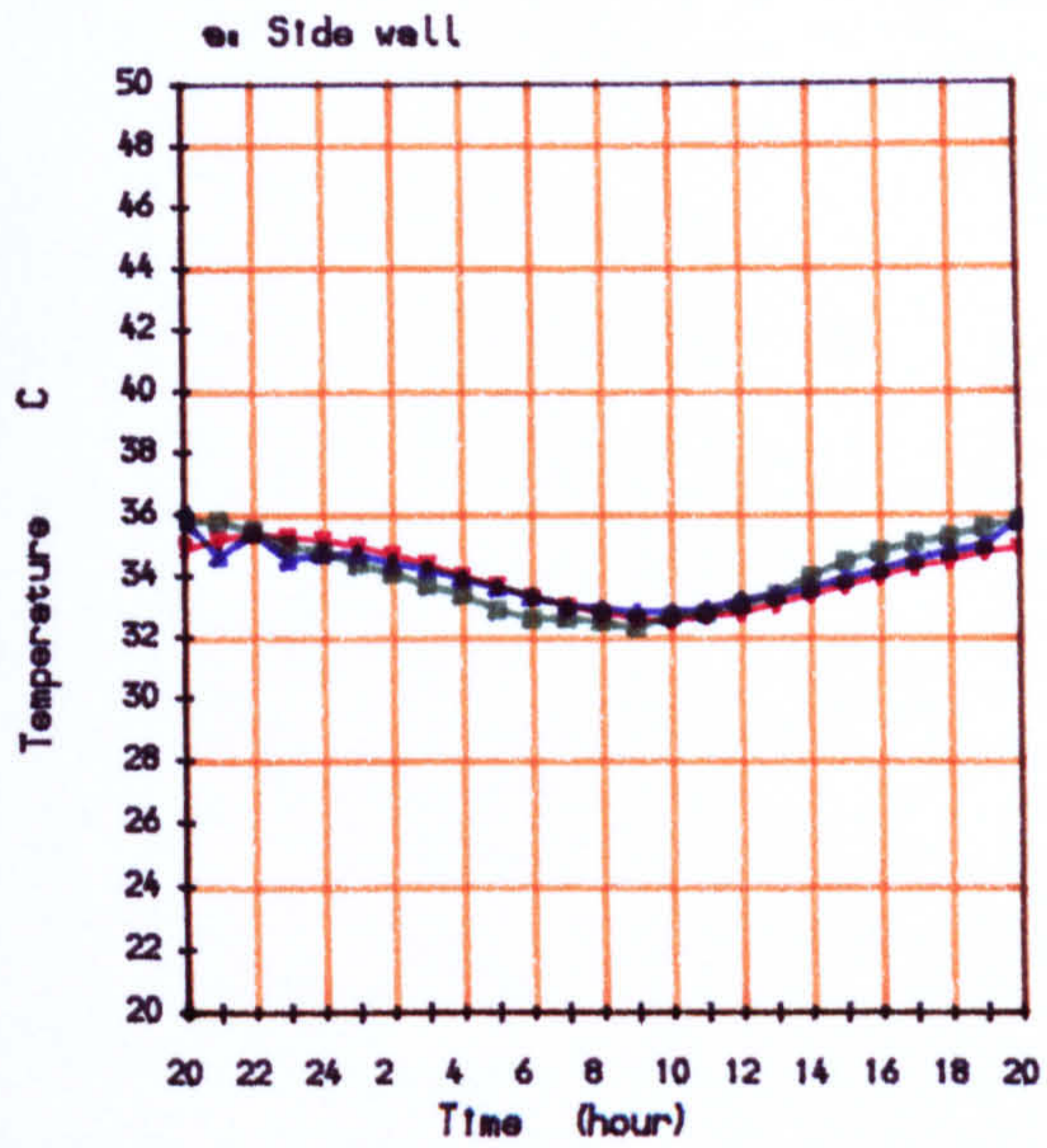


Figure 7.4. Comparison of measurements and predictions of the Finite Difference and the Response Factor Method  
 30 air changes per hour for four hours (from 2000 to 2400 hours)



—x—x Finite Difference Method     
 —■—■ Measurements     
 —▲—▲ Response Factor Method

Figure 7.5: Comparison of measurements and predictions of the Finite Difference and the Response Factor Method

3 air changes per hour for ten hours (from 2000 to 0600 hours)

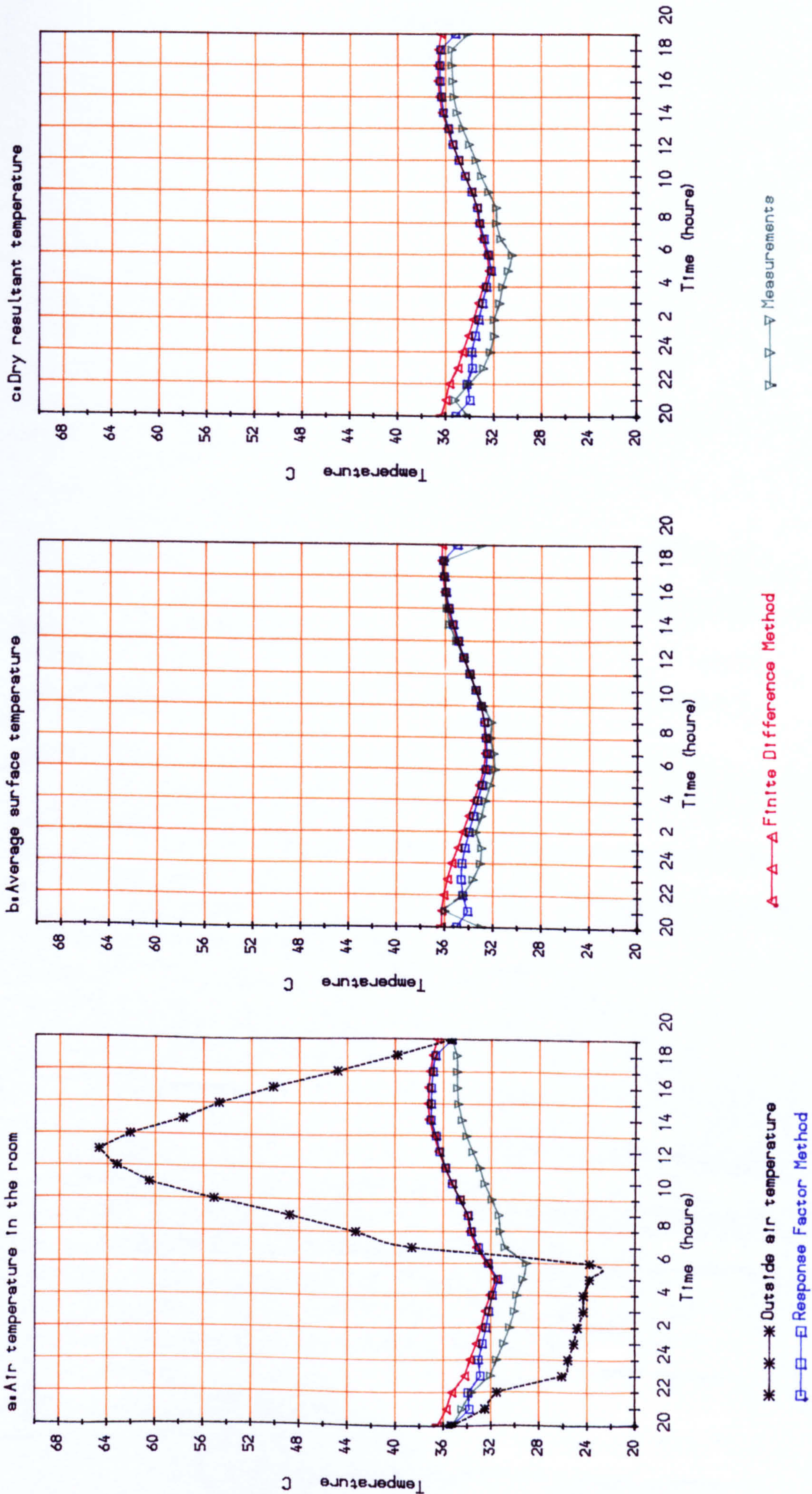


Figure 7.6: Comparison of measurements and predictions of the Finite Difference and the Response Factor Method  
3 air changes per hour for ten hours (from 2000 to 0600 hours)

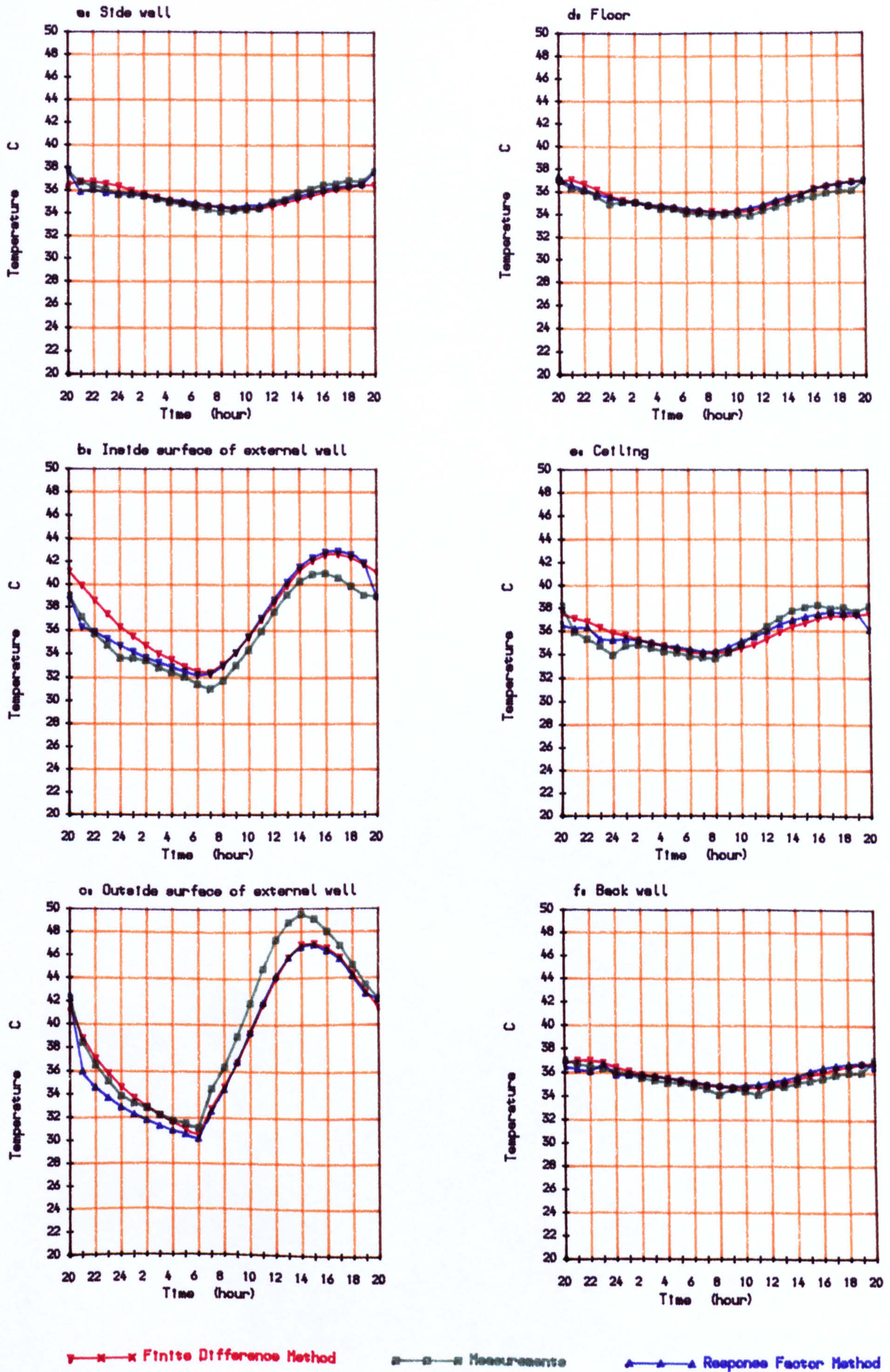


Figure 7.7: Comparison of measurements and predictions of the Finite Difference and the Response Factor Method

3 air changes per hour for four hours (from 2000 to 2400 hours)

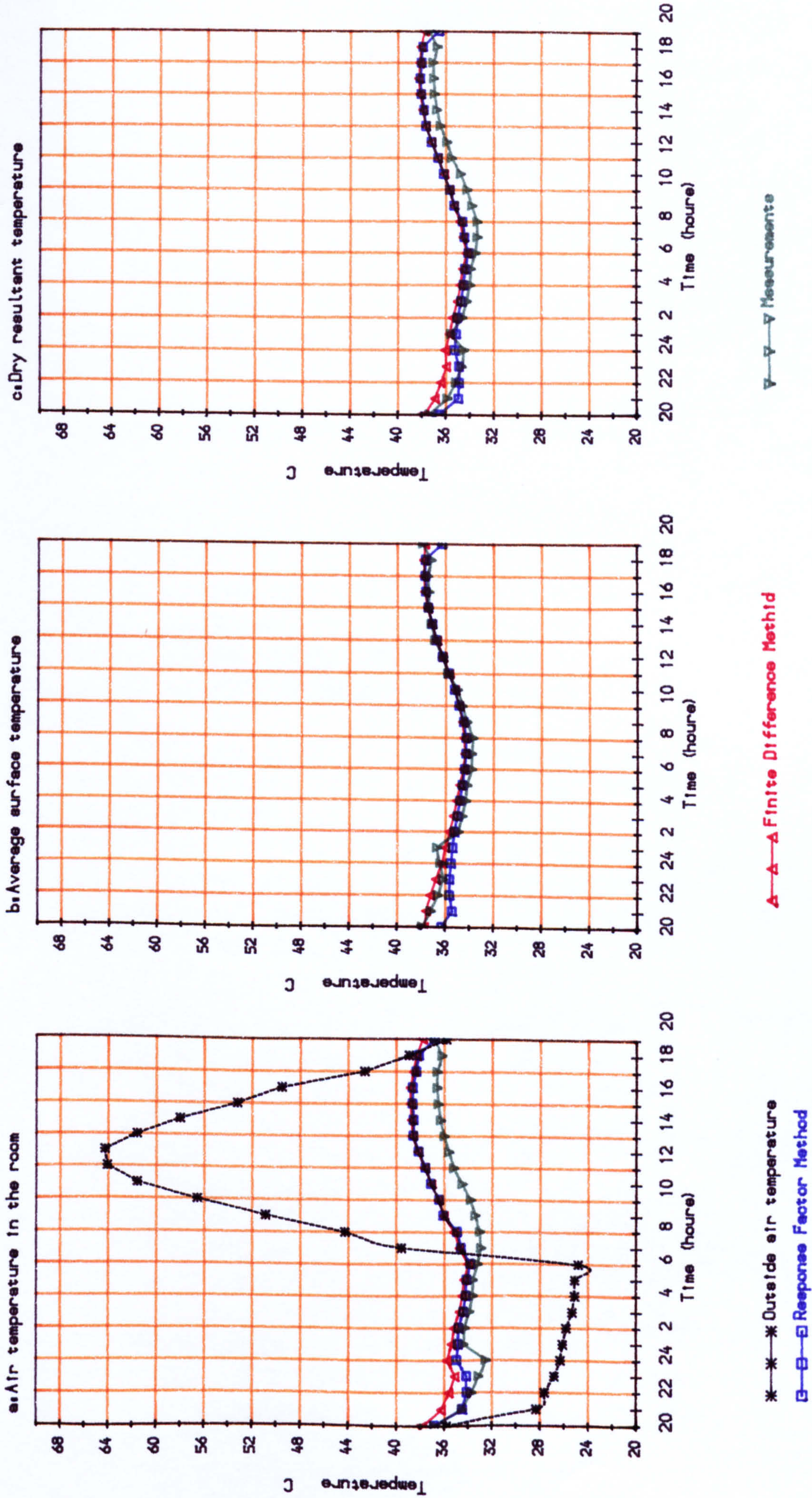


Figure 7.8: Comparison of measurements and predictions of the Finite Difference and the Response Factor Method  
 3 air changes per hour for four hours (from 2000 to 2400 hours)

size of the opening. As discussed above (see 5.2.3) this might happen in three ways. Two different unknowns have contributed to the difficulty in prediction of air temperature: the mechanism of air mixture and its efficiency in replacing the air in the room, and the rate of estimated infiltration. (CIBSE Guide chapter 8 suggests one air change per hour for cross ventilation). With regard to the evaluation of comfort, as one of the major purposes of investigation, use of the dry resultant temperature (mean of air and average surface temperature) as an index temperature, the general agreement of air temperature is within acceptable precision.

### 7.3.1 Results from different models:

The differences between measured and calculated air and average surface temperatures, in different models are presented in figures 7.9 to 7.11. As was predicted above, it is the inside air temperature which is more sensitive than the average surface temperatures to different assumptions. (8 and 6 surface models). Different assumptions in the nine and seven nodes models have not resulted in any better agreement in the average surface temperatures.

Comparison of model "Finit 9.1", "Finit 7.1" and "Finit 9.2" and "Finit 7.2" (i.e. time dependant  $h_c$  with fixed  $h_c$ ) shows that using a variable  $h_c$  did not result in better agreement in the nine and seven element model. In fact with a fixed  $h_c$  slightly better agreement than with predicted  $h_c$  is obtained.  $h_c$  in model "Finit 9.1" and "Finit 7.1" is calculated using a correlation suggested by Alamdari and Hammond (discussion is detailed in 2.2). As expected with the range of ventilation rate used in the observations; the natural convection was predominant inside the room. It seems that the predicted value underestimates  $h_c$ . The calculated  $h_c$  at different times of the day for different surfaces of the room is given in table 7.5. During ventilation, for a higher rate of ventilation the predicted temperatures of model 9.1 and 7.1 were more accurate while for lower rates of ventilation the model with a calculated  $h_c$ , of models 9.2 and 7.2 is closer to the observed values. The procedure for the calculation of  $h_c$  is independent of the ventilation rate, and is based only on the temperature difference between the air and the surfaces. It is clear that the air flow rate will affect the convection coefficient. This requires further investigation.

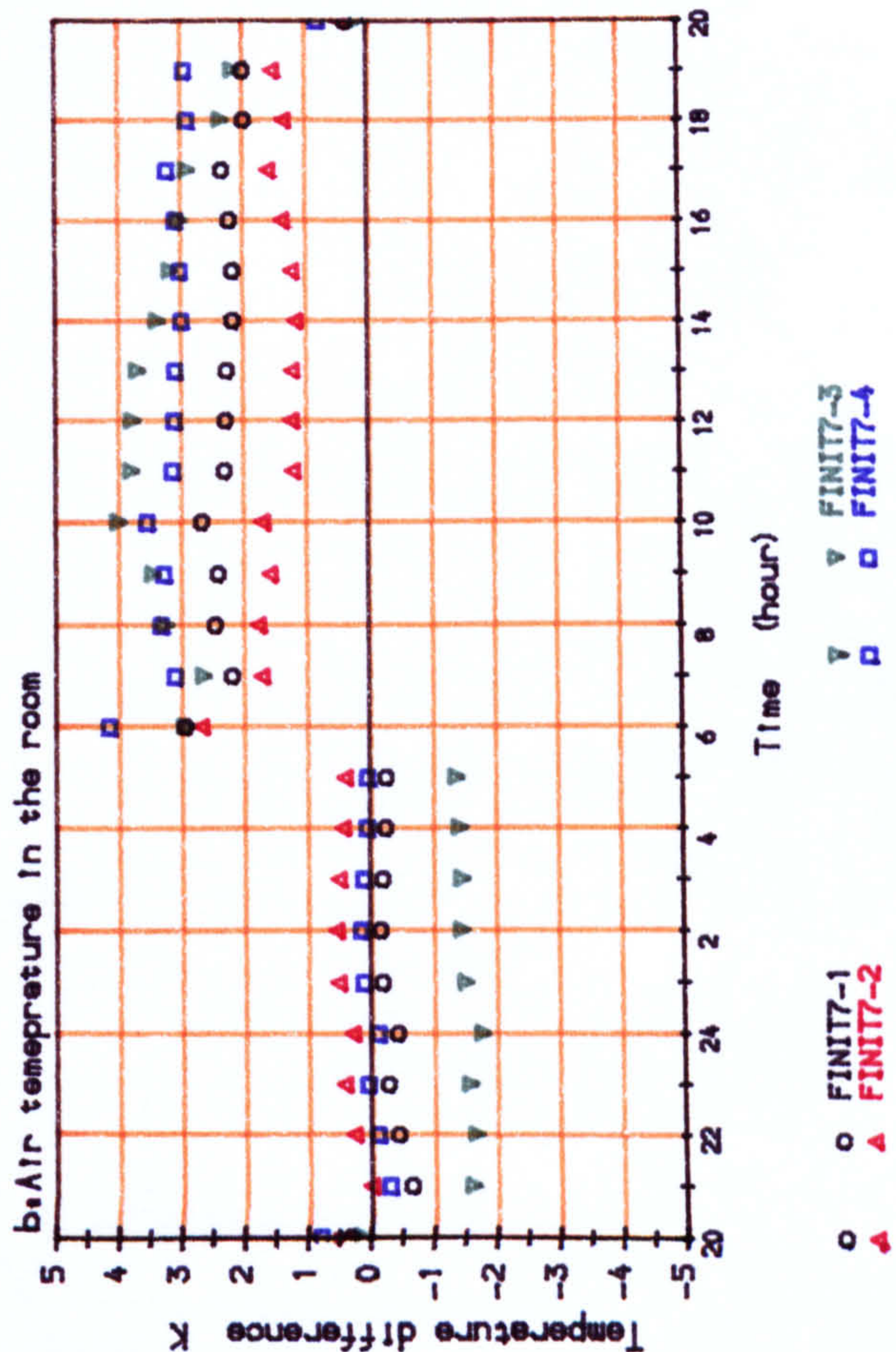
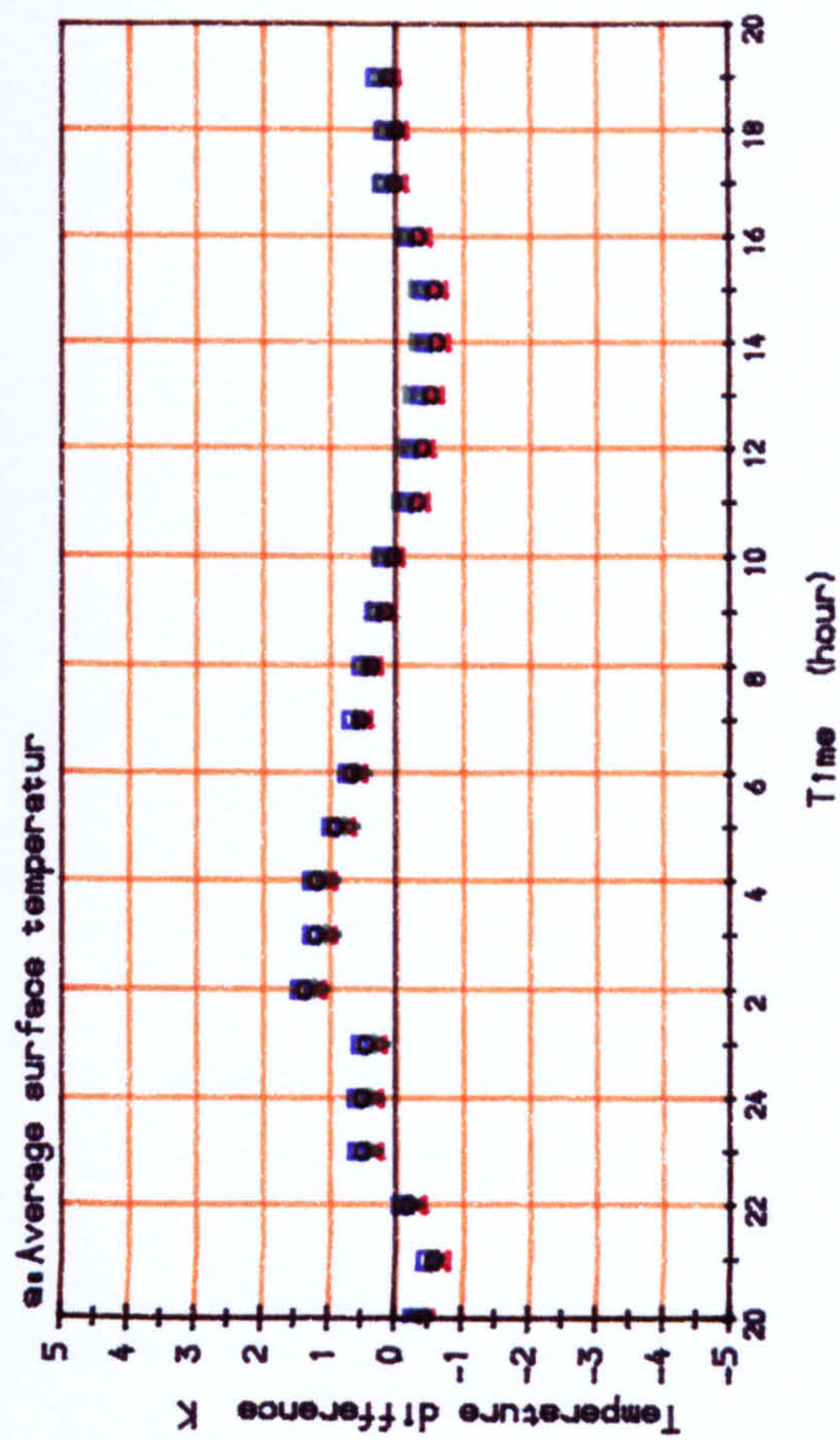
Comparison of model "Finit 9.1" and "Finit 7.1" with "Finit 9.3" and "Finit 7.3", which are different in treatment of air mixing, show



**Table 7.5: Convective heat transfer coefficient,  $h_c$ , for internal Surfaces calculated by correlations, Suggested by Alamdari and Hammond**

time	front wall	side wall	back wall	ceiling	floor
20	2.25	0.96	0.82	0.50	1.27
21	2.54	2.15	2.05	0.69	2.63
22	2.54	2.34	2.25	0.72	2.85
23	2.48	2.41	2.33	0.73	2.93
24	2.42	2.45	2.38	0.73	2.97
1	2.33	2.44	2.37	0.73	2.94
2	2.28	2.44	2.38	0.73	2.93
3	2.21	2.43	2.36	0.72	2.90
4	2.13	2.39	2.32	0.71	2.85
5	2.05	2.35	2.28	0.71	2.79
6	1.46	1.47	1.23	0.36	1.26
7	1.46	1.23	0.96	0.76	0.18
8	1.43	0.99	1.25	1.49	0.51
9	1.21	1.46	1.58	1.73	0.58
10	1.73	1.73	1.81	1.86	0.63
11	1.38	1.87	1.94	1.93	0.66
12	1.75	1.93	2.00	1.97	0.66
13	2.00	1.95	2.01	1.94	0.66
14	2.18	1.91	1.97	1.82	0.65
15	2.27	1.84	1.91	1.66	0.62
16	2.32	1.74	1.81	1.46	0.59
17	2.35	1.58	1.68	1.14	0.55
18	2.32	1.40	1.55	0.69	0.51
19	2.21	1.38	1.54	0.97	0.50

Seven nodes model



Nine nodes model

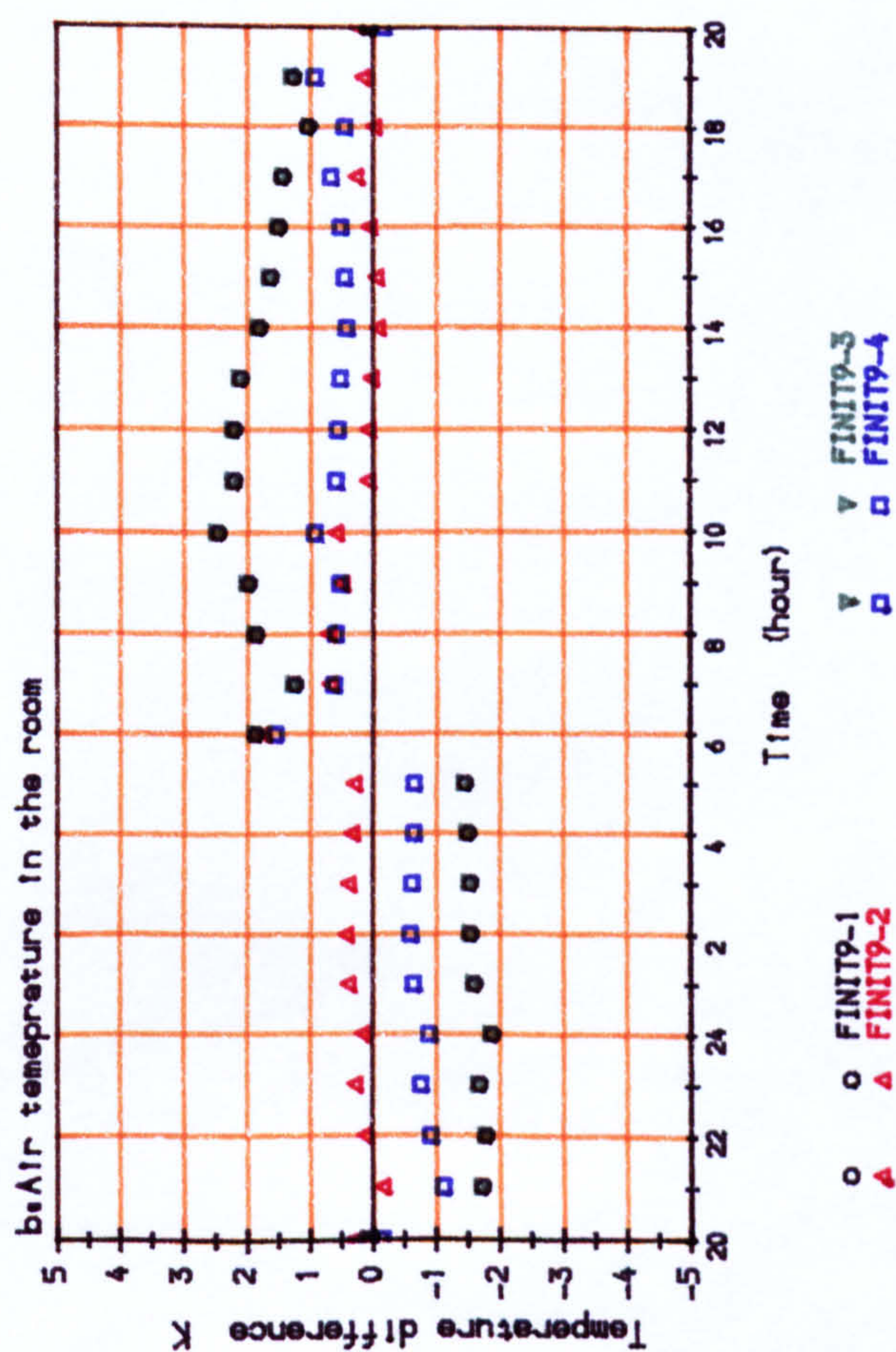
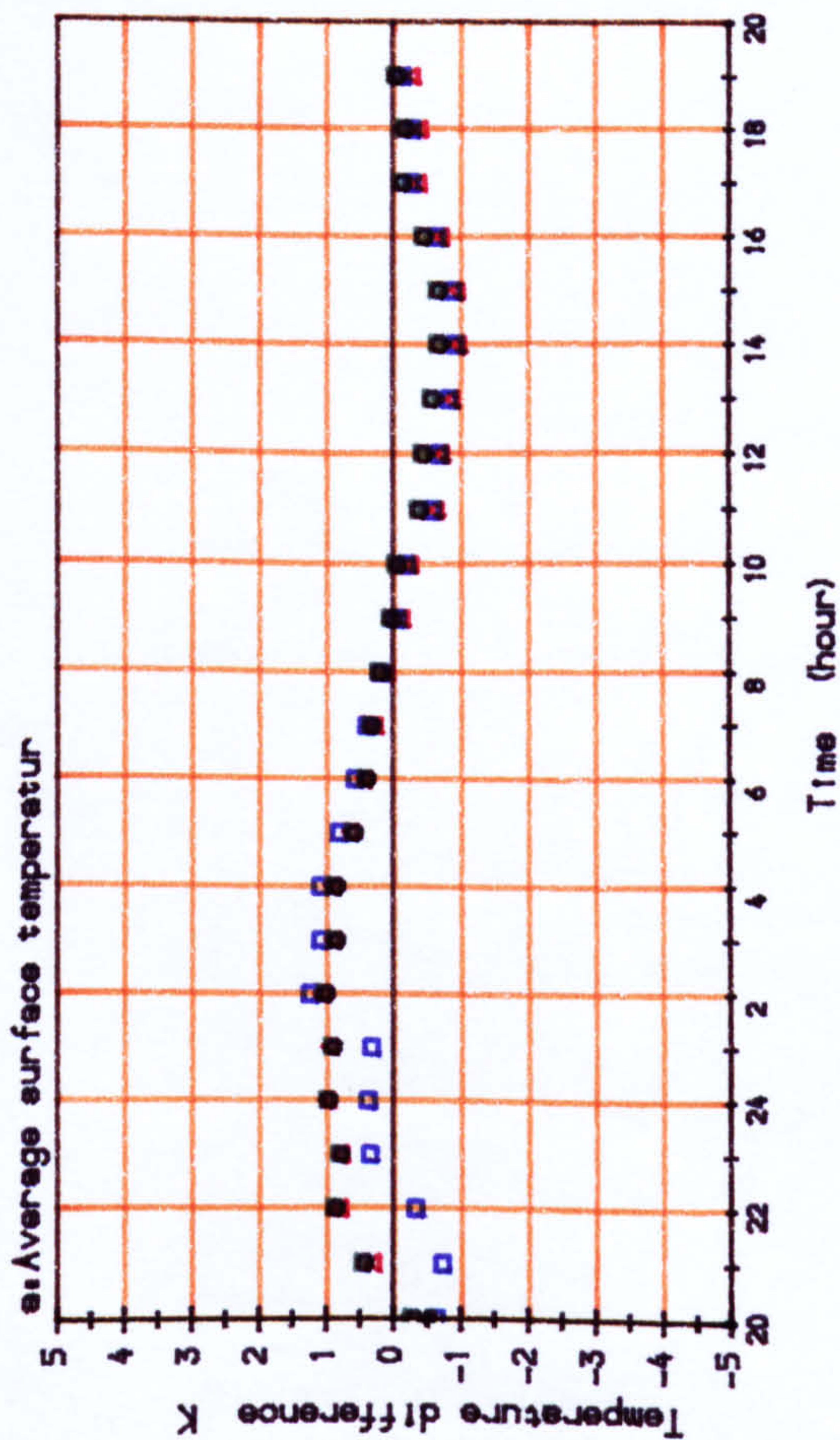
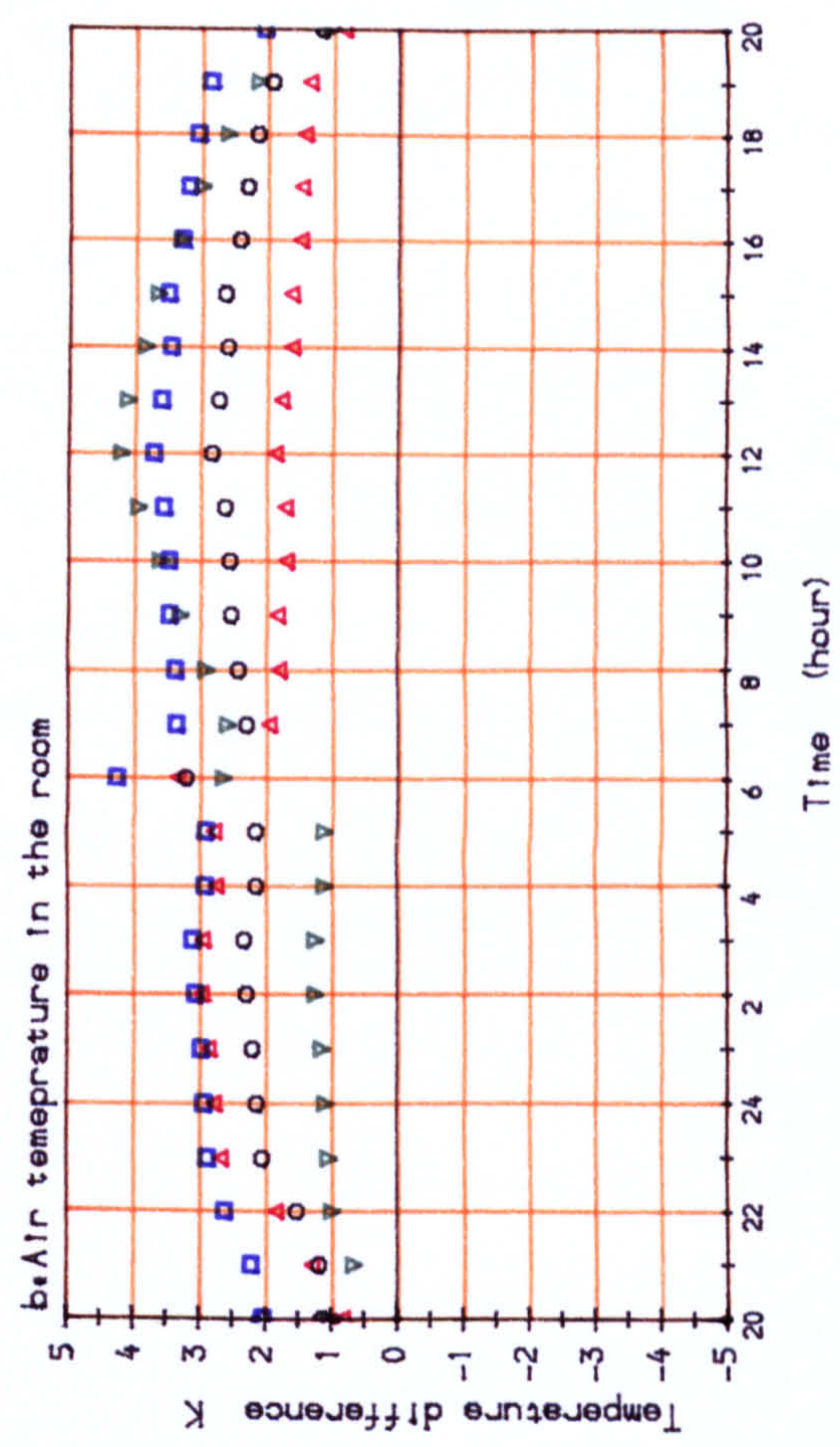
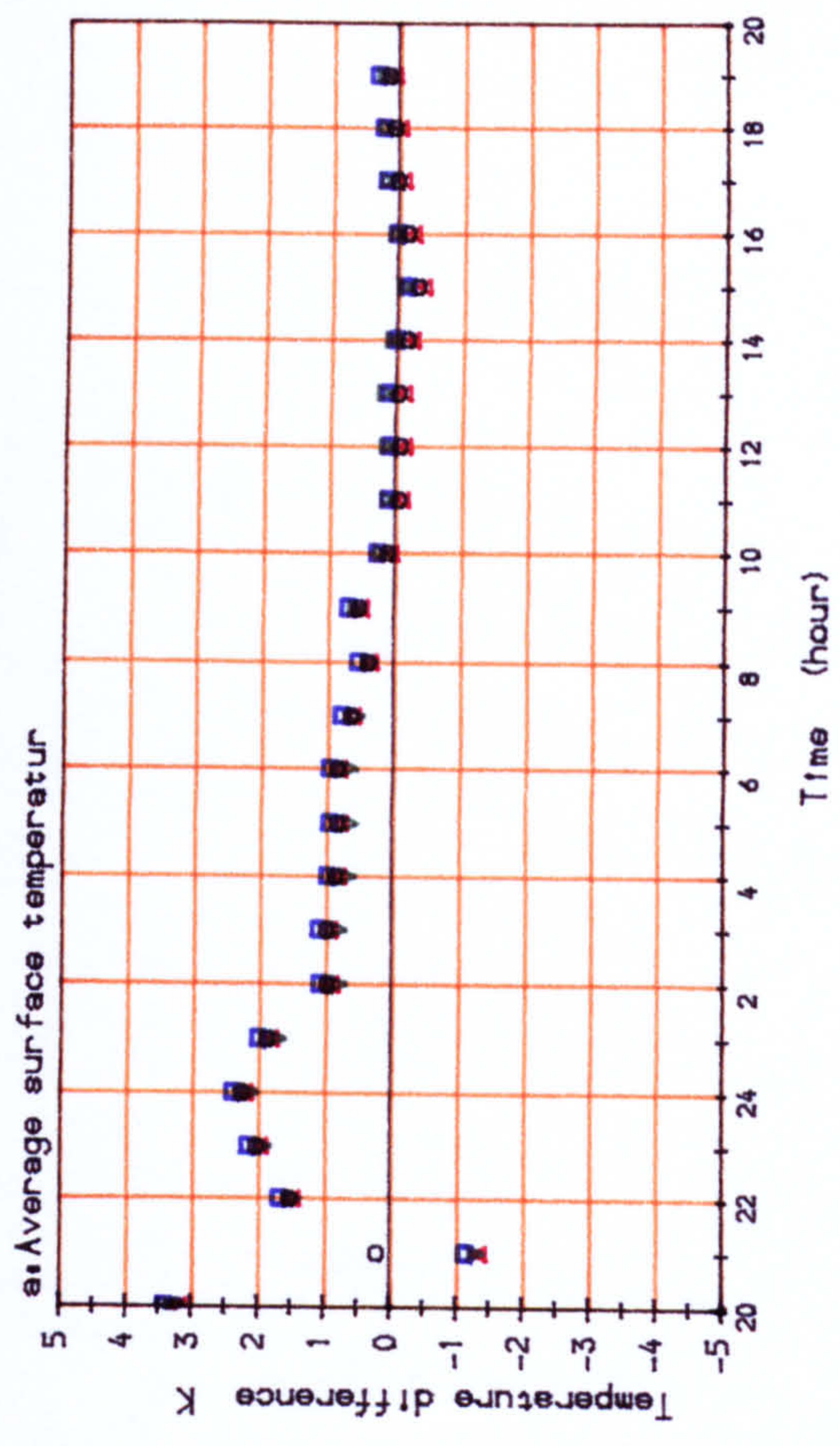


Figure 7.9: Temperature differences between observations and the Finite Difference models

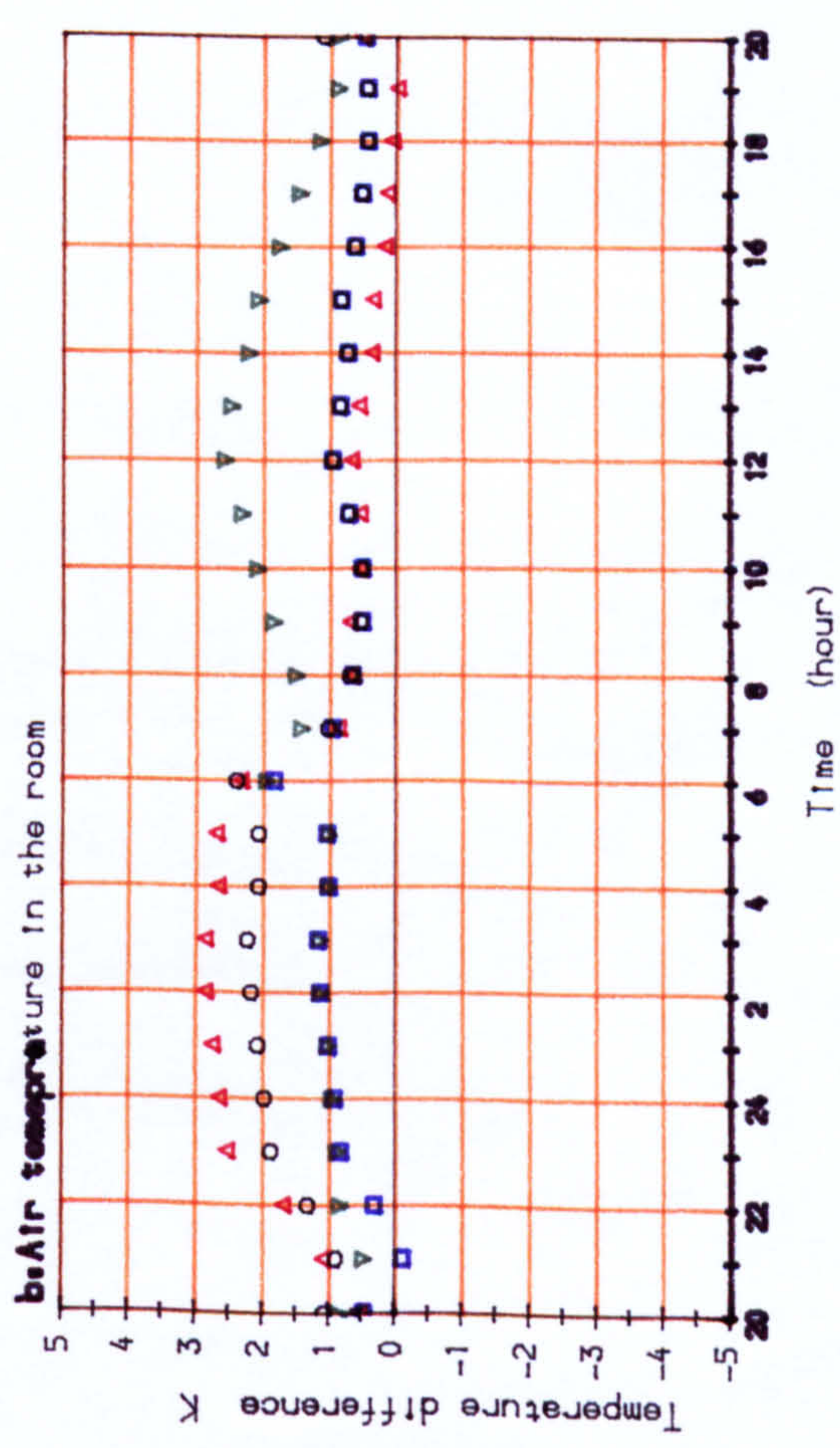
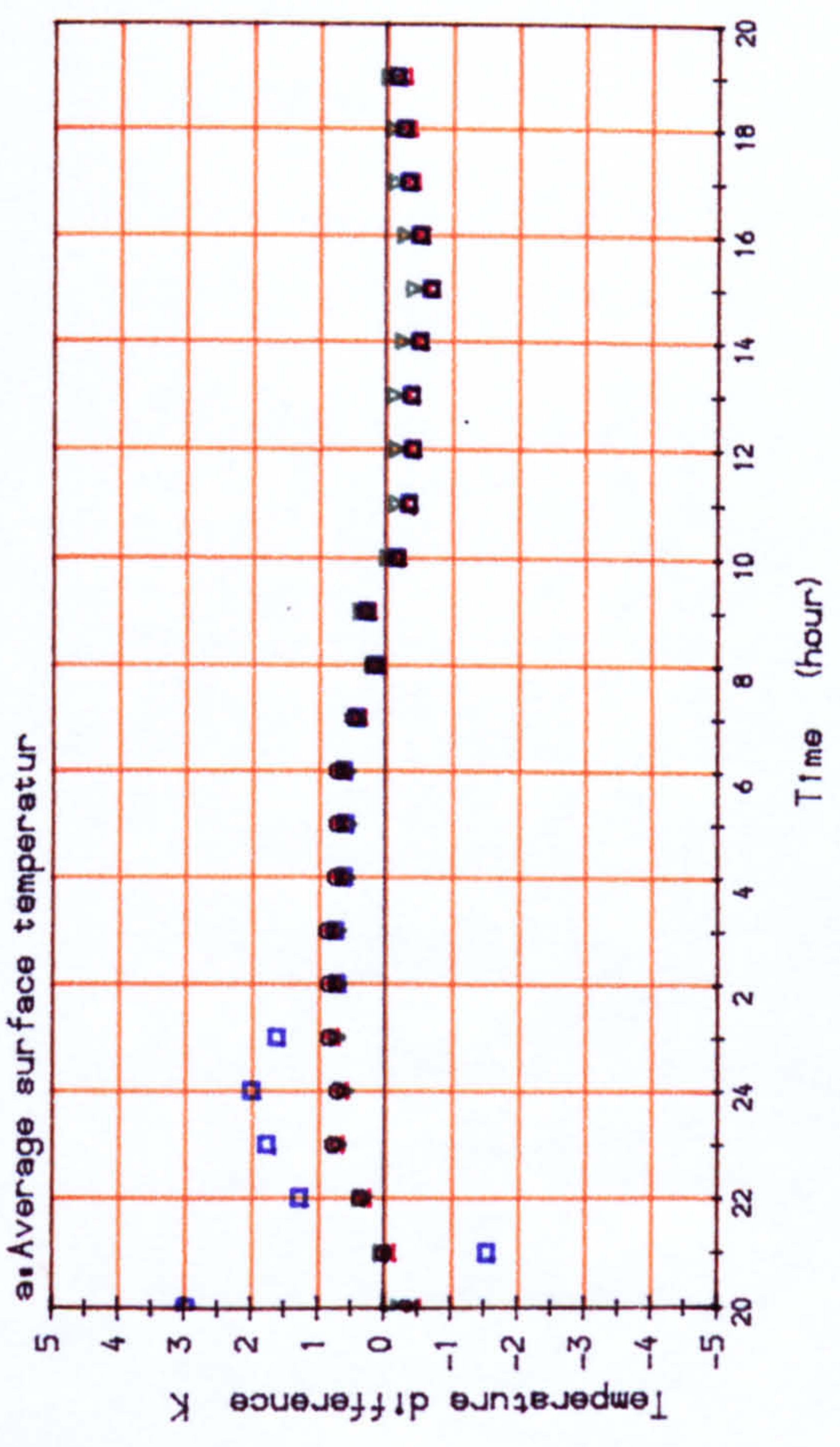
30 air changes per hour for ten hours (from 2000 to 0600 hours)

Seven nodes model



○ FINIT7-1  
 △ FINIT7-2  
 ▼ FINIT7-3  
 □ FINIT7-4

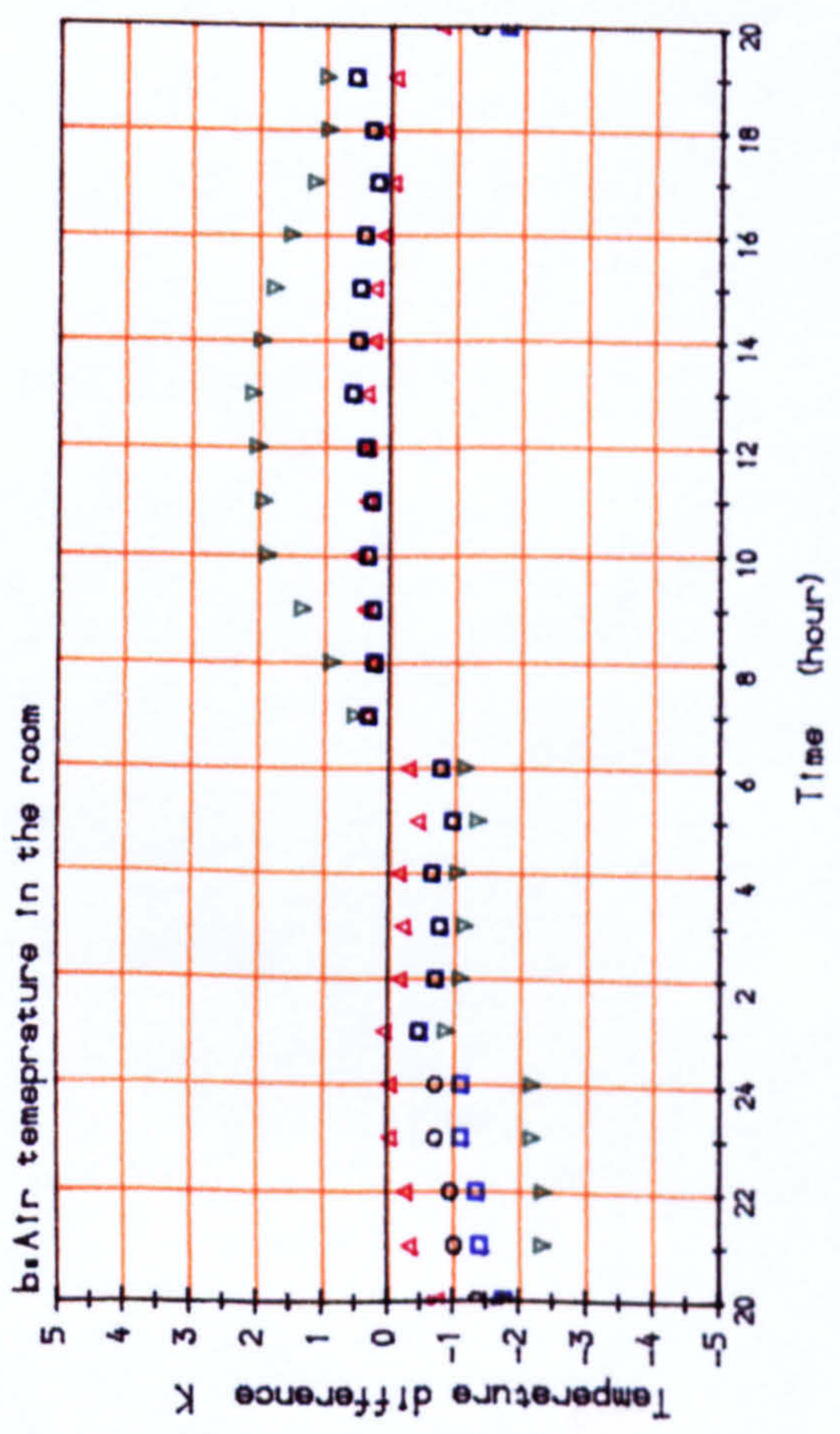
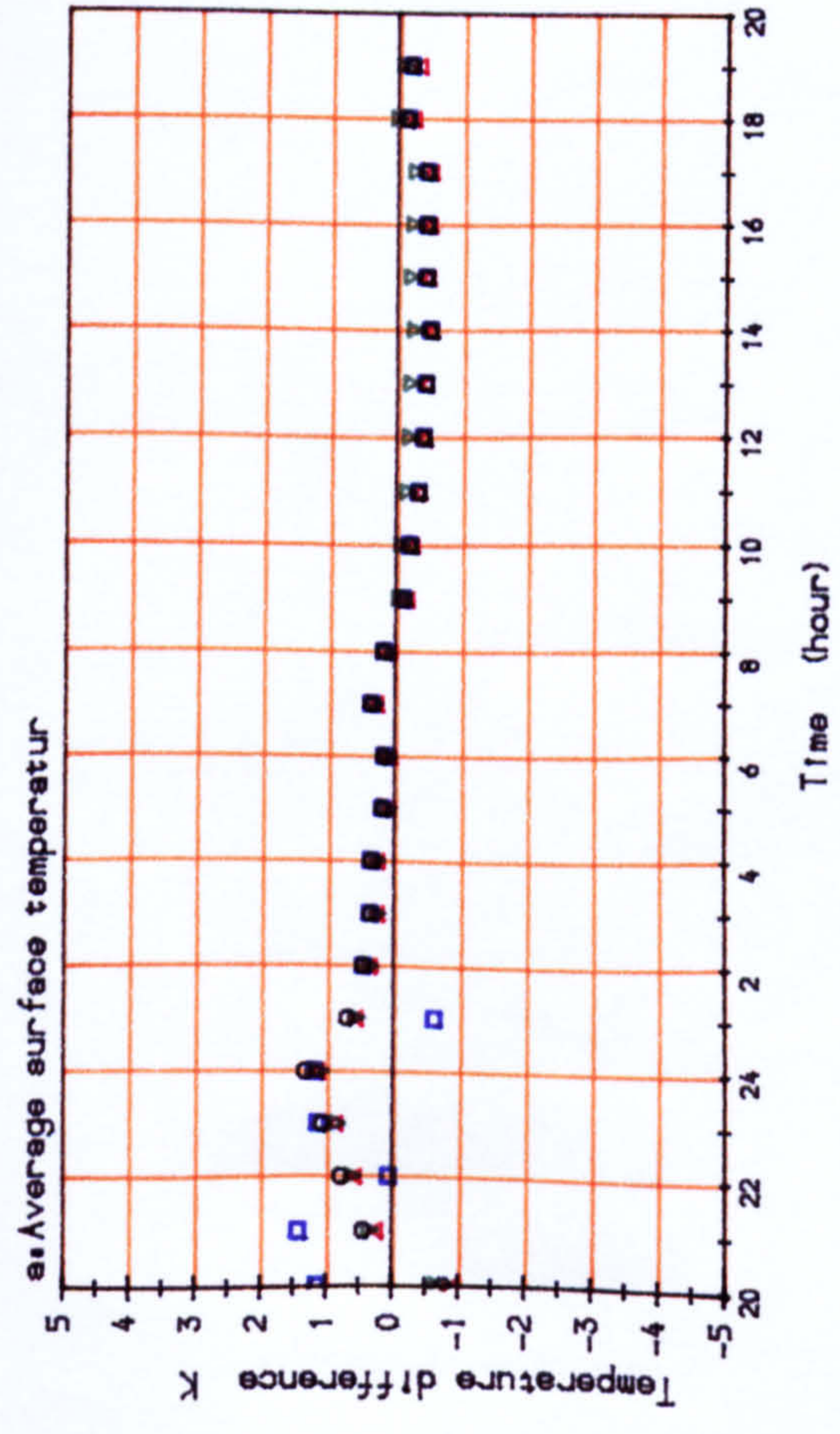
Nine nodes model



○ FINIT9-1  
 △ FINIT9-2  
 ▼ FINIT9-3  
 □ FINIT9-4

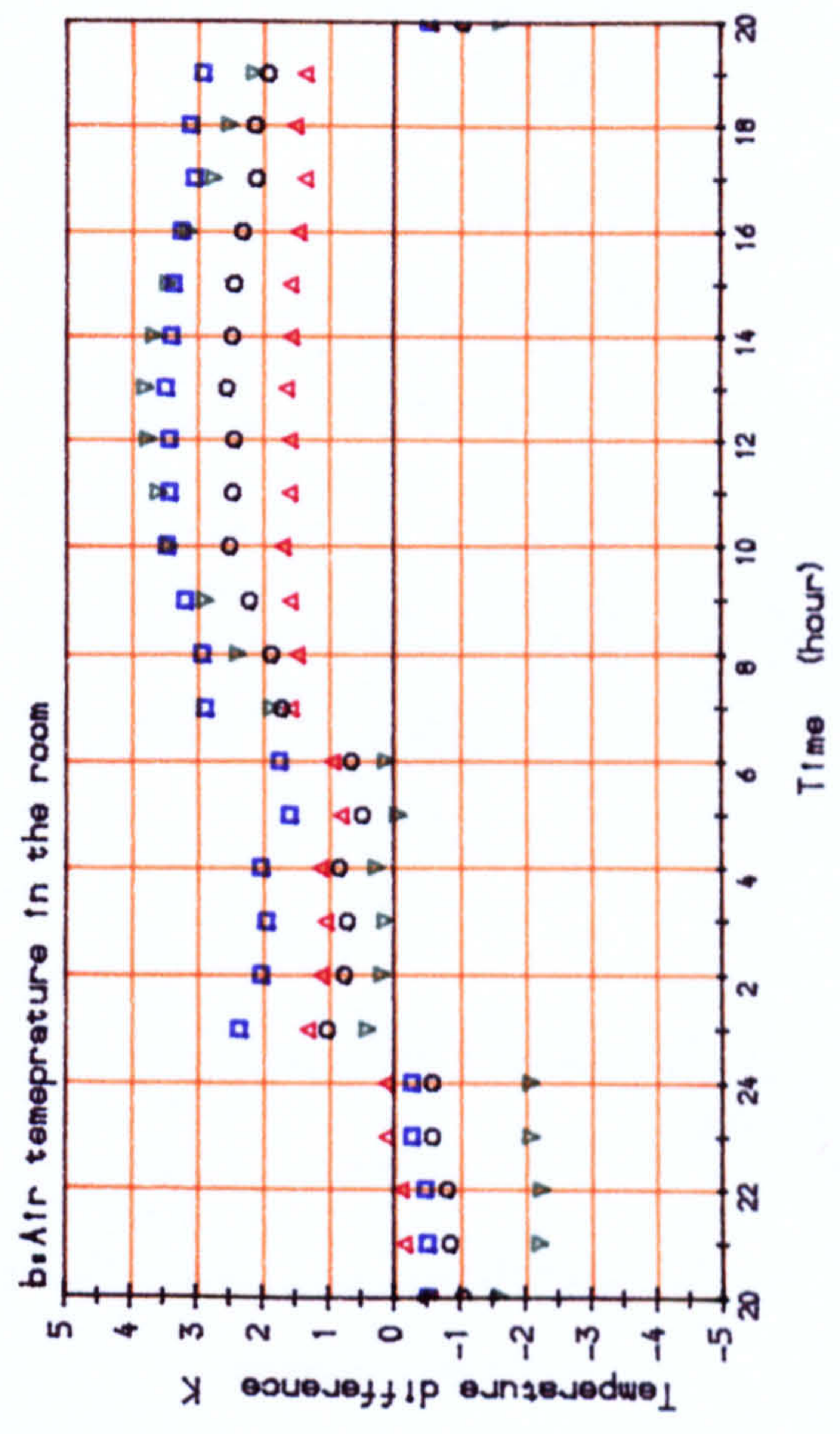
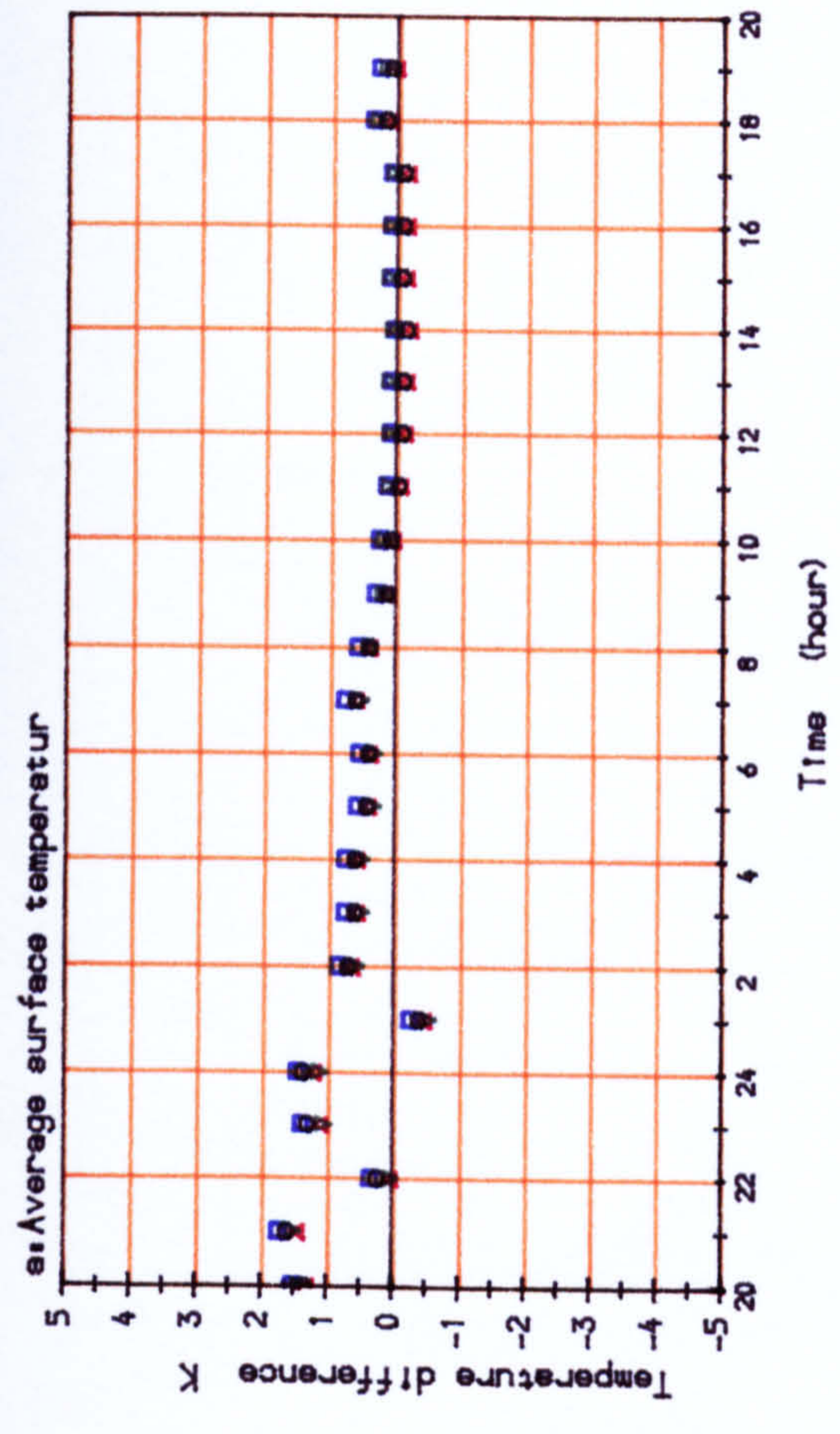
Figure 7.10: Temperature differences between observations and the Finite Difference models  
 30 air changes per hour for ten hours (from 2000 to 0600 hours)

Nine nodes model



○ FINIT9-1  
 ▲ FINIT9-2  
 ▼ FINIT9-3  
 □ FINIT9-4

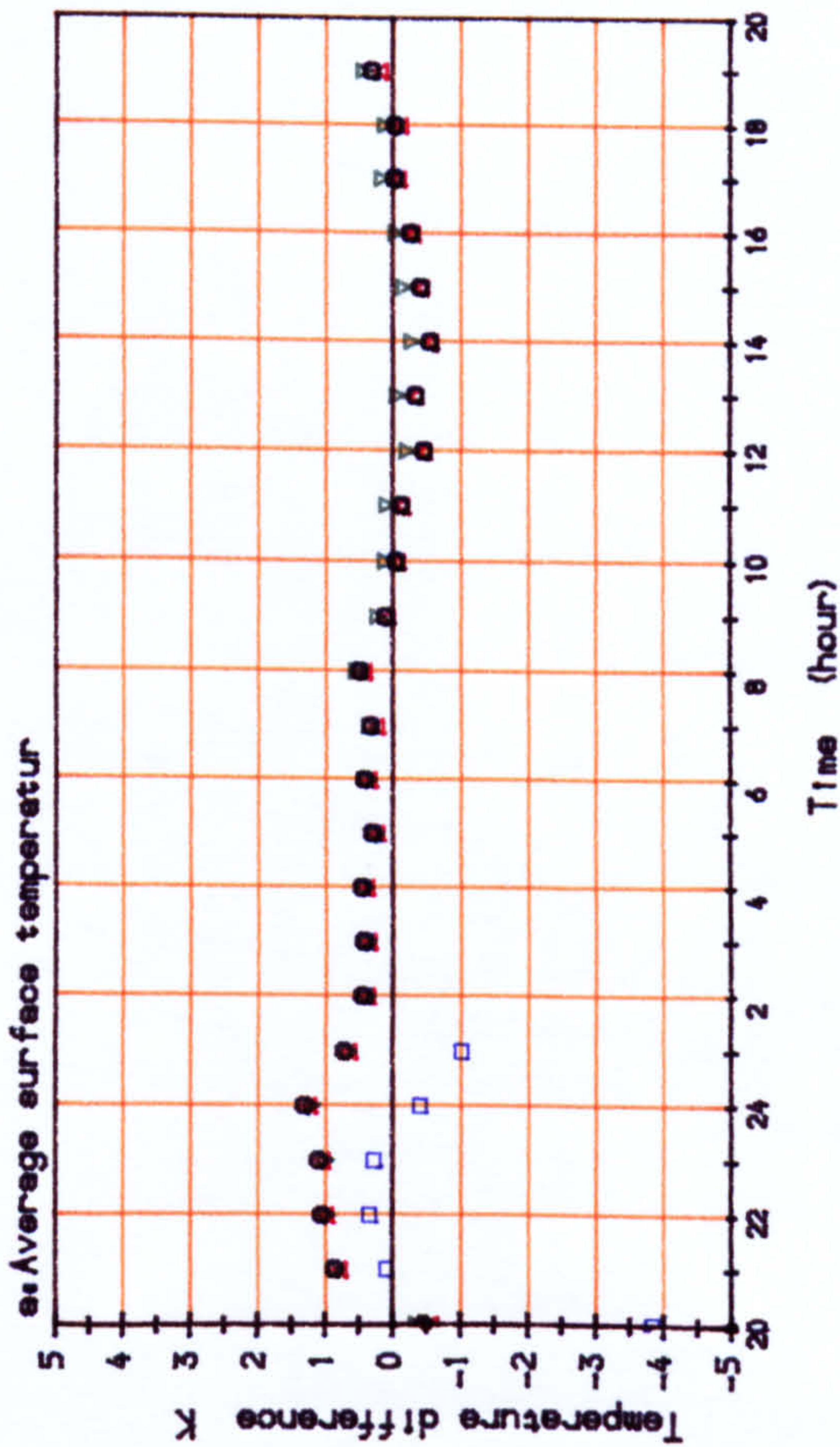
Seven nodes model



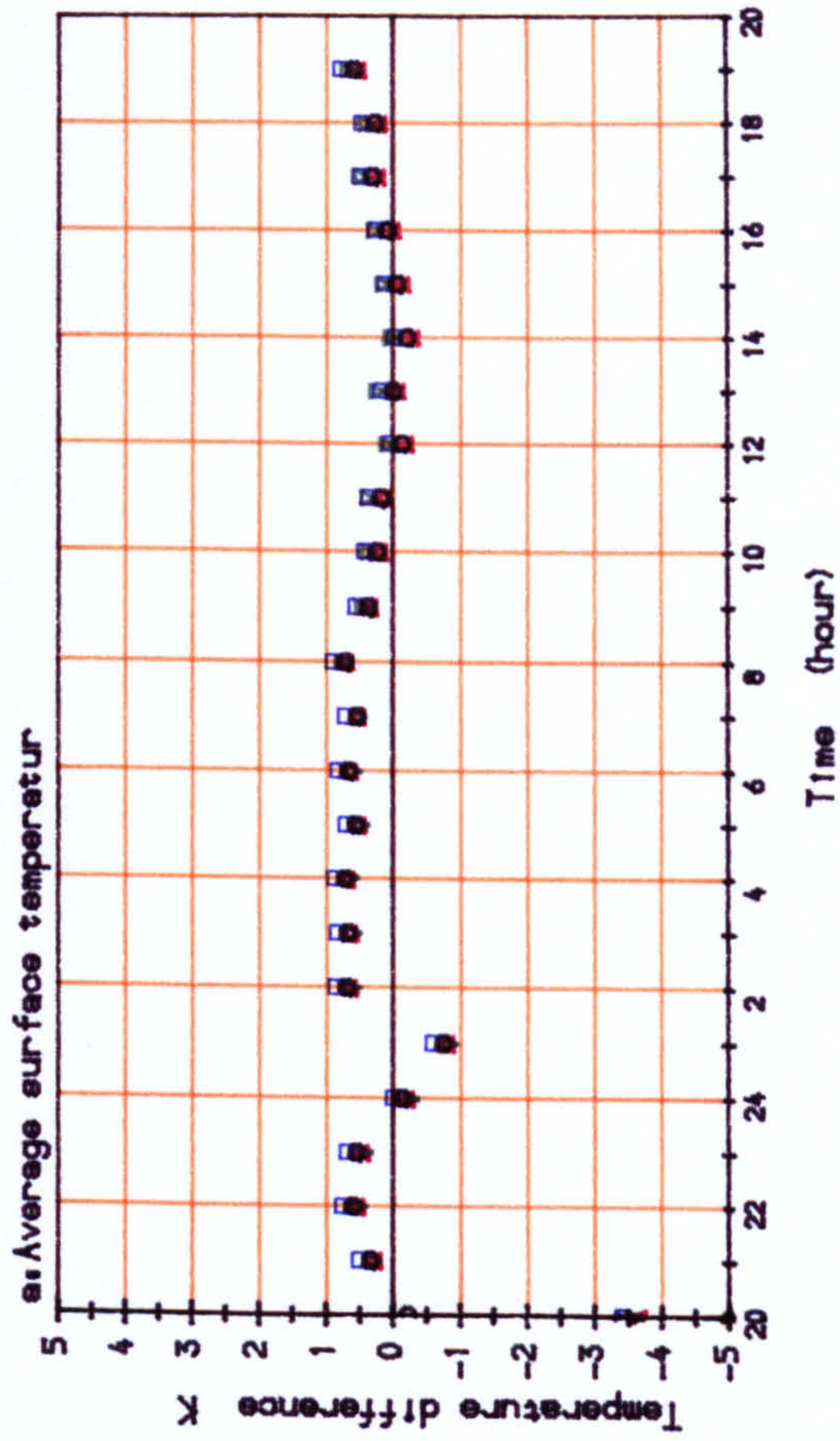
○ FINIT7-1  
 ▲ FINIT7-2  
 ▼ FINIT7-3  
 □ FINIT7-4

Figure 7.11. Temperature differences between observations and the finite difference models  
 30 air changes per hour for four hours (from 2000 to 2400 hours)

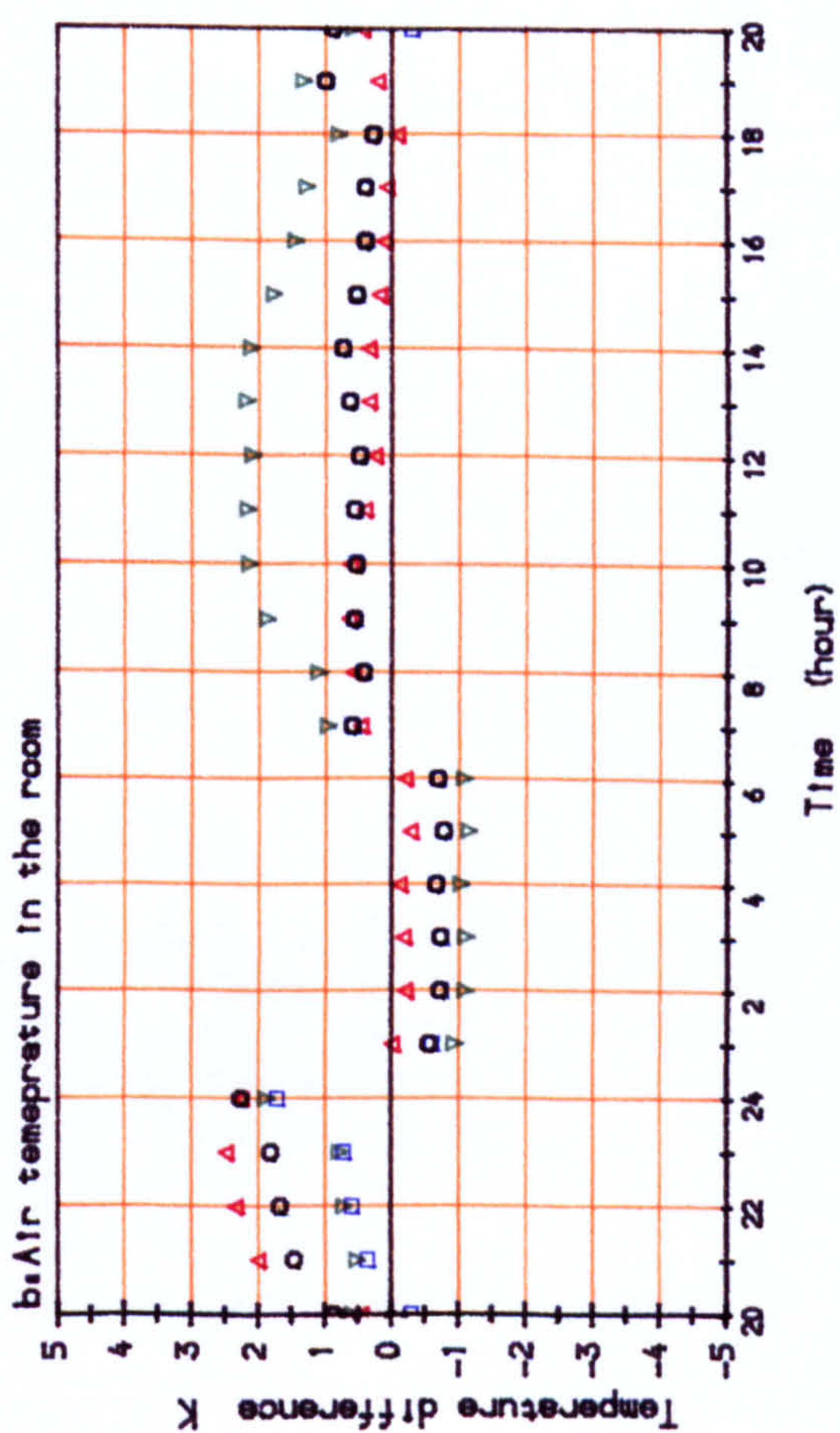
Nine nodes model



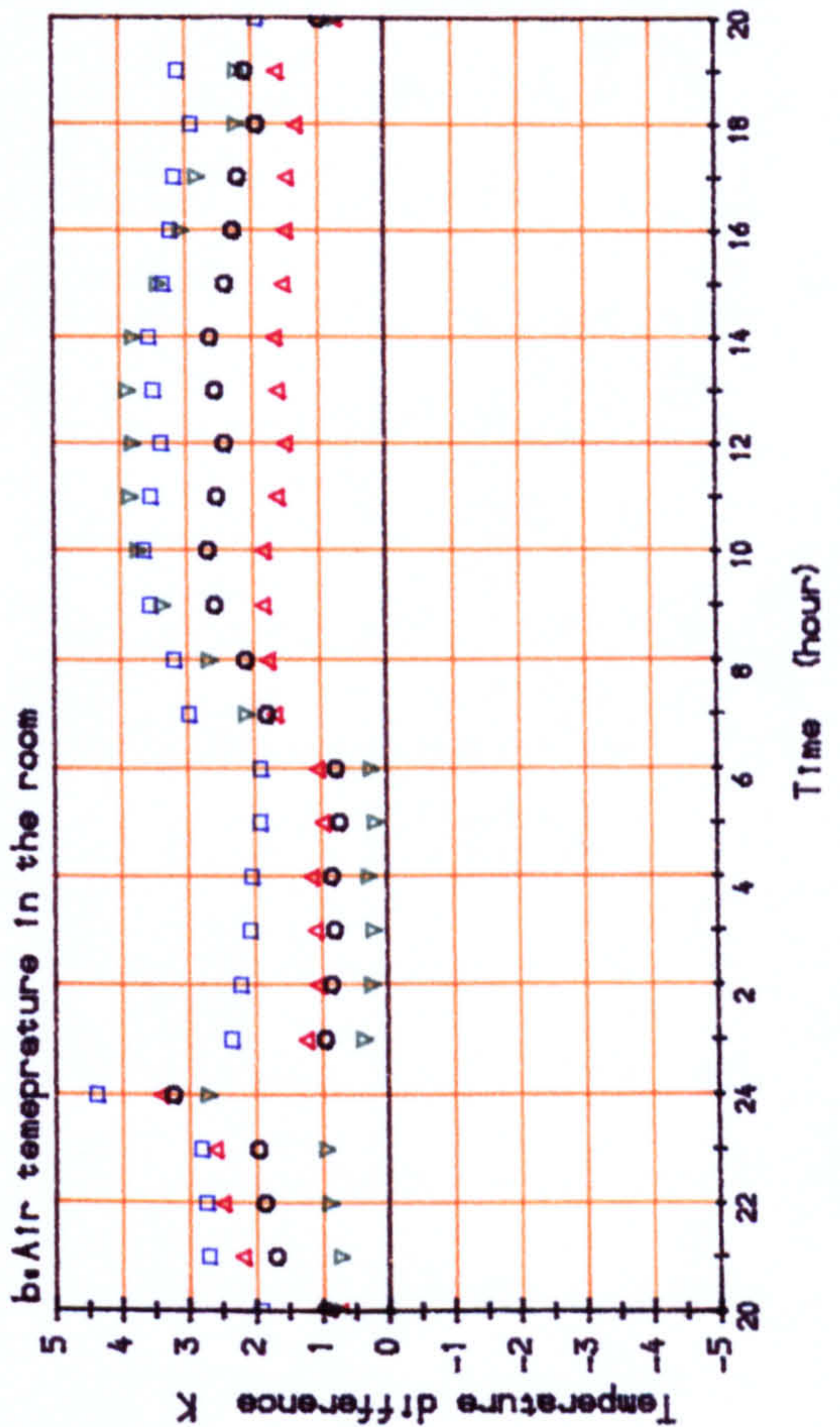
Seven nodes model



air temperature in the room



air temperature in the room



○ FINIT9-1    △ FINIT9-2    ▽ FINIT9-3    □ FINIT9-4  
 ○ FINIT7-1    △ FINIT7-2    ▽ FINIT7-3    □ FINIT7-4

Figure 7.12. Temperature differences between observations and the Finite Difference models  
 3 air changes per hour for four hours (from 2000 to 2400 hours)

that for higher rates of ventilation the assumption of perfect air mixing during ventilation results in better agreement with observation. For lower rates of ventilation, the assumption of partial displacement flow is in better agreement. All cases of models 9.1 and 7.1 have shown more accurate results when there is infiltration.

Comparison of models "Finit 9.1" and "Finit 9.4" shows that the separate calculation of radiation heat loss through open windows does not contribute to better results for the prediction of air temperature during the night. The separate treatment of radiation is not worth the cumbersome calculations with regard to the uncertainties of the parameters used in the calculation such as the temperatures, convective coefficient etc.

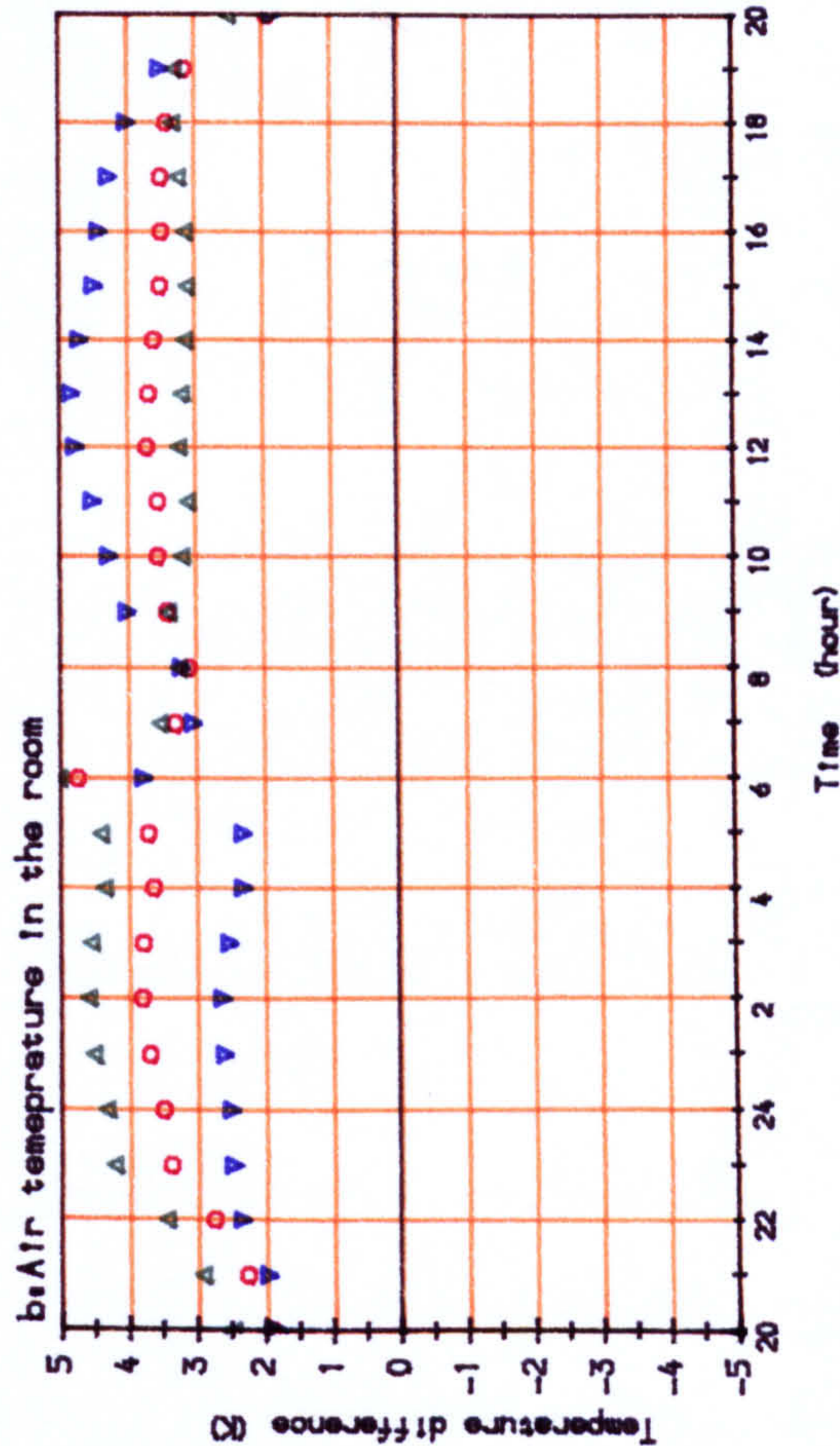
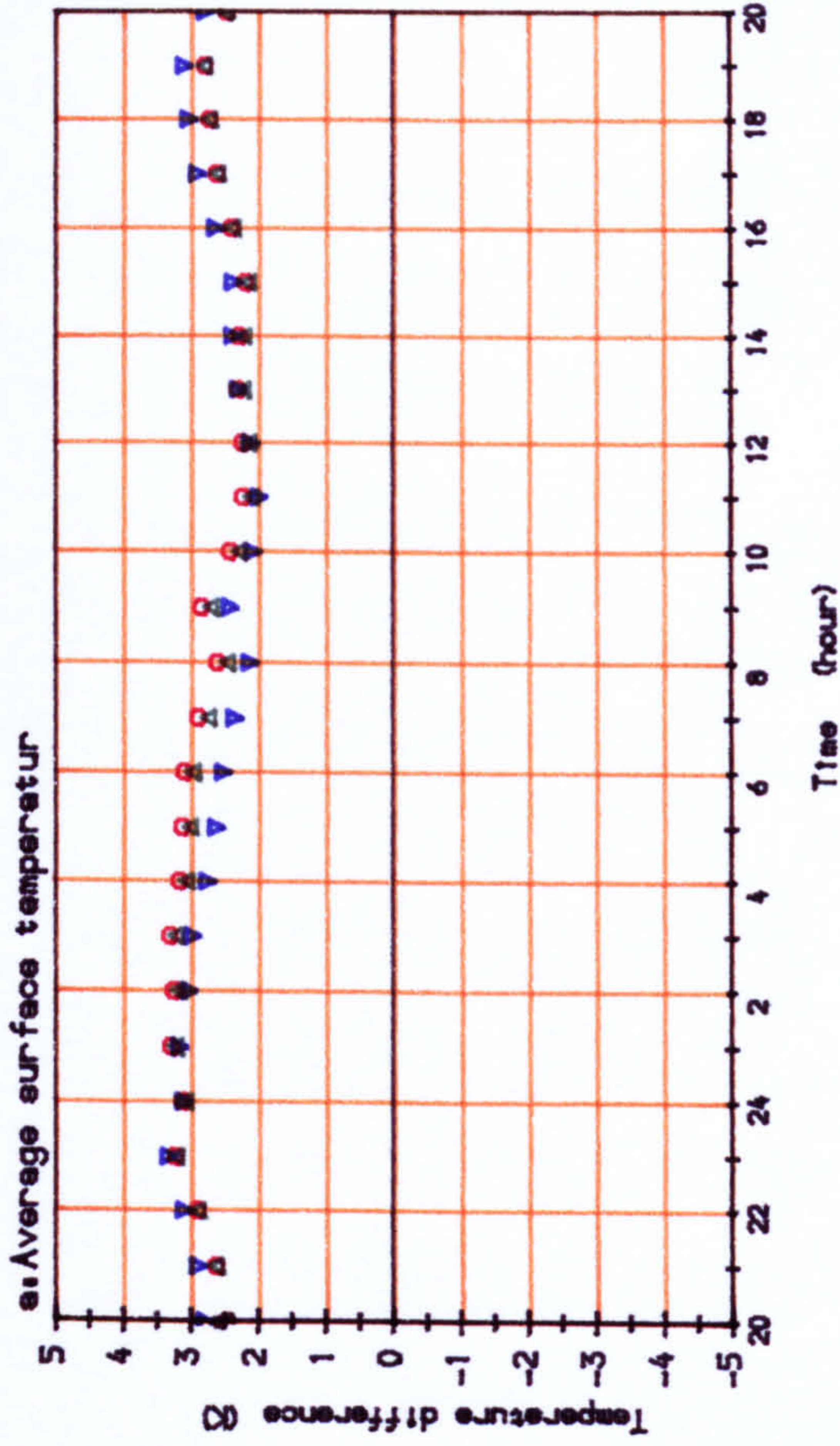
The difference between models "Finit 7.1" and "Finit 7.4" is in the way the air thermal capacity is treated. It is shown that the consideration of air thermal capacity has resulted in slightly higher internal air and surfaces temperatures. As the ventilation rate increases the difference becomes smaller for the time of ventilation. For higher rate of ventilation it is negligible.

Comparison between the seven nodes model and the nine nodes model in general shows that, in similar models (9.1 and 7.1 ,9.2 and 7.2 and 9.3 and 7.3) , the predicted temperatures for low rates of ventilation show better results in the nine nodes model, while for higher rate of ventilation, both nine and seven nodes models gave satisfactory results. For higher rates of ventilation, the nine nodes models give values closer to observations by about 1 K during the day.

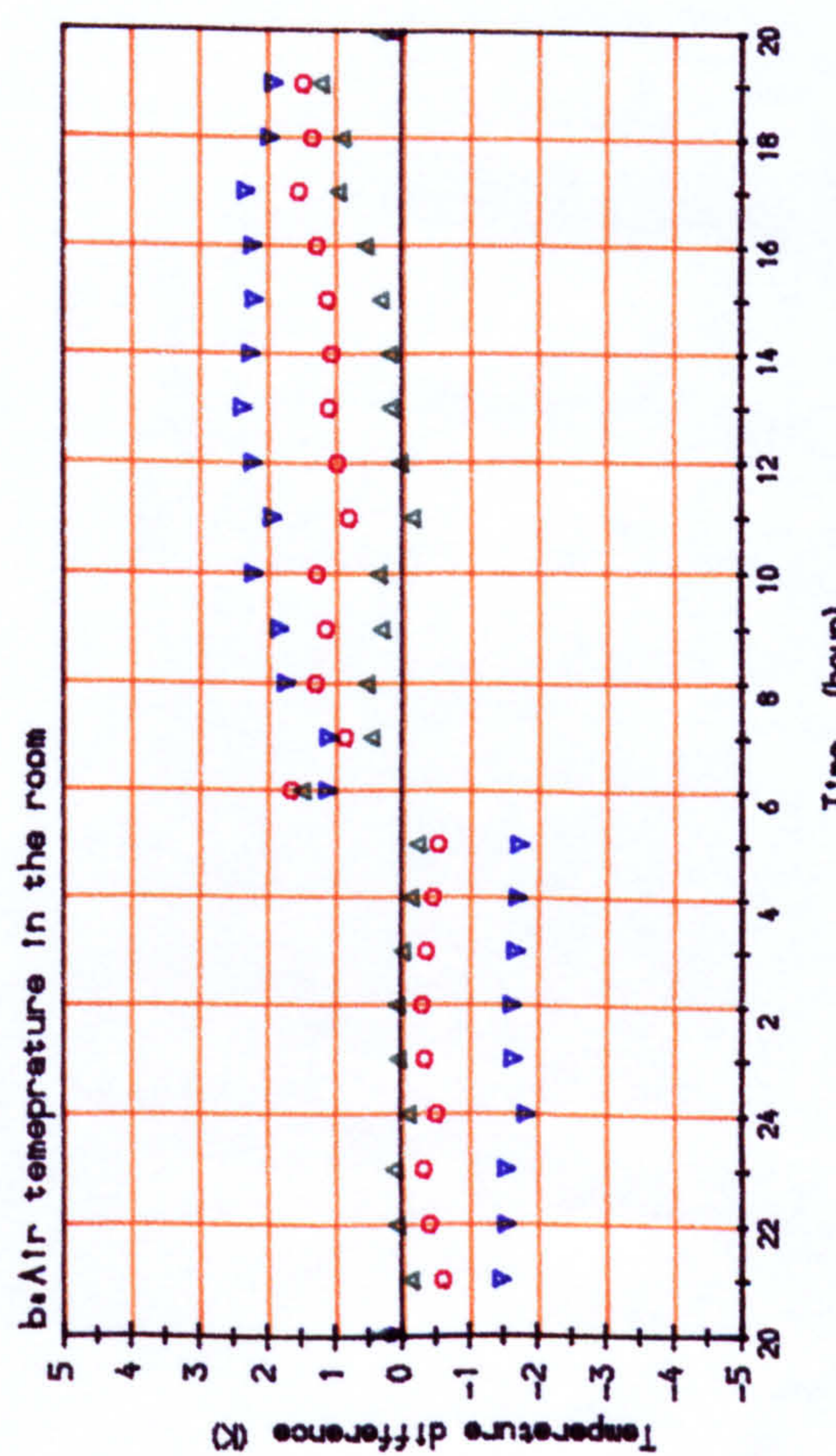
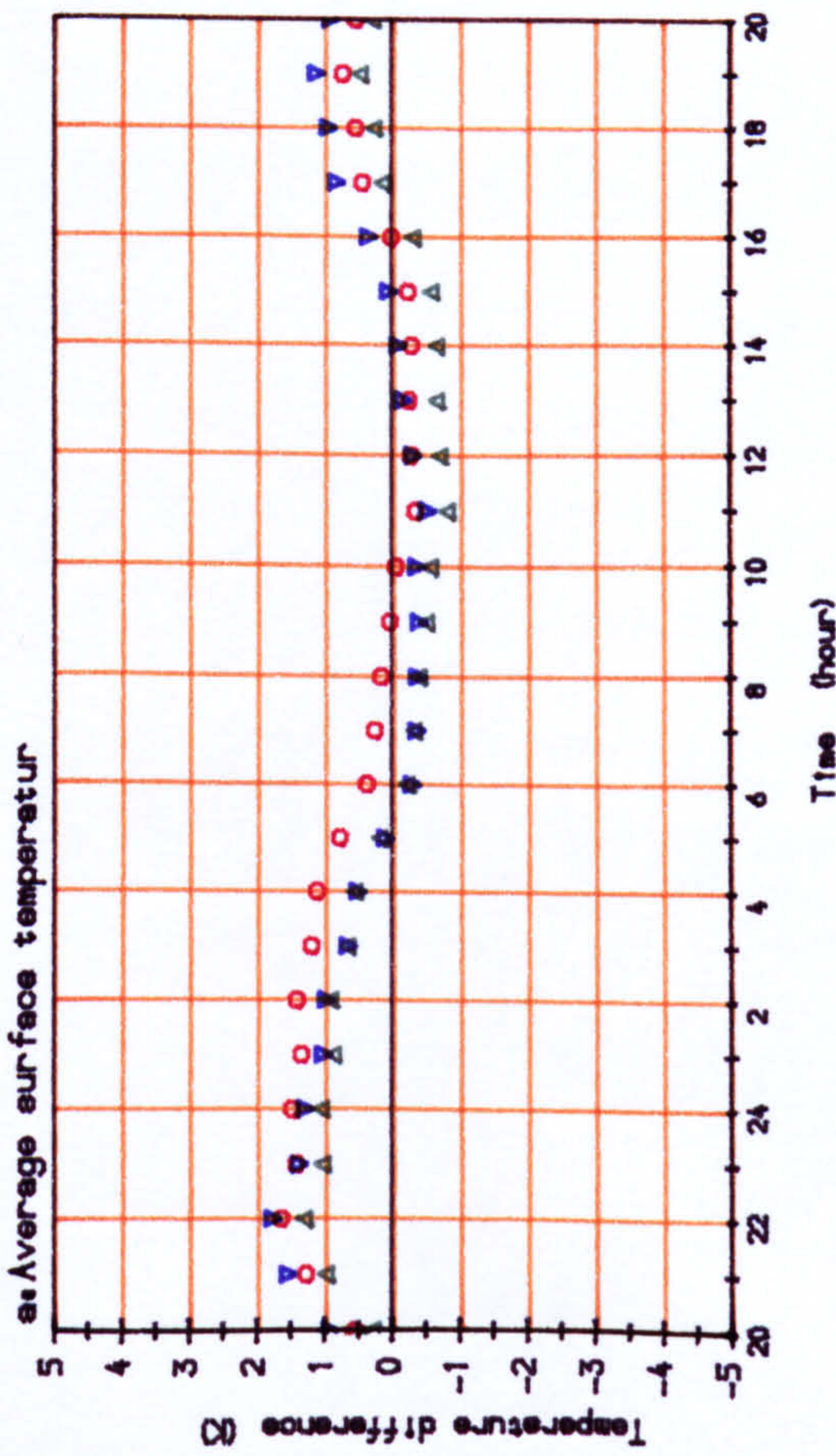
Figures 7.13 to 7.14 show the difference between the temperatures calculated by the three nodes model and observations.

As far as the treatment of the convection coefficient and air mixing are concerned, trends similar to the nine and seven nodes models are also found in the three nodes models. Figure 7.13a and 7.14a show the results of the three nodes models for 30 air changes per hour for ten hours and for four hours of ventilation. The difference between predicted temperatures and observed values are little greater than those from seven nodes model. Figures 7.13b and 7.14b show the same results but for 3 air changes per hour. The temperature difference is higher by about 1 degree. As the ventilation rate decreases, the disagreement between the calculated temperatures and experimental results increases. Temperatures

3 air changes per hour for ten hours (from 2000 to 0600)



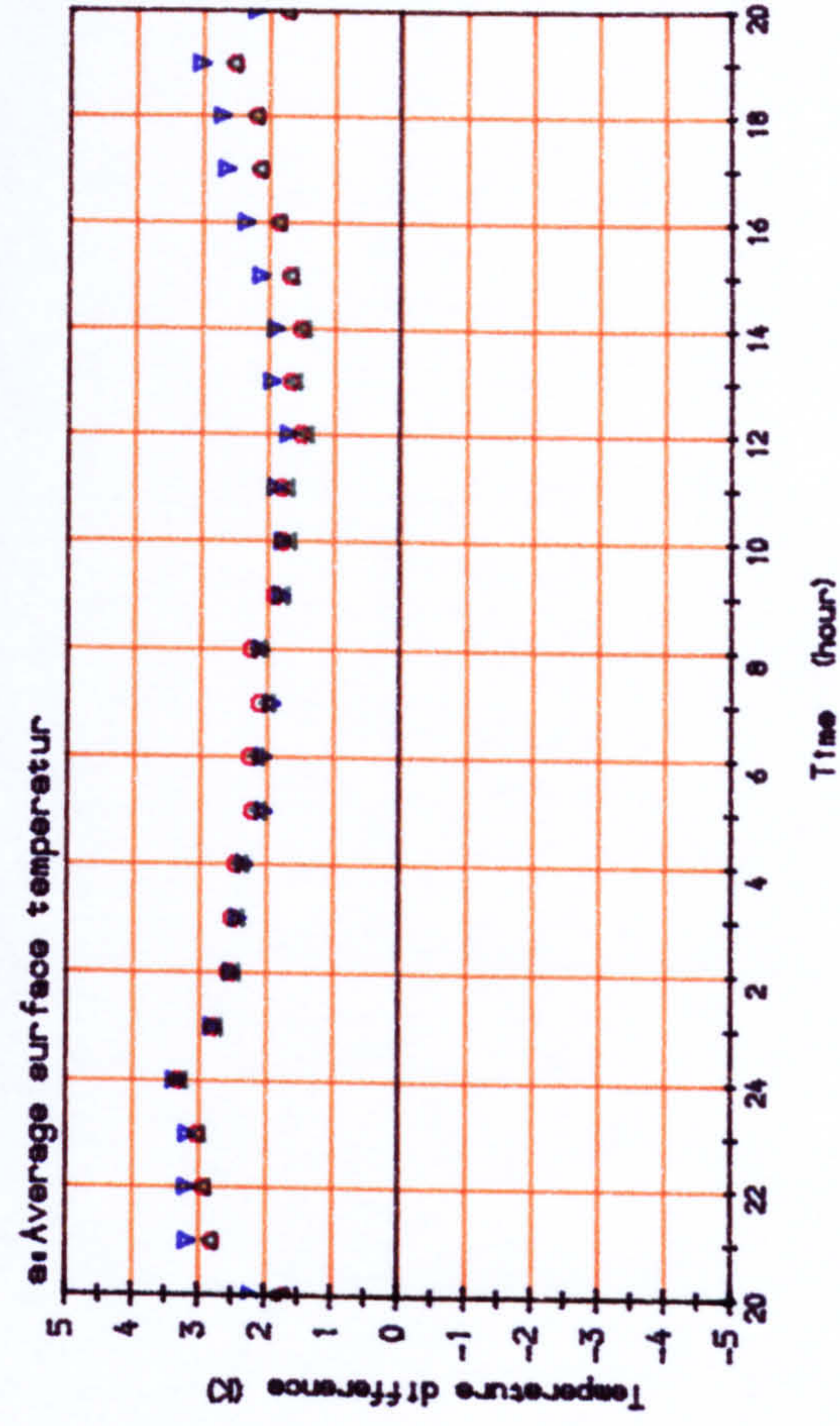
3 air changes per hour for ten hours (from 2000 to 0600)



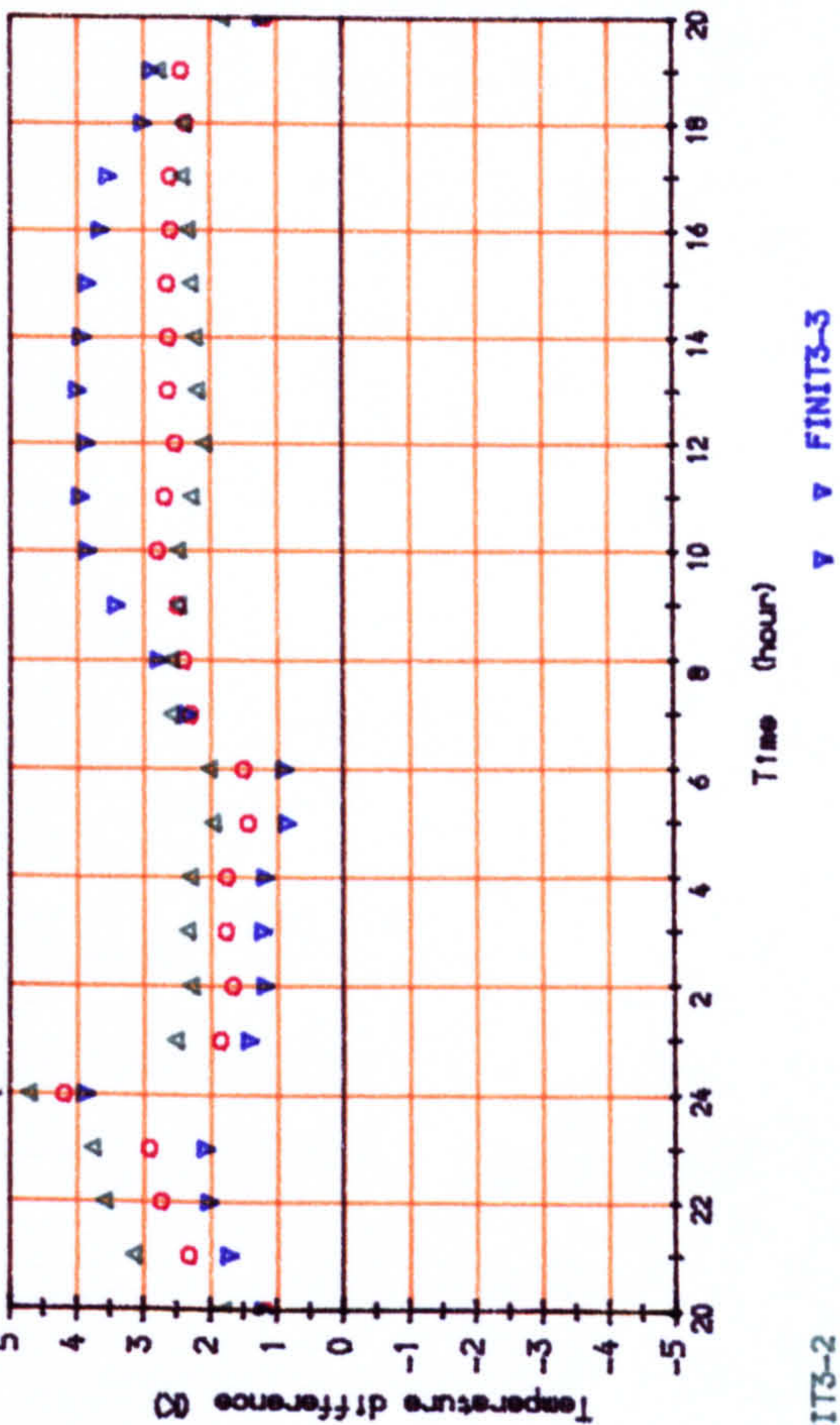
○ FINIT3-1    △ FINIT3-2    ▽ FINIT3-3

Figure 7.13. Temperature differences between observations and the Finite Difference models

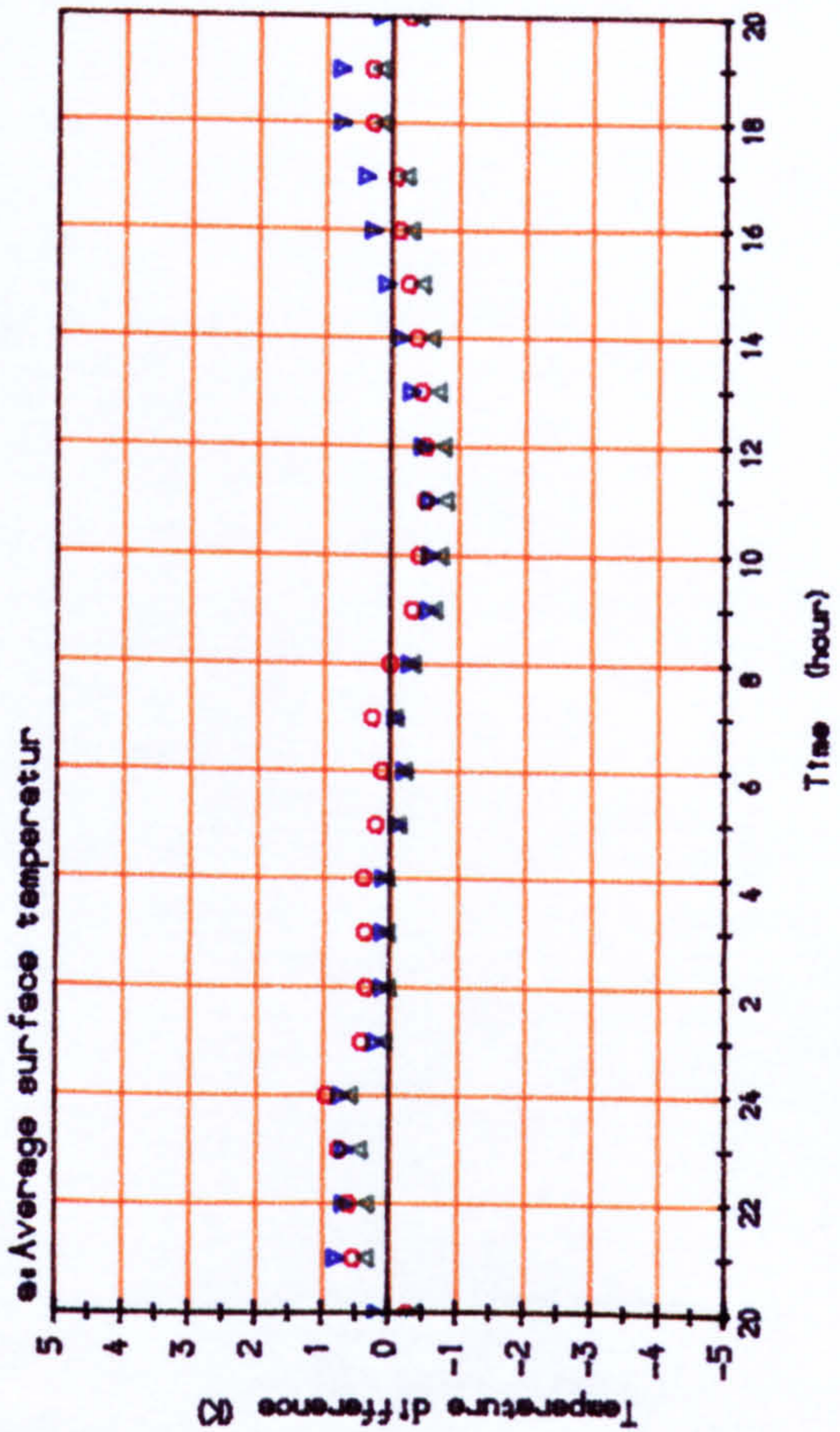
3 air changes per hour for four hours (from 2000 to 2400)



3 air changes per hour for four hours (from 2000 to 2400)



3 air changes per hour for four hours (from 2000 to 2400)



3 air changes per hour for four hours (from 2000 to 2400)

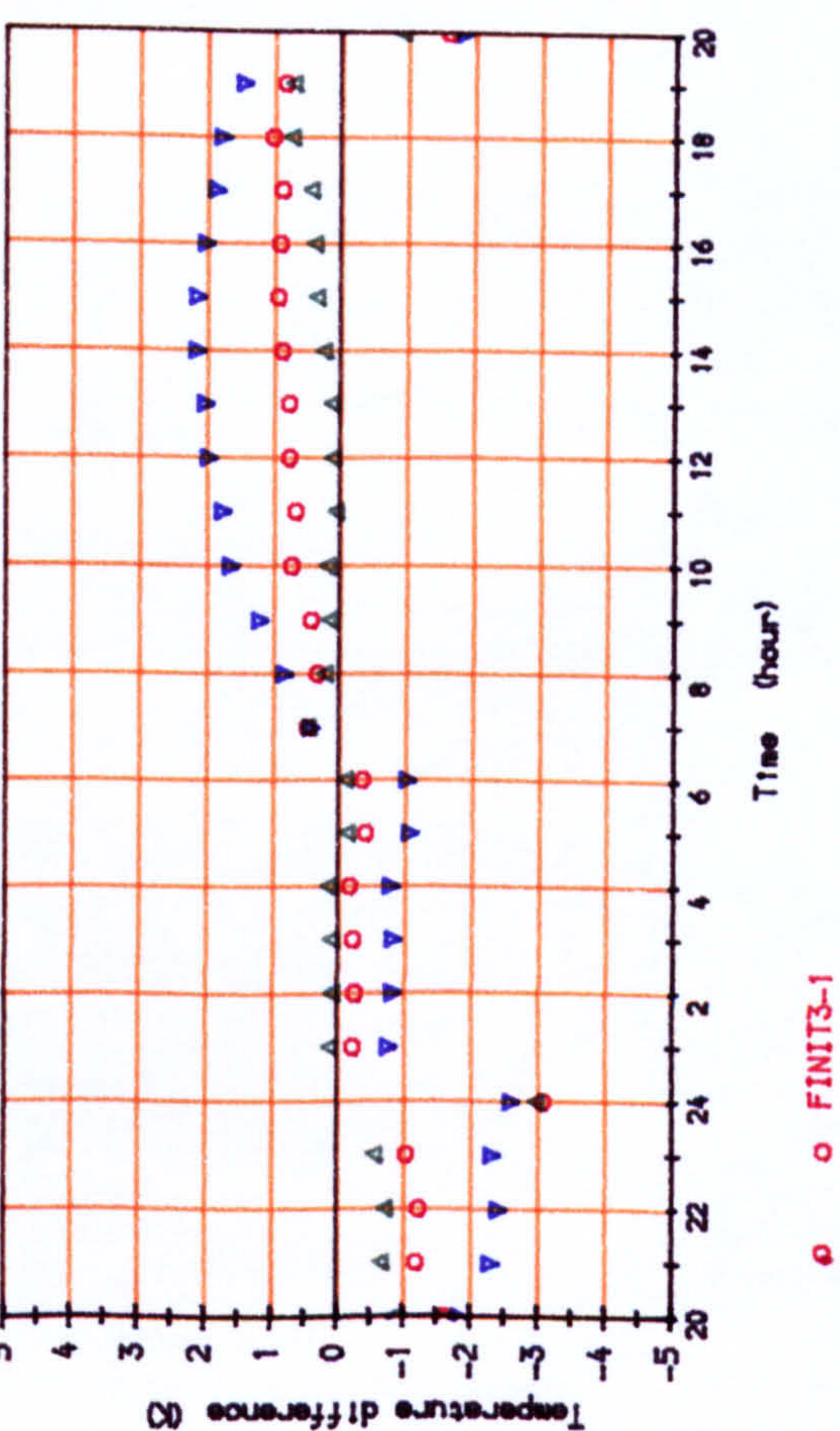


Figure 7.14: Temperature differences between observations and the Finite Difference models

○ FINIT3-1    
 △ FINIT3-2    
 ▽ FINIT3-3



calculated by different models and the full range of observed values for 15,10,7,4 ac/h and for ten and four hours of ventilation are presented in Appendix C.

### 7.3.2 Discussion and conclusion:

The use of different assumptions in the nine ,seven and the three nodes models makes no significant change to the prediction of average surface temperature , but the air temperature is more sensitive.

Comparison of the nine and seven nodes model, shows that the evaluation of the thermal response of buildings,( for example for the evaluation of comfort) , is not significantly improved by increasing the number of nodes from seven to nine.

Radiation loss through open windows during the night is negligible, and the cumbersome and laborious calculation is thus thought to be unnecessary. A fixed value of  $h_c$  has given satisfactory results. The correlation used in the present study cannot take into account the effect of the ventilation rate, although from the observations it is clear that the convection coefficient will change with the rate of ventilation. The values obtained from the correlation (table 7.5) underestimate the convection coefficient. The fixed  $h_c$  (e.g.  $3.0 \text{ W/m}^2\text{K}$  for vertical surfaces) is greater than the mean  $h_c$  obtained from the correlation .

When a high rate of ventilation is introduced to a room the new air is believed to mix fully with the room air, but for low rates of ventilation the new air does not properly mix with the room air. This is shown by the comparison between the two different assumptions and the results of the observations. The results of different rates of ventilation on the observation show that as the ventilation rate decreases the way the ventilation is treated becomes important.

In the three nodes model with higher rates of ventilation, the agreement was satisfactory and there is no great advantage in increasing the number of nodes from three to seven or nine. For lower rates of ventilation, the air temperature is more sensitive to the way the room is presented.

Generally with a high rate of ventilation, a simple model is capable of predicting the response of buildings and a complicated model will not provide better results as far as the architect and building engineer are concerned.

#### 7.4 Harmonic method

Figures 7.15 to 7.18 compares values obtained from the two harmonic methods with observed values. As the environmental temperature model was used it is not possible to present the individual surface temperatures directly from the calculations. As with the finite difference and response factor methods, the results of 30 and 3 ac/h for ten and four hours of ventilation are presented. The results of the observations between these two extremes are presented in Appendix C.

Two different approaches are used. The first used the model developed by BRE based for the Admittance Method (which is the standard method suggested by the CIBSE Guide). In the BRE model, the actual outside air temperature is used. All thermal factors are obtained from the first harmonic solution to the heat conduction equation, here referred to as BRE model. The second approach uses the actual temperature analyzed into the first six harmonics with relevant frequencies (24, 12, 6 hours) and employed the factors related to each harmonic. This is referred to as the HAR6 model. (for a detailed discussion see chapter 5).

Figure 7.15 shows the case of 30 air changes per hour for 10 hours. The general agreement between both models and observation for both average surface and air temperatures is good. During the day the BRE model overestimates the air temperature. In the BRE model, the outside air temperature is presented to the model as a mean and "swing" above below the mean (mean to extreme) and the time the maximum temperature occurs. (The same procedure is used in chapter 8 of the CIBSE Guide in the calculation of internal mean and swing temperatures). In hot climates the outside air and solair temperature is peaky stable during the night and rapidly increasing during the day. This approximation leads to some significant errors. In the case of night ventilation, as shown in fig 7.15, it results in a large error in air temperature compared with the first six harmonic approximation. As the ventilation rate decreases this error becomes less important.

As the ventilation rate decreases the disagreement between HAR6 and the BRE model in predicting the night air temperature also decreases, but the general disagreement of both models with observation increases.

With four hours of ventilation, the disagreement between the BRE model and HAR6 is significant. The prediction of the time of peak

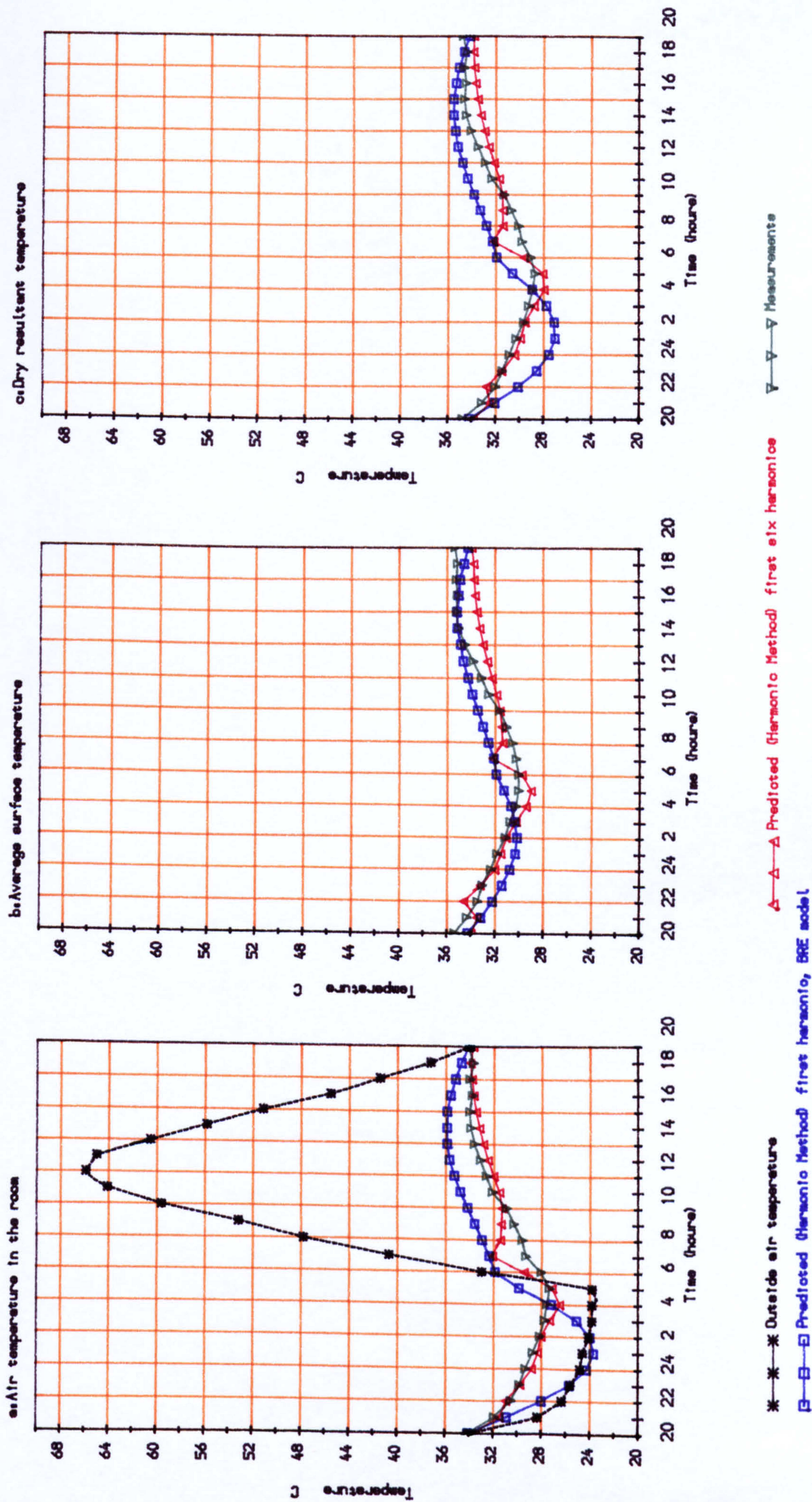


Figure 7.15: Comparison of measurements and predictions of the Harmonic Methods

30 air changes per hour for ten hours (from 2000 to 0600 hours)

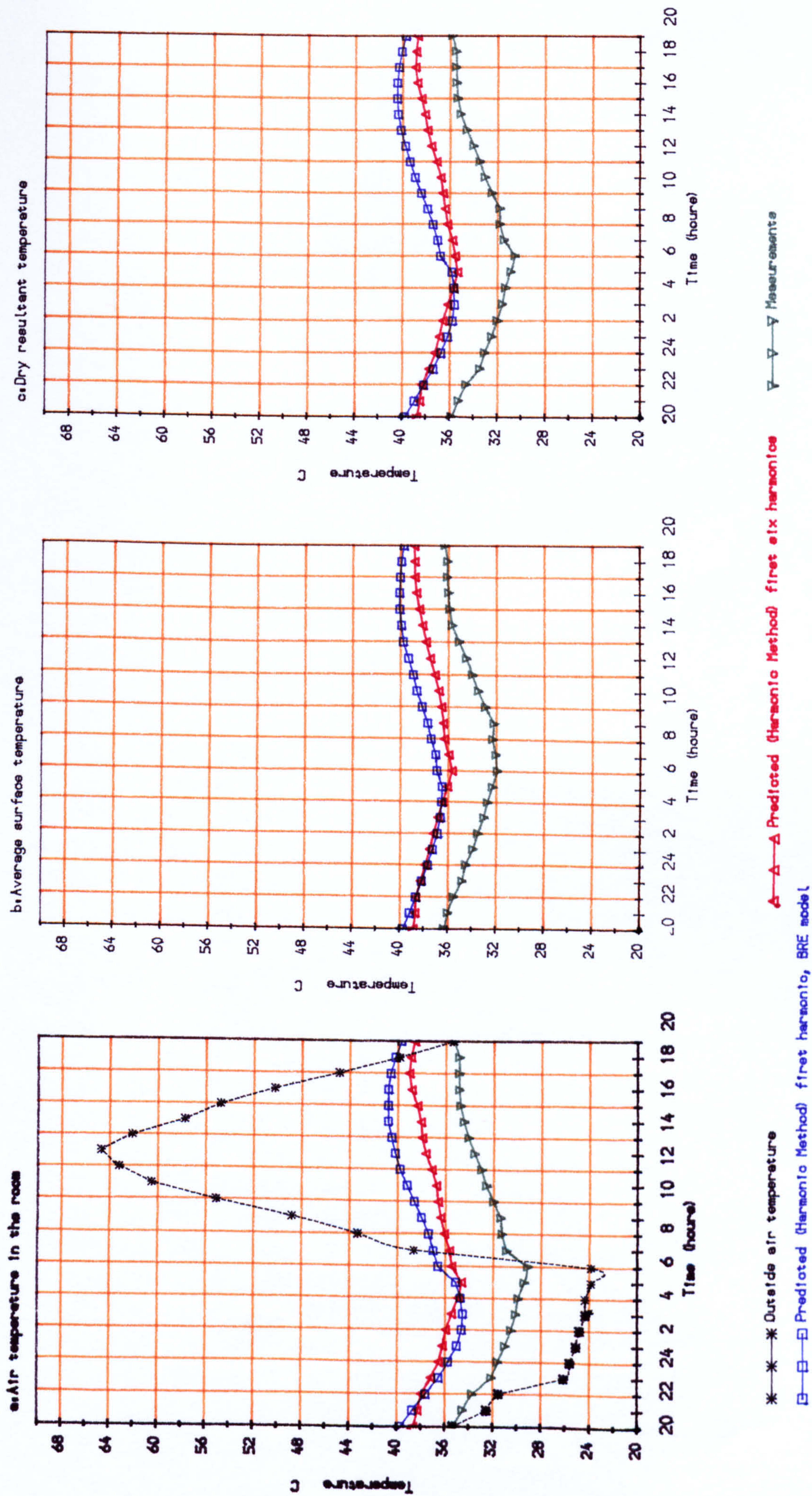


Figure 7.16. Comparison of measurements and predictions of the harmonic methods

3 air changes per hour for ten hours (from 2000 to 0600 hours)

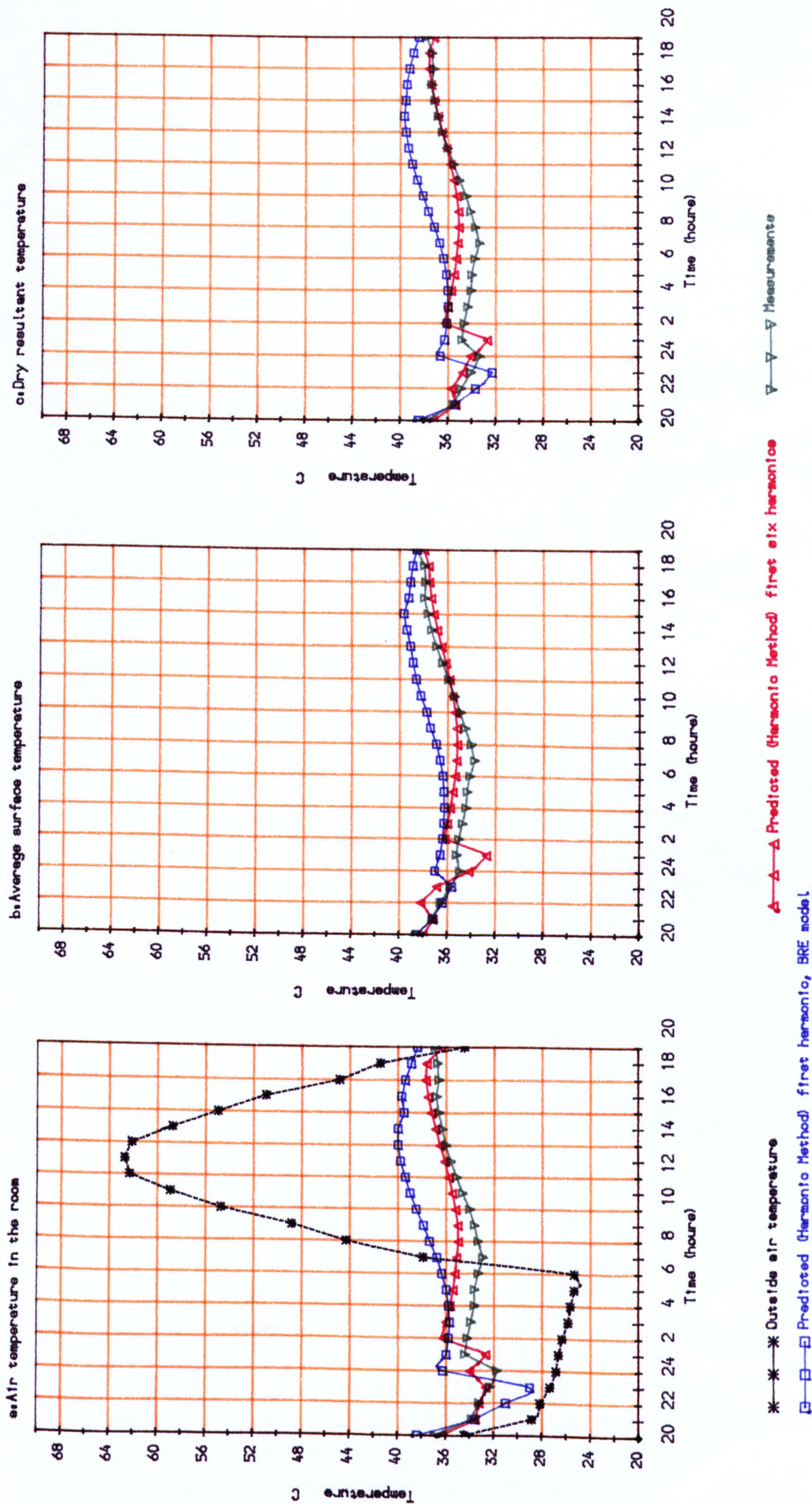


Figure 7.17. Comparison of measurements and predictions of the harmonic methods 30 air changes per hour for four hours (from 2000 to 2400 hours)

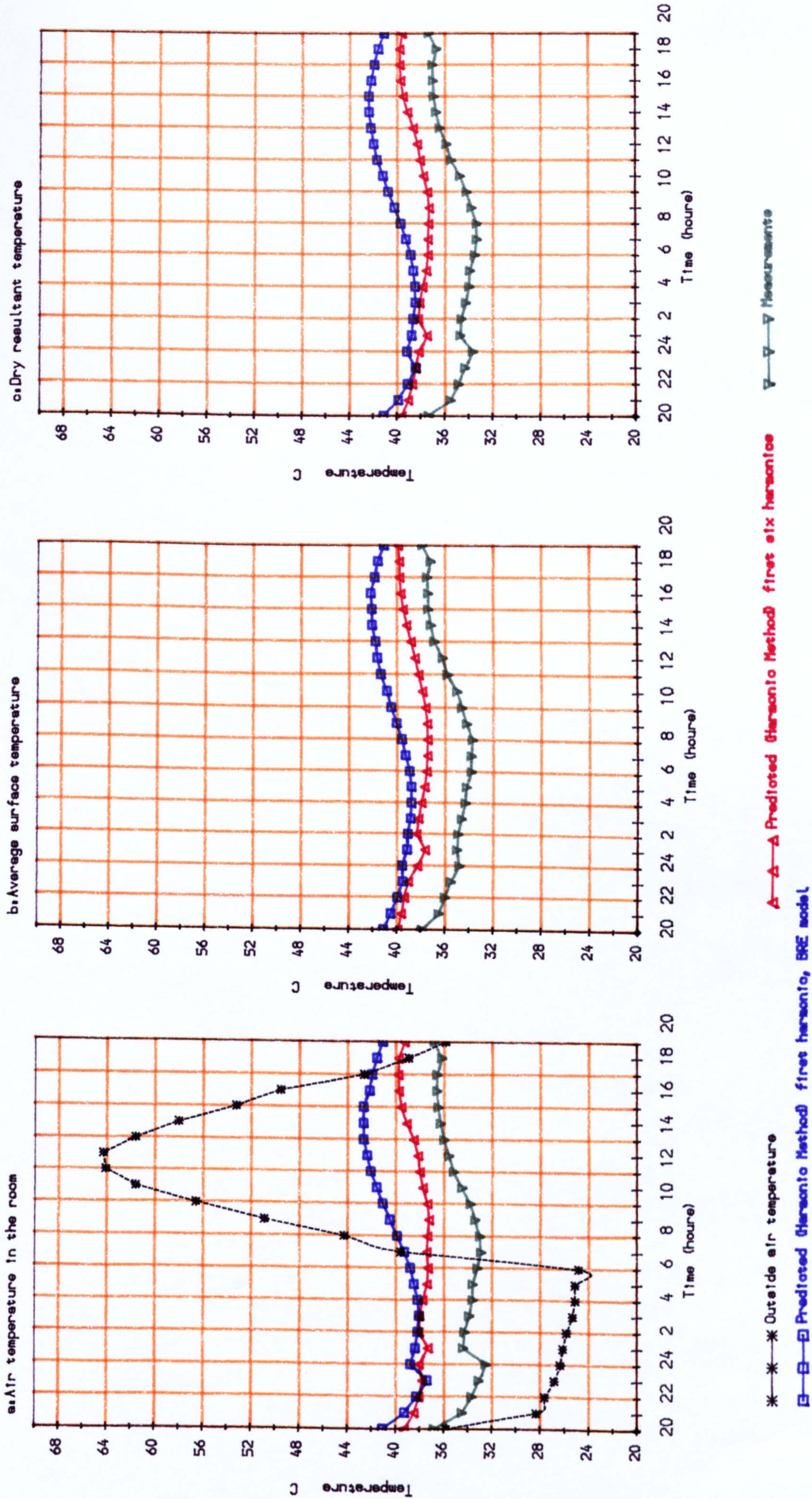


Figure 7.18. Comparison of measurements and predictions of the harmonic methods

3 air changes per hour for four hours (from 2000 to 2400 hours)

temperature in the BRE model is different from both HAR6 and observation, and as the ventilation rate decreases, this difference becomes larger. This is because of the crude treatment of time lag in the BRE model. The BRE model does not consider the time lag associated with the admittance. (BLOOMFIELD 1985) In the case of heavy structures with poor insulation, (similar to the apparatus used in the observations), as the ventilation rate increases the response of the building is more like that of light structures. The effect of time lag therefore becomes less important. As the ventilation rate decreases the building responds more like a heavy structures, and the treatment of the time lag becomes significant. This is thought to be one of the sources of disagreement between the two methods. The dual behaviour of buildings subjected to variable ventilation, that is to say the difference of characteristics of a building during period of ventilation as light structures, and heavy without ventilation, is the source of serious error caused by the crude way of the BRE model. The error will be significant for lower rates of ventilation and heavy structures.

For lower rates of ventilation both models over-estimate the internal temperatures of the air and the average temperature of the surfaces, although the general agreement shape of the results are more or less similar, and as the ventilation rate increases improvement is seen. This might be due to the fact that the environmental temperature model is used in the approach. The treatment of long wave radiation is crude. The temperature difference between the room surfaces could be as high as 12 K as suggested by figure 6.9 so that the long wave radiation exchange among different nodes in the model might play an important role in the overall result of temperatures in the room.

In the cases of high rate of ventilation, the main energy exchange will occur between the room air and surfaces and the inside and the outside air, and consequently long wave radiation becomes less significant.

## CHAPTER EIGHT

## CONCLUSIONS AND SUGGESTIONS FOR FURTHER WORK

Various extant thermal simulation methods for the prediction of hourly indoor air and surfaces temperatures in buildings in hot arid climates with natural nocturnal ventilation are experimentally verified. From the analysis of the data obtained, a deeper insight is gained of how buildings behave thermally under these circumstances.

The models developed in this study are based on:

the Harmonic Method used in the BRE and HARG model

the Response Factor Method

the Finite Difference Method

They differ in the treatment of:

-unsteady heat conduction

-radiative heat transfer

-convective heat transfer

-ventilation air

-long wave radiation heat transfer through open windows

Comparison of simulations and measurements show that:

-the Response Factor and Finite Difference Method, which are mainly computer techniques, showed similar results and are closest to the observations.

-in the case of a high rate of ventilation, a simple model of three nodes produced data that agreed reasonably with observations. As the ventilation rate decreased the disagreement between calculations and observations increased.

-in the case of a high rate of ventilation the BRE model underestimated the air temperature. This is thought to be caused by the way the outside air is presented. The BRE model simulates the outside air temperature as a pure sine wave, using the mean and the 'swing' value. This is the cause of error in the prediction of the air



temperature. It could be corrected by the use of hourly values of air temperature.

-the use of the first six harmonics in HARG model and the proper treatment of time lead and time lag associated with dynamic thermal factors improved the predictions. The improvement does not justify the complications, and the great advantage of the BRE model of being a manual method would be lost.

-the similarity of the results obtained from the three nodes model employing the Finite Difference technique and the BRE model suggests that the main shortcoming of the BRE method is in the way the internal heat exchange between the elements is tackled. Nevertheless in the case of a high rate of ventilation a simple model is capable of predicting the air and surface temperatures with sufficient accuracy.

-the seven-nodes models produced data that were in good agreement with the observations. The nine nodes models improved the accuracy. Considering the uncertainties associated with the input data the increase of accuracy was not enough to justify the complexity of the nine nodes model. The improvements were mainly in the prediction of air temperature, only one of the temperature relevant to comfort.

-by using existing correlations it was found that natural convection is the dominant regime of convection in all ranges of air flow used in this study. The correlation used to predict the convective heat transfer coefficient ( $h_c$ ) resulted in its being underestimated. Where the value of  $h_c$  was assumed to be fixed at a higher value, the agreement with the observations improved.

-in the case of high rate of ventilation during the night, the data obtained from models which assumed a perfect mixing of incoming air with the room air, showed better agreement with observations than models assuming a partial mixture of air. While with a low rate of ventilation the air temperature predicted by models assuming a partial mixture of air were closer to observations.

-the calculation of radiation through open windows was performed in the nine-nodes models. In the cases studied this did not result in significant improvement. Its precise evaluation requires direct field measurements.

A computer model was developed to analyze the error resulting from uncertainties in input data. The results are used to investigate

the sensitivity of internal air temperature and average surface temperature due to variations of each parameter. It is found that:

- the uncertainties in the rate of infiltration, outside air and outside surface resistance, were the most important sources of error in the prediction of temperature in all models.

- in Finite Difference Method, with high rates of ventilation the uncertainty in  $h_c$  was more significant than case of low rate of ventilation. Difference technique.

- with low rates of ventilation the internal air and average surface temperatures showed sensitivity to the variations of internal surface resistance.

- the uncertainties associated with the physical properties of the structure (i.e. thermal conductivity, thermal capacity and density) had the least significant effect on the predictions of internal temperatures.

Natural ventilation through open windows is also investigated. From the results theoretically obtained of natural cross flow in multi-zone buildings, a nonlinear relation is found which relates the ratio of external/internal opening area to the rate of flow. A procedure using this relationship is suggested, which could greatly simplify the calculations of cross air flow in multi-zone buildings.

The experimental observations show that the duration of ventilation is more effective in cooling the structure than its rate.

A better understanding of the thermal behaviour of a building with night ventilation is gained. This is achieved by the inter-model comparison and empirical validation. Computer models developed in this study and by BRE are experimentally validated and evaluated. The effect of shortwave radiation and very high rates of ventilation are not investigated due to difficulties of laboratory simulations. Their inclusion requires field measurements.

## SUGGESTIONS FOR FURTHER WORK

Solar radiation plays an important role in the overheating problems of buildings in hot climates during the summer period. The boundary conditions of the external surface of buildings in these regions are also complicated. They include the radiation loss to the sky during the night (which might be 20 K below the outside air temperature), and the absorbed solar radiation during the day. Their simulation is very difficult under laboratory conditions. Some field data are required to test the models. This should include radiation loss to the sky and absorbed solar radiation.

The effect of high rates of ventilation on the thermal response of the buildings also needs further investigation. When a building is subjected to a high rate of ventilation, say above 200 ac/h, it is expected that the convective heat transfer coefficient will change considerably, consequently the cooling effect of night ventilation will increase. This increase in the convective heat transfer coefficient and the cooling effect is expected to be nonlinear. Further investigation could reveal its effect and also evaluate the optimum rate of ventilation. This will affect the design of a building for the optimum rate of natural ventilation. The investigation might be performed with the same method of experimentation as used in this study.

The internal surfaces of a room might lose some energy through open windows to the outside. The rate of this source of passive cooling depends on the configuration between the surfaces and the outside and temperature difference between them. Because of the low water vapour pressure in the atmosphere and its clarity, the sky temperature in hot climates drops greatly during the night. With regard to the fact that the coefficient for heat transfer by long-wave radiation is larger than for convection, its rate of heat loss by this source might be significant. It depends on the geometry of the building surfaces and area of openings. More theoretical and empirical investigation are needed. This could be achieved by the development of a dynamic model similar to the nine-node model used in the present study and including real climatic data. The experiment could be done by comparing the thermal performance of similar buildings with and without open windows

during the night, either in an existing building or in specially built test rooms.

Equations 4.13 and 4.14 suggest correlations which will simplify the calculation of cross air-flow in multi-zone buildings. These are totally based on theoretical examination. An empirical verification of the above equations is required. This might be performed by a wind tunnel study of cross-ventilation in a multi-zone building with different configurations of internal partitions and different ratios of external openings.

The present knowledge of pressure coefficients for the calculation of wind induced pressures on buildings is limited. The same  $c_p$  values are used irrespective of whether the infiltration is through a normal crack or ventilation through a window sized openings. Further field and wind tunnel studies are required to examine the effect of large external open areas in buildings on the pressure coefficients. This might be done both on existing buildings and wind tunnel studies in the laboratory

To achieve a high rate of ventilation some design facilities such as waffle walls, domed roofs and large areas of windows might be employed. By comparing the performance of different architectural facilities their suitability might be examined.

Traditional passive cooling techniques such as wind towers (Baud Geers), large terraces in front of buildings (Eivans), domed roofs etc., have served to help provide comfort for many years. The present knowledge of their performance is mostly restricted to descriptive studies. More quantitative and qualitative investigations into their performance would help to exploit their use with new types of construction. The study may include direct field measurements as well as laboratory simulations to investigate the effect of design parameters in order to increase their efficiency.

The combined effect of natural night ventilation and evaporation would increase the rate of cooling. They may be studied by the same experimental technique as the present study, with appropriate adaptation to include the effect of evaporation.

## REFERENCES

- Alamdari F. & Hammond G.P. 1985 "Improved data correlation for buoyancy driven convection in rooms" *Building Services Engineering Research and Technology* vol. 4 no. 3 pp. 106-112
- Alamdari F. Hammond G.P. & Muhammad W.S. 1986 "Computation of air flow and convective heat transfer with space conditioned rectangular enclosure" *Proceedings of the 5th. International Symposium of the use of computer for Environmental engineering related to buildings* Chartered Institute of Building Services Engineers Garston Watford U.K.
- Al-Awa S. 1981 "Housing design in extreme hot and arid zones with special reference to thermal comfort" Department of Building Science Lth. University of Lund Lund Sweden
- ASHRAE 1985 "ASHRAE Handbook of Fundamentals" *American Society of Heating Refrigerating and Air Conditioning Engineers* Atlanta U.S.A.
- Bahodori M.N. 1978 "Passive cooling systems in Iranian architecture" *Scientific American* vol. 238 no. 2 pp 114-150
- Bahadori M.N. 1979 "Natural cooling in hot regions" in "Solar energy in buildings" edited by Sayigh A.A.M. Academic Press London
- Bauman F. Gadgil A. Kammerud R. Altmayer E. Nansteel M. 1983 "Convective heat transfer in buildings recent results" *ASHRAE Transactions* vol. 89 (1a) pp. 215-233
- Baxter A.J. 1975 "The use of index temperature" *Building Services Engineers* vol. 43 pp183-19
- Billington N.S. 1976 "Thermal insulation and thermal capacity of buildings" *Building Services Engineers* vol. 43 pp. 226-233
- Billington N.S. 1987 "The evolution of Environmental temperature" *Building and Environment* vol. 22 no. 4 pp. 241-249
- Bloomfield D. 1985 "Appraisal techniques for method of calculating the thermal performance of buildings" *Building Services Engineering Research & technology* vol. 6 no. 1 pp. 13-20
- Bloomfield D. 1983 "Thermal design of buildings: prediction of building temperature and heating/cooling loads using the admittance method" Building Research Establishment Garston Watfor U.K
- Bowman N.T. Lomas K.J. 1981 "Empirical Validation of dynamic thermal computer models for buildings" *Building Services Engineering Research & Technology* vol. 6 no. 4 pp. 153-162

- British Standar Institute 1980 "BS 5925 Code of Practice: Design of buildings for natural ventilation"
- British Standar Institute 1982 "BS 1042 Measurement of fluid flow in closed conduits Part1: Pressure difference devices section 1.1: Orifice plated, nozzles and venturi tubes inserted in circular cross-sectional conduits running flow"
- Buchberg H. and Naruishi J. 1967 "A rational evaluation of thermal protection alternative for shelter" *Building Science* vol. 2 pp. 37-57
- Buchberg H. 1967 "Sensitivity of the thermal response of buildings to perturbation in the climate" *Building Science* vol. 4 pp 43-61
- Buchberg H. 1971 "Sensitivity of room Thermal response to inside radiation exchange and surface conductance" *Building Science* vol. 6 pp. 133-149
- B.R.E. 1986 "BRE Digest 210: Principles of natural ventilation" Building Research Establishment Garston Watford U.K.
- Chandra S. & Bowman A. Cermak J.E. 1981 "Passive cooling by natural ventilation a review and research plan" Contract report no: FSEC-CR-81-27 prepared for DOE Washington USA
- Chandra S. and Kerestecioglu 1984 "heat transfer in naturally ventilated rooms: data from full scale measurements" *ASHRAE Transactions* vol. 90 (B) pp. 211-223
- Chandra S. and Fairey P.W. 1986 "Wind tunnel and full scale data on air flow from natural ventilation and ceiling fans" *ASHRAE Transactions* pp. 804-816
- Chatfield K. 1975 "*The analysis of time series theory & practice*" Chapman and Hall London
- CIBSE 1980 "The calculation of energy demands and targets for the design of buildings" Chartered Institute of BUilding Services Engineers Watford U.K.
- CIBSE 1986 "*CIBSE Guide Book A*" Chartered Institute of Building Services Engineers Watford U.K.
- Clarke J. 1985 " The effect of space and time steps in finite difference computation of building energy flow" ABACUS Occasional paper Glasgow University of Strathclyde
- Clarke J. 1985 "*Energy simulation in building design*" Adam Hilger Ltd. Boston
- Cockroft J.P. Robertson P. 1976 "Ventilation of a building through a single opening" *Building and Environment* vol. 11 pp. 29-35
- Cornell A.A. 1976 "Environmental temperature and comfort" *B.S.E.* vol. 32 pp. 219-225
- Crabb J.A. Murdoc H.M. and Renman J.M. 1987 "A simplified

- thermal response model" *Building Services Engineers Research & Technology*
- Crommelin R.D. and Urins E.M. 1988 "Ventilation through a single opening in a scale model *Air Infiltration Review* vol. 9 no. 3 pp. 11-15
- Danter E. 1960 "Periodic heat flow characteristic of simple walls and roofs". *Journal of Institution of Heating Ventilating Engineers* vol. 28 pp 136-147
- Danter E. 1974 "Heat exchange in a room and definition of room temperature " *Building Services Engineers* vol. 41 pp. 232-246
- Danter E. 1983 "Room response according to CIBSE Guide procedure" *Building Services Engineering Research and Technology* vol. 4 no. 2 pp 46-51
- Davies M.G. 1974 "Presentation of environmental temperature in a room" *Building Services Engineering* vol. 41 pp.246-249
- Davies M.G. 1978 "On the basis of environmental temperature" *Building Science* vol. 13 PP 29-46
- Davies M.G. 1984 "An approximate expression for room view factor" *Building and Environment* vol. 19 no. 4 pp.217-220
- Davies M.G. 1986 "A critique of environmental temperature" *Building Science* vol. 21 pp 155-170
- Davies M.G. 1987(a) "Room internal heat exchange : new design method" *Building Services Engineering Research & Technology* vol. 8 pp. 47-60
- Davies M.G. 1987(b) "The reduction of room radiant and convective exchange to star based system" *Numerical methods in thermal problems Proceedings of the 5th. International Conference Montreal Canada*
- Dow M.R. 1984 "Calculation of peak temperature in multizone buildings using Admittance method" *Building Services Engineering Research and Technology* vol. 6 no. 2 pp. 63-66
- Fanger p.o. 1970 "Thermal comfort , an analysis and application in environmental engineering" Mc. Graw Hill London
- Givoni B. 1981 "Cooling buildings by passive systems" *Proceedings of the International Conference on passive cooling* Miami Beach Florida pp 588-596
- Givoni B. 1981 "Man climate and architecture " Applied Science Publications London
- Golneshan A.A. and Yaghoubi M.A. 1984 "Natural cooling of a residential room with ventilation in hot arid regions"
- Gupta C.L. Muncey R.W.R. Spencer J.W 1976 "A conceptual survey of computer oriented of thermal calculation methods"

- Gupta C.L. 1964 "A matrix method for predicting thermal response of unconditioned buildings" *Journal of Institution of heating & ventilating Engineers* vol. pp. 159-165
- Gupta C.L. 1970 "Heat transfer in buildings: A review" *Architectural science review* vol. 1 pp. 1-8
- Haghighat F. and Bahadori M.N. 1985 "Passive cooling in hot arid regions in developing countries by employing domed roofs and reducing the temperature of internal surfaces" *Building and Environment* vol.:20 no:2 pp 103-113
- Hanna G.B. 1974 "Development of models to estimate the temperature response of an enclosure" Ph.D. Theses University of Liverpool
- Hanna G.B. 1977 "computer analysis to estimate the temperature response of an enclosure by finite difference" *Building Services Engineers* vol. 45 PP 59-68
- Harrington-Lynn J. 1974(a) "Admittance procedure, variable ventilation" *Building Services Engineers* vol. 42 pp 190-200
- Harrington-Lynn J. 1974(b) "Admittance procedure, intermittent plant operation" *Building Services Engineers* vol. 42 pp. 219-221.
- Harris-Bass J. 1980 "Computing indoor temperature in hot climate" *The International Journal of Ambient Energy* vol. 2 pp. 47-53
- Harris-Bass J. 1981 "Cooler homes for hot climates" *Middle East Construction* vol. 6 part 6 pp. 86-88
- Hassan K.E. & Hanna G.B 1972 "Effect of walls on indoor temperature" *Build International* vol. 5 pp. 220-228
- Herlin M. 1988 "A multizone Infiltration and ventilation simulation program" *Air Infiltration Review* vol. 9 no. 3 pp. 3-6
- Humphreys M.A. 1974 "Environmental temperature and thermal comfort" *Building Services Engineers* vol. 42 pp. 77-81
- Incropera F.P. & Dewit D.P. 1985 "Introduction to heat transfer" John Willey & Sons New York
- Iranian Meteorological Office 1981 "Meteorological Year Book" Iranian Ministry of Road Tehran Iran
- Irving A.D. 1988 "Validation of dynamic thermal models" *Energy and Building* vol. 10 pp. 213-220
- Kaas-Petersen C. 1987 "PATH - User's Guide" Department of Applied Mathematical & Centre for Nonlinear Studies, University of Leeds, 59 pages.
- Kaas-Petersen C. 1988 "Technique to trace curves of bifurcation points of periodic solutions of dissipative systems, Revised manuscript submitted to SIAM Journal of Scientific and Statistical Computing, 42 pages.



- Kusuda T. 1976 "Computer programs for heating and cooling loads in buildings" Building Environment Division National Bureau of standard Washington D.C. USA
- Lee J.R.G. 1979 "Development and optimization of Tromb's wall" Ph.D. University of Leeds
- Loudon A.G. 1970 "Summertime temperature in building without air conditioning" *Journal of Institution of heating & ventilating Engineers* vol. 37 pp.280-292
- Loudon A.G. 1968 "U Values in the 1970 Guide" *Journal of Institution of Heating & Ventilating Engineers* vol. 38 pp 167-174
- Liddament M.W. 1987a "A review and bibliography of ventilation effectiveness" AIVC Technical note 21 Air Infiltration and Ventilation Centre Bracknell U.K.
- Liddament M.W. 1987b "Power law O.K." *Air Infiltration Review* vol. 8 no. 2 pp. 4-6
- Liddament M.W. 1987 "Air infiltration calculation techniques- An Application Guide " Air ifiltration and Ventilation Centre Bracknell U.K.
- Mathews E.H. 1986 "Thermal analysis of naturally ventilated buildings" *Building and Environment* vol. 21 no. 1 pp. 35-39
- Milbank J. & Harrington -Lynn J. 1970 "Estimation of air conditioning Load" Building Research Station Current Paper CP 13/70 Garston Watfors U.K.
- Milbank J. & Harrington -Lynn J. 1974 "Thermal response and Admittance procedure *Building Services Engineers* vol. 42 pp.38-51
- Mitalas G.P. 1965 "An assessment of common assumption in estimating cooling loads and space temperature" *ASHRAE Trans.* vol.71 pp 72-80
- Muncey R.W.R. 1953 "The calculation of temperature inside buildings having variable external conditions" *Australian Journal of Applied Science* vol. 4 PP. 189-199
- Muncey R.W.R. 1979 "Heat transfer calculations in buildings" Applied Science Publishers London
- Mc Adams W.H. 1958 "Heat transmission" 3rd edition McGraw Hill Tokyo
- Narasaki M. and Yamanaka T. "Influence of turbulent wind on ventilation" "Proceedings of the 4th International conference on Indoor Air Quality" Institute of water soil and air hygiene" West Berlin Germany
- Nicol J.F. 1975 " An analysis of some observations of thermal comfort in Roorkee India and Baghdad Iraq" Building Research Establishment Garston Watford U.K.

- O'Callaghan 1980 "building for energy conservation " Pergamon Press Oxford
- Phaff J.C. Gids W.E. Ton J.A. Ree D. Schijndil L.L.M. 1980 "The ventilation of buildings: Investigations of consequence of opening one window on the internal climate of a room" Institute of Environment Hygiene and Health Technology
- Peavy B.A. Powell F.J. Burch D.M. 1974 " Dynamic Thermal performance of an experimental masonry building" Building Environment Division National Bureau of Standard Washington USA
- Pipes 1957 "Matrix analysis of heat transfer Problem" *Journal of Franklin Institute* vol. 263 pp 195-205
- Sodha M.S. Bansal N.K. & Kumar A. 1986(a) "Solar passive buildings" Pergamon Books Ltd. London
- Sodha M.S. Bansal N.K. & Kumar A. 1986(b) "A comparison of the admittance and the Fourier method for predicting heating or cooling loads" *Solar Energy* vol. 36 no. 2 pp. 125-127
- Stephenson D.G. Mitalas G.P. 1967(a) "Cooling load calculation by response factor method" *ASHRAE Transactions* vol. 73 III pp. 1.1-1.7
- Stephenson D.G. & Mitalas G.P. 1967(b) "Room thermal response factor" *ASHRAE Transactions* vol. 73 (II) pp. 2.1-2.10
- Swami M.W. Chandra S. 1987 "Procedure for calculating natural ventilation air flow in buildings" *ASHRAE Final Report FSEC-CR-163-86 USA*
- Tavassoli M. 1976 "The architecture of hot arid climate" Peyvand Publications Ltd. Tehran 'in Persian'
- Taylor J.R. 1982 "An introduction to error analysis: the study of uncertainties in physics" Oxford University Press USA
- Tinker J.A. Stuckes A.D. Simpson A. 1986 "The effect of moisture on the thermal conductivity of lightweight aggregate concrete" *Building Services Engineering Research & Technology* vol. 7 no. 1 pp. 27-32
- Ullah M.B. & Long Worth 1977 "A single equivalent decrement factor and a single equivalent lag for the effect of multiple harmonics in a solair temperature cycle" *Building Services Engineers* vol. 45 pp. 139-146
- Warren 1986 "The analysis of single sided ventilation and measurements" *Air Infiltration Review* vol. 7 no. 2 pp. 3-6
- Waters J.R. 1977 "The derivation and experimental verifications of a computer aided thermal design method" Ph.D. Lanchester Polytechnic

Waters J.R. 1981 "Using admittance method to calculate energy consumptions during intermittent plant operation"  
*Building Services Engineering Research & Technology* vol. 2  
no. 4 pp. 181-187

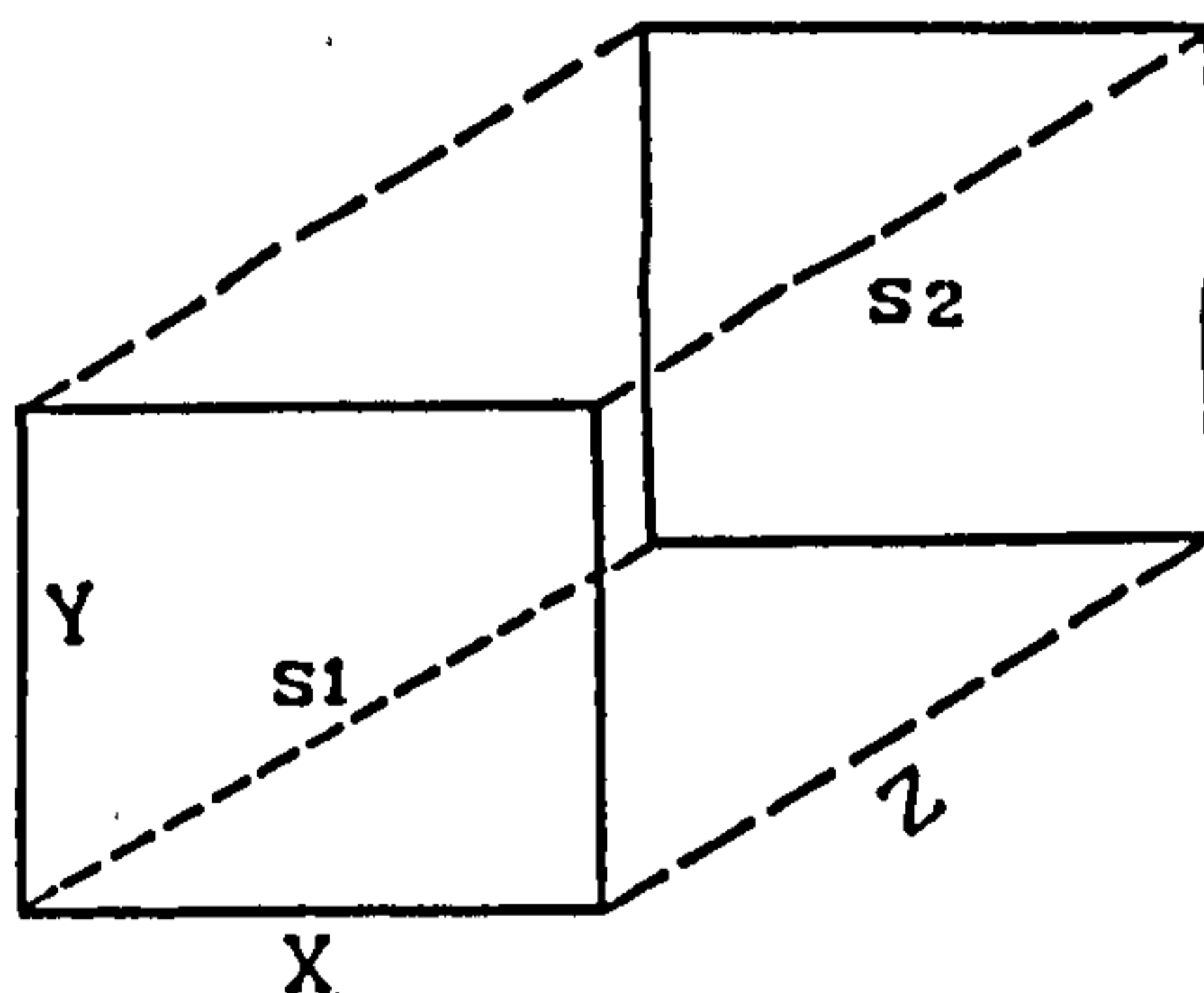
Wong H.Y. 1977 "heat transfer for engineers " Longman Group Ltd.  
London

## APPENDIX A

## CALCULATION OF VIEW FACTOR IN A ROOM

The following is a general approach to calculate the view factor between surfaces of the room, most suitable for computer calculations.

For two parallel walls (DEWITT & INCROPERA 1985)



$$\begin{aligned}
 F_{II}(X, Y, Z) = \frac{2}{xy\pi} & \left\{ \text{Log} \sqrt{\frac{(1+x^2)(1+y^2)}{(1+x^2+y^2)}} + (\sqrt{1+y^2}) \arctan\left(\frac{x}{\sqrt{1+y^2}}\right) \right. \\
 & \left. + \sqrt{1+x^2} \arctan\left(\frac{y}{\sqrt{1+x^2}}\right) - x \arctan(x) - y \arctan(y) \right\} \quad (A-1)
 \end{aligned}$$

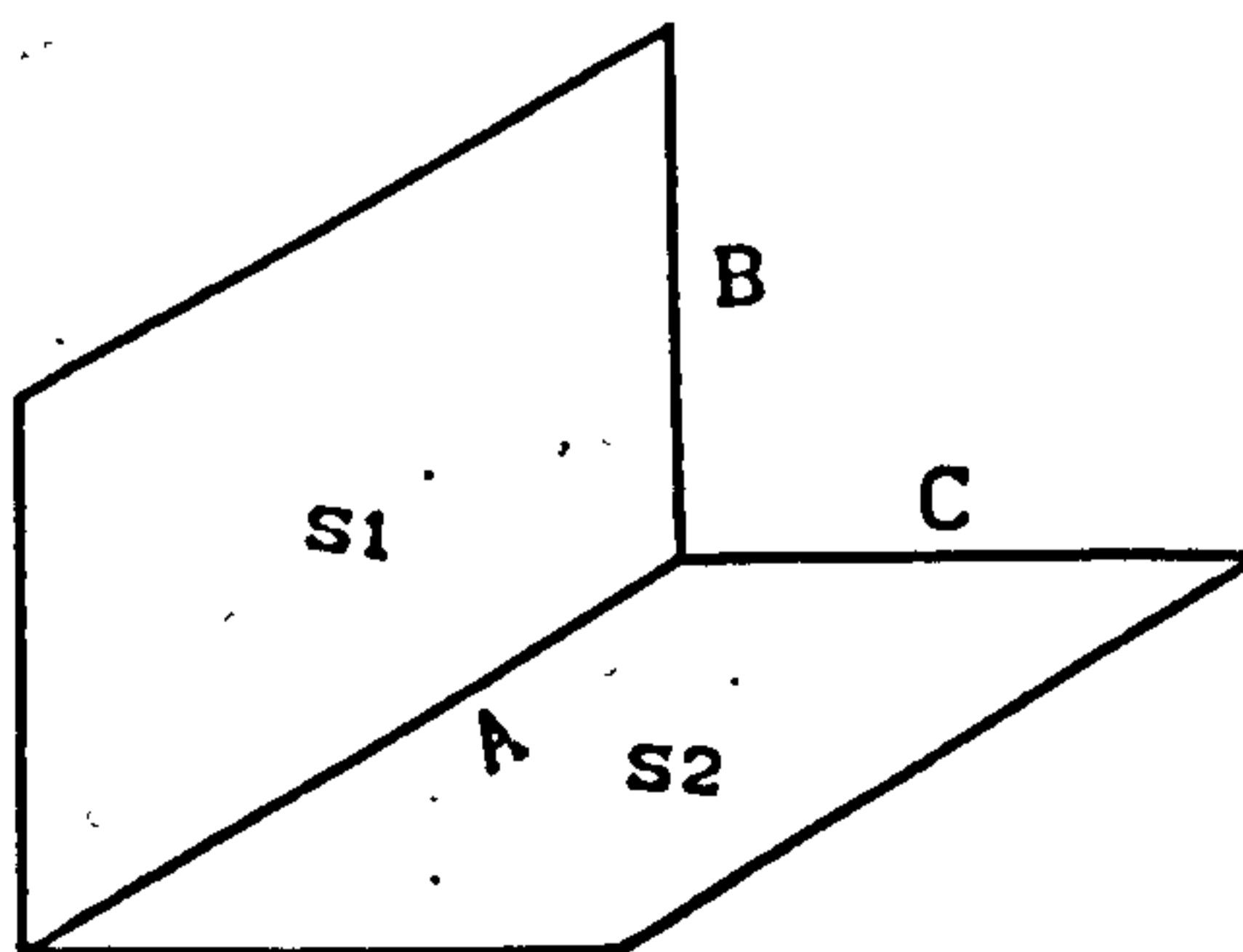
where

$F_{II}(X, Y, Z)$  is the view factor between surface 1 and 2 in

$$x = X/Z$$

$$y = Y/Z$$

For two perpendicular walls (DEWITT & INCROPERA 1985)



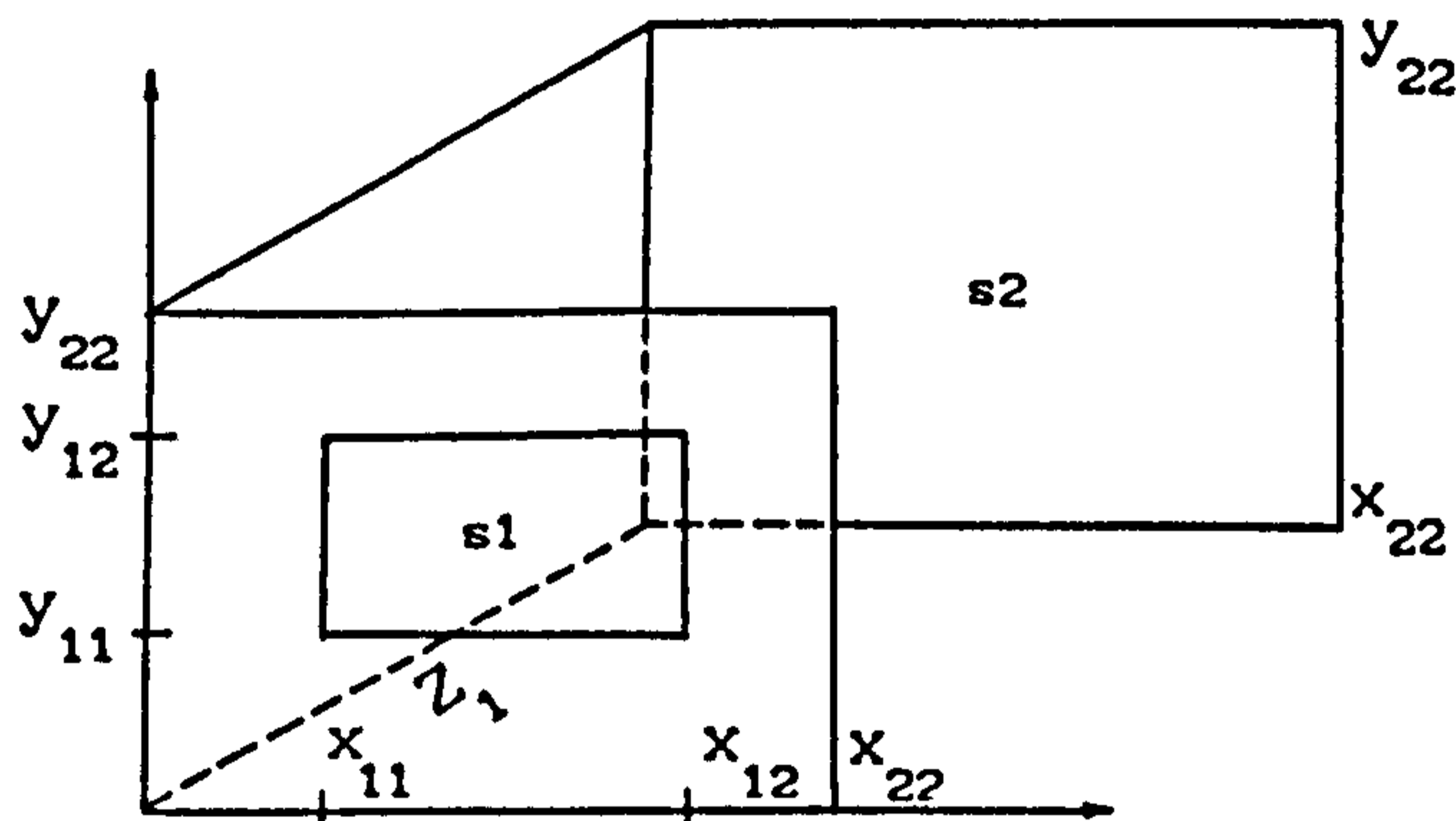
$$\begin{aligned}
 FL(A, B, C) = & \frac{1}{\pi H} \left[ \left\{ H \arctan\left(\frac{1}{H}\right) + W \arctan\left(\frac{1}{W}\right) - \sqrt{W^2 + H^2} \arctan\left(\frac{1}{\sqrt{W^2 + H^2}}\right) \right\} \right. \\
 & \left. + 0.25 \operatorname{Log} \left[ \frac{(1+H^2)+(1+W^2)}{1+W^2+H^2} \times \left[ \frac{H^2(1+H^2+W^2)}{(1+H^2)(1+W^2)} \right]^{H^2} \times \left[ \frac{W^2(1+H^2+W^2)}{(1+H^2)(1+W^2)} \right]^{W^2} \right] \right]
 \end{aligned}
 \tag{A-2}$$

where

$$H = B/A$$

$$W = C/A$$

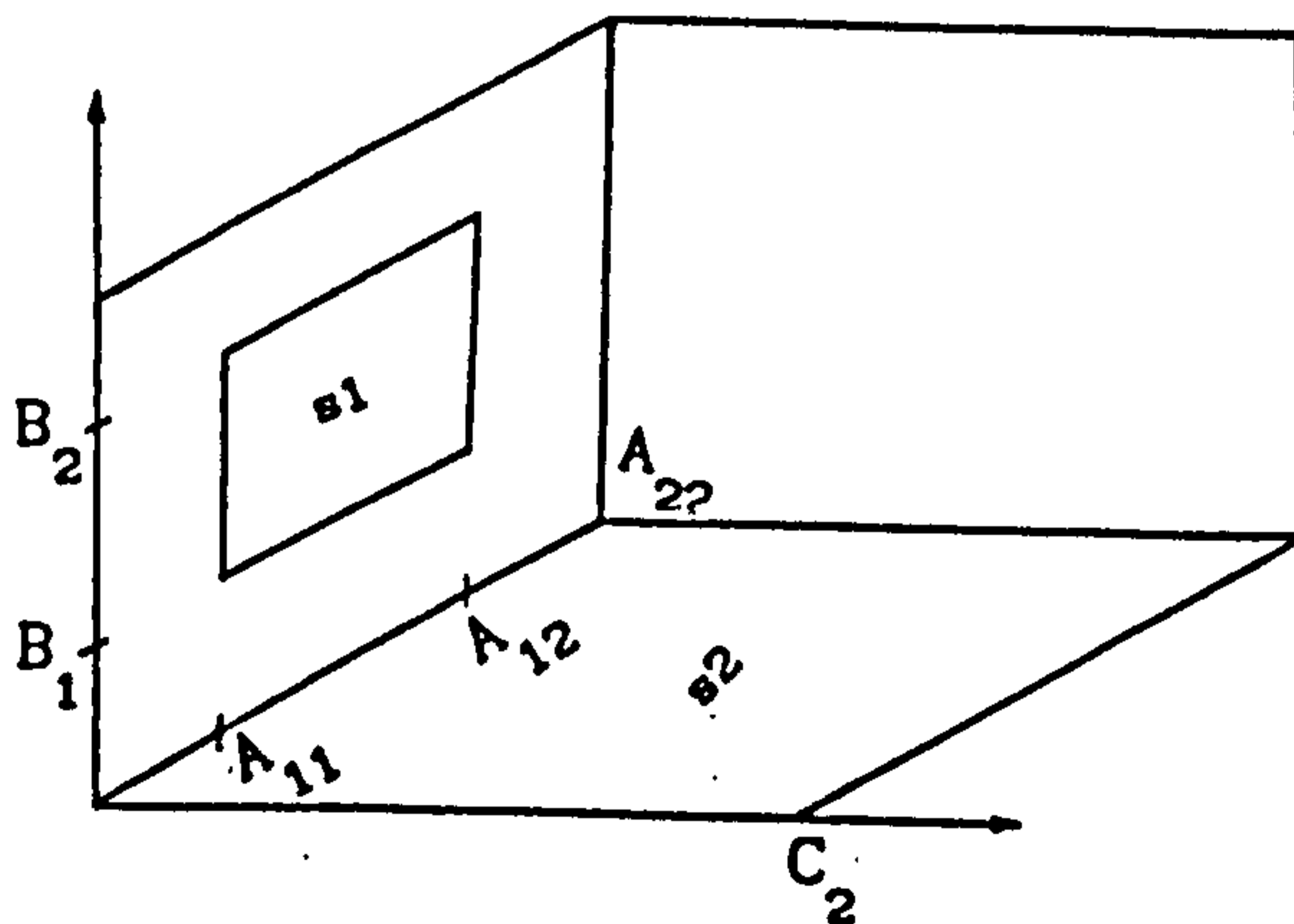
For a window or door Parallel with a wall



$$\begin{aligned}
 F_{s1, s2} = & F_{II}(x_{12}, y_{12}, z_1) + F_{II}(x_{22} - x_{11}, y_{12}, z_1) + F_{II}(x_{12}, y_{22} - y_{11}, z_1) \\
 & + F_{II}(x_{22} - x_{11}, y_{22} - y_{11}, z_1) - F_{II}(x_{12}, y_{11}, z_1) - F_{II}(x_{11}, y_{12}, z_1) \\
 & - F_{II}(x_{22} - x_{11}, y_{11}, z_1) - F_{II}(x_{22} - x_{12}, y_{12}, z_1) - F_{II}(x_{11}, y_{22} - y_{11}, z_1) \\
 & - F_{II}(x_{12}, y_{22} - y_{12}, z_1) - F_{II}(x_{22} - x_{12}, y_{22} - y_{11}, z_1) \\
 & - F_{II}(x_{22} - x_{11}, y_{22} - y_{12}, z_1) + F_{II}(x_{11}, y_{11}, z_1) + F_{II}(x_{22} - x_{12}, y_{11}, z_1) \\
 & + F_{II}(x_{11}, y_{22} - y_{12}, z_1) + F_{II}(x_{22} - x_{12}, y_{12} - y_{12}, z_1)
 \end{aligned}$$

(A-3)

For a window or door perpendicular to a wall



$$\begin{aligned}
 FL_{s_1, s_2} = & FL(A_{12}, B_2, C_2) + FL(A_{22} - A_{11}, B_2, C_2) - FL(A_{12}, B_1, C_2) \\
 & - FL(A_{22} - A_{11}, B_1, C_2) - FL(A_{11}, B_2, C_2) - FL(A_{22} - A_{12}, B_2, C_2) \\
 & + FL(A_{11}, B_1, C_2) + FL(A_{22} - A_{12}, B_1, C_2)
 \end{aligned}$$

(A-4)

## APPENDIX B

*Derivation of thermal Response Factors*  
(MITALAS & STEPHENSON 1967)

The thermal response factors for a homogeneous slab can be expressed directly in terms of the thermal properties and thickness of the slab and the time interval.

The temperature at any point in the slab is given by the following equation

$$T_{d,\tau} = A \left[ \frac{d^3 - d}{6} + d \frac{\tau}{\alpha} + \frac{2}{\pi^3} \sum_{m=1}^{\infty} \frac{(-1)^{m-1} e^{-m^2 \pi^2 \tau} \sin(m\pi d)}{m^3} \right] \quad (B-1)$$

when

$$T_{d,0} = 0$$

$$T_{0,\tau} = 0$$

and

$$T_{1,\tau} = A\tau$$

where

$d = l/l$ ; dimensionless time

$\tau = \alpha t/l^2$ ; dimensionless time

$\alpha$  = thermal diffusivity

$t$  = time

$A$  = rate of surface temperature rise

$$T_{1,\tau} = A\tau \quad \text{or} \quad T_{1,t} = A \frac{\alpha}{l^2}$$

The heat flux through any plane at the distance  $d$  is simply the product of temperature gradient at the plane  $d$  and thermal conductivity  $\lambda$  i.e.

$$Q_{d,\tau} = \lambda \frac{\partial T_{d,\tau}}{\partial d} \quad (B-2)$$

Selection of  $A$  so that the surface temperature is one unit at  $t=\Delta$ , i.e.  $A=\frac{1^2}{\alpha\Delta}$  and substituting  $t=n\Delta$  and  $\tau=\frac{\alpha n\Delta}{2}$  gives

$$Q_{0,n\Delta} = \frac{\lambda}{\alpha} \frac{1}{\Delta} \left[ -\frac{1}{6} - \frac{\alpha n\Delta}{1^2} + \frac{2}{\pi^2} \sum_{m=1}^{\infty} \frac{(-1)^m \gamma_m^n}{m^2} \right] \quad (\text{B-3})$$

$$Q_{1,n\Delta} = \frac{\lambda}{\alpha} \frac{1}{\Delta} \left[ \frac{1}{3} - \frac{\alpha n\Delta}{1^2} - \frac{2}{\pi^2} \sum_{m=1}^{\infty} \frac{(-1)^m \gamma_m^n}{m^2} \right] \quad (\text{B-4})$$

where

$$\gamma_m = \exp\left(-m^2 \pi^2 \frac{2\alpha\Delta}{1^2}\right) \quad (\text{B-5})$$

Thus the surface heat flux through the surfaces due to the triangle surface temperature variation i.e. thermal response factors for a homogeneous slab are:

$$x_0 = -\frac{\lambda}{1} \frac{1^2}{\alpha\Delta} \left[ -\frac{1}{3} - \frac{\alpha\Delta}{1^2} + \frac{2}{\pi^2} \sum_{m=1}^{\infty} \frac{\gamma_m}{(m)^2} \right] \quad (\text{B-6})$$

$$x_1 = -\frac{\lambda}{1} \frac{1^2}{\alpha\Delta} \left[ \frac{1}{3} + \frac{2}{\pi^2} \sum_{m=1}^{\infty} \frac{\lambda_m^2 - 2\gamma_m}{(m)^2} \right] \quad (\text{B-7})$$

$$x_n = -\frac{\lambda}{1} \frac{1^2}{\alpha\Delta} \frac{2}{\pi^2} \sum_{m=1}^{\infty} \frac{\gamma_m^2 - 2\gamma_m^n + \gamma_m^{n-1}}{(m)^2} \quad (\text{where } n \geq 2) \quad (\text{B-8})$$

$$y_0 = -\frac{\lambda}{1} \frac{1^2}{\alpha\Delta} \left[ \frac{1}{6} - \frac{\alpha\Delta}{1^2} + \frac{2}{\pi^2} \sum_{m=1}^{\infty} \frac{(-1)^m \gamma_m^m}{(m)^2} \right] \quad (\text{B-9})$$

$$y_1 = -\frac{\lambda}{1} \frac{1^2}{\alpha\Delta} \left[ \frac{1}{6} + \frac{2}{\pi^2} \sum_{m=1}^{\infty} \frac{(-1)^m (\gamma_m^2 - 2\gamma_m)}{(m)^2} \right] \quad (\text{B-10})$$

$$x_n = -\frac{\lambda}{1} \frac{1^2}{\alpha\Delta} \frac{2}{\pi^2} \sum_{m=1}^{\infty} \frac{(-1)^m (\gamma_m^2 - 2\gamma_m^n + \gamma_m^{n-1})}{(m)^2} \quad (\text{where } n \geq 2) \quad (\text{B-11})$$



**Multi-layer slab:**

If the surfaces of a two layer slab are designated as A B and C (figure C-1)

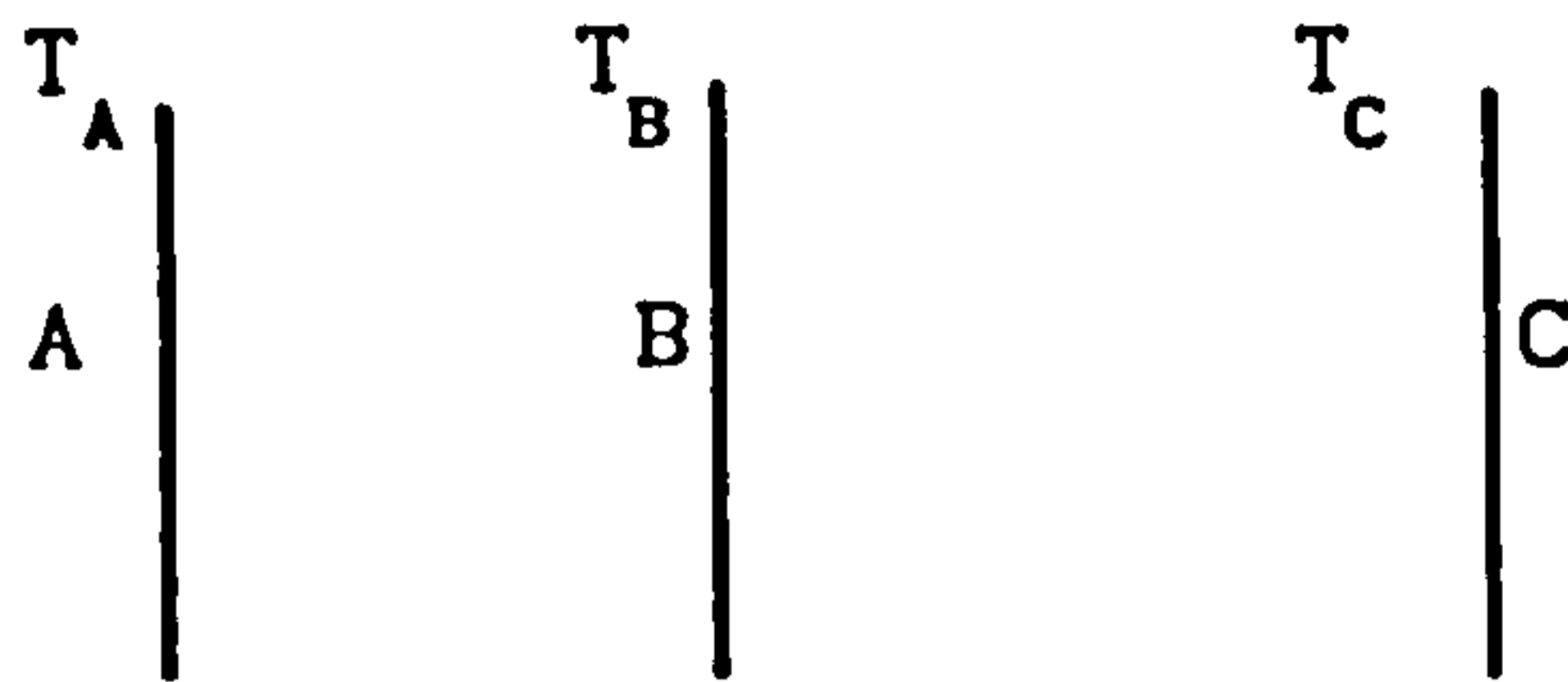


Figure B-1

$$Q_A = T_A X_1 - T_B Y_1$$

$$Q_B = T_A Y_1 - T_B Z_2$$

$$= T_A X_2 - T_C Y_2$$

$$Q_C = T_B Y_2 - T_C Z_2$$

Thus

$$T_B = \frac{T_A Y_1 + T_C Y_2}{Z_1 + X_2} \quad (B-12)$$

and

$$Q_A = T_A \left\{ X_1 - \frac{Y_1^2}{Z_1 + X_2} \right\} - T_C \left\{ \frac{Y_1 \cdot Y_2}{Z_1 + X_2} \right\} \quad (B-13)$$

$$Q_B = T_A \left\{ \frac{Y_1 \cdot Y_2}{Z_1 + X_2} \right\} - T_C \left\{ Z_2 - \frac{Y_2^2}{Z_1 + X_2} \right\} \quad (B-14)$$

The sets in brackets are the response factors for the composite slab. This process can be repeated for as many the number of layers in the slab.

APPENDIX C

*COMPARISON OF MEASUREMENTS AND PREDICTIONS OF DIFFERENT MODELS*

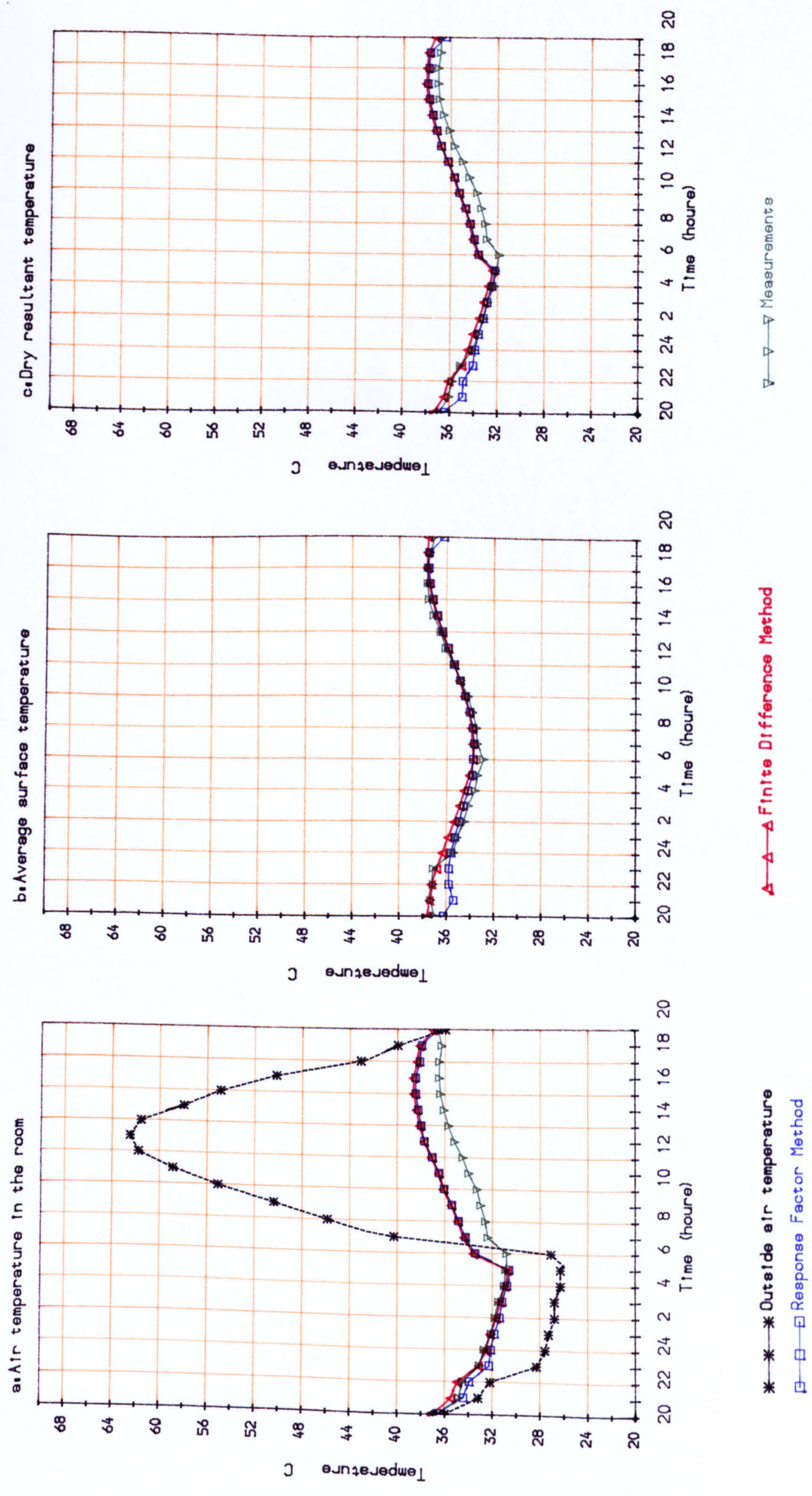


Figure C.1. Comparison of measurements and predictions of the Finite Difference and the Response Factor Method 15 air changes per hour for ten hours (from 2000 to 0600 hours)

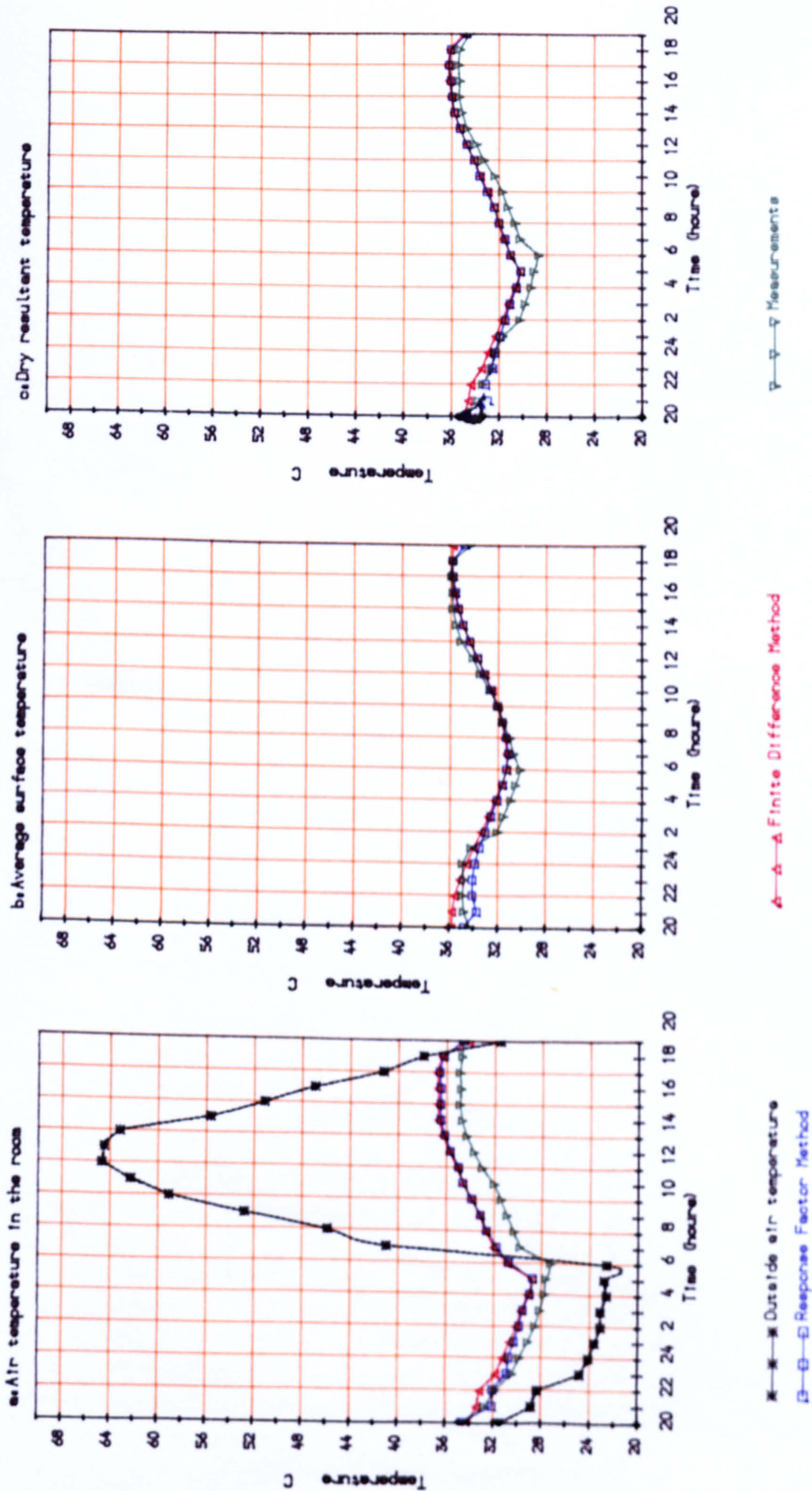


Figure C.2: Comparison of measurements and predictions of the Finite Difference and the Response Factor Method

10 Air changes per hour for ten hours (from 2000 to 0600 hours)

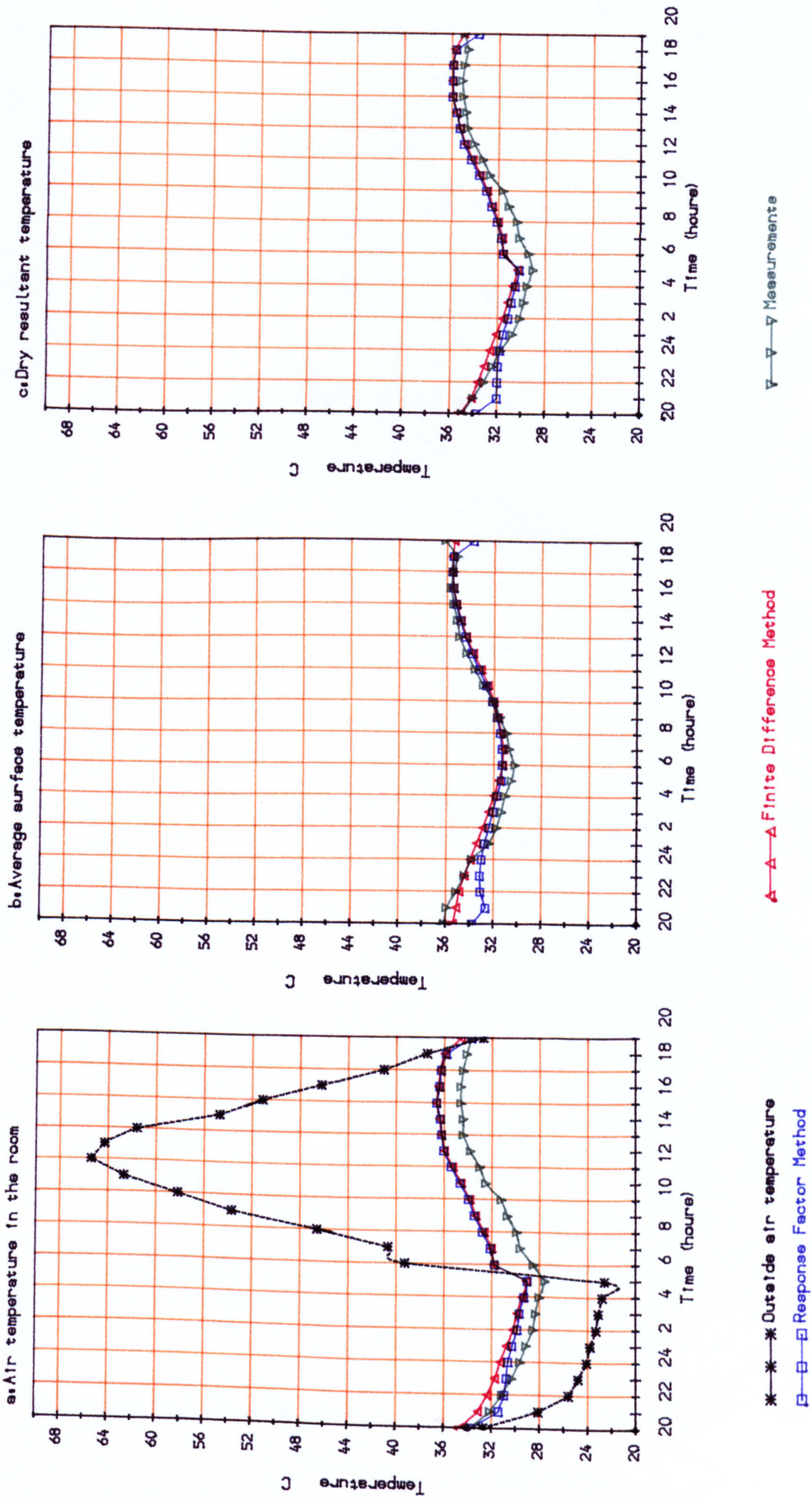


Figure C.3. Comparison of measurements and predictions of the Finite Difference and the Response Factor Method

7 Air changes per hour for ten hours (from 2000 to 0600 hours)

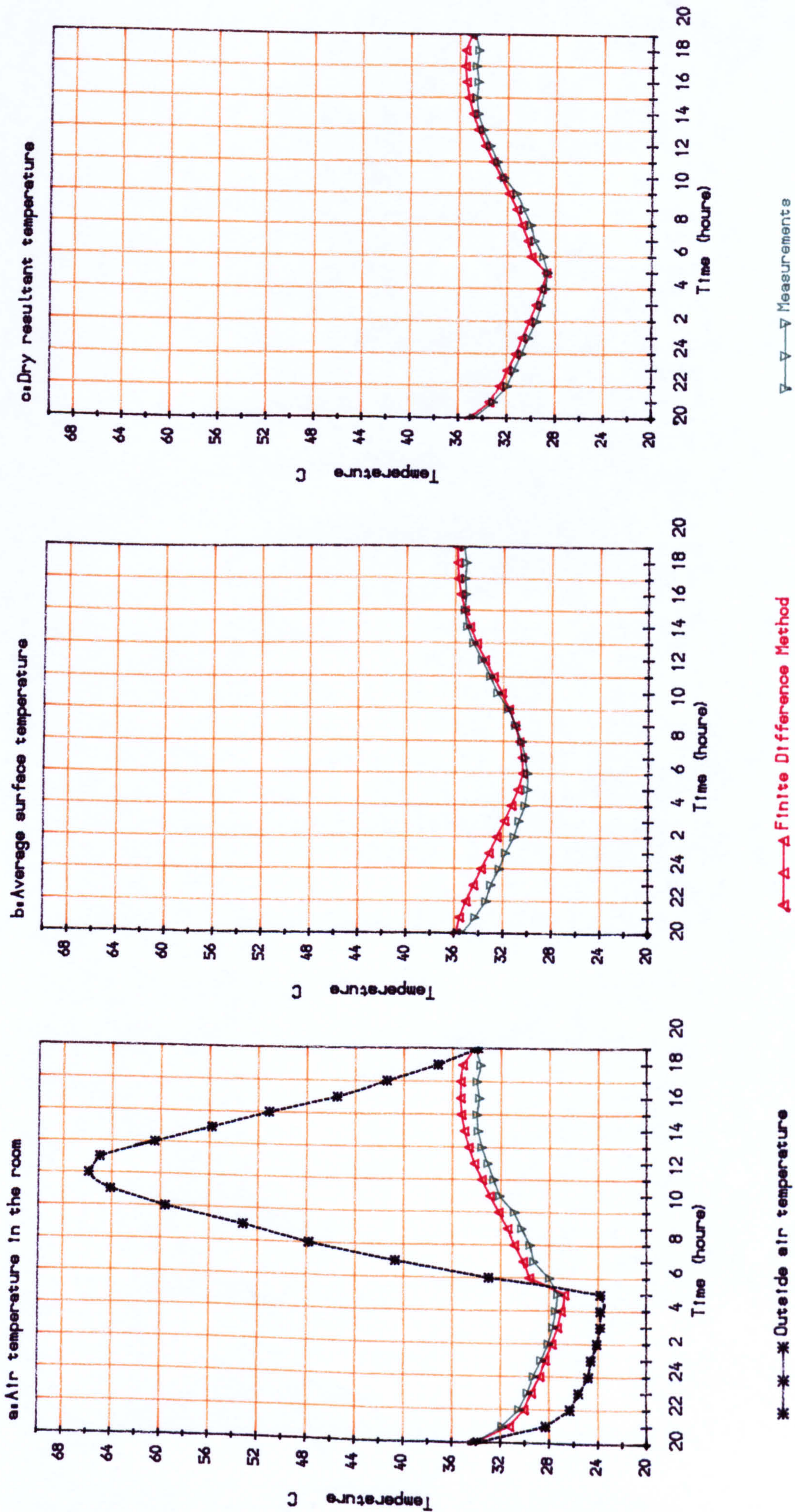


Figure C.4: Comparison of measurements and predictions of the Finite Difference Method, Three-node model (FNIT3.1) 30 air changes per hour for ten hours (from 2000 to 0600 hours)

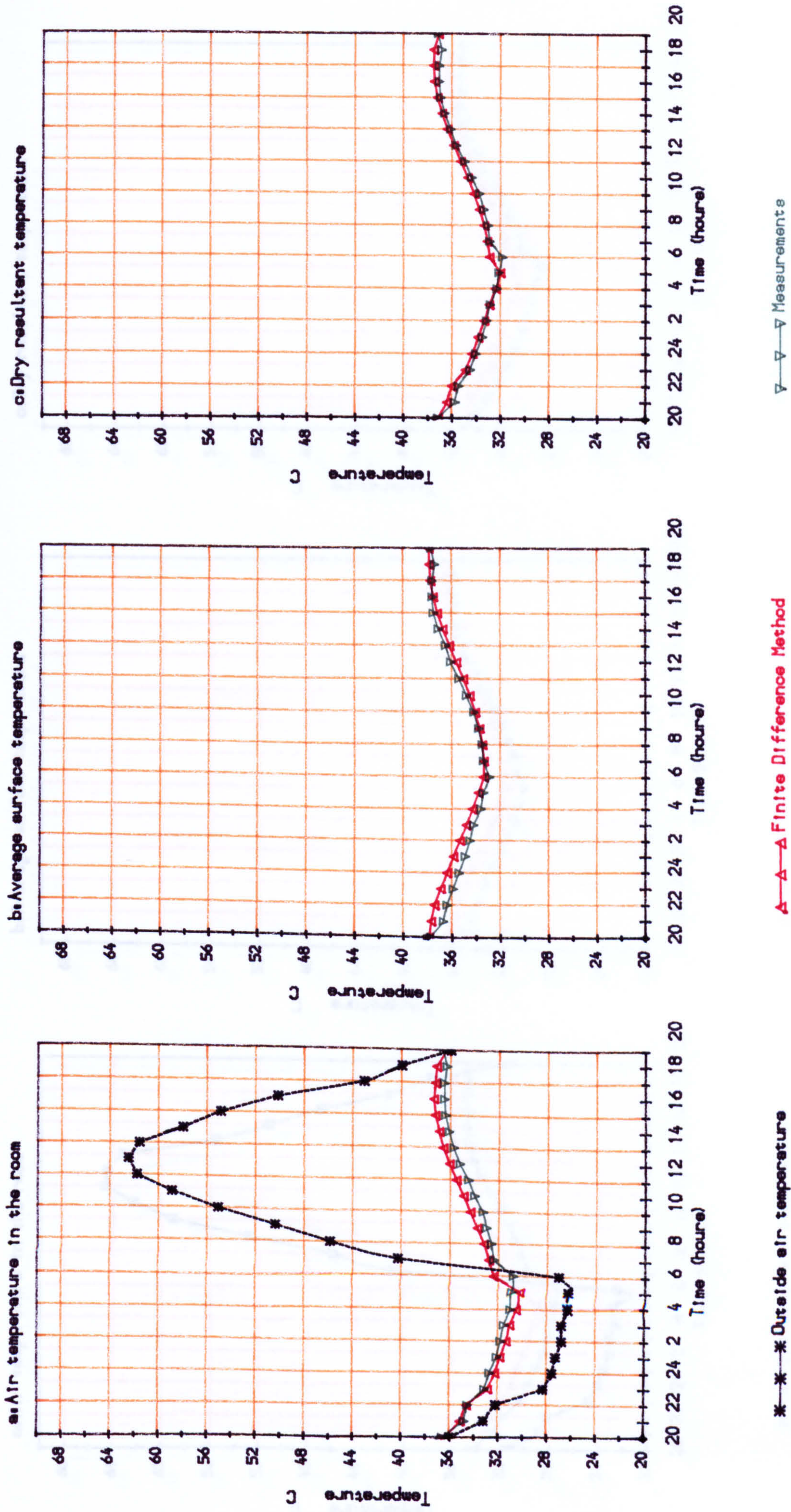


Figure C.5: Comparison of measurements and predictions of the Finite Difference Method, Three-node model (FNIT3.1) 15 air changes per hour for ten hours (from 2000 to 0600 hours)

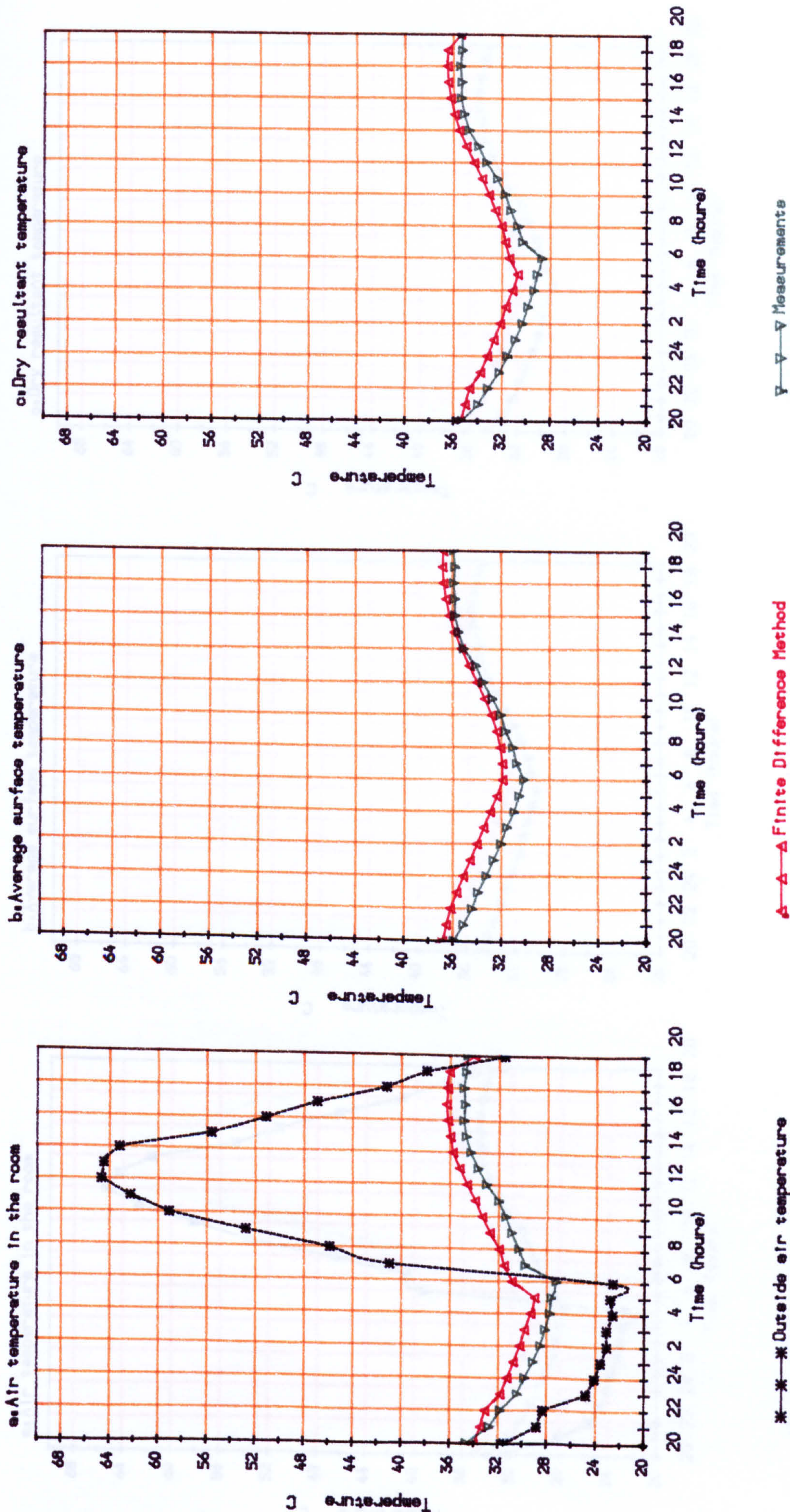


Figure C.6: Comparison of measurements and predictions of the Finite Difference Method, Three-node model (FNIT3.1) 10 air changes per hour for ten hours (from 2000 to 0600 hours)



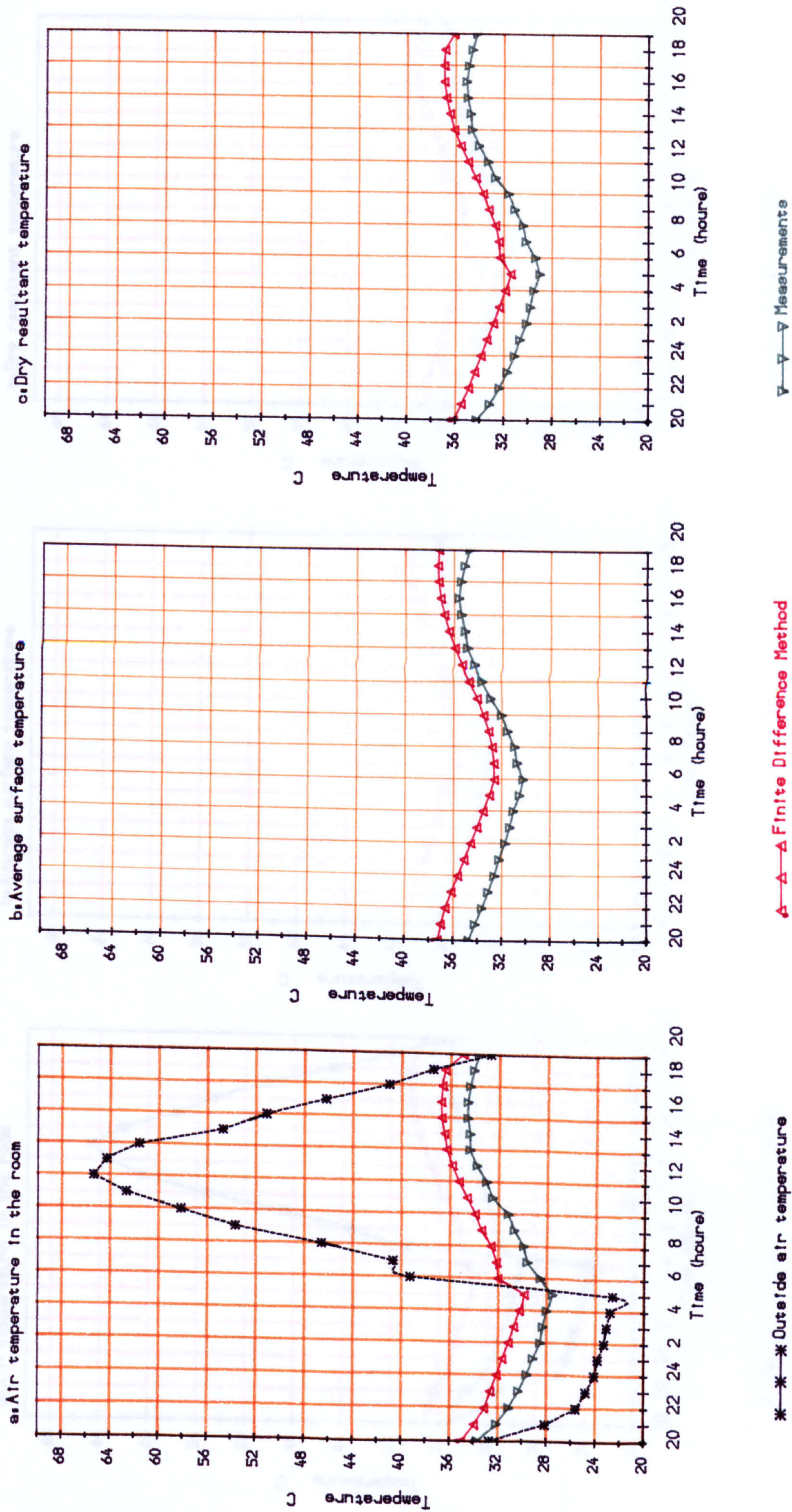


Figure C.7. Comparison of measurements and predictions of the Finite Difference Method, Three-node model (FNIT3.1)

7 air changes per hour for ten hours (from 2000 to 0600 hours)

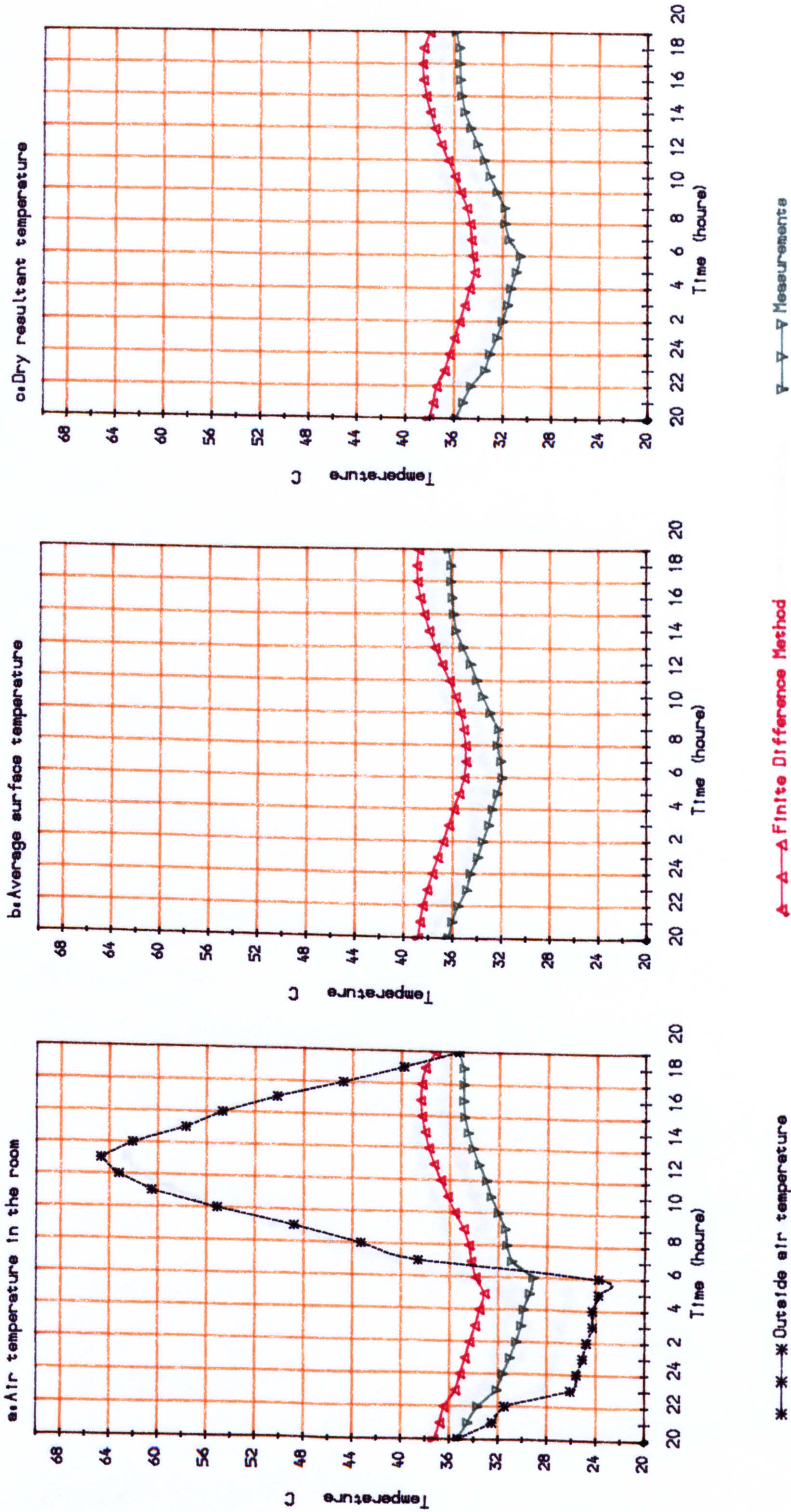


Figure C.8. Comparison of measurements and predictions of the Finite Difference Method, Three-node model (FNIT3.1)

3 air changes per hour for ten hours (from 2000 to 0600 hours)

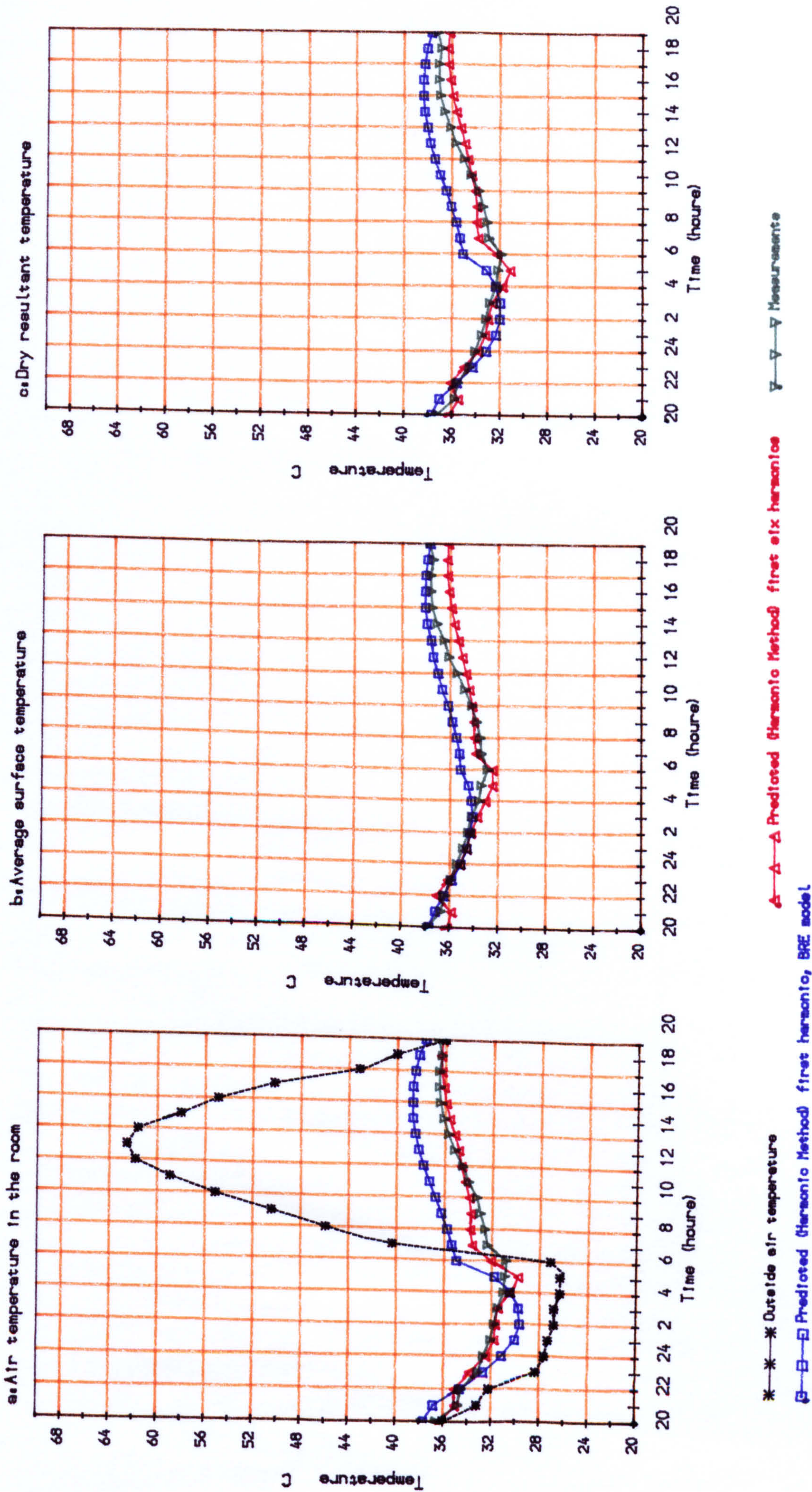


Figure C.9. Comparison of measurements and predictions of the harmonic methods

15 air changes per hour for ten hours (from 2000 to 2400 hours)

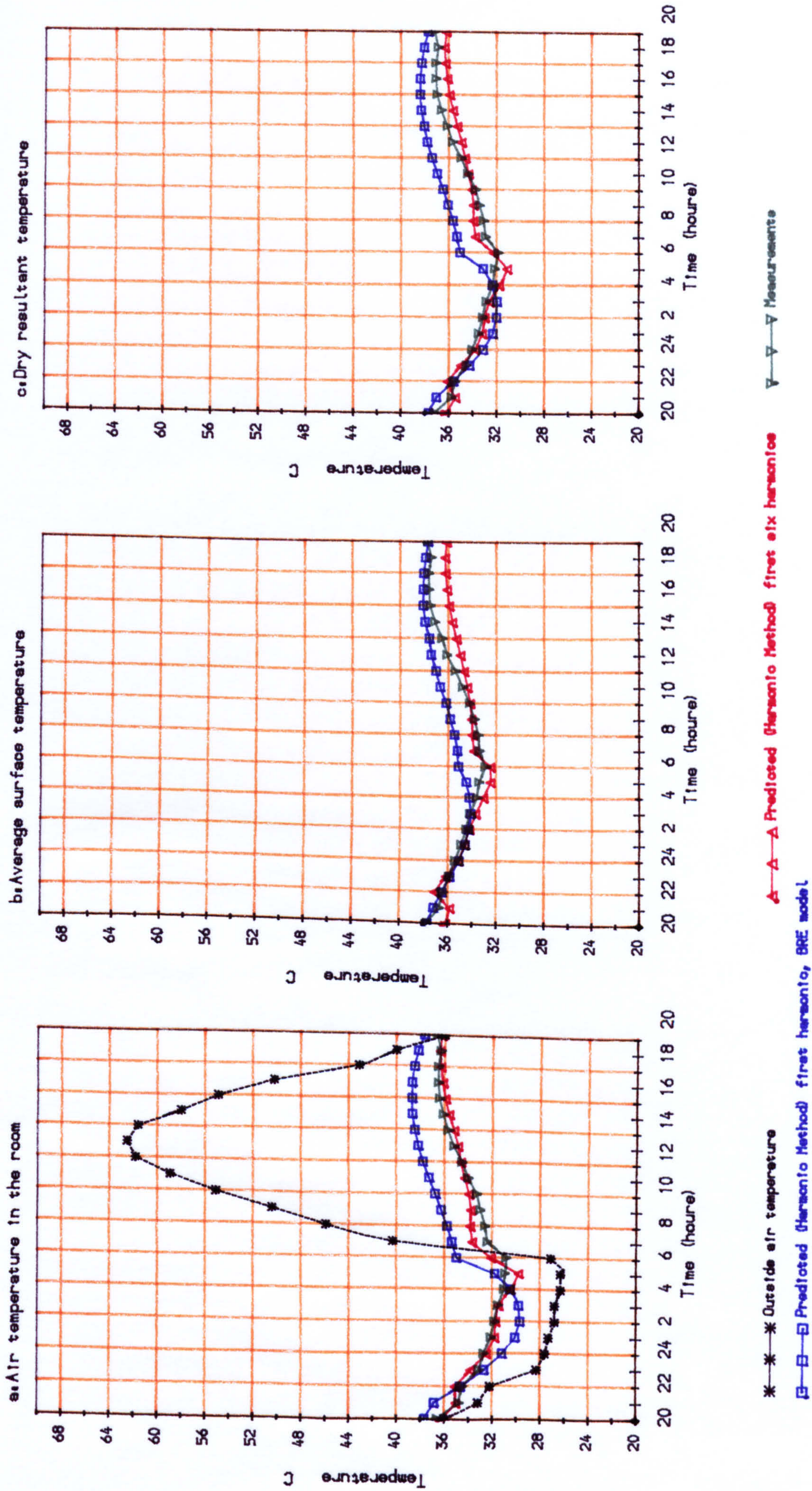


Figure C.10. Comparison of measurements and predictions of the harmonic methods 10 air changes per hour for ten hours (from 2000 to 2400 hours)

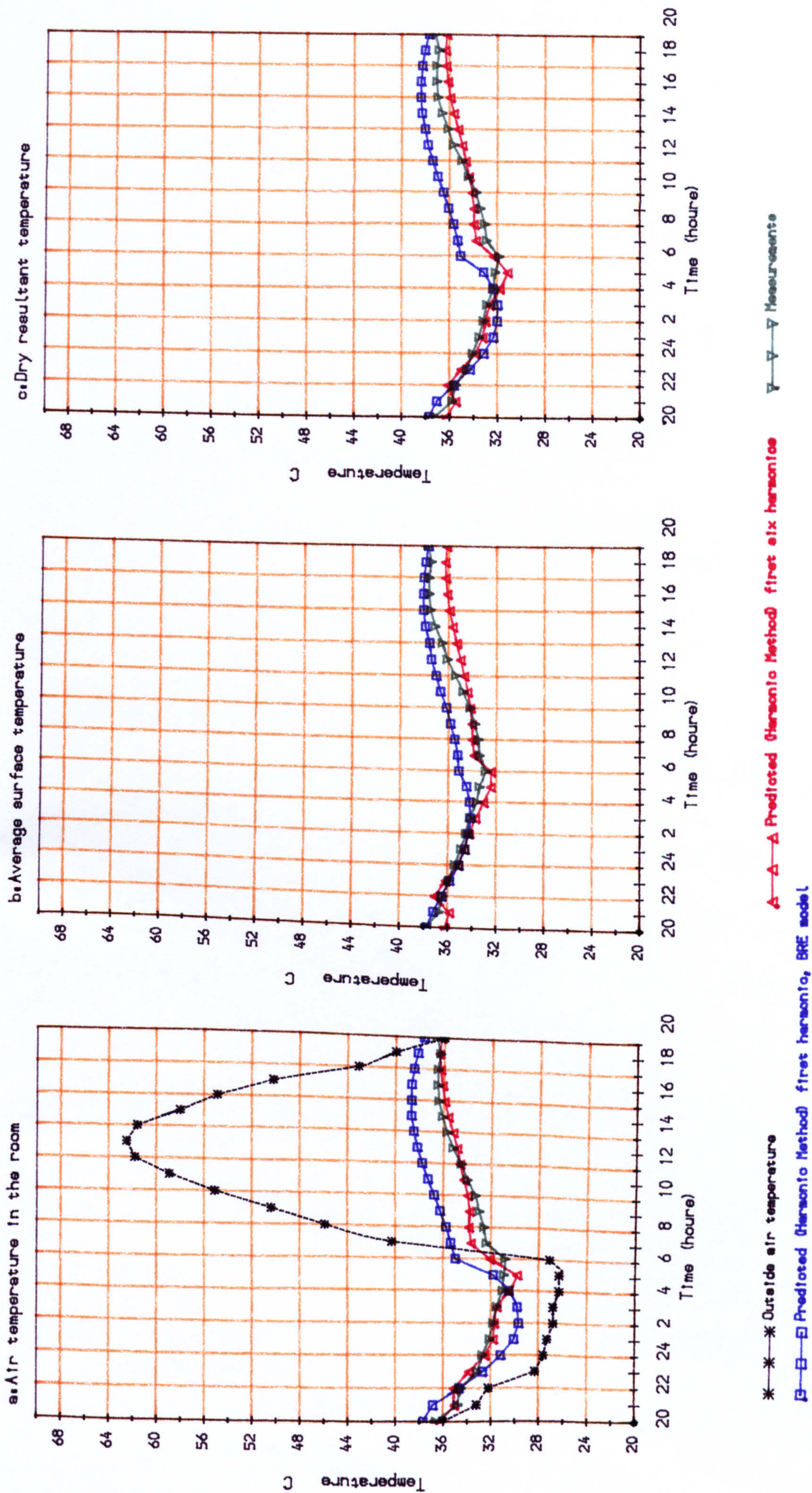


Figure C.11. Comparison of measurements and predictions of the harmonic methods  
 7 air changes per hour for ten hours (from 2000 to 2400 hours)